UNIVERSITY 0F KWAZULU-NATAL

AN INVESTIGATION OF THE HYDRODYNAMICS OF THE TEETERED BED SEPARATOR FOR FINE COAL RECOVERY

2005

L. MAHARAJ

AN INVESTIGATION OF THE HYDRODYNAMICS OF THE TEETERED BED SEPARATOR FOR FINE COAL RECOVERY

Lakesh Maharaj

BSc.Eng (University of Natal)

Submitted in fulfilment of the academic
Requirements for the degree of
MSc.Eng
In the
School of Chemical Engineering
University of KwaZulu-Natal, Howard College Campus, Durban

December 2005

PREFACE

The work in this dissertation was performed at the University of KwaZulu-Natal, School of Chemical Engineering, Howard College Campus, Durban, from February 2004 to December 2005. The project supervisor was Dr. Jon Pocock.

I hereby declare that all work performed in this dissertation is my own, unless otherwise stated in the text, and that it has not been submitted, in whole or in part, for a degree to any other University or Institution.

Lakesh Maharaj

As supervisor of the above-mentioned student, I am satisfied with his work, and hereby approve this dissertation for submission.

Dr. Jon Pocock

ACKNOWLEDGEMENTS

I would like to thank the following people for all their motivation and support, which contributed to the completion of this research project:

- MINTEK for sponsoring the project, in particular Mr. V. Deeplaul and Mr. R. Tait.

- My supervisor, Dr. Jon Pocock, for all his assistance and guidance during the project.

- My co-supervisor, Prof. B.K. Loveday and MINTEK supervisor Mr. David Powell.

- My colleagues in the Mineral Processing Research Group, Allen Hemphill and Nhlanganiso Talent Mabuza, for their assistance and motivation during the project.

- Ms. Ashma Singh (MINTEK) for her assistance with TBS design and operation.

- The workshop technicians at the School of Chemical Engineering for the construction of TBS, in particular, Mr. Kelly Robertson and Mr. Ken Jack.

- The Laboratory Technicians, Mrs. Rekha Maharaj and Mr. Sadha Naidoo, for their assistance with obtaining laboratory chemicals and equipment,

- A special thanks to members of staff, Conrad Sydney, Dhavaraj Naidoo, Niri Naidu and Venishree for all their assistance.

- Ms. Tzu-Hua Huang (Jenny) for all her assistance with the use of CFD package, Fluent 6.1 and Gambit 2.1.6.

- Mr. Chris Brouckaert for his help with multiphase simulations in Fluent.

- The workshop staff, Elliott, Patrick and Congo.

- My fellow postgraduate students in particular, Avin Manilal, Omasha Naicker, Viran Pillay, Denny Mwasiswebe, Yash Nanoolal, Prelan Gounder, Shailendra Rajkumar, Scott Clifford, Etienne Wilson, Jason Knock, Milan Soni, Salvannes George, Vivek Gododia and Thishendren Naidoo.

- Special thanks to Deepesh Gopal, Pranesh Luckan, Deshen Naidoo, Sudashen Moodley, Kevin Naicker and Kumarasen Pillay for their motivation.

- I would like to thank my family for all their love, support, and motivation in particular my father Mr. A.S. Attwarie for making sure that I met all my deadlines, for his constant inspiration, prayer, and wisdom, and to my late mother for her support from above. Special thanks also to Premilla, my sisters, Rajeshree and Yogita, my brother-in-laws', Mistri and Rakesh and my cousin Saksha. I would also like to thank my girlfriend Sandhya, for her love, understanding, patience and support. Love you all.

- Finally but most importantly to my Gods and Pitars for making everything I dream possible.

ABSTRACT

The South African coal industry produces a large quantity of coal per annum. The rejects from various unit operations, such as spirals, consist of fine coal that joins the plants tailings dam waste. As existing high quality resources become depleted, the need to improve recovery of this fine coal grows. This project investigates the use of a teetered bed separator (TBS); a hindered settling gravity concentration device for fine coal recovery. This device has proven successful in the United Kingdom and in Australian collieries for fine coal separation in the size range between 2mm and 0.3mm. It has also been used for decades as a classifying device for silica sand and tin.

The TBS operates in the size range of water-only cyclones and spiral concentrators, and could potentially be used to separate a broader size range of coal fines so as to offer a lower footprint device for the fines recovery section of a plant. Spiral concentrators cannot always be operated efficiently at a separating specific gravity of lower than 1.6; a TBS may also extend the density range for separation and thus improve recovery.

The objective of this project was to gain a full understanding of the TBS from fundamental particle interaction and develop a lab scale unit, which is capable of separation to about 0.1mm at optimum conditions. This involved the development of design parameters based on the various distributor plates and flow pattern modelling. The hydrodynamics of the separator were investigated using the Eulerian-Eulerian modelling approach of commercial CFD package, Fluent 6.1. Seven distributor plates of varying aperture size and geometric arrangement were considered.

Coal and shale particles, sized between 2mm and 0.038mm with a specific gravity (SG) range of 1.2 to 2.0, were separated using the laboratory scale unit. The results of both the simulations and the laboratory tests were then compared.

The simulations revealed that Plate 3 was the best option for implementation. It had an even upward velocity profile compared to the other plates, with minimum wall effects and disturbances. The upward water flow rate (teeter water) was varied experimentally and the composition of the teeter bed, underflow and overflow were analysed using 1.5, 2 and 5mm cubic density tracers with an SG range of 1.2-2.0. Analysis of the partition curves of the distributor plates revealed that Plate 3 had the lowest Ecart Probable (Ep) and cut-point

densities. The comparison of simulated results and experimental results show that the simulator could predict the distributor plate design with the lowest Ep in practical tests. The simulator could be beneficial when optimising an industrial scale unit, by allowing prediction of improved segregation patterns and thus separation efficiency.

TABLE OF CONTENTS

LIST OF TABLES

LIST OF FIGURES

NOMENCLATURE

SYMBOL	DESCRIPTION	UNITS
A	Bed cross sectional area	m^2
C_i	Concentration of particle of type i	kg/m^3
D	Diffusivity coefficient	m^2/s
α	Empirical correction factor	-
ε	Voidage	-
ε_i	Voidage for single particle of type i	-
ΔP	Pressure Drop	Pa
d	Particle diameter	m
d_i	Particle diameter of species i	m
g	Acceleration due to gravity	m/s^2
ρ_s	Solid density	kg/m^3
ρ_i	Solid density of species i	kg/m^3
ρ_f	Liquid density	kg/m^3
ρ_m	Suspension density	kg/m^3
μ	Liquid viscosity	Pa.s

ϕ	Volume fraction of solids	-
ϕ_i	Volume fraction of particle type i	-
u	Velocity	m/s
u_{mf}	Minimum fluidization velocity	m/s
u_t	Terminal settling velocity	m/s
Re	Reynolds Number	-
Re_t	Reynolds Number at terminal settling velocity	-
M	Mass of material in the bed	kg
V	Volume	m^3
n	Richardson-Zaki parameter	-
z	Bed height	m

CHAPTER 1: INTRODUCTION

1.1. Background

The Teetered Bed Separator (TBS) was developed from the hydrosizer concept in 1934 (Drummond et al, 2002). The TBS is a hindered settling gravity concentration device for minerals recovery. These units have been employed for coal recovery since the 1960s and utilised in the UK since the 1980s (Drummond et al, 2002). In recent years, the TBS has been introduced into the Australian and the South African coal industries.

The Australians have performed intensive research on the TBS in an attempt to convince industry that it is the best option. This has proven extremely successful. Companies like Eriez Magnetics and Minerals Engineering Processes Ltd (MEP) have also developed and tested units in an attempt to sell their product. QVA Process Technologies (Pty) Ltd introduced the TBS to South Africa in 2002 and compared the MEP Hydrosizer and its advantages over spirals and other hindered settling devices (Craddock and Hand, 2002). It has been adopted in certain coal mines due to its proven advantages over the current spirals circuits however many still question its capabilities.

The TBS has proven successful in the -2mm + 0.3 mm particle size range (Nicol, 1998). Although density effects dominate the separation process, other variables such as size, shape, fluid properties, operation parameters and distributor design have significant roles in the separation (Nicol, 1998). The TBS operates in the size range of water-only cyclones and spiral concentrators, and could potentially be used to separate a broader size range of coal fines so as to offer a lower footprint device for the fines recovery section of a plant.

1.2. Uses of the TBS

Teetered bed separators have a range of uses for fine coal treatment in new plants, in upgrade situations for the reprocessing of spiral product, mineral sand processing, tailings recovery and run of mines (ROM) coal processing. Over 200 units exist worldwide which take advantage of its capabilities, which include low cut-points, previously unattainable efficiencies and short payback periods (Nicol, 1998). The hindered bed separator is widely applied in the mineral processing industry due to its high separation efficiency, simple structure and low operational cost (Nicol, 1998). The TBS has several advantages compared to the spiral separators, which include, a high solids handling capacity – a 3m diameter TBS will handle 150 t/h solids, a small footprint area with a minimum feed slurry distribution problem (Nicol, 1998).

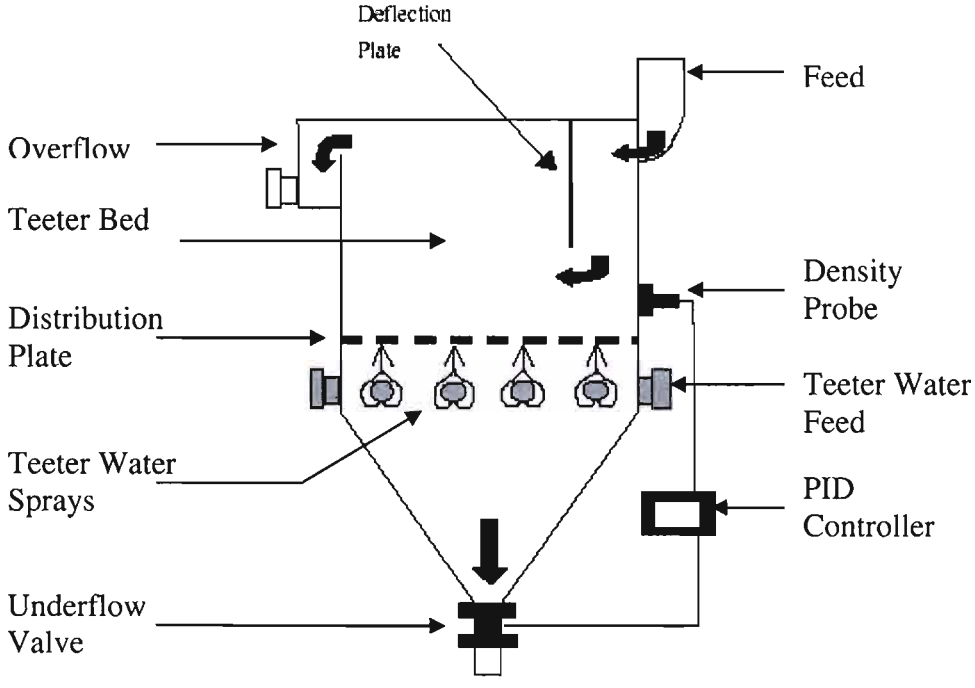

Figure 1.1: Diagram representing a Teetered Bed Separator (Nicol, 1998)

1.3. Operation of the TBS

The TBS operates similar to an elutriator, which permits separation by particle size. Since it is a hindered bed classifier, separation is based on density rather than particle size. The coal slurry is fed tangentially from the top of the cylindrical vessel in this continuous process. The feed is met by an evenly distributed upward water current (teeter water). Particles of a higher settling velocity report to the underflow whereas those with a lower settling velocity report to the overflow. A valve controls the underflow outlet.

The deflection plate or baffle prevents any feed disturbances to the system. By restricting the underflow outlet, the lower section forms a bed of particles, called a teeter bed. This bed acts as an autogenous dense medium due to a high particle concentration, so particles experience a density gradient. This creates the condition of hindered settling. Controlling the teeter water flow enhances the fine coal separation. The density of the bed is controlled using a PID controller on the underflow exit valve.

1.4. Objectives of the project

The main aim of this research project was to investigate the hydrodynamic behaviour, fundamental particle interactions and internal velocity profiles within the TBS in response to changes in the distributor plate configurations to achieve fine coal recovery below 0.1mm.

These objectives could be achieved by considering the following investigations:

- An extensive literature review on gravity concentration, hindered settling, recent TBS Technology and liquid-solid hydrodynamics.

The research focused on the effects of the general settling theory and the concentration criterion on the separability of the process. The fluidisation theory was extremely significant in this investigation due to the operational similarities of the TBS to fluidised bed systems, in particular liquid-solid fluidisation. Other factors such as the pressure-velocity relationship, mixing and segregation were discussed. The fundamental concepts of hindered settling were researched, in order to interpret the particle interactions and behavioural patterns, within the packed bed of the TBS in terms of mathematical relations.

- The design and operation of a lab scale TBS unit, with various distributor plate configurations, in order to perform density tracer tests to determine particle circulation patterns, tracer profiles through the bed and determine the efficiency of separation.

The study investigates the use of a broad size range of coal particles of between 2mm and 0.038mm with a specific gravity range of 1.2, 1.4, 1.6, 1.8 and 2.0 SG, to determine the separation capabilities of the TBS based on the various distributor plate designs. The density tracer particles were used to monitor the particle behaviour in response to these variations and obtain a density profile through the teeter bed.

- Modelling of the laboratory system on a commercial Computational Fluid Dynamics (CFD) Package, and perform simulations to determine the velocity profiles within the separator with respect to each plate configuration.

The simulations would be beneficial in determining the hydrodynamic profiles through the teeter bed due to the effect of the distributor plate configurations.

- Compare experimental and simulated results to determine if CFD would be a useful tool in industrial scale up.

The comparison would serve as an indication of the benefits of CFD for optimisation of existing technology, and to observe if it may be a more beneficial tool for improving plant efficiency. This was observed by testing different distributor plate configurations with the simulation package, and in the laboratory scale TBS.

CHAPTER 2: LITERATURE REVIEW

This chapter provides a critical review of previous researchers' work in the field of Gravity Concentration, Fluidisation and fundamental concepts of Hindered Settling. Conclusions and comparisons have been made based on the different systems considered.

2.1. Settling Theory

Gravity separation is applied to processes in which particles are separated from each other due to different settling rates in fluids e.g. water. The classical theory of particle separation by differential settling velocity is properly applied only to motion in a fluid.

Free settling refers to the sinking of particles in a volume of fluid which is large with respect to the total volume of particles, hence particle crowding is negligible (Wills, 1985). Free settling predominates for a solids content less than 15%.

Consider a spherical particle of diameter d and density ρ_s falling under gravity in a viscous fluid of density ρ_f, under free settling conditions. The particle is acted upon by a downward gravitational force, an upward buoyancy force due to the displaced fluid and a drag force D acting upwards. The equation describing the particle motion is:

$$mg - m'g - D = m\frac{du}{dt} \tag{1}$$

Where m is the mass of the particle m' is the mass of displaced fluid and u is the particle velocity.

At terminal velocity: $$\frac{du}{dt} = 0 \quad (2)$$

and hence $$D = (m - m')g \quad (3)$$

The volume of a sphere is defined as: $$V = \frac{\pi d^3}{3} \quad (4)$$

Since $$m = \rho_s V \quad (5)$$

And $$m' = \rho_f V \quad (6)$$

Therefore $$D = \frac{\pi}{6} g d^3 (\rho_s - \rho_f) \quad (7)$$

Stoke assumed that the drag force on a spherical particle is due to the viscous resistance and deduced the following expression:

$$D = 3\pi d\mu u \quad (8)$$

Substituting in equation (6)

$$3\pi d\mu u = \frac{\pi}{6} g d^3 (\rho_s - \rho_f) \quad (9)$$

and

$$u = \frac{gd^2(\rho_s - \rho_f)}{18\mu} \tag{10}$$

This expression is known as Stoke's Law (Wills, 1985). It is valid for particles below 50 microns in diameter up to a Reynolds number based on the diameter of the sphere of about 0.1. Above this laminar range its predictions of the drag force is about 10 percent lower (Bird et al. 1960).

It can be simplified to

$$u = k_1 d^2(\rho_s - \rho_f) \tag{11}$$

where k_1 is a constant.

Newton assumed that the drag force was entirely due to the turbulent resistance, and deduced,

$$D = 0.055\pi\ d^2 u^2 \rho_f \tag{12}$$

Substituting in equation (6) gives,

$$0.055\pi\ d^2 u^2 \rho_f = \frac{\pi}{6} g d^3(\rho_s - \rho_f) \tag{13}$$

thus

$$u = \left(\frac{gd(\rho_s - \rho_f)}{0.33\rho_f} \right)^{\frac{1}{2}} \tag{14}$$

This is Newton's Law for turbulent resistance (Wills, 1985). It is valid for particles larger than 5mm in diameter.

It can be simplified as follows:

$$u = k_2[d(\rho_s - \rho_f)]^{\frac{1}{2}} \tag{15}$$

Where k_2 is a constant.

Both Laws are invalid for the intermediate size range. This is the size range in which most wet classification is performed. Newton and Stokes Laws' have also been derived assuming that the particles are spherical. Since this investigation is based on coal, which is composed of irregular sized, porous particles of varying size and density, the above relationships will not be representative of the settling velocity. These relationships have been modified by a number of researchers as shown in Chapter 2.3 and 2.4.

Concentration Criterion

Consider two particles of mass m_a and m_b, density ρ_a and ρ_b, radii r_a and r_b, settling in a fluid of relative density ρ_f. For equal settling velocities in Stoke's range,

$$Kr_a^2(\rho_a - \rho_f) = Kr_b^2(\rho_b - \rho_f) \tag{16}$$

The ratio of particle sizes

$$\frac{r_a}{r_b} = \left[\frac{\rho_b - \rho_f}{\rho_a - \rho_f}\right]^{\frac{1}{2}} \quad (17)$$

Using Newton's Law:

$$\frac{r_a}{r_b} = \left[\frac{\rho_b - \rho_f}{\rho_a - \rho_f}\right] \quad (18)$$

This ratio (Eq. (18)) reveals the separability of particles of differing density known as the Settling Ratio or Concentration Criterion. If this ratio is greater than 2.5, then gravity concentration will be easy. Separation is virtually impossible if the ratio is less than 1.25 and a process such as dense medium separation must be employed (Wills, 1985).

The Concentration Criterion shown above relates to free settling. When hindered settling occurs, the fluid displaced by one particle will create an upward current for the adjacent particles since particles are closer together and interfere with one another. The suspension density must be considered in place of the fluid relative density ρ_f when determining the ratio. This considers the fluid and the particles effect on the suspension (Horsfall, 1993).

Horsfall (1993) stated that the criterion is actually the ratio of sizes of equal settling particles and explained the significance to the separation process. He explained that the ratio showed the size range to be treated in the gravity concentrator. This means that the particles within such a size ratio will separate from each other because of their different settling rates, i.e. at that ratio, all the high density particles will settle faster than the low density particles.

If a feed containing coal of 1.3 SG and shale of 2.4 SG with a Concentration Criterion ratio of 4.7 is sized between 46mm and 10mm, all the shale particles will settle faster than the coal particles, by a simple gravity-processing unit. If however, 50mm coal particles were used, it would settle faster than the 10mm shale. An undersize shale particle say 8mm, will settle more slowly than a 10mm coal particle, and so report to the clean coal.

This resulted in feeds to gravity units being closely sized to improve the efficiency. As the density of the particles to be separated gets closer, so does the size range, making certain separations impractical.

The settling ratio of the coal sample depends on the sink float analysis of the feed. The majority of the coal in this investigation falls in the 1.3 and 1.4 specific gravity range resulting in a ratio of 2 assuming a suspension density of 1.2 SG. Thus, separation would be difficult and inefficient in the TBS or any water-only unit. Coal of higher specific gravity is present, however it contributes a smaller mass fraction compared to the lights. The coal feed size distribution is presented in the Coal Properties in Chapter 4.7.

Chapter 2.2 introduces the fluidisation theory, which is significant to the operation of the TBS. The TBS is essentially a fluidised bed separator however due to the high particle concentration, the cross flow feed and teeter water flow, the particles experience a density and hindered settling effect. The TBS feed has particles of varying size and density, thus every particle phase experiences a specific minimum fluidisation velocity. The various phenomena associated with fluidised beds such as the pressure-velocity relationship, mixing and segregation also apply to the TBS.

2.2. Fluidised Beds

Fluidisation occurs when a bed of solid particles is met by an upward fluid flow with an intermediate range of flow rates (Couderc, 1985). The particles experience a fixed state when the flow rate is low and lie on one another. At high velocities, the particles experience a pneumatic or hydraulic transport. The bed is fluidised when the particles are suspended in the fluid and the bed is stationary relative to the unit. This occurs in the intermediate flow regime.

2.2.1. Pressure-Drop –Velocity Relationship

Ideal behaviour is noted for particles of uniform shape and size. As the fluid flows through a packed bed of solid particles, the frictional resistance increases and the pressure drop across the bed can be measured. The velocity is proportional to the pressure drop during the fixed bed stage.

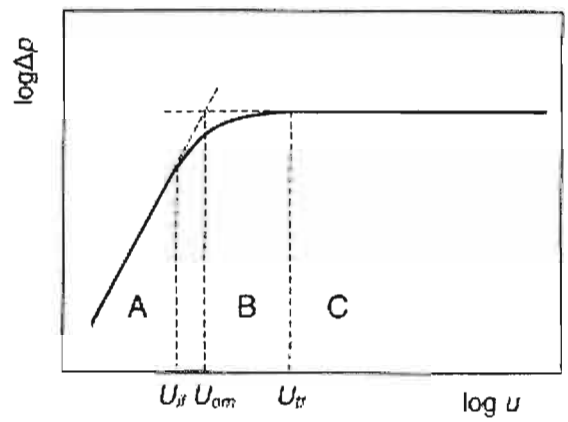

Figure 2.1: Relationship showing Pressure Drop versus Superficial Velocity in a binary system (Carsky, 2002)

Figure 2.1 represents a binary system with three distinctive points and fluidisation regions. U_{if} represents the incipient fluidisation velocity. U_{om} is the hypothetical minimum fluidisation, which occurs between the regions A and C and U_{tf} is the total fluidisation velocity. Most fluidised beds lie between these extremities (Carsky, 2002).

During the fluidisation process, the upper surface of the bed becomes horizontal and the inside layers move more slowly and rearrange. As the velocity is increased, the pressure drop begins to stabilise and remains constant, however the bed height increases. When the flow rate is decreased, a point is reached where the pressure drop becomes equivalent to the buoyant weight of solid particles per unit area of the cross-section of the column. The incipient fluidisation or minimum fluidisation (u_{mf}) conditions occur between the fixed and fluidised states (Davidson et al., 1985).

The pressure drop is described by the following expression:

$$\Delta P = \frac{M}{\rho_s A}(\rho_s - \rho_f)g \tag{19}$$

$$\Delta P = (\rho_s - \rho_f)(1-\varepsilon)zg \tag{20}$$

Where A is the cross sectional area (m^2), M is the mass of particles (kg), ε is the bed porosity and z is the bed height (m).

2.2.2. Liquid-Solid Fluidisation

Liquid-solid fluidisation gives rise to particulate behaviour, which has been described as homogenous (Davidson et al., 1985). Many deviations occur from the ideal behaviour and are briefly described below.

Locally organized solid movements with vertical upward motion cause channelling in particular regions and downward motion in other cases (Davidson et al., 1985). Handley et al. (1966) and Couderc and Angelino (1970) have shown that channelling is caused by poor liquid distribution at the base of the bed. It can be avoided by using a distributor with a uniform velocity profile. Couderc and Angelino (1970) carried out several experimental tests on channelling. They found that channelling results in differences in the local pressure drop. This causes velocity fluctuations in the bed. The low velocities would result in dead zones in certain regions of the bed whereas the high velocities cause turbulent zones and particle entrainment.

Parvoids are low-density strata in liquid fluidised beds (Hassett, 1961), which result from solids mixing. The authors describe them as high-voidage horizontal bands about one centimetre wide that form near the distributor plate. They can occupy the whole cross section of the column

depending on the liquid flow rate and tend to result in large dead zones near the distributor, lowering the liquid velocity.

Particulate fluidisation occurs in a liquid-solid system when the bed continues to expand as the velocity is increased above the minimum velocity. The teeter bed separator operates similar to a fluidised bed. As the teeter water velocity increases the particles in the teeter bed begin to rise and fluidise. The TBS operates best at a low water fluidisation velocity to minimize the particle mixing due to dispersion and attain a sharp segregation effect in order to increase the suspension density, which enhances the gravity separation process. The relationships described by Richardson and Zaki (1954) relating to bed porosity and particulate fluidisation for fluidised beds are also used to describe the particle interaction in the TBS.

2.2.3. Mixing and Segregation

The particle behaviour in a fluidised bed is due to diffusion and classification. Diffusion describes the random mixing of particles in a fluidised bed. Classification is the tendency of particles to segregate based on their difference in size and density. The Kennedy and Bretton diffusion model (1966) was used to account for mixing, segregation and diffusion in nature.

$$D_i \frac{dC_i}{dz} = C_i(\frac{u}{\varepsilon} - u_{pi}) = C_i \bar{u}_{pi} \qquad (21)$$

Where D_i is the axial dispersion coefficient of particles of the i^{th} type, $\frac{u}{\varepsilon}$ is the interstitial liquid velocity and $\bar{u}_{pi}$ is the convective particle velocity or slip velocity.

In a bi-disperse fluidised bed, Equation (21) written for a two-component system constitutes a coupled set of non-linear first order equations in which the local bed porosity is expressed in terms of total solid concentration:

$$\varepsilon = 1 - (C_1 + C_2) \tag{22}$$

Kennedy and Bretton (1966) based their model on a diffusional flux generated in the direction of decreasing concentration. At steady state, the diffusional flux is counterbalanced by a convective flux. This results from the relative motion between particles and the fluidising liquid. They used a steady state mass balance with boundary conditions to estimate a dispersion coefficient, thus yielding the axial concentration and porosity.

Juma and Richardson (1983) showed that between two completely segregated zones there exists a transition zone caused by bed porosity fluctuations from one end to the other. Size and density changes increase the complexity of the model. They used a direct method of integration of Equation (21). The slip velocity $\bar{u}_{pi}$ was expressed as a linear function of axial position in the transition region.

$$\bar{u}_{pi} = \frac{u}{\varepsilon} - u_{pi} = a_i + b_{iz} \tag{23}$$

using the Richardson-Zaki relationship for u_{pi}:

$$u_{pi} = u_{ti}\varepsilon^{n_i - 1} \tag{24}$$

The coefficients a_i and b_i were evaluated by fitting experimental axial porosity data. Mono-component boundary compositions were used as boundary conditions.

Pattwardhan and Tien (1985) used an alternative method based on the computation of the locus of admissible concentration pairs for the concentration and porosity profile in the bed. Gibilaro et al. (1986) used the same method with concentration pairs. (C_1, C_2).

Dutta et al. (1988) discussed the dependence of the Kennedy Brenton model (1966) on liquid velocity, particle size and density. Complete or partial segregation occurs depending on the flow regime. Their experimental work yielded valuable results. They found that the dispersion coefficient was dependent on the liquid velocity. An increase in dispersion coefficient occurred, as the liquid velocity and bed porosity was increased. Their analysis on a coke sample concluded that the dispersion coefficient was smaller for smaller particles.

Juma and Richardson (1983) also expressed the same results. They found that larger size, lower density particles, overshadows porosity. The main factors affecting segregation are liquid velocity, bed porosity, particle size, and density and shape factors.

2.2.4. Particle interactions and pressure drop in a fluidised bed

The total pressure in a fluidised bed due to a single particle species increases down through the bed.

$$P_T = \phi_i \rho_i g H + (1-\phi_i)\rho_f g H \tag{25}$$

The total pressure gradient is given as:

$$\frac{dP_T}{dH} = \phi_i(\rho_i - \rho_f)g + \rho_f g \tag{26}$$

The pressure gradient consists of two terms. The first is due to the weight of the particles in the liquid and the dissipative drag force and secondly the hydrostatic head of the liquid.

The dissipative pressure gradient is,

$$\frac{dP}{dH} = \phi_i(\rho_i - \rho_f)g \tag{27}$$

The Ergun Equation (1952) was used to determine the voidage of the bed in the TBS. The Ergun equation is derived based on spherical particles in fixed bed region of the pressure drop-velocity relationship. The effective particle diameter was corrected by using the sphericity of coal and the average particle diameter from the size distribution of the feed coal.

$$\frac{(-\Delta P)}{\rho} = \frac{150(1-\varepsilon)^2 \mu u_0 L}{\varepsilon^3 d_p{}^2 \rho} + \frac{1.75(1-\varepsilon) u_0{}^2 L}{\varepsilon^3 d_p} \tag{28}$$

Where ρ is the density of water, μ is the viscosity of water, ε is the bed porosity, u_o is the superficial water velocity (m/s), L is the bed length (m) and ΔP is the pressure drop (Pa).

Foscolo et al. (1983) aimed to obtain a theoretical relationship for velocity and voidage since the pressure drop in a fluidised bed may be equated to the buoyant weight of suspended particles in a unit area of the bed cross section. They developed this relationship for laminar and turbulent flow.

$$\Delta P(u, \varepsilon) = u^a \varepsilon^{\ b} \tag{29}$$

$$\Delta P(u, \varepsilon) = c \tag{30}$$

Where c is a constant.

$$d\Delta P = \frac{\partial \Delta P}{\partial u} du + \frac{\partial \Delta P}{\partial \varepsilon} d\varepsilon = 0 \tag{31}$$

They related the drag force of a single particle to the global pressure drop i.e. (the floating weight of the suspension). They also investigated the dependency of tortuosity i.e. (diffusion in porous solids) and the turbulent kinetic energy.

2.3. Hindered Settling

Due to the presence of a large quantity of particles of varying size and density, particle to particle collisions or 'near misses' occur (Littler, 1987). Particle size can be directly related to the settling velocity since a decrease in particle size causes a decrease in the settling velocity. Littler (1987) developed a simple rule of thumb, which stated that hindered settling, occurs at a particle concentration of 20% solids by mass.

Zimmel (1990) concluded that as the volume fraction of particles (ϕ) in the slurry increases, the following occur.

- There is a decrease in the cross-sectional area for teeter water.
- An increase in settling velocity occurs.
- The viscosity of the pulp increases.
- The apparent specific gravity increases towards the specific gravity of the particles, thus reducing the effect of the force of gravity on the individual particles.
- There is also an increase in the wall hindrance and hydrodynamic diffusion.

The apparent viscosity (μ_{ap}) of the slurry is required to determine the hindered settling velocity of a particle. Many equations have been developed to determine slurry viscosity. Other factors which influence hindered settling are the volume concentration of solids, particle size and shape. The size ratio of particle components is an important factor when determining the maximum packing of solids. ϕ_{max} is empirical in most cases unless particles are ideally spherical.

McGeary (1961) performed measurements on ideal spherical particles. He approximated that the packed density of mono-sized spherical particles was 62.5% that of the crystal density of the solid. Low and Bhattacharya (1984) found that ϕ_{max} could be estimated by direct and graphical methods. Sudduth (1993) made attempts to predict the optimum size distribution of packing material. They used size ratios from the 1st to nth order size fraction of the dry mineral samples and matched McGeary's work. They found that the packing density depends on the solids volume and particle size distribution.

2.4. Hindered velocity of a particle: (Slip Velocity u_t)

Particle slip velocity is defined as the velocity of the particle relative to the fluid. Richardson and Zaki (1954) were the first to describe hindered settling velocities in equation form. Others have modified it based on different parameters. Hindered settling mostly occurs in transitional flow regimes.

Richardson and Zaki (1954) related the particle velocity to volume fraction of solids. The equation is as follows,

$$u_i = u_{ti}(1-\phi)^{n_i-1} \tag{32}$$

Where u_{ti} is the particle terminal velocity, ϕ is the volume fraction of solids and n_i is found empirically. $n_i = 4.65$ for spherical particles at low $Re < 0.1$.

For a system of particles of different size and density, the suspension density is defined as follows:

$$\rho_m = \rho\left(1-\sum_{j=1}^{n}\phi_j\right)+\sum_{j=1}^{n}\rho_j\phi_j \tag{33}$$

Where ρ_m is the suspension density (kg/m^3), ρ_j is the density of the jth particle.

Smith (1966) developed a cell model to account for differences in volume fraction of each species. He recognised that each species was subject to a common pressure gradient.

Brauer and Thiele (1973) (cited by (Kohmuench, 2000)) showed the dependence of hindered settling on free settling. Their expression accounted for two phenomena that occurred due to hindered settling. These were as follows:

- The upward fluid flow against the settling particle is a function of the particle volume.
- Particles settling in a dense multi-species suspension result in variable flow profiles with profile interactions, which cause turbulence referred to as cluster turbulence.

Thus their hindered settling velocity u_{hij}, can be obtained by applying these two factors to the free settling velocity u_o of each particle in the ith particle size and jth density fraction.

$$u_{h_{ii.j}} = u_0 k_{f_{i.j}} k_{c_{i.j}} \tag{34}$$

Where $u_{hi,j}$ = hindered settling velocity

u_o= free settling velocity

k_{fij}= fluid counter flow factor

k_{cij}= particle cluster turbulence factor

k_f and k_c are a function of overall particle population and particle size, d and density distributions, ρ.

$$k_{i,f} = \left(1+\left[(1-\phi)((d_i^*)^2 \rho_i^* / \sum(\phi_j)(d_j^*)^2 \rho_j) - 1\right]\right)^{-1} \tag{35}$$

$$k_{ic} = (1-\phi)\left\{ 1 + \left(1+1.05\ \phi\ \frac{d_i^*}{d_1^*}\right)\left[0.25\left(1+\frac{d_{21}^*}{d_1^*}\right)\right]^2 + \frac{2\ \pi\ /\ 3\ n^2}{\phi\left(1+\frac{d_2^*}{d_1^*}\right)^2} + \left(\frac{d_i^* - \sum\ d_j^*}{2\ d_j^*(n-1)}\right)^{-0.5} \right\}^{-1} \tag{36}$$

Where j is from 1 to n, $\rho_I^* = (\rho_i-\rho_f)/(\rho_n-\rho_f)$, and $d_i^* = d_i/d_n$, for particle size groups $d_1, d_2, \ldots, d_n$, f represents the fluid medium and ϕ is the volumetric fraction of solids.

Lockett and al-Habbooby (1974) derived an equation for systems containing particles, which differ according to size only. This was based on the Richardson and Zaki (1954) equation (eqn. (32)). It was relevant for general design purposes. For a three particles species the equation was as follows:

$$u_i = u_{ti}(1-\phi_i-\phi_j-\phi_k)^{n_i-1} \tag{37}$$

Where ϕ_i, ϕ_j and ϕ_k are the species volume fractions.

The hindered settling equation for moving spherical particles for a mono-dispersed system in the low Reynolds number region was, (Masliyah, 1979):

$$u_t = \frac{gd^2(\rho_s-\rho_f)\alpha_f}{18\mu_f}F(\alpha) \tag{38}$$

Where d is the particle diameter (m), g is the acceleration due to gravity (m/s^2), ρ_s is the particle density (kg/m^3), ρ_f is the fluid density (kg/m^3), μ_f is the viscosity of the fluid (Nm), α_f is the suspension voidage and $F(\alpha)$ accounts for the particle concentration.

When α_f and $F(\alpha) \rightarrow 1$, the equation takes the form of Stokes Equation.

Masliyah (1979) corrected the above equation for non-stokes flow to obtain the following expression:

$$u_t = \frac{gd^2(\rho_s-\rho_f)\alpha_f}{18u_f(1+0.15\mathrm{Re}^{0.687})}F(\alpha) \tag{39}$$

Masliyah (1979) developed an equation for hindered settling in a multivariable system:

$$(u_i - u_f) = \frac{g d_i^2 F(\alpha_f)}{18\mu_f}\left[(\rho_i - \rho_f)(1 - \alpha_i - \sum_{k=1}^{N}(\rho_k - \rho_f)\alpha_k)\right] \tag{40}$$

This expression was further a simplified to obtain a generalised form of the slip velocity for the i^{th} particle species in a multi-species system (Masliyah, 1979):

$$(u_i - u_f) = \frac{g d_i^2 F(\alpha_f)}{18\mu_f}(\rho_i - \rho_{susp}) \tag{41}$$

This equation shows that the slip velocity of i^{th} particle species in a suspension is governed by the density difference between the i^{th} particle species and the suspension, the i^{th} particle species diameter, the fluid volumetric concentration and the fluid velocity.

Masliyah (1979) also proposed the following equation

$$u_{pi} = u_{ti}\varepsilon^{n_i - 2}\frac{\rho_i - \rho_m}{\rho_i - \rho_f} \tag{42}$$

Where ρ_m is the medium density. The experimental results from his research indicated that the slip velocity in a fluidised bed containing particles of different densities could be fitted using a quadratic equation.

$$\bar{u}_{pi} = \frac{u}{\varepsilon} - u_{ti}\varepsilon^{n_i - 2}\frac{\rho_i - \rho_m}{\rho_i - \rho_f} = a_i + b_i z + c_i z^2 \tag{43}$$

Where, the concentration of each species, C_i is obtained by substituting Equation (43) into (21) and integrating:

$$C_i = A_i \exp\left[\left(a_i z + \frac{b_i}{2} z^2 + \frac{C_i}{3} z^3\right) / D_i\right] \tag{44}$$

The integration constants are evaluated using boundary conditions.

Richardson and Zaki (1954) defined $F(\alpha) = (1-\phi)^{\beta}$ where β is an unknown function of particle size and shape. They defined β for the following Reynolds Numbers.

$$\beta = 4.36\ Re^{-0.03} \qquad \text{for } 0.2 < Re < 1$$

$$\beta = 4.4 / Re^{0.1} \qquad \text{for } 1 < Re < 500$$

Barnea and Mizrahi (1973) used another form of $F(\alpha)$.

$$F(\alpha_f) = [1 + (1 - \alpha_f)^{1/3} \exp(5(1 - \alpha_f)/3\alpha_f)]^{-1} \tag{45}$$

Al-Dibouni and Garside (1979) formed an equation for the dependence of n on the Reynolds number. The explicit form is,

$$n = \frac{5.1 + 0.2 Re^{0.9}}{1.0 + 0.1 Re^{0.9}} \tag{46}$$

In 1981, Zigrang and Sylvester derived an equation for terminal velocities for particles of different size and density. The Reynolds number of the particle at its terminal velocity, u_t, is,

$$\mathrm{Re} = [(14.51 + (g(\rho_s - \rho)\rho)^{0.5} 1.83 d^{1.5} / \mu)^{0.5} - 3.81]^2 \tag{47}$$

Where g is the acceleration due to gravity (m/s^2), ρ_s is the density of the particle (kg/m^3), d the particle diameter (m), and μ the viscosity of the fluid (Ns/m^2).

The particle Reynolds number, Re is defined as:

$$\mathrm{Re} = \frac{\rho_f d u_t}{\mu} \tag{48}$$

Where, ρ_f is the density of water ~ 1000 kg/m^3, μ is the viscosity of water 0.001 Pa.s. d is the particle diameter (m), and u_t is the terminal settling velocity (m/s).

Swanson (1989) derived a mathematical model for free and hindered settling for transitional flow regime. He used the hindered settling model of DeVaney and Shelton (1939) for heavy media separation. This was based on the Oliver's General model (1961) that accounted for backflow effects. Swanson's main assumptions were that, the settling rate of a particle is influenced the boundary layer of the fluid, the volume fraction of solids, the apparent viscosity of the slurry and the effect of backflow and side flow.

The General Model (Oliver) $$M = 0.5\left(1 - \left(\frac{CV}{CVM}\right)^9\right) \tag{49}$$

Where CV is the volume fraction of solids over the total volume, CVM is the maximum obtainable volume fraction of solids and M is an exponential term for modifying f, (cm^3/g).

Swanson's Model (1989) $$u_c = \frac{u_N}{\alpha(\tanh(N_s\sqrt{48}) + \frac{1}{N_s})} \quad (50)$$

Where M = 0.5 for the hindered settling model, u_c is the calculated velocity, u_N is the Newtonian velocity and α is the boundary layer drag coefficient. N_S is the Swanson number, which accounts for the inverse of the boundary layer thickness and is defined as follows,

$$N_S = \frac{N_R\sqrt{f_d}}{\beta\sqrt{48}} \quad (51)$$

Where β is the boundary layer thickness coefficient = 3.2312 for spheres and N_R is the Reynolds number and f_d is the friction factor. Newton and Stoke's Law for free settling are the boundary limits.

Swanson (1989) also estimated the apparent viscosity η. This was semi-empirical expression.

$$u = u_w(2\phi_{max} + \phi)/2(\phi_{max} - \phi) \quad (52)$$

Lee (1989) developed a hindered settling model. He incorporated several empirical parameters based on statistical analysis. This considered the bi-directional motion.

The equation is as follows:

$$u = \frac{20.52\mu_f}{d\rho_p} f_1(\phi) \left\{ [1 + 0.092\ (d^3|\rho_s - \rho_p|\rho_p g/0.75{\mu_f}^2)^{0.5} f_2\ (\phi)]^{0.5} - 1 \right\}^2 \quad (53)$$

Where $$f_1(\phi) = C_1 C_2{}^2 / (1 - 1.45\phi)^{1.83}(1 + 2.25\phi^{3.7}) \quad (54)$$

And $$f_2(\phi) = (1 - 1.45\phi)^{1.83}(1 + 2.25\phi^{3.7}) / C_1 C_2 \quad (55)$$

$$C_1 = (1 + 0.75\phi^{1/3})(1 - \phi) \quad (56)$$

$$C_2 = (1 - 1.47\phi + 2.67\phi^2) \quad (57)$$

$f_1(\phi)$ and $f_2(\phi)$ are empirical functions that account for the effects of solids concentration by volume, ϕ on the settling velocities of the particles in diameter d, μ_f is the fluid viscosity, g the acceleration due to gravity, ρ_s, ρ_f and ρ_p are the particle, fluid and pulp density respectively.

Asif (1997) formulated a dynamic model for a fluidised bed containing two or more solid particle species of different size and density. It incorporated particle mass transfer, and transport mechanisms such as convection and dispersion. His model describes bed expansion, concentration profiles of individual species, the bulk density profile and the occurrence of the layer of inversion. He evaluated the particle relative velocity (slip velocity) as follows:

$$u_{ri} = u_{ti}\left(\frac{\rho_{si} - \rho}{\rho_{si} - \rho_f}\right)^{n_i - 1} \quad (58)$$

Where u_{ti} is the terminal velocity of species i, u_{ri} is the relative velocity, ρ_f is the fluid density and ρ is the local bulk density of the bed.

He used the Khan and Richardson's correlation (1990) to evaluate the terminal Reynolds Number, Re_t and the Index n.

$$\mathrm{Re}_t = \left(2.33Ga^{0.018} - 1.53Ga^{-0.016}\right)^{13.3} \tag{59}$$

Where the Galileo Number, Ga was defined as

$$Ga = \left(\frac{(\rho_s - \rho_f)\rho_f d_p^3 g}{\mu^2} \right) \tag{60}$$

Where d_p is the particle diameter, μ is the fluid viscosity and g is the acceleration due to gravity.

$$\mathrm{Re}_t = \left(\frac{u_t \rho_f d_p}{\mu} \right) \tag{61}$$

The index, n was calculated as follows:

$$\frac{4.8 - n}{n - 2.4} = 0.043Ga^{0.57} \tag{62}$$

Asif (1997) also derived the correlations for the dispersion coefficient in terms of the Froude Number and Peclet Number.

2.5 Conclusion

The information gathered from previous research work provided a better understanding of the concepts involved in gravity concentration and hindered settling. The extensive fluidisation theory highlights the effect of the particle interactions and fluid phase phenomena on the separation process. Most equations and correlations mentioned in this Chapter have not been utilised for the experimental investigation, however the modification of the fundamental equations derived by Stoke, Richardson and Zaki have been clearly illustrated. The Khan and Richardson correlations (1990) were used for the prediction of the hindered settling velocities from the Asif model (1997).

Previous research work indicated that the main factors contributing to the improved segregation patterns for the hindered settling within the separator are, particle size, shape factor, sphericity, particle density, the upward teeter water velocity, suspension density, and in the case of a significant amount of fine particles, the liquid viscosity (Joshi, 1983). These findings indicate the limiting parameters required for effective fine coal separation.

The equipment design and operation discussed in Chapter 4 was based on the theoretical concepts reviewed in Chapter 2 and 3. The experimental work serves as an excellent comparison of the actual performance of the unit with literature findings.

The research work was concentrated on investigating the internal velocity profiles for the density separation process. The equations derived in this Chapter have a significant relevance to the fundamental particle interactions and liquid-solid hydrodynamic behaviour that is prevalent in the TBS. The simulations performed using the CFD package, Fluent 6.1 described in detail in Chapter 4, were a direct result of the fundamental concepts defined in this Chapter. The hydrodynamic behaviour is best described using a simulation package to obtain a visual interpretation of the actual behaviour that occurs in the TBS column.

CHAPTER 3: INDUSTRIAL DEVELOPMENTS IN TBS TECHNOLOGY

The first TBS in Australia was installed in the Stratford Coal preparation plant in 1997. An eighty ton per hour unit was designed to re-treat spiral product to produce an enhanced yield of low ash coking coal. The unit treated coal between 1.2mm and 0.35mm fines and had a payback period of two months. A second unit was installed in Bayswater Colliery in Australia. The plant yield increased by 2% and the throughput rate increased by 100 tph. This resulted in a reduction in normal and overtime operating hours. There was also an increase in the washed product tonnage and export quality of the coal (Drummond et al 2002).

Nicol (1998) found that the TBS had many operational advantages over other units. These include controllable density cut points as low as 1.38, a good separation efficiency (E_p) of approximately 0.06 compared to spirals which ranged between 0.07-0.12, and a high solids handling capacity in a single unit. The unit also covered a small footprint area with minimal feed slurry distribution. Due to these findings, it was proposed to use the TBS instead of spirals in industry as it yielded a higher recovery of coarse particles and could be easily upgraded.

Hyde (1998) investigated hindered settling classifiers in fine coal washing. He conducted experiments comparing the Stokes Hydrosizer to a spiral on a pilot scale. Water was added at a rate to ensure that the coarsest coal was held in suspension and reported to the overflow. He used a water box at the bottom of the cell to ensure an even water distribution. The test work was conducted at different teeter water and feed flows. He found that the hydrosizer had a higher mass yield, ash rejection and recovery to the overflow compared to the spiral. Spirals were found to be sensitive to feed variations. When the volumetric feed rate is lower than normal, material was lost to the tailings. The separation efficiency of the spiral was greater however a significant loss of coarse low density material was noted.

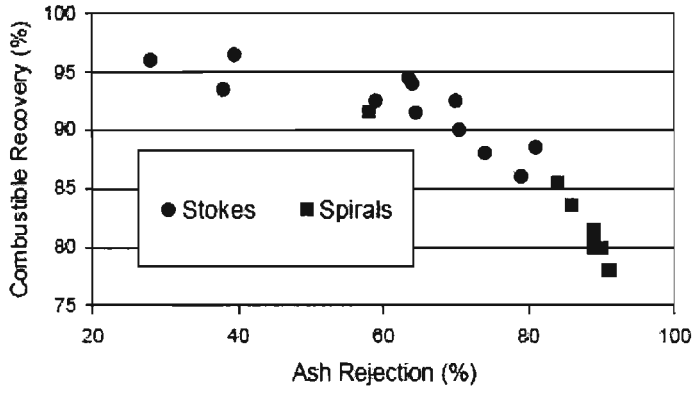

Figure 3.1: A comparison of the separation performances achieved on the basis of ash rejection from the testing of the Stokes Hydrosizer and the existing Spirals Circuit. (Hyde, 1998)

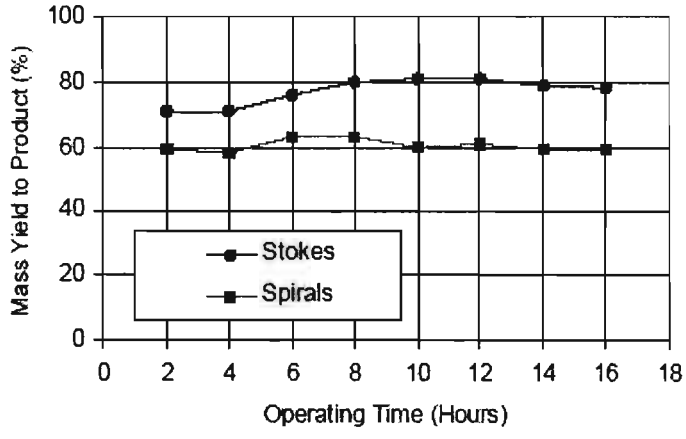

Figure 3.2: Mass yield data obtained from tests carried out on the Stokes Hydrosizer and the Spirals circuit. (Hyde, 1998)

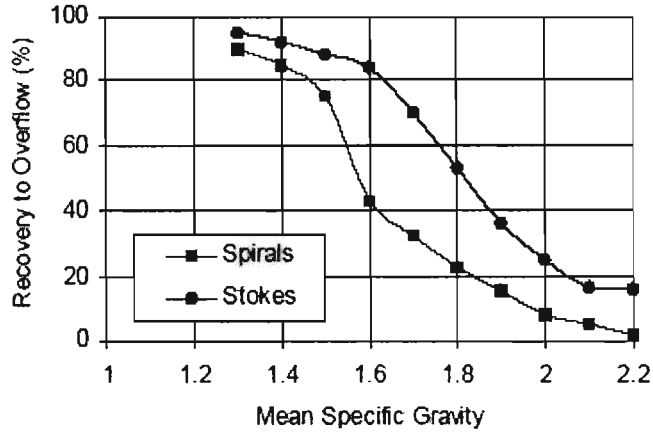

Figure 3.3: Partition Curves obtained from tests carried out on the Stokes Hydrosizer and Spirals circuit (Hyde, 1998)

Galvin et al (1999), have conducted most of the work in TBS technology in recent years. The research was conducted at the University of Newcastle, Australia. They related the suspension density to the settling velocities. This explained how the slip velocity was dependent on the hydrodynamic resistance. It was noted that as the volume fraction of the species was increased, the slip velocity decreased. This was used to develop an equation for slip velocity by modifying the Richardson and Zaki equation (1954).

The equation relating the pressure drop to the hindered settling velocity was as follows:

$$u_i = u_{ti}\left(1-\frac{\frac{dP}{dH}}{(\rho_i-\rho)g}\right)^{n_i-1} \tag{63}$$

Where, $\frac{dP}{dH}$ is the pressure gradient term.

They stated that only data required for the model was the mono-component fluidisation data for each species. The pressure gradient is common to all particle species and is a consequence of the drag forces produced by the liquid to support the weight of all the particle species.

The authors also presented a more generalised form of the Richardson and Zaki equation that is useful for all suspensions whether it be a single species, different size or density. This equation describes a dimensionless density parameter used to describe hindered settling.

$$u_i = u_{ti}\left(\frac{\rho_i - \rho_m}{\rho_i - \rho}\right)^{n_i - 1} \tag{64}$$

Where ρ_m is the density of the suspension medium (kg/m^3)

This slip velocity equation (eqn. (64)) was similar to the equation (58) formulated by Asif (1997). Galvin used this for experiments on the TBS. The slip velocity equation converts to the equation (32), and equation (37) for identical particles. This was however only applicable when the particles are of the same density but differing size.

If $\rho_m > \rho_i$, the suspension will be unstable and generate streaming or lateral effects (Galvin et al. 2000). Galvin used a fluidised bed to conduct experiments. From the analysis of the solids volume fraction, he proposed that the slip velocity of a multi-species suspension, involving particles of different size and density could be used.

Galvin et al. (Sept, 1999) investigated the effect of dense medium separation using a TBS by varying the suspension density. They used three different types of media, namely clean coal, clean coal with mineral matter and clean coal, mineral matter and magnetite. They used a low fluidisation rate with the heavy media having a settling velocity similar to the particle settling velocity.

A lab scale TBS was used with an internal diameter of 0.173m, 1.36m high. The coal feed was obtained from the hydrocyclone underflow. Galvin stated that according to theory, high suspension densities as close as possible to low ash coal particles yield the best separation and these are achieved by operating at low fluidisation velocities.

From their investigations, they concluded that at a low suspension density, separation is governed by particle size, however at a high suspension density, it is dependent on particle density. When the system is fluidised, the underflow discharge rate governs the separation. They concluded that the selected particles for the dense medium should be of a density higher than the coal feed, with a more narrower size range, and with the settling velocity of the dense particles in the bed being as close as possible to the desired cut point velocity. This would make it possible to generate a higher suspension density resulting in an improved separation efficiency.

The error of separation (Ecart Probable, E_p) of a feed with a continuous distribution of sizes and densities is usually defined as:

$$E_p = \frac{(D_{25} - D_{75})}{2} \tag{65}$$

Where, D_{25} and D_{75} are the densities at which particles have a 25% and 75% probability respectively of reporting to the overflow and effective density of separation (D_{50}), is the cut point density at which 50% of the feed reports to the overflow. It can be reported on the overall feed or on specific size fractions. It is therefore the error or deviation from ideal separation (Wills, 1985).

Pilot studies using the TBS, questioned industries use of the E_p, since the efficiency of hydrocyclones were found to be similar to a TBS, however the hydrocyclones had a higher amount of fine low-density coal rejection. The only problem experienced by the Australians, were process disturbances due to the feed. This affected the closed loop density control. It caused a cyclical density response due to oversize material causing fines to be lost in the tailings

during feedback control. Screening the feed, before running the process, solved the problem (Galvin et al, Sept. 1999).

Kohmuench (2000) developed a modified separator, called the Crossflow separator. It utilises a tangential low velocity feed entry system that introduces slurry at the top of separator using a feed well. It has parallel-perforated pipe spargers rather than a distributor plate for the teeter water supply. It has an innovative feed presentation system. The velocity of the feed flow is reduced, by allowing the feed to enter a side well before entering the chamber. This approach allows the water to travel across the top of the unit and report to the overflow launder with minimal disturbance of the fluidsation water within the separation chamber (Kohmuench, 2000). Peng et al. (2004) found that this eliminates the excess feed water rapidly, thus a higher handling capacity and separation efficiency is achieved.

Nuyentranlam and Galvin, (2001) found the Reflux classifier to be an innovative device for both particle classification and density separation. Their research provided key findings on the operational advantages of the reflux classifiers over conventional gravity separation devices. They stated that within the inclined channels between the plates, particles of coarser size or higher density, having a higher settling velocity, settle short distances within the channels and onto the upward-facing plates, form sediment layers and rapidly slide down below. Finer or less dense particles are carried through the channels by the fluidisation liquid into the overflow zone.

They explained that the reflux action develops as a result of the fluidised particles segregating onto the inclined plates, and returning to the fluidised zone below. This self-recycling effect should eliminate misplaced materials, thus enhancing the separation quality. Fine high-density material fails to pass through the upper inclined plates and accumulates in the system. This creates the high suspension density without an excessively high volume fraction of solids. The authors stated that since conventional liquid fluidised beds such as the TBS have a one to one correspondence between the suspension concentration and the fluidisation rate, they are forced to operate at the lowest possible fluidisation rate in order to effect satisfactory gravity separation.

Galvin et al. (2002) did a pilot trial on a reflux classifier. The Ludowici LMPE reflux classifier was designed for classifying and separating particles on a size and density basis. The unit had 3 sets of plates inclined at 60 ^{0}. The reject plates were 0.6m long and 100mm apart. The middling plates were 0.6m long and 50mm apart. The overflow plates were 1.2m long and 30mm apart. The authors investigated the gravity separation and throughput performance using coal mineral matter less than 2mm in size. The plates significantly increased the throughput of the device compared to conventional systems.

Water flows up through the distributor plate at the base of the vessel. This suspends particles within the vessel. The feed slurry was delivered through the side of the vessel. Fluidised mixing zones are created between each set of plates. This permitted the option of withdrawing a stream from each zone above and below each set of plates if multiple sets of inclined sections were used. The particle trajectory within the inclined channel is parallel and normal to the plate. The parallel plates act as classification zones as described by Nguyentranlam and Galvin (2001).

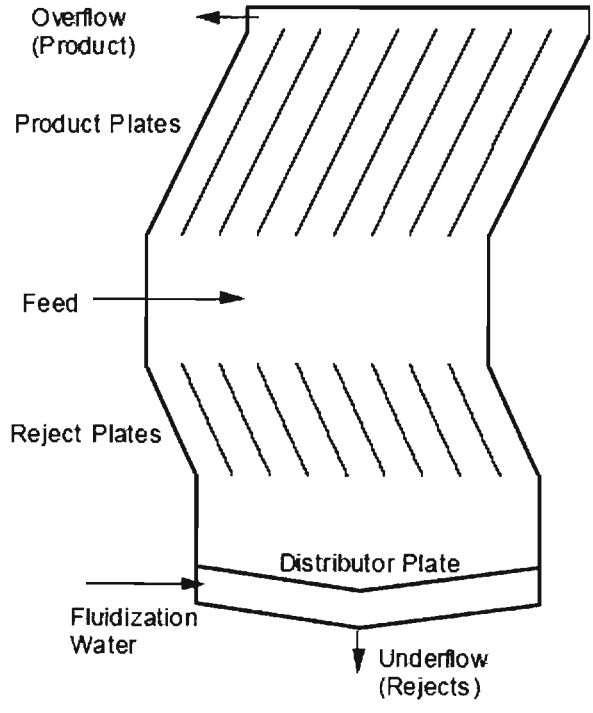

Figure 3.4: Diagram representing a Reflux Classifier. (Galvin.et al. 2002)

The results showed that the reflux classifier had a higher solids loading (33-47 t/m^2h) than the TBS. Honaker and Mondal (2000) found the nominal solids throughput of the TBS to be 14 t/m^2h. This was three times lower than the reflux classifier (RC). The TBS had a higher pulp density in the overflow (35 – 41%). The RC could be run with a lower feed pulp density and hence overcame the need to install cyclones as a pre-concentration step. A feed washability curve was plotted for the RC. This indicates the maximum possible yield for a given ash product. In this case it indicated a high combustible yield. Partition curves were also plotted for the RC. This curve indicates the probability of a particle of a given density reporting to the product stream. The authors found a shift towards higher densities as particle size decreased. A comparison was also made between the TBS and RC on the effect of increasing the fluidisation rate.

The TBS would suffer a decrease in suspension density (Galvin et al. 2002). This would cause a larger low-density material to report to the underflow. The RC however operates at high fluidisation rates, high slip velocities, and has a higher recovery of large, low-density material. More fine high-density particles report to the product stream. The RC has a greater degree of flexibility and according to the authors, reduces the loss of large low ash coal compared to the TBS.

Galvin and Nguyentranlam (2002) found that parallel inclined plates within a liquid fluidised bed permit a broad range of suspension concentrations at the one-fluidisation rate. This allows suspensions to form at fluidisation rates higher than the particle terminal velocities, which would benefit a broad range of systems.

Galvin et al. (2002) also investigated the influence of a jigging action on the gravity separation achieved in a TBS in order to extend the operating size range. The authors conducted this study in order to determine an operating size range of a TBS by cyclic variations in fluidisation water supply.

They used a 0.174 internal diameter, 1.36 m high TBS. The vessel was designed for a steady state or pulsed flow. The particles were of varying size range determined by the authors. Coal and other minerals were used as feed material. Despite several tests, only a subtle change in

separation was noted (Galvin et al, 2002). No changes were noted by the jigging action. If the jigging improved the separation, the rate of change of the D_{50} versus Particle Size would have been less and the E_p would be lower. The effective density of separation (D_{50}) is a function of particle size, and since the D_{50} increased as the size range increased, it showed that jigging was insignificant in improving the separation performance over a broad size range. The authors noted that the jigging action did improve the separation efficiency of fine particles from rejects, however it resulted in a loss of large low ash coal to the rejects.

Eriez Magnetics (2003) developed two types of classifiers, the high capacity Crossflow separator and the air-assisted Hydrofloat Separator. The Crossflow Separator is capable of sizing and concentrating minerals in slurry form having various sizes and density. As stated by Kohmuench (2000), the crossflow design eliminates efficiency losses to the feed water. Other benefits include a high capacity, (0.28-0.84 tph/m^2), with online cut point control, a fully automated discharge control system with a capability of handling high and low density variations.

The Hydrofloat is an air assisted Density Separator. The efficiency of the gravity separation is enhanced by the density difference. It is typically suited to a feed with a broad size distribution or a narrower range of densities. It is a low maintenance, low operating cost separator with a high throughput (0.19 – 0.46 tph/m^2). Fine air bubbles introduced in the system rise with the upward water current and selectively attach to the particles. The Hydrofloat incorporates flotation concepts with density separation. Selective attachment can be made on low-density coarse particles, which is normally entrained to the underflow. As a result, the separation efficiency can be increased significantly.

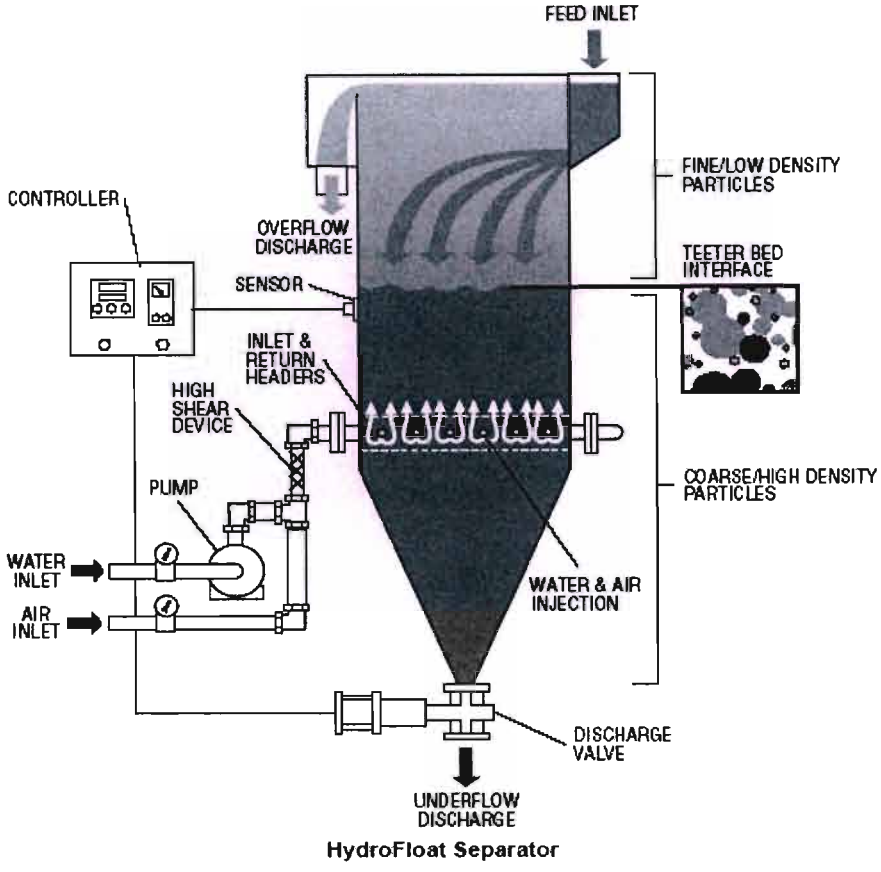

Figure 3.5: Diagram representing a HydroFloat Separator. (Eriez Magnetics, 2003)

This chapter was beneficial in providing a detailed summary of recent research conducted industrially to improve the density separation process of the TBS. Various modified separators were developed to improve the separation efficiency, cut point densities and size range that the unit can separate. Chapter 4 will deal with the design, operation and modelling of the laboratory scale TBS. The information gathered from this Chapter was significant in respect to the design criteria considered.

CHAPTER 4: EXPERIMENTAL EQUIPMENT, PROCEDURE AND MODELLING OF THE TBS

This Chapter gives a description of the equipment design including all design considerations. The main equipment required for the project was the Teetered Bed Separator (TBS). A description of the experimental procedure, analysis methods and tools is outlined in this chapter.

4.1. Equipment

A TBS was constructed in the Chemical Engineering Workshop by the workshop technicians. It consists of a cylindrical, blue PVC column, 0.2 m internal diameter and 1.5 m in height with four distributor pipes, a distributor plate, an overflow launder and an underflow exit valve. The teeter bed region was divided in to sections for experimental work. Perspex and clear PVC were also considered as potential vessel material however the blue PVC had the most appropriate strength and durability properties. The unit was designed in sections in order to analyse slices of the bed for density tracers. Using a bed height of approximately 300mm above the distributor plate, the teeter bed was partitioned into five sections of 60mm each. The grooves had to be drilled on the circumference so that O-rings could be fitted. The O-rings enabled the unit to seal tightly together with no leaks during operation. After each experiment it could be opened and reassembled. Since the primary and secondary phases consisted of water and coal particles respectively, no additional considerations were required for the vessel material as both are non-corrosive. The unit was also open to atmosphere; therefore no design considerations were necessary for pressure vessels.

The framework consists of four rods with wing nuts and an open lid, which seals the unit tightly together. A baffle was fitted on the top section, 50mm away from the feed entry. Its purpose was to minimise the feed disturbances on the teeter bed. The teeter water flow rate entering the distributor was controlled using a rotameter. The coal samples consisted of different densities and ash content in a size range of – 2mm + 0.1mm. MINTEK supplied a 100kg sample for the experimental work. It was proposed to insert a feed well adjacent to the column. The feed would overflow tangentially into the column minimising the disturbances to the bed however the system behaviour noted during preliminary experiments suggested that the baffle sufficiently reduced the disturbances.

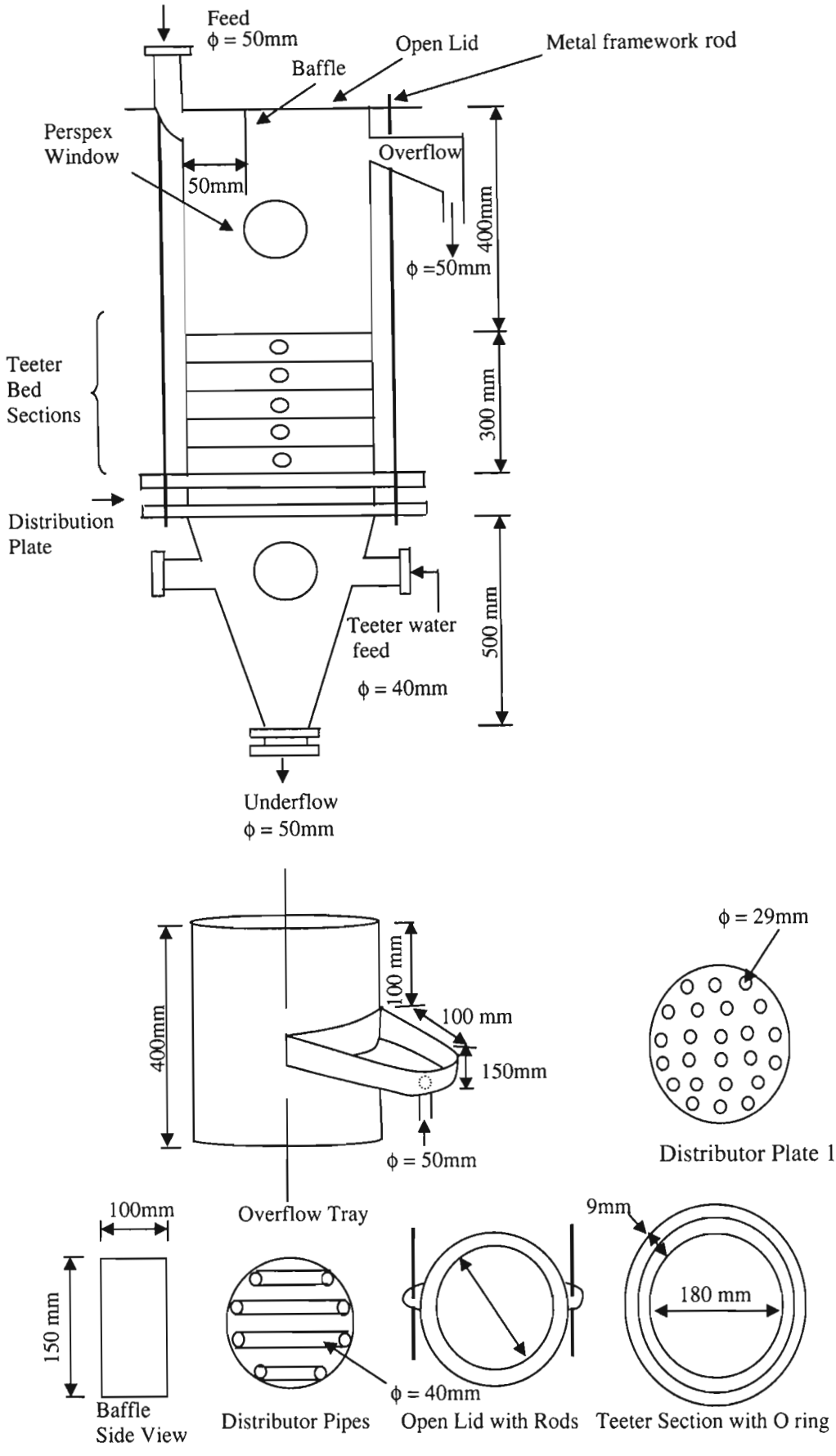

Figure 4.1. Diagram of the Teeter Bed Separator

The TBS has distributor pipes below the distributor plate. The pipes have their holes facing downwards. The advantage of this configuration is that it reduces the clogging of the teeter water pipes and since the upward momentum is from the bottom of the unit (above the underflow valve), any coarse or fine low-density particles that are entrained below the distributor can be pushed upwards provided that the bed voidage is not too low. An additional advantage is that the flow patterns would only arise due to the distributor effects. The velocity profile would be more even below the plate since there are minimum flow disturbances which would occur in that region. The drawback is that the teeter water flowrate has to be increased when the outlet valve is opened slightly or the upward flow would terminate. If the outlet were opened fully the unit will just empty out. Since the underflow is only opened when the pressure drop rises above a certain range determined from the Ergun Equation, no operational problems have arisen.

The feed solids content was consistently between 25 – 45 % in-order to facilitate hindered settling. The underflow valve was closed during operation. The top of the column has an overflow tray about 100mm below the feed entry. This may have an effect on the separation efficiency due to the manner in which the particles overflow the unit. The effect of the feed disturbances on the overflow would be investigated. The bed height was monitored through Perspex windows that were inserted on each section.

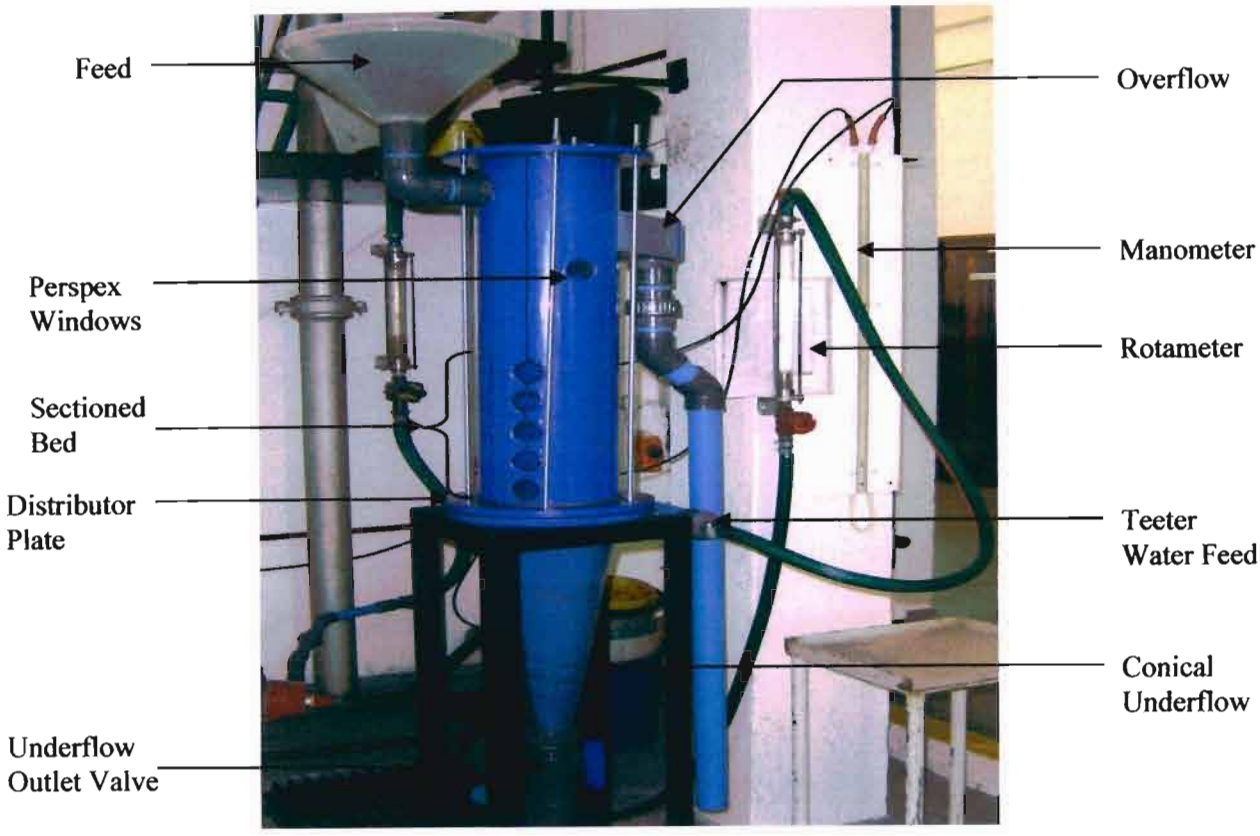

Figure 4.2: Picture of the Teeter Bed Separator

4.2. Distributor Plates

The design of the distributor or orifice plate plays a significant role on the overall hydrodynamics in a fluidised bed. The distributor effects can cause severe distortions in the fluidised-bed hydrodynamics, which would lead to incorrect estimation of the design parameters (Asif et al, 1991).

Asif et al. (1991) performed experiments in liquid fluidised beds on low-density particles. They formulated a few guidelines on the distributor plate design criteria:

- For low-density solid particles (ρ_s = 1050 kg/m^3) care should be taken to eliminate dead zones in the distributor region. To avoid the presence of dead zones, a distributor with a hole density (N_{or}) as large as possible should be used.

- Care must be taken at the same time to ensure even liquid distribution at the minimum possible cost which increases as the number of distributor apertures increase.

- The Distributor Pressure drop (ΔP_d) is an important variable of distributor design and can be controlled by varying the hole density. Low pressure drop distributors result in large-scale convective circulation patterns in the bed.

- The distributor fractional open area (F_{or}) should be optimised to attain good distribution without causing excessively high-pressure drops.

- Perforated plate distributors are less susceptible to clogging.

Asif et al. (1992), defined distributor parameters that were considered when designing the various distributor configurations for the TBS in this project.

Hole Density:
$$N_{or} = \left(\frac{No.\ of\ holes, n}{Area\ of\ column, A} \right) \tag{66}$$

Orifice Diameter:
$$D_{or} = \left(\frac{4F_{or}A}{\pi N_{or}} \right)^{0.5} \tag{67}$$

Orifice Velocity:
$$U_{or} = \left(\frac{U_o}{F_{or}} \right) \tag{68}$$

Distributor Pressure Drop:
$$\Delta P_d = 0.5\rho_f \left(\frac{U_{or}}{C_d} \right)^2 \tag{69}$$

Where, C_d is the orifice coefficient ((Kunii and Levenspiel, 1969) cited by (Asif et al, 1992)). The scaleup parameter for distributors is hole density not the number of holes.

Seven distributor plates were designed with varying aperture arrangements to test the flow profile and observe the hydrodynamic behaviour through the column. The plate specifications were as follows. PVC plastic was used as the plate material. The plate diameter and thickness was 200mm and 5mm respectively. Figure 4.3 to 4.8 represent the seven different configurations considered. These choices were based on the effect of pressure drop, geometric arrangement, and aperture size. The choice of minimum aperture size was dependent on the feed size distribution. 65.4% of the feed passed through 1400μm and 100% passed through 4000μm. Based on those figures, the minimum aperture size was designed at 5000μm to reduce the possibility of clogging of the plates due to particle agglomeration. This would affect the cut-point suspension density due to the accumulation of high-density material in the bed.

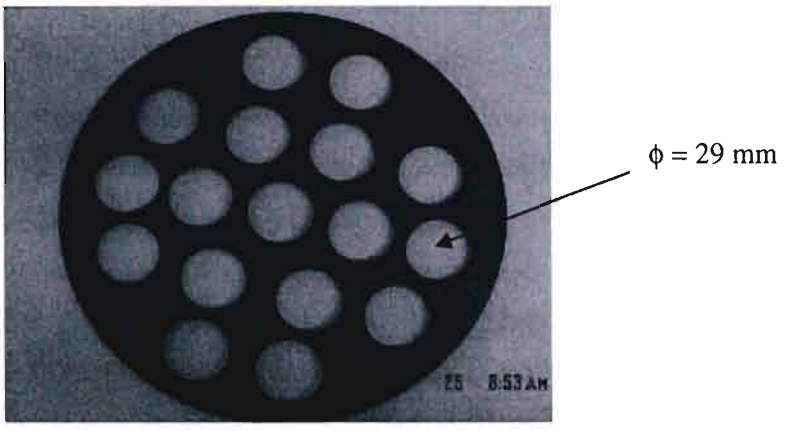

Figure 4.3: Picture of Distributor Plate 1

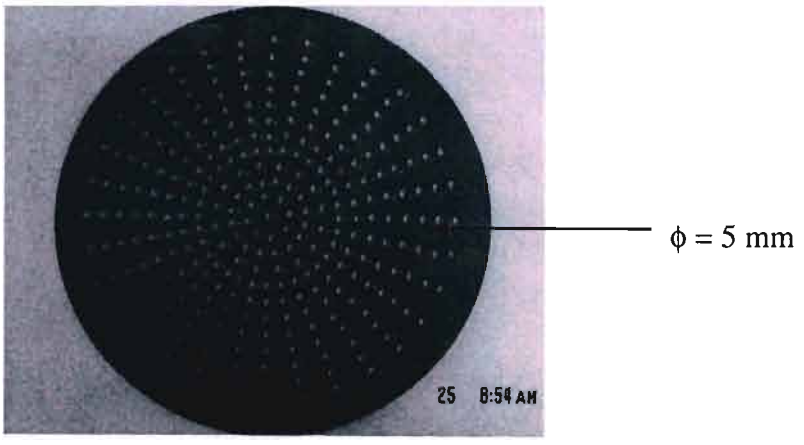

Figure 4.4: Picture of Distributor Plate 2

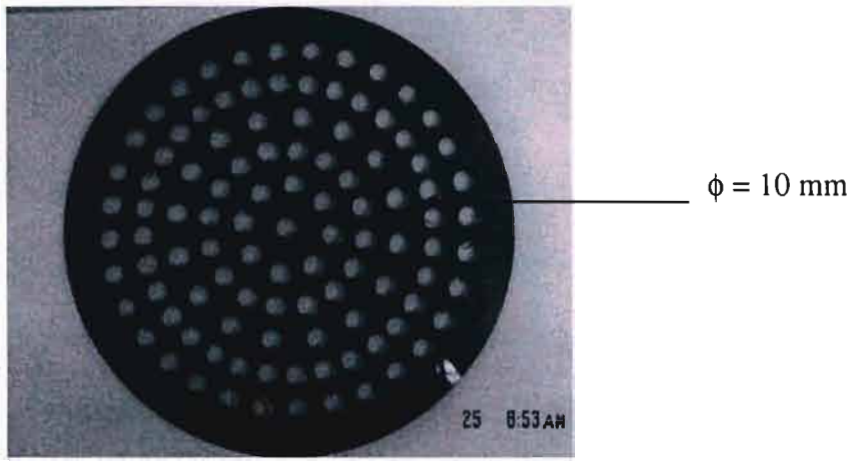

Figure 4.5: Picture of Distributor Plate 3

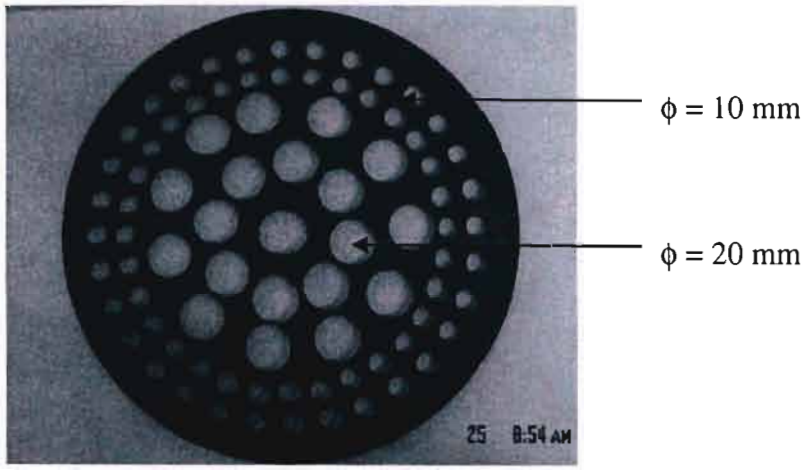

Figure 4.6: Picture of Distributor Plate 4

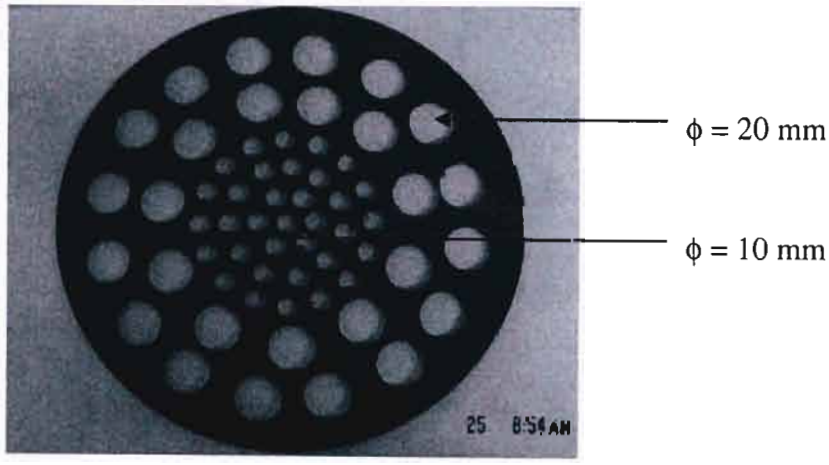

Figure 4.7: Picture of Distributor Plate 5

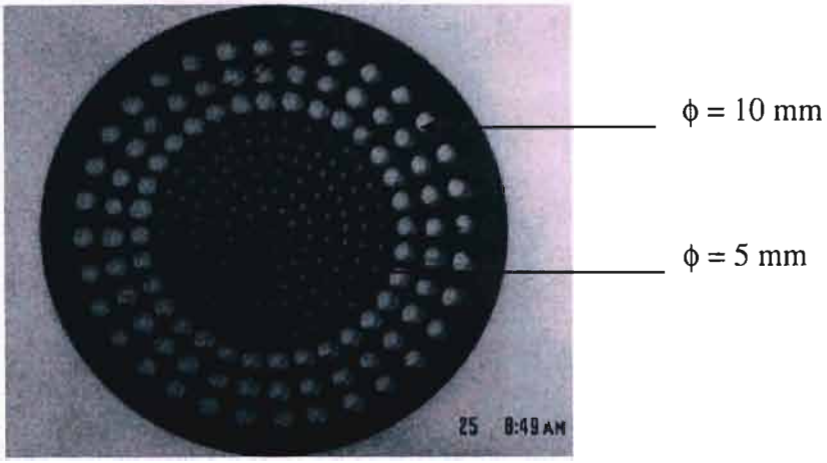

Figure 4.8: Picture of Distributor Plate 6

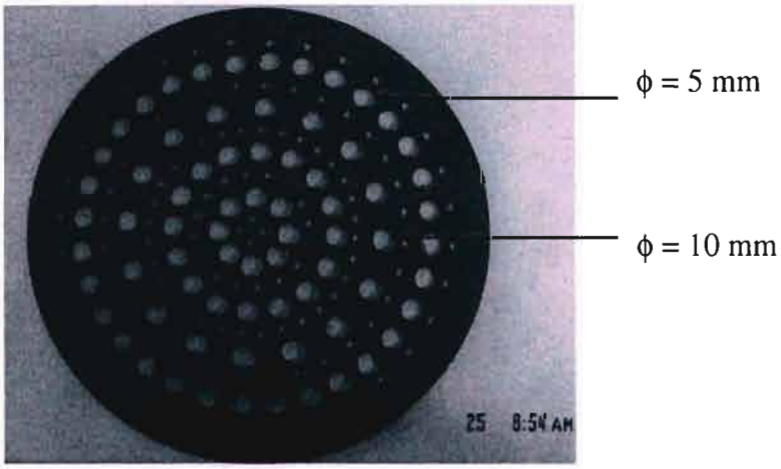

Figure 4.9: Picture of Distributor Plate 7

Plate No.	Apertures	Diameter (mm)	Area (m^2)	% Open
1	17	29	1.123E-02	44.1
2	296	5	5.812E-03	22.8
3	105	10	8.247E-03	32.4
4	20	20	6.283E-03	
	64	10	5.027E-03	44.4
5	27	20	8.482E-03	
	34	10	2.670E-03	43.8
6	96	10	7.540E-03	
	137	5	2.690E-03	40.2
7	116	5	2.278E-03	
	72	10	5.655E-03	31.2

Table 4.1: Summary of Plate Configuration

Plate No.	F_{or}	N_{or}	D_{or} (mm)
1	0.441	0.0668	46.3
2	0.228	1.16	7.98
3	0.324	0.413	15.9
4	0.444	0.330	20.9
5	0.438	0.916	12.5
6	0.402	0.511	15.9
7	0.312	0.738	11.7

Table 4.2: Calculation of the theoretical Aperture Diameters using Asif et al. (1991) from Equation 64 & 65.

A circular arrangement was favoured generally in order to keep the number of holes per unit area uniform throughout the distributor. A square arrangement was used for Plate 1 however due to the large aperture size a non-uniform arrangement was evident.

Plates 2 and 3 may improve the flow distribution and reduce entrainment of large low-density material. The maintenance of the packed bed during the withdrawal of the underflow was also considered. Plates 2 and 3 could reduce the disturbances on the teeter bed by providing extra support during density control.

The percentage area open for Plates 2 and 4 represent the two extremities of the geometric arrangement. Plates 4 to 7 were designed with an intention to reduce dead zones near the wall or boundary regions. The effect of turbulence was also investigated by varying the aperture size for each plate. This gave an indication of the pressure drop relation through the unit. These four configurations may cause more radial interactions in the teeter bed, which could hinder density segregation.

Wall effects have a significant effect on the flow pattern within the column. They result in velocity fluctuations within the bed, the radial effects are more pronounced and the particles experience an increased hinderance. The flow pattern would be unstable with more circulative random velocity movements, which would result in increased bed disturbances.

Plate 4 and 6 were designed with a reduced aperture area near the wall to reduce the effect of dead zones. Plate 5 was designed with a large aperture area near the wall to investigate the wall effects due to the reduced teeter-water velocity. Plate 7 investigated the effect of alternating the aperture size throughout the plate with 5mm and 10mm apertures respectively to observe if this would reduce both wall effects and dead zones in the teeter bed. Plate 1, 2 and 3 investigated the variation in the extreme aperture sizes of the plate together with the circular and square aperture arrangement.

4.3. Experimental Procedure

The experimental work conducted on TBS technology was subdivided into 3 main sections. The first set of experiments dealt with the density tests on the lab scale unit using the cubic density tracers. The second part involved retrieving the tracers from the overflow, underflow, tops and 5 sectioned slices and thus determining the tracer position in the unit. The third investigation was the sink-float analysis and ash analysis on the samples from Experiment 2 in order to plot partition curves for each run. The distributor configurations were tested at 3 flow rates (3, 6, 8 l/min) to attain a better understanding of the operational capabilities of the TBS. These flow rates were based on the hindered settling model by Asif (1997).

Observations of the particle interactions and water circulation patterns in the column were difficult to view physically, due to the dark colour of the water caused by the fine coal particles, however the tracer positions do provide evidence of the particle circulation patterns. A detailed experimental procedure is outlined in Appendix A. The experimental data and detailed graphs are presented in Appendix B and Appendix C respectively. A summary of the main results and outcomes are presented with a detailed discussion in Chapter 5.

4.4. Experimental Approach

The unit was run with tracer elements in the feed coal. Slices of the teeter bed were analysed at the end of each run.

Two operational scenarios were used initially. In the first method, the unit was initially empty, and run from the start-up stage, with time allocated for bed formation. Sample collection only commenced once the unit began to naturally overflow. In the second method, the unit was refilled with the particles in the appropriate parts that they were removed from the sectioned bed during the tracer analysis of the previous run before commencing with the new run. The second method requires a high water flow rate initially to mix and fluidise the particles. Then a lower velocity is be adopted to allow the particle to segregate and settle according to their density and settling velocities, with the highest density at the bottom of the bed since a highly segregated bed of particles will improve the density separation process.

The second method has the advantage of reducing the water wastage since only fines end up in the overflow during the startup process. The startup process takes around 10 minutes and with high flows, a loss of 150 litres of water is possible. This water would be recycled in a real process, but is quite significant in an experimental setup with no recycle. The first method was chosen for subsequent runs since the project is based on fundamental flow concepts of the distributor plates and these are more correctly investigated by considering the total run and all phenomena that may occur.

The tracers used were cubic, brightly coloured plastic, of a specific gravity range of 1.2, 1.4, 1.6, 1.8 and 2.0. Three size fractions were considered, namely, 5mm, 2mm and 1.5 mm particles. 0.8 mm cubes were also used to improve the understanding of fine particle interactions, however their retrieval proved difficult. The tracer elements provided necessary information on the density distribution in the bed. A tracer shape similar to the coal particles would have been more beneficial to the study; however the costs of these tracers were high and proved unfeasible for the laboratory scale investigation. Since the TBS has already proven successful in industry, other factors needed to be investigated to obtain specific design parameters. The radial position of the tracers in the bed and entrainment in the overflow or underflow caused by the changing distributor plates, give an indication of the dependence on the column height, diameter and other factors required for an effective separation of low-density fine coal.

Figure 4.10: Density Tracers (BATEMAN, 2005)

4.5. Sample Analysis

The dry samples from each section of the bed were analysed to retrieve the density tracers. The heavy liquid test or sink-float analysis was chosen to determine the density distribution of the experimental samples. Standard solutions of varying densities (1.2, 1.4, 1.6, 1.8 and 2.0 SG) were mixed in 120ml batches and used for the analysis. An organic liquid, Tetrabromoethane (TBE) and Acetone were used to prepare the density standards. Since acetone is extremely volatile, test work was usually performed directly after mixing these solutions in order to minimise errors. Sink-float analysis is more conclusive for a coarse size range. The coal sample from MINTEK contained large amounts of fine particle, which occur mostly as middlings when performing the analysis. Screening of the samples into size fractions reduced the problem of middlings. The Riffling Sampling Technique was used to obtain the sub-samples for analysis purposes. Samples from each section were taken and sink-float tests were performed. The detailed procedure is outlined in the experimental procedures in Appendix A.

4.6. Data Analysis

Partition curves were plotted to obtain the percentage recovery, cut-point density and the Ecart Probable (E_p). It was initially decided that the partition curves would be generated using a tracer count method. This method is based on the ratio of the amount of tracers recovered in each SG range and not on the amount of tracers initially present in the feed. Due to an insufficient number of tracers due to tracer costs, tracer losses and insufficient tracer recovery to the overflow, the tracer plots would have misrepresented the cut-point. A tracer profile through the bed was plotted for each run to obtain a distribution through the TBS. These profiles were then compared to the bed profile curve from the sink-float in order to determine the validity and accuracy of the tracer investigations.

4.7. Coal Properties

4.7.1. Feed Size Distribution

The coal supplied by MINTEK was tested using simple laboratory techniques to determine the feed specifications. Several size analyses were performed on the coal samples. The data below represents the average size distribution.

Aperture Size (μm)	% Retained	% Cumulative Passing
1700	34.59	65.41
1400	28.66	36.75
1000	12.23	24.52
710	11.74	12.79
300	7.35	5.44
106	3.95	1.48
38	1.42	0.06
-38	0.06	0.00

Table 4.3: Feed Size Distribution

4.7.2. Rosin-Rammler Distribution Method

The size distribution data was used to obtain the average particle size for the batch sample used for experiments. The Rosin- Rammler Method uses the fractional cumulative passing to obtain the average particle size (Fluent User Manual, 2003). The following plot was obtained from the data.

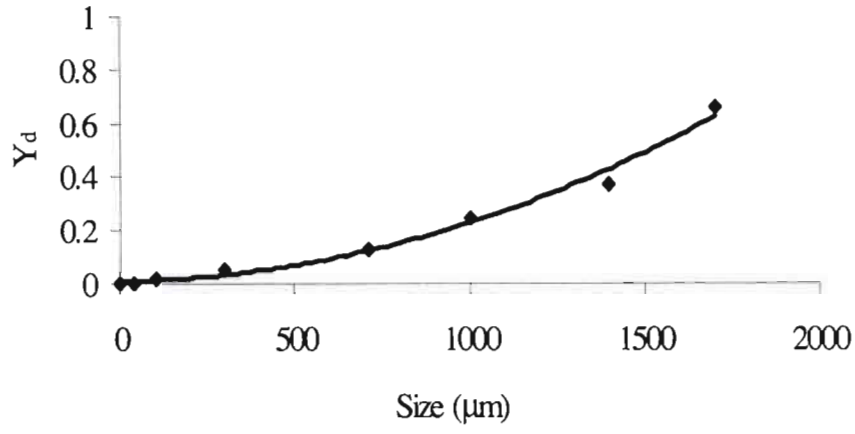

Figure 4.11: Rosin-Rammler Diameter Distribution Graph

From the graph above, the Rosin-Rammler method for the average diameter was obtained at the point where the fractional cumulative passing (Y_d) = e^{-1} = 0.368. It was calculated to be 1352 μm from the equation of the distribution graph. The average diameter was used in the Ergun Equation for the Pressure Drop calculations and for the slip velocity model.

4.7.3. Feed Density of Coal

SG	Coal (g)	Mass Fraction
2.2	0.15	0.03
2.0	0.20	0.03
1.8	0.43	0.08
1.6	0.77	0.14
1.4	2.59	0.46
1.2	1.49	0.26
Total	5.64	1.00

Table 4.4: Density Distribution of Feed Coal from Sink- Float Analysis

From the data above, it is evident that a density gradient exists. This was necessary to facilitate the process of gravity separation discussed in the Concentration Criterion in the Literature Review.

4.7.4. Average Feed Specific Gravity

The Density-Bottle Method (Wills, 1985) was used to obtain the average SG of the feed. This was used in the calculation of the feed flow rate for each run. Six runs were performed and the average SG was found to be 1.51. The experimental procedure for this method is available in Appendix A. The data tables are presented in Appendix B.

4.7.5. Feed Moisture Content

The moisture content of the coal particles under investigation was obtained experimentally. The experiments were performed at 105°C. The average moisture content was found to be 3.97 %, which was extremely low. According to Carsky, (IFSA 2002), the use of a correction factor (f_r) is necessary for the calculation of the minimum fluidisation velocities for wet coal particles if the moisture content is greater than 25%. The coal under investigation was far below the criterion so no correction factors were introduced. It must be noted that these tests performed, were necessary, since the fluidisation behaviour of highly porous material differs. The tables of raw data are presented in Appendix B for further investigation

4.8. Slip Velocity Calculations

The slip velocity equation derived by Asif (1997) was used to obtain preliminary data for the experimental work on the lab scale TBS. A suspension density of 1350kg/m^3 was assumed and using a particle density of range of 1400, 1600, 1800 and 2000 kg/m^3, the theoretical slip velocities were calculated. The suspension density assumption was based on the desired cut-point for the coal particles. From this data, an approximate operating range (0.002 – 2.8 cm/s) for the teeter water flow was established. This was performed for both the correlations in Tables 4.5 and 4.6. Both sets of results are similar however the Khan and Richardson correlations (1990) produced slightly improved results for the very fine material. This was attributed to the value of the index n, which is lower as seen in the Figure 2.2 for the particle sizes between 0 and 0.5 mm. Since the fine particle regime was relevant to this study, the Khan and Richardson correlations (1990) were favoured.

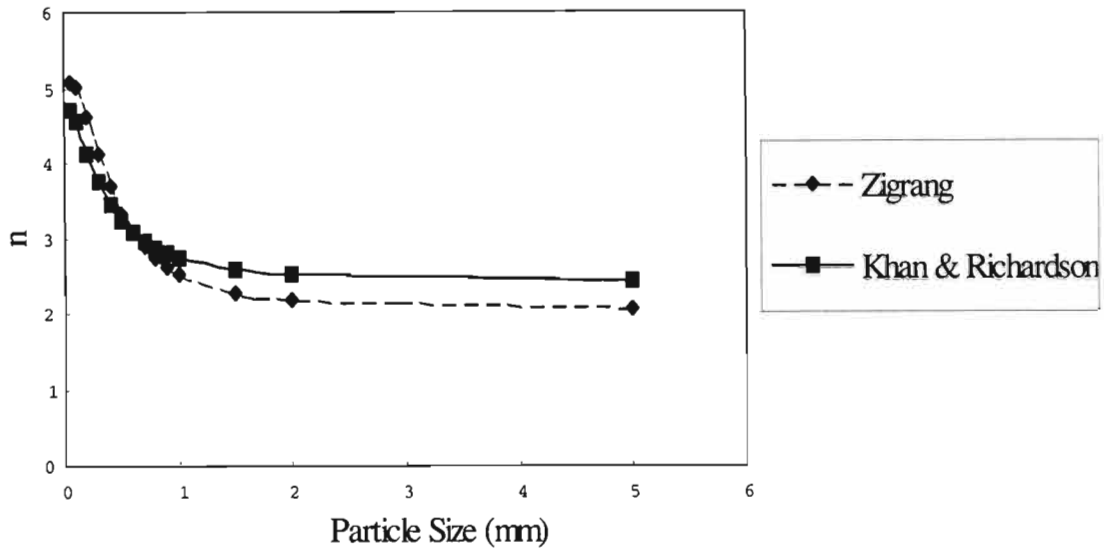

Figure 4.12: Relationship of n vs. D_p using two different Models

Size(mm)	Re	u_t (m/s)	n	u_i (m/s)	u_i (cm/s)
2.0	243.6	0.12	2.21	0.03	2.85
1.0	66.2	0.07	2.58	0.01	0.99
0.5	15.4	0.03	3.43	0.002	0.17
0.1	0.2	0.003	5.01	0.00002	0.002

Table 4.5: Preliminary Calculations of Particle Slip Velocities (u_i) in operating size range using the Zigrang and Sylvester Correlations (1981).

Size(mm)	Galileo No.	Re_t	u_t (m/s)	n	u_i (m/s)	u_i (cm/s)
2.0	39240.0	278.3	0.14	2.53	0.02	2.21
1.0	4905.0	72.2	0.07	2.77	0.01	0.86
0.5	613.1	16.5	0.03	3.30	0.002	0.21
0.1	4.9	0.3	0.003	4.57	0.00004	0.004

Table 4.6: Preliminary Calculations of Particle Slip Velocities (u_i) in operating size range using the Khan and Richardson Correlations (1990).

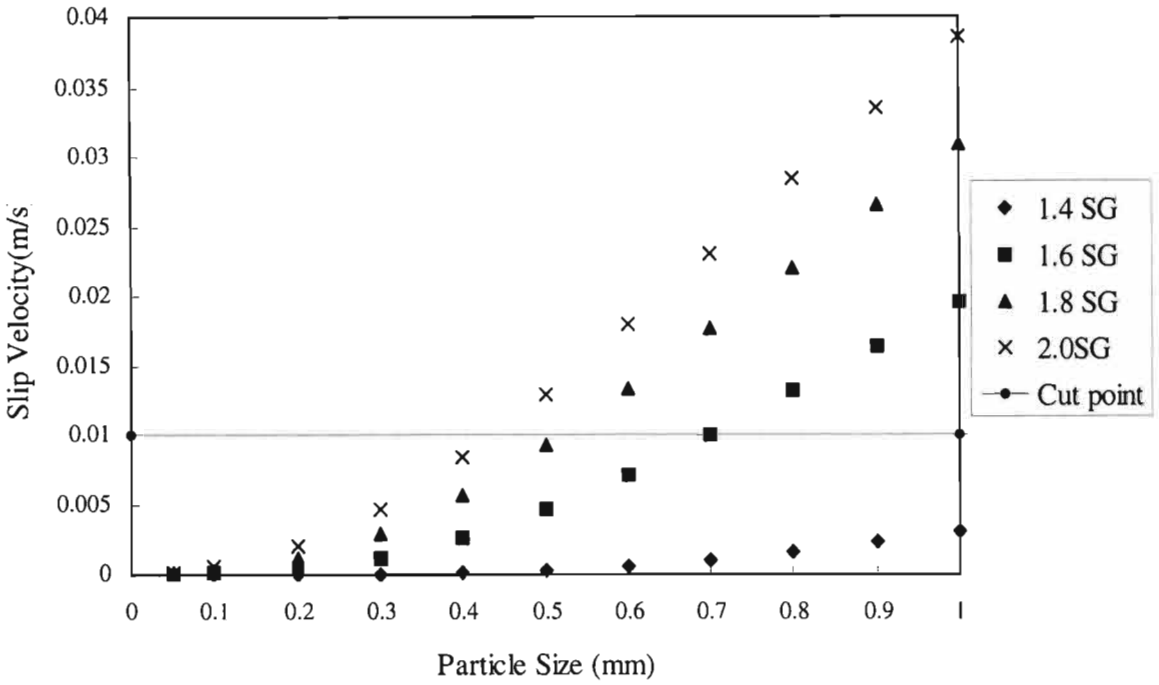

Figure 4.13: Slip Velocity as a function of Particle Size and Density - Suspension Density of 1350 kg/m³

The slip velocity relationship shown in Figure 4.13 provides a theoretical prediction of the two main factors that govern the separation process. This plot shows how a variation in the slip velocity changes the composition of the overflow and cut-point density.

The Chapter thus far focused on the design of the TBS and the various distributor plate configurations. The experimental approach and analysis techniques were explained in the relevant sections and the coal supplied by MINTEK was analysed to obtain the feed properties for the experimental investigations. The sections that follow, detail the hydrodynamic behaviour, the governing equations that describe the flow patterns within the TBS column, the simulation method and the modelling of the TBS. This would form the basis of the comparison with of the experimental and simulation work conducted to determine the best distributor plate configuration for the unit.

4.9. Hydrodynamics of the TBS

4.9.1. Introduction

The liquid phase flow pattern and the behaviour of particles in the fluid phase is essential in understanding the processes, interactions and the factors that influence the separation. The hydrodynamic model will provide further information on the gravity separation process, taking place within the TBS.

4.9.2. Previous Work

There have been many hydrodynamic models derived for the hindered bed separator. The following models are examples of the recent work carried out by various researchers, highlighting the different aspects considered.

Honaker and Mondal (2000) developed a dynamic population balance model for the separation in a Floatex, Crossflow separator. This unit was divided into six zones. The feed, lower intermediate, thickening, underflow, upper intermediate and overflow zone. A mass balance equation was derived for each zone including concentration, size and density variations.

Kim et al. (2003) formulated a convection-diffusion model for the motion of spherical, solid particles of varying size and density. The authors were able to account for the movement of particles within the separator. The equation is as follows:

$$\frac{\partial \phi(x,\rho,z,t)}{\partial t} = D\left[\frac{\partial^2 \phi(x,\rho,z,t)}{\partial z^2}\right] - \frac{\partial (V(x,\rho,z,t)\phi(x,\rho,z,t))}{\partial z} \tag{70}$$

Where $\phi(x,\rho,z,t)$ is the volume fraction of particles of size x to x + dx , density ρ to $\rho + d\rho$ in the element z + dz, at time t with respect to the wall of the column. The first term on the right hand side represents the rate of accumulation due to convection. The mass balance shows that if a given volume of particles moves in the z direction, then the same amount of liquid will move in the opposite direction. The hindered settling velocities were calculated empirically. A finite difference technique was utilized to attain the solution of this mathematical model.

Peng et al. (2004) took into account the interaction of the liquid phase and the particles together with the particle-particle collisions in a 2-D model. This was integrated into a momentum transfer equation to characterise the fluidising flow pattern and the equation of motion of particles.

The Euler-Lagrange approach of Computational Fluid Dynamics (CFD) is used to obtain the separation performance of the unit. The modelling of the hindered settling separator was based on the liquid governing equations. The parameters that they considered included particle size effects, particle density compositions, feed rate, feed water flow rate and upward fluidisation flow rates. They investigated the flow patterns effects using two methods of feed input, namely side cross-flow and centre downward flow.

A major difference between their system and the conditions of the current system under investigation was the flow regime. Their study concentrated on turbulent flow of hard spheres and binary collisions. This introduces particle phenomena such as particle-fluid coupling and inter particle collisions where fluid-particle interactions are much more significant. The simulated results from their model, were in good agreement to actual plant tests carried out. The TBS was operated in the laminar and intermediate flow regime for the current investigation. Turbulent effects were neglected, however viscous effects were considered. The particles were non-spherical as opposed to hard spheres.

The effect of operational parameters was quite useful in their study and provided some excellent guidelines when running the unit. The effect of the fluidising water flow rate was found to be the most important parameter. An increasing flow rate was found to cause a higher drag force, causing a coarser size separation and a higher specific gravity and vice versa. The solids feed

rate was found to influence the settling characteristics. A high solids concentration increases the apparent viscosity and specific gravity of the slurry, thus reducing the settling velocities producing a coarser size product. A dry feed was found to have a minor effect on size separation. The side cross-flow feed system showed a low specific gravity of separation compared to the centre downward flow configuration.

4.9.3. Eulerian Model

The hydrodynamics of the distributor plate and the region above the plate were modelled using a CFD program, Fluent 6.1. Fluent is a control-volume based code with divides the calculation domain into a finite number of control volumes. It incorporates the multiphase model for granular solids using the Eulerian model. The Eulerian model accounts for the conservation equations for momentum and continuity for both solid and liquid phases, together with the mechanism for the exchange of momentum between phases. It solves these equations based on the initial conditions. The Eulerian model generally offers better accuracy than the mixture model, as it solves separate sets of equations for each individual phase, rather than modelling slip velocity between phases.

Lift Forces have not been included in the hydrodynamic model of the TBS. Fluent can include the effect of lift forces on the secondary phase coal particles due to the effect of the velocity flow field of the primary phase (water). Fluent assumes that the particle diameter is much smaller than the inter-particle spacing therefore for a closely packed bed of particles the lift forces are insignificant and were neglected in this case.

The following equations were obtained form the Fluent User Manual (2003).

Interphase Exchange Coefficients

The momentum exchange for granular flow is based on the fluid-solid and solid-solid exchange coefficients, K_{sl}.

Fluid-Solid Exchange Coefficient

General Form:

$$K_{sl} = \frac{\alpha_s \rho_s f}{\tau_s} \tag{71}$$

Where f is defined from the different exchange-coefficient models and τ_s is the particulate relaxation time, defined as:

$$\tau_s = \frac{\rho_s d_s^2}{18\mu_l} \tag{72}$$

Where, d_s is the diameter of particle of phase s.

All definitions of f include a drag function (C_D) are dependent on the Reynolds Number (Re). It is the drag function that differs in the exchange coefficient model.

The Syamlal-O'Brien model (Fluent User Manual, 2003) was used to calculate the drag coefficient in Fluent. This model was based on measurements of terminal settling velocities in fluidised beds. The correlations are a function of volume fraction and Reynolds Number (Re). This model was recommended in the multiphase modelling guide in Fluent for liquid-solid systems.

$$f = \frac{C_D \, \mathrm{Re}_s \, \alpha_l}{24 v_{r,s}^2} \tag{73}$$

The drag function was derived by Dalle Valle (Fluent User Manual, 2003).

$$C_D = \left(0.63 + \frac{4.8}{\sqrt{\mathrm{Re}_s / v_{r,s}}} \right)^2 \tag{74}$$

$$\mathrm{Re}_s = \frac{\rho_l d_s \left| \vec{v}_s - \vec{v}_l \right|}{\mu_l} \tag{75}$$

Where l is the subscript for the l^{th} liquid phase, s is the subscript for the s^{th} solid phase and d_s is the diameter of the s^{th} solid phase particles.

The Fluid-Solid Coefficient has the form

$$K_{sl} = \frac{3\alpha_s \alpha_l \rho_l}{4 v_{r,s}^2 d_s} C_D \left(\frac{\mathrm{Re}_s}{v_{r,s}} \right) \left| \vec{v}_s - \vec{v}_l \right| \tag{76}$$

Where $v_{r,s}^2$ is the terminal velocity term for the solid phase in this case the coal particles of varying size and density.

$$v_{r.s} = 0.5(A - 0.06\mathrm{Re}_s + \sqrt{(0.06\mathrm{Re}_s)^2 + 0.12\mathrm{Re}_s(2B - A) + A^2}) \tag{77}$$

with

$$A = \alpha_l^{4.14} \tag{78}$$

and

$$B = 0.8\alpha_l^{1.28} \quad \text{for } \alpha_l \leq 0.85 \tag{79}$$

and

$$B = \alpha_l^{2.65} \quad \text{for } \alpha_l > 0.85 \tag{80}$$

This model is used when solid shear stresses are defined according to the Syamlal et al. (Fluent User Manual, 2003)

Wen and Yu formulated a model for the dilute systems.

The fluid–solid coefficient is defined as follows

$$K_{sl} = \frac{3}{4} C_D \frac{\alpha_s \alpha_l \rho_l \left| \vec{v}_s - \vec{v}_l \right|}{d_s} \alpha_l^{-2.65} \tag{81}$$

$$C_D = \frac{24}{\alpha_l \, \mathrm{Re}_s} \left[1 + 0.15 (\alpha_l \, \mathrm{Re}_s)^{0.687} \right] \tag{82}$$

and Re_s is defined by Eq (73).

The Gidaspow model is a combination of the Wen and Yu model and the Ergun Equation. The Fluent User Manual specified its use for dense fluidised beds. Both the Syamlal O' Brien and Gidaspow Model were compared in the simulations and discussed in Chapter 5 to determine which drag law model best described the velocity magnitude for the multiphase simulations.

When $\alpha_l > 0.8$, the fluid-solid exchange coefficient K_{sl} is given by Eq. (71) & (81).

When $\alpha_l \leq 0.8$, the fluid-solid exchange coefficient K_{sl} is given by

$$K_{sl} = 150\frac{\alpha_s(1-\alpha_l)\mu_l}{\alpha_l d_s^2} + 1.75\frac{\rho_l \alpha_s \left|\vec{v}_s - \vec{v}_l\right|}{d_s} \quad (83)$$

This model is appropriate for dense fluidised beds for gases thus not relevant.

Dispersed Turbulence Model

This effect was neglected in the TBS model since it is only appropriate when the secondary phase is dilute. This is not the case in the TBS since the volume fraction was always above 30%. The dispersed turbulence model also neglects interparticle collisions.

Solution Method for Pressure Fluctuations

The Eulerian multiphase model used a phase coupled simple (PC-Simple) algorithm for its pressure-velocity coupling. The velocities are solved in phases in a segregated form. The coupled solver solves a vector equation of all phases simultaneously.

4.9.4. Grid Geometry and Meshing

The geometry of the system is most important when simulating in Fluent. The program that was used to create this geometry was Gambit 2.1.6. Gambit is used to build and mesh models for CFD packages. Boundary zones and continuum phase properties for the unit are incorporated in the geometry before being exported to Fluent 6.1. The TBS grid was initially created from vertices. These vertices were used to create the various edges (outlining structures). These edges were then used to create faces (the feed, overflow & distributor plate) and finally all the faces were joined to form the main control volume (an open shell) for meshing, boundary specifications and continuum fluid property definitions.

The TBS geometry was created in Gambit with the specified boundary conditions for the overflow, underflow, teeter water and feed slurry. The region above the distributor plate was analysed to determine the flow characteristics of each plate configuration considered. A drawback of this method is the inability of Fluent 6.1 to simulate cross flow through the distributor plate.

The holes in the distributor cannot be specified both as an inlet and an outlet. This was overcome by considering two cases. In the base case, water was used as a single phase in the unit to determine the distributor profile. In the second case, a two-phase model was adopted, with the solids phase introduction. The distributor acted as a teeter water inlet and the settling solids would settle above the plate forming a packed bed. The underflow region was neglected since the separation from literature was found to be purely dependent on the teeter bed region.

When meshing the TBS grid the following methodology was utilised:

- The number of nodes on each vertex was chosen.
- The faces (overflow, distributor holes and feed) were meshed first.
- The volume was then meshed. This meshes all other parts of the geometry, refines the mesh and gives a node count.
- In order to reduce the computation time however still obtain accuracy, the number of nodes were varied depending on the degree of accuracy required in the specific regions.
- The meshes in the distributor region are finer. More nodes were used in that region since the investigation was based on the distributor effects.

The figures below illustrate the TBS grid and meshing for each plate in Gambit 2.1.6.

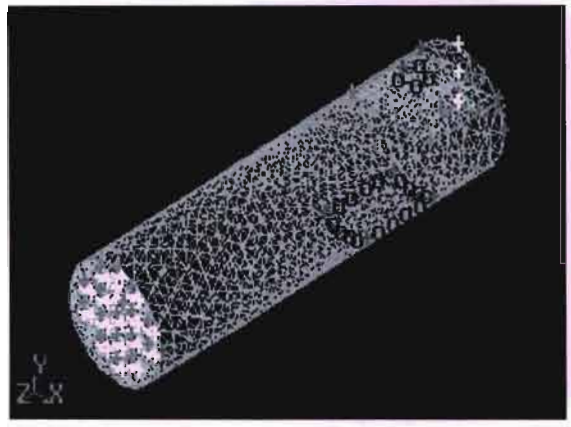

Figure 4.14: 3D Mesh of Plate1

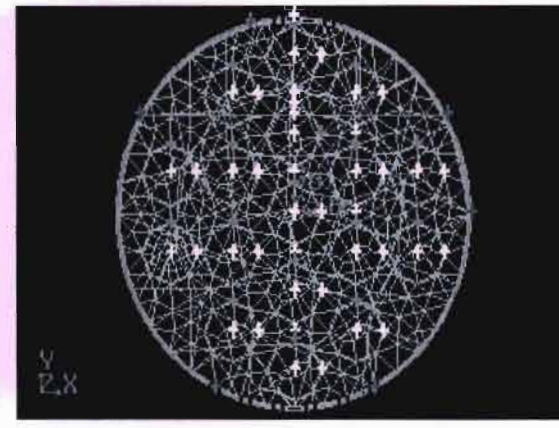

Figure 4.15: Top View Mesh of Plate1

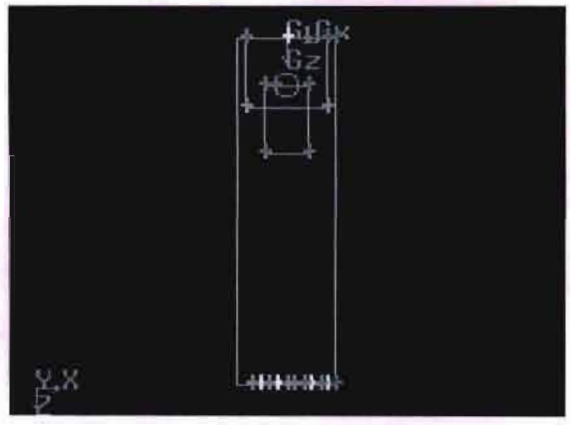

Figure 4.16: Front View of Plate1

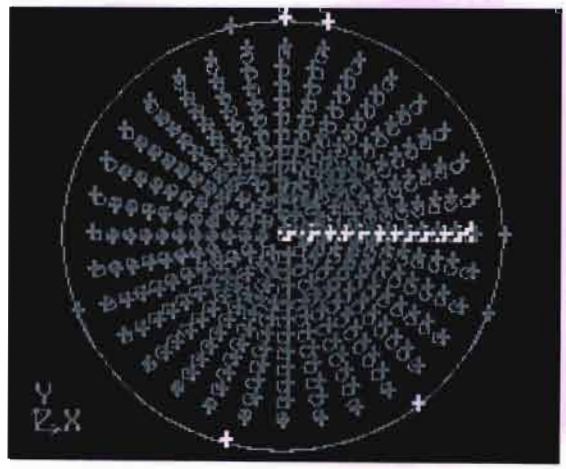

Figure 4.17: Top View of Plate 2

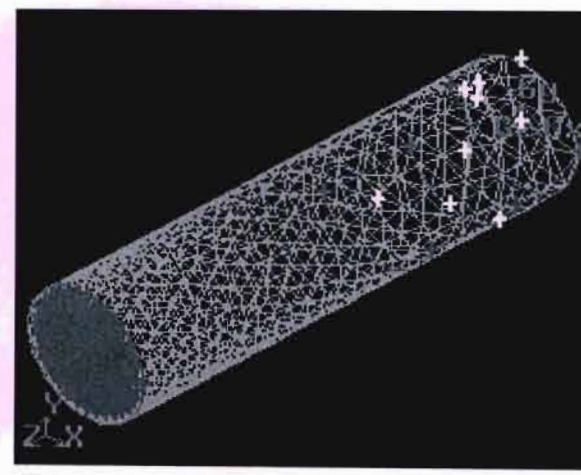

Figure 4.18: 3D Mesh of Plate 2

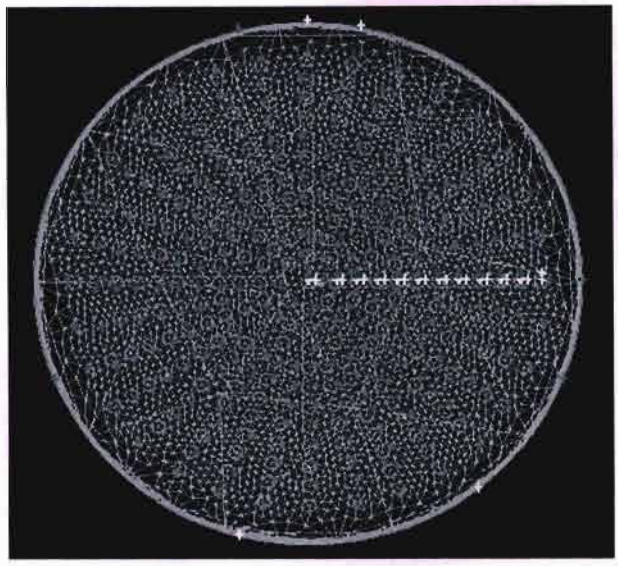

Figure 4.19: Top View Mesh of Plate 2

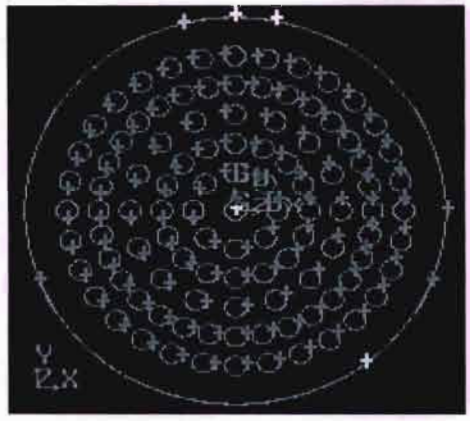

Figure 4.20: Top View of Plate 3

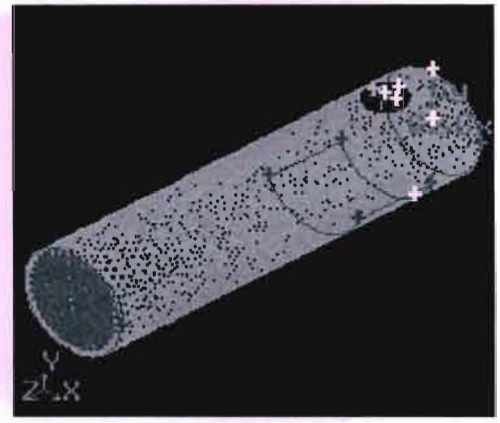

Figure 4.21: 3D Mesh of Plate 3

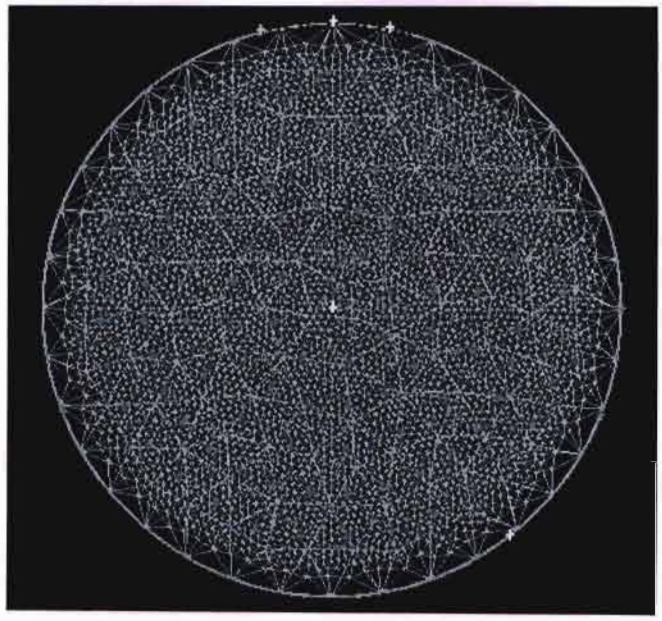

Figure 4.22: Top View Mesh of Plate 3

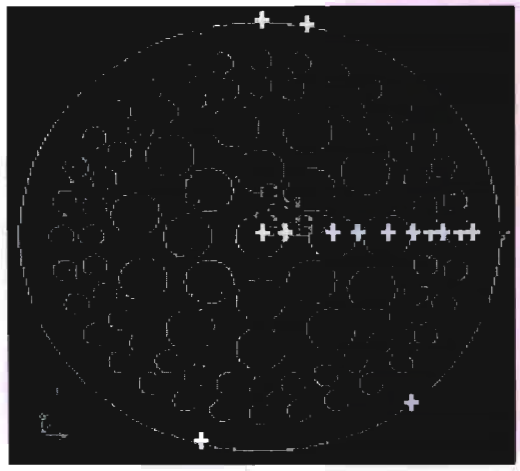

Figure 4.23: Top View of Plate 4

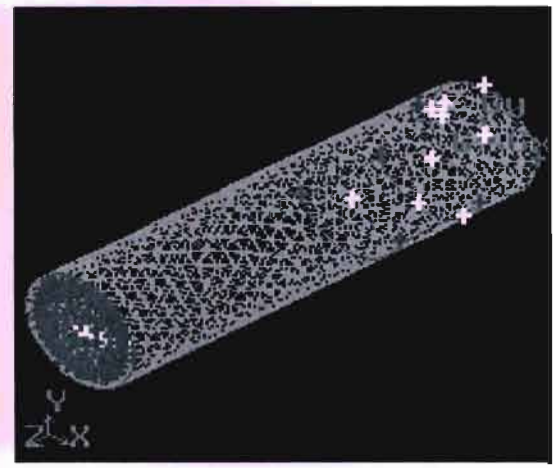

Figure 4.24: 3D Mesh of Plate 4

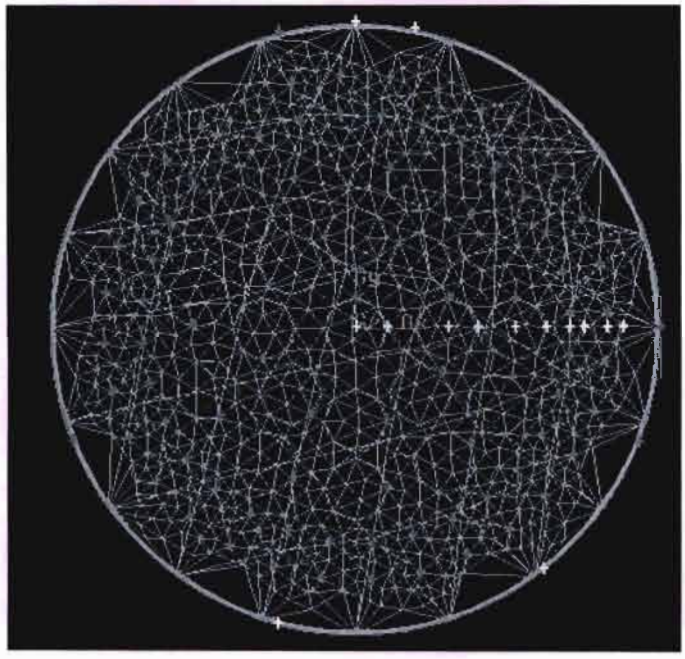

Figure 4.25: Top View Mesh of Plate 4

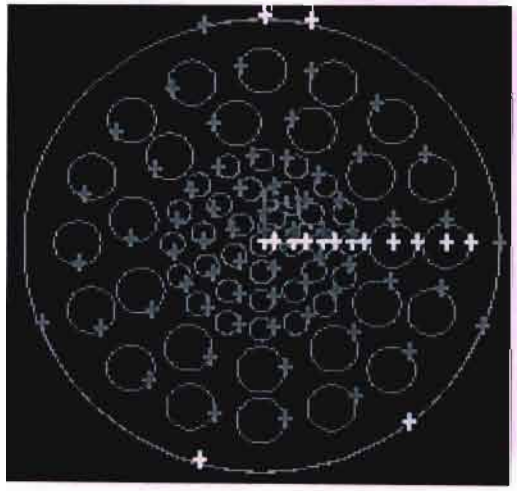

Figure 4.26: Top View of Plate 5

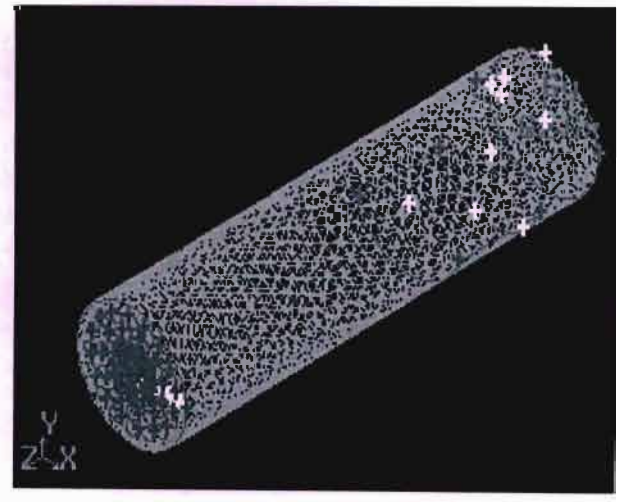

Figure 4.27: 3D Mesh of Plate 5

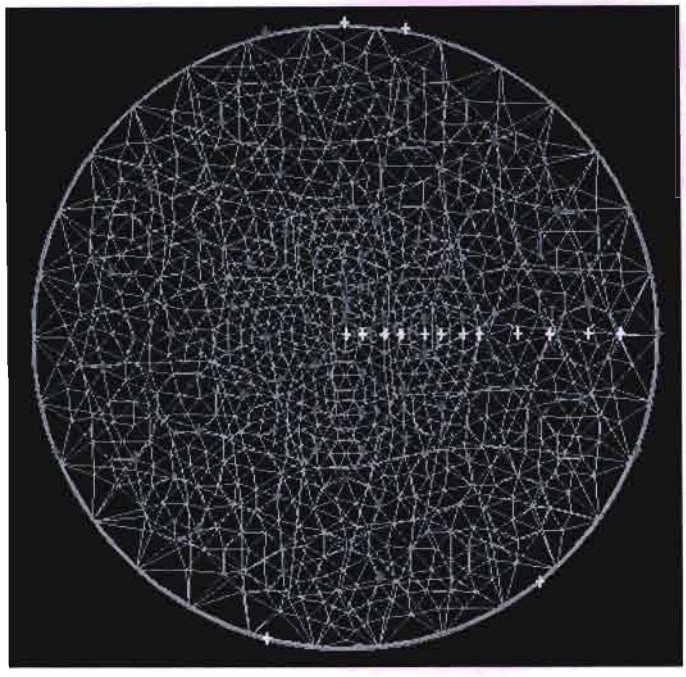

Figure 4.28: Top View Mesh of Plate 5

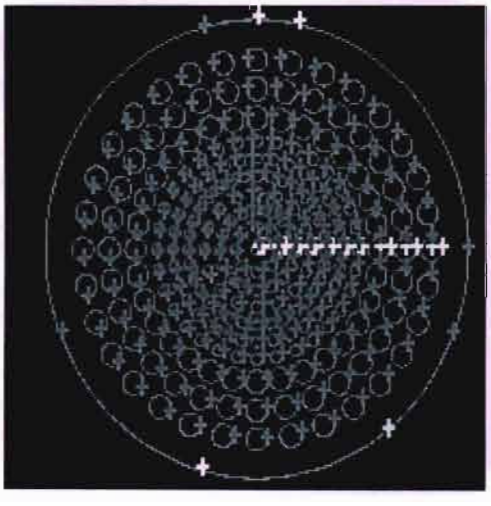

Figure 4.29: Top View of Plate 6

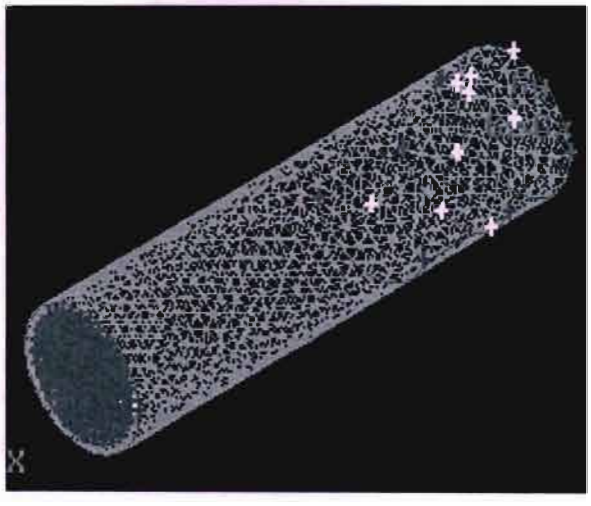

Figure 4.30: 3D Mesh of Plate 6

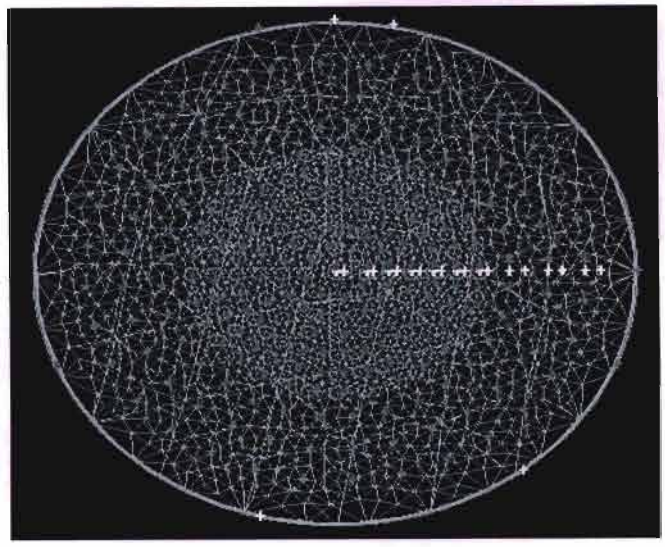

Figure 4.31: Top View Mesh of Plate 6

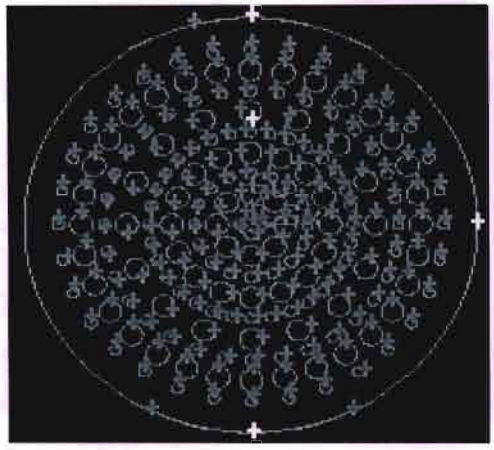

Figure 4.32: Top View of Plate 7

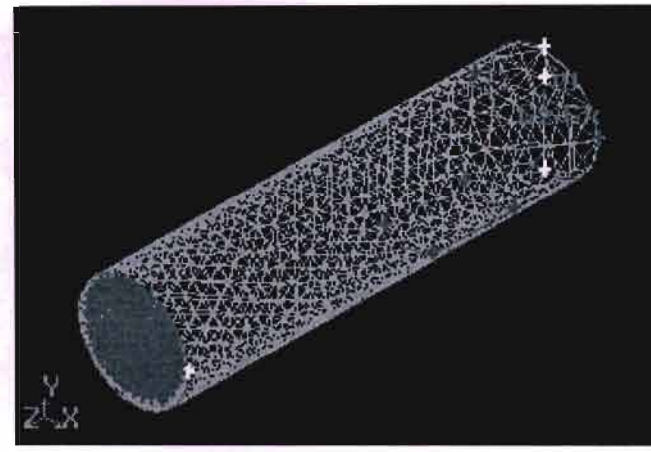

Figure 4.33: 3D Mesh of Plate 7

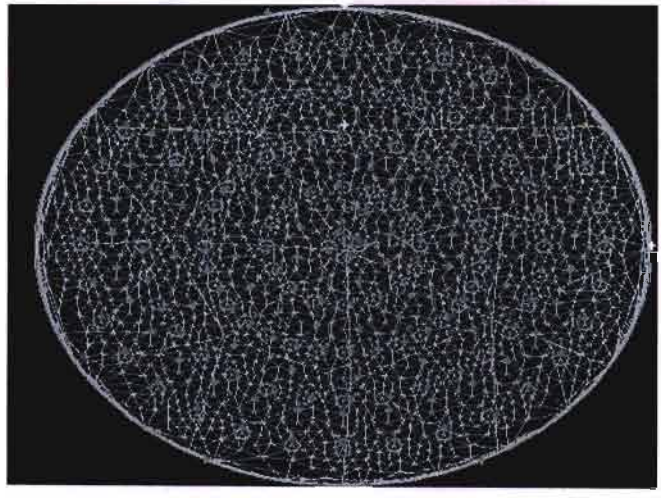

Figure 4.34: Top View Mesh of Plate 7

4.9.5. Fluent Simulation Method

The granular multiphase simulation method required the following inputs in Fluent.

- The geometry created in Gambit 2.1.6 was exported to Fluent.
- The meshed grid was checked to ensure that the minimum volume was greater than zero.
- The grid was drawn in millimetres; therefore, it had to be scaled to metres.
- The grid was smoothened to remove any skewness caused by incorrect meshing of the control volume.

The following specification methods were used when formulating the TBS simulation.

Define Panel:

The type of solver was initially specified as followed:

- Segregated Solver
- Implicit Formulation
- 3D Space
- Unsteady Time
- Absolute Velocity Formulation
- 1st Order Implicit Unsteady Formulation
- Cell based gradient option
- Porous Formulation,
- Superficial velocity

Multiphase Model:

- Eulerian
- Mixture

In instances here, the Eulerian Model did not converge and the Mixture Model was used to obtain a solution. Both models accounted for multiphase granular particles. The Mixture Model had solution controls for Momentum (Flow), Volume Fraction, Slip velocity and Turbulence. Convergence was easily achieved. This method was used for Plates 2, 5, 6 and 7 since the Eulerian Model diverged during simulation runs. The Mixture Model does not produce plots of the secondary phase velocities. It only accounts for the primary phase, the mixture velocity profile and velocity vectors.

Number of Phases:

- 16 (1 liquid phase, 15 solid phases), where 3 size fractions were considered, 0.8; 2; 5 mm particles each in the specified density range.

Mass Transfer:

- None

Viscous Model:

- Laminar to intermediate flow.
- There was no need to account for k-epsilon since turbulence was not considered in the low Reynolds flow regime.

Materials Panel:

From the materials database, water was chosen with all its properties. The coal particles were defined as Coal 1 – Coal 15. The density range was 1200 – 2000 kg/m^3 for each size fraction mentioned above. The viscosity was fixed at 0.015Pa.s

Phases Panel:

- The materials were classified as phase 1 – phase 16. Water was defined as phase1. Coal 1- 15 occupied Phases 2-16.
- For each solid phase, it was specified that the material properties be of granular particles with packed beds.
- The particle diameters were also specified for each phase.

The following models were chosen for each of these variables in the simulation from the Fluent User Manual (2003).

- Granular Viscosity (kg/ms): Syamlal & O Brien Model
- Granular Bulk Viscosity (kg/ms): Lun et al.
- Granular conductivity (kg/ms): Syamlal & O Brien Model
- Packing Limit: 0.72

Phase Interaction:

Two methods were initially tested. The Syamlal & O Brien and Gidaspow Model were compared. The Syamlal O Brien model predicts a large primary phase velocity of 25 cm/s, which increases the cut-point density. The Gidaspow model is generally preferred for dense fluidised bed and was set as default in the simulations.

Operating Conditions:

- Pressure: Atmospheric
- Gravitational Acceleration: 9.81 m/s^2 in the Z direction.

Boundary Conditions:

Feed:

- The velocity magnitude (m/s) and volume fraction for each phase was required. It was assumed that an equal proportion of each SG and size was fed into the unit.

Feed Velocity Specification:

- Magnitude normal to boundary

Reference Frame:

- Absolute
- Teeter-water:
- The velocity input was required for the upward water flow.
- Wall: No slip at boundary
- Overflow: Flow rate weighting of 1
- Feed, Teeter-water: Specified as Velocity inlets
- Overflow: Specified as an outflow
- Continuum Fluid: Water – Applies continuity equations on unit.
- Default Interior: Specified as interior

Solve

Solution Controls

When simulating using the Eulerian Model, there are solution controls for, Flow, Volume Fraction, Pressure, Density, Body Forces and Momentum. Pressure, Momentum and Volume Fraction were usually kept low to quicken the convergence. It produces velocity plots for both primary and secondary phases

Discretisation

- Pressure-Velocity coupling- Phase Coupled Simple
- Momentum – Second Order Upwind
- Volume Fraction – Second Order Upwind

Initialising Solutions

- All the variables were set to zero.

Monitors

- The monitors were Residual Plots and Data Print Outs to observe the solution convergence.

Iteration of the solution

- The Step size, Number of steps and Time Stepping Method was be specified
- Time Step Size (s): 1
- Number of Steps: 200
- Time Stepping Method: Fixed
- Max iterations per Time Step: 30
- Relaxation Factors for Solution Control Equations
- The relaxation factors range from 0 to 1. For the Momentum, Pressure and Volume Fraction equations, it was varied between 1 and 1e-29.
- The Density and Body Force factors were left at their default settings of 1.

- For the Mixture Model and single-phase simulations, a relaxation factor of 1e–25 was used to achieve quick convergence.

Chapter 4 described the both the TBS and distributor plate design criteria for the experimental investigations and outlined the hydrodynamics model developed in Fluent6.1 for the simulation work. Chapter 5 would provide a detailed discussion of the results of both the experimental and multiphase simulations with necessary conclusions regarding the comparisons of the investigations.

CHAPTER 5: RESULTS AND DISCUSSION

In this Chapter, the results from the experimental work on the TBS and the Fluent simulations are represented for each distributor plate configuration. The partition curves for each plate, together with the Fluent velocity vectors and axial velocity profiles were compared. The tracer and sink-float density profiles have also been plotted to compare the effectiveness of the tracer tests. All the data has been tabulated and can be referenced in Appendix B. Appendix C contains additional graphs from the repeat runs on the unit and additional Fluent profiles which have been referred to in the discussion.

It is appropriate to begin the discussion of the TBS results with Table 5.1 and 5.2, which summarise the actual velocities developed through the seven distributor plates at the desired set-point flow rates. It is evident from Table 5.2 that the majority of the runs were performed in the laminar region for the experimental investigation. This is appropriate for the recovery of fine coal particles since higher fluidisation velocities result in higher cut point densities. The tables below indicate the velocities, Reynolds Numbers and the flow regime for each run. It serves as a comparison with the simulated profiles when observing the various phase 1 velocity vectors and axial velocity profiles in Fluent.

The plate configurations were tested at various flow rates relevant to the cut-point density range. The effect of the pressure-drop across the distributor plates were also investigated however due to the minimal plate thickness, the pressure-drop effect is shown in relation to percentage area open. The experiments were conducted at three flow rates; Run 1 was performed at 6 l/min, Run 2 at 3 l/min and Run 3 at 8 l/min. The teeter-water velocities were dependent on the fractional open area of each plate. This resulted in the Reynolds Numbers overlapping into a higher flow regime for certain plates at the set point flow rates. Run 1 was in the laminar and intermediate flow regime; Run 2 was performed in the laminar regime only and Run 3 was predominantly performed in the intermediate flow region. Plate 2 experienced turbulent effects at 8 l/min. This was due to the reduced aperture area, which resulted in a turbulent liquid velocity at this flow rate.

Flow (l/min)	Plate 1 (m/s)	Plate 2 (m/s)	Plate 3 (m/s)	Plate 4 (m/s)	Plate 5 (m/s)	Plate 6 (m/s)	Plate 7 (m/s)
3	4.5E-03	8.6E-03	6.1E-03	4.4E-03	4.5E-03	4.9E-03	6.3E-03
6	8.9E-03	1.7E-02	1.2E-02	8.8E-03	9.0E-03	9.8E-03	1.3E-02
8	1.2E-02	2.3E-02	1.6E-02	1.2E-02	1.2E-02	1.3E-02	1.7E-02

Table 5.1: Teeter water velocities through the Distributor Plates

	Run 1: 6 l/min		Run 2: 3 l/min		Run 3: 8 l/min	
Plate no.	Reynolds No.	Flow Regime	Reynolds No.	Flow Regime	Reynolds No.	Flow Regime
1	1603	Laminar	802	Laminar	2137	Intermediate
2	3097	Intermediate	1549	Laminar	4129	Turbulent
3	2183	Intermediate	1091	Laminar	2910	Intermediate
4	1592	Laminar	796	Laminar	2122	Intermediate
5	1614	Laminar	807	Laminar	2152	Intermediate
6	1760	Laminar	880	Laminar	2346	Intermediate
7	2269	Intermediate	1135	Laminar	3026	Intermediate

Table 5.2: Reynolds Number & Teeter-water Flow Regime

5.1. Interpretation of Figures

The velocity vector profiles and axial velocity profiles displayed in the subsequent sections illustrate the flow patterns within the column. The TBS geometry was created in Gambit 2.1.6 with the top of the unit denoted as the point (0,0,0) in the x, y and z directions respectively. The velocity vector profiles display the front view of the unit in the positive z direction with the top of the unit positioned at zero metres. The colour scheme on the left hand side of these figures, indicate the different velocity regions visible through the unit. The maximum and minimum velocity vectors (m/s) are displayed on these plots with specific shades of colour denoting each velocity region. From these plots, the magnitude and direction of the liquid phase flow could be determined.

The axial velocity profiles were placed adjacent to the velocity vectors to make it possible to observe the magnitude and direction of the liquid phase and its specific position in the teeter bed. Fluent plots the axial velocity profiles in the positive z-direction. This resulted in the distributor region being positioned at the top, since its corresponding axial position was 0.75m in relation to the feed position of zero metres. The axial velocity plots were inverted and this resulted in the position (m) on the z-axis being reflected as negative values. The distributor region was denoted by -0.75m in these plots.

The axial velocity profiles indicate the velocity magnitude range (m/s) of the particles present in each section of the column. Ideally, the velocities should be consistent through the column in order to improve the density separation process, however it is evident from the profiles in this chapter that certain regions of the unit are affected by turbulence and dead zones which are a direct relation to the distributor plate configuration. The arrangement of these profiles clearly describes the flow patterns and circulation effects within the TBS for each plate configuration at the set point flow rates.

5.2. Results from Plate 1

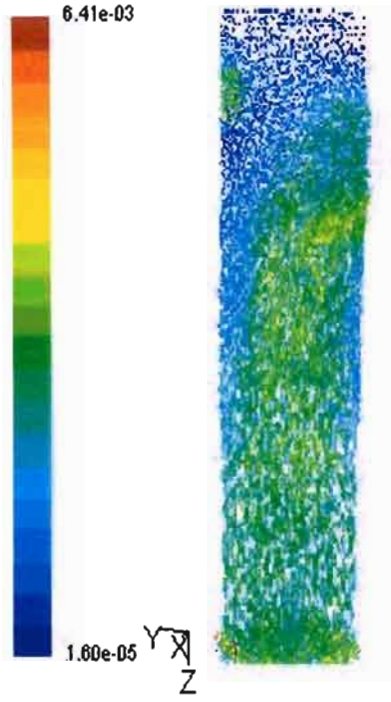

Figure 5.1: Velocity Vector Profile for Plate 1 – 6 l/min

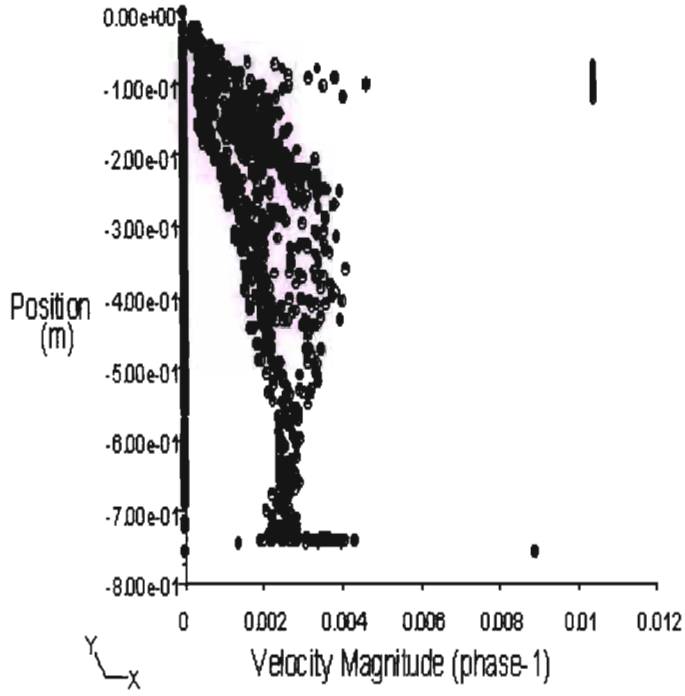

Figure 5.2: Axial Velocity Profile for Plate 1 – 6 l/min

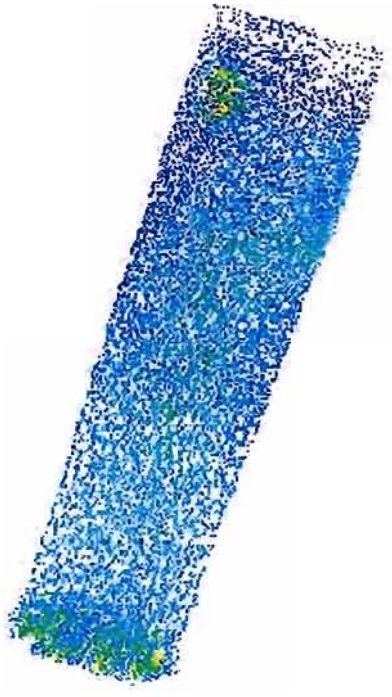

Figure 5.3: Velocity Vector Profile for Plate 1 – 3 l/min

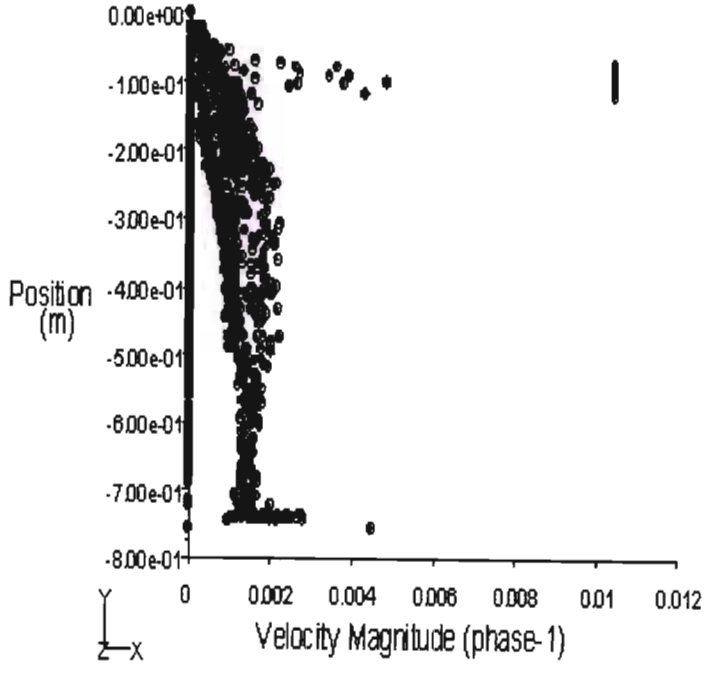

Figure 5.4: Axial Velocity Profile for Plate 1 – 3 l/min

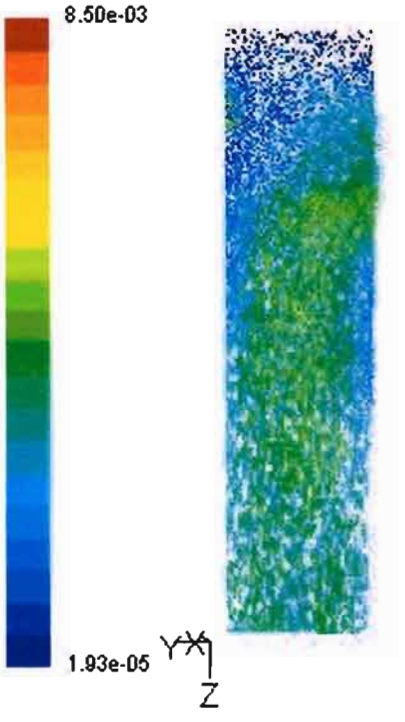

Figure 5.5: Velocity Vector Profile for Plate 1 – 8 l/min

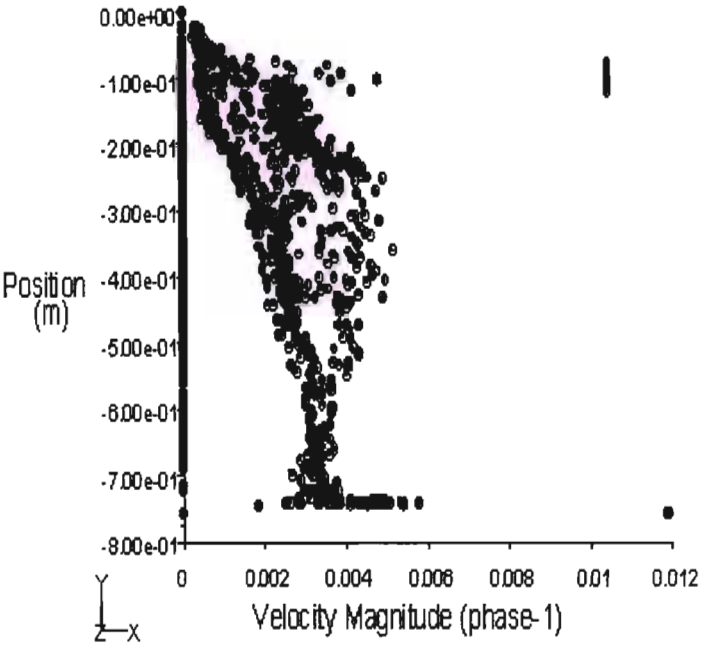

Figure 5.6: Axial Velocity Profile for Plate 1 – 8 l/min

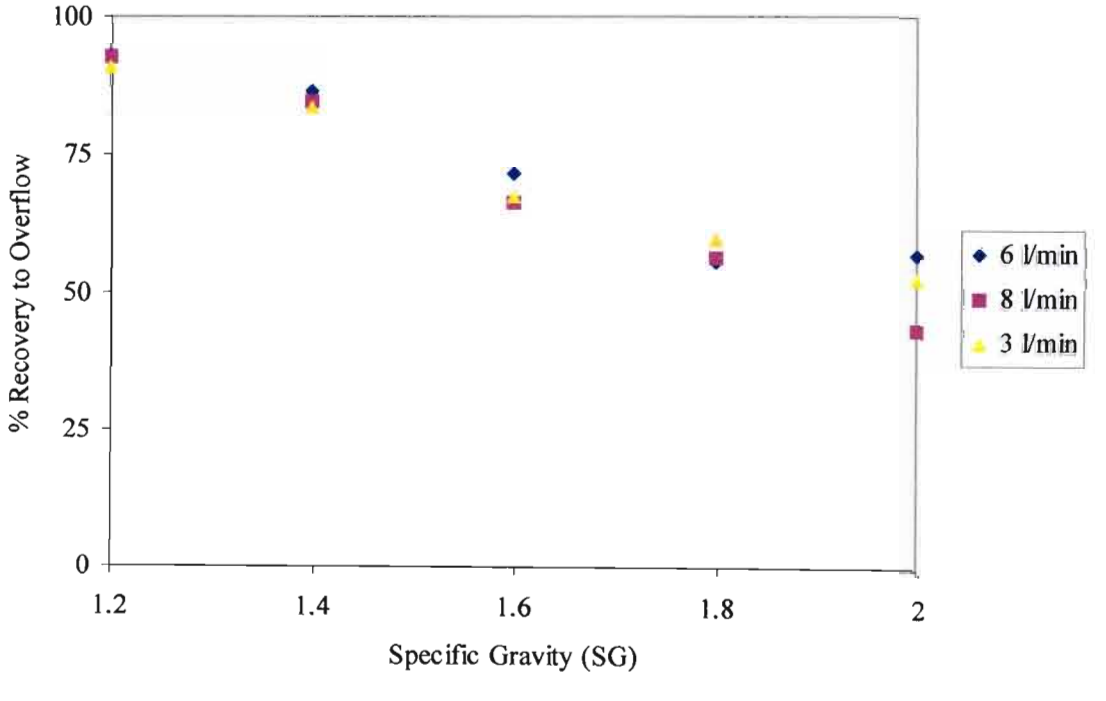

Figure 5.7: Partition Curves for Plate 1

The velocity vector profile in Figure 5.1 illustrates the primary phase velocity profile within the column. It is evident from this profile that Plate 1 has a higher velocity within the centre of the column, with minimum wall effects in that region. The distributor and teeter bed region (-7.5e-01 to –1.5e-01 m) have an intermediate flow profile with some wall effects. The region near the feed has dead zones represented by the dark blue contours. However this was ideal as it limited the feed disturbances on the overflow. Figure 5.2 illustrates the z-component velocity of phase-1, which was the teeter-water velocity magnitude. The feed entry was the region on the graph between 0 and –1.5e-01 metres. The zero velocity magnitude seen on the y-axis was due to the assumption of no-slip on the boundary walls. The PVC column material was assumed to be smooth and thus resulted in a zero wall resistance. The velocity range was between 0.002-0.004 m/s compared to the set point from Table 5.1 of 0.0089 m/s.

The Run 2 simulation represented by Figure 5.3 showed a more even vector profile. This is expected due to the low water flow rate, however slight turbulence was still noted near distributor region. The contrast between the previous run was that feed turbulence is prevalent in Run 2. The result of which may cause an increased settling velocity and thus resulted in a higher product cut. The general trend observed with the both Figures 5.2 and 5.4 is the reduction of the phase velocities compared to the theoretical values. This may be attributed to the comprehensive phase interactions models accounted for in the Fluent simulation which would reduce the upward liquid velocity compared to the theoretical model.

The vector profile in Figure 5.5 is more pronounced due to the intermediate teeter-water flow. An irregular velocity pattern is evident through the column. From the simulations of Plate 1, it is evident that the variation in the circulation patterns resulted due to the reduced pressure resistance.

The partition curves above for Plate 1 reveal that the D_{50} values are 1.98, 1.92 and 2.06 SG for Runs 1, 2 and 3 respectively, with an Ep of 0.45, 0.37 and 0.53 for each run respectively. Normally this would be classified as a totally inefficient process, however due to the nature of the research work, which concentrated on the study of the fundamental particle interactions due to hindered settling, a broad feed size and density range was required.

Furthermore, the hydrodynamic pattern of each plate at different flow rates was also a major contributing factor to the variation in parameters. The sink-float data does suggest however that the unit was operating consistently close to the cut-point density of 1.35 SG. Due to the varying the size fraction of the feed material, the settling rates varied causing the fine high-density particles to be carried into the overflow. From Figure 4.13 it is evident that at the 1.35 SG, fine high-density material would overflow.

Wills (1985) outlined a few possibilities that would cause the effective density of separation (D_{50}) and the error of separation (Ep) to vary. This was used to analyse completed the experimental work on the TBS. There was a significant size discrepancy in the feed material, which normally causes variations in the Ep. A higher percentage of the coal material was greater than 1mm and since Ep decreases with size, this could have contributed to the high experimental values. The concentration criterion suggested that the separation would be difficult due to the average material density being too close to the cut-point density. The size distribution in the unit may have also caused the medium viscosity to increase, thus increasing the Ep and D_{50}.

From the literature on separation efficiency, it is evident that the Ep was not a common method of assessing the efficiency of units that have many operating variables, such as spirals and cones. The TBS falls into this category since it is a cross-flow separator with two inlets and outlets. The teeter-water flow, feed water and feed coal fluctuations could have also contributed to the Ep and D_{50} variations.

5.3. Results from Plate 2

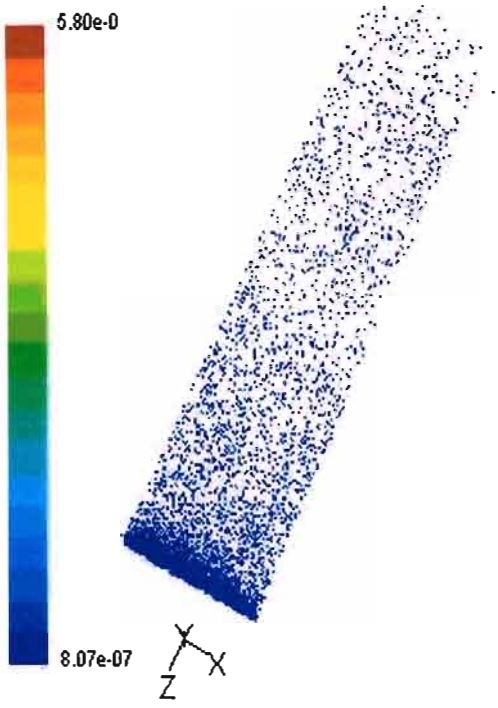

Figure 5.8: Velocity Vector Profile for Plate 2 – 6 l/min

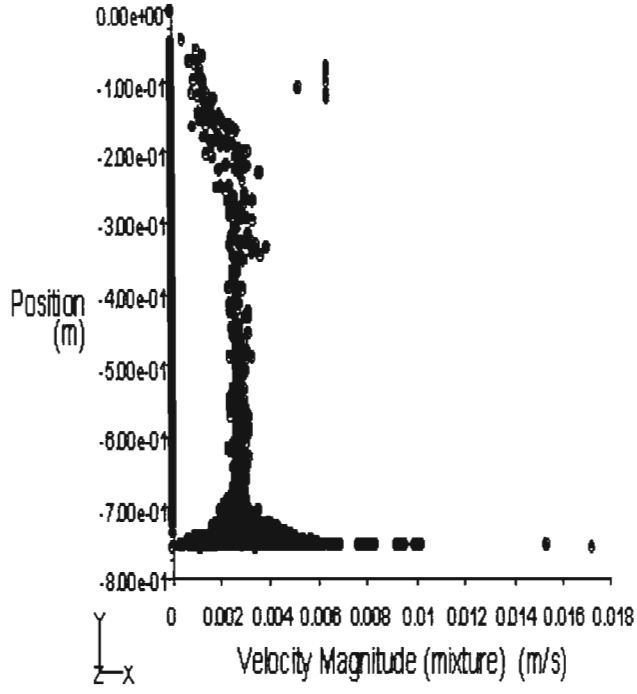

Figure 5.9: Axial Velocity Profile for Plate 2 – 6 l/min

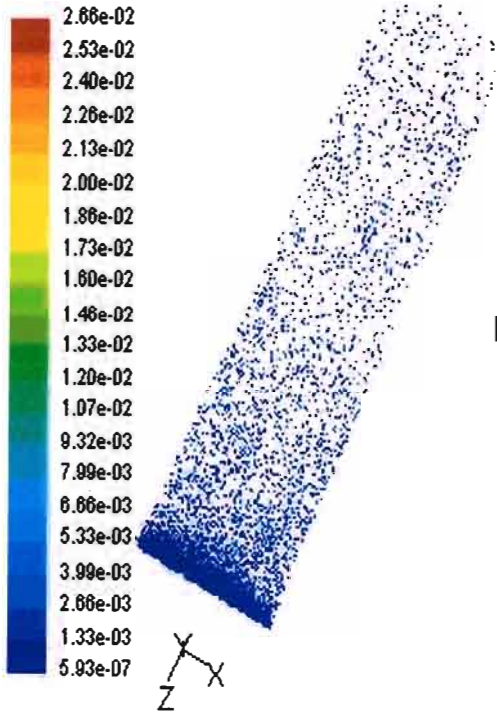

Figure 5.10: Velocity Vector Profile for Plate 2 – 3 l/min

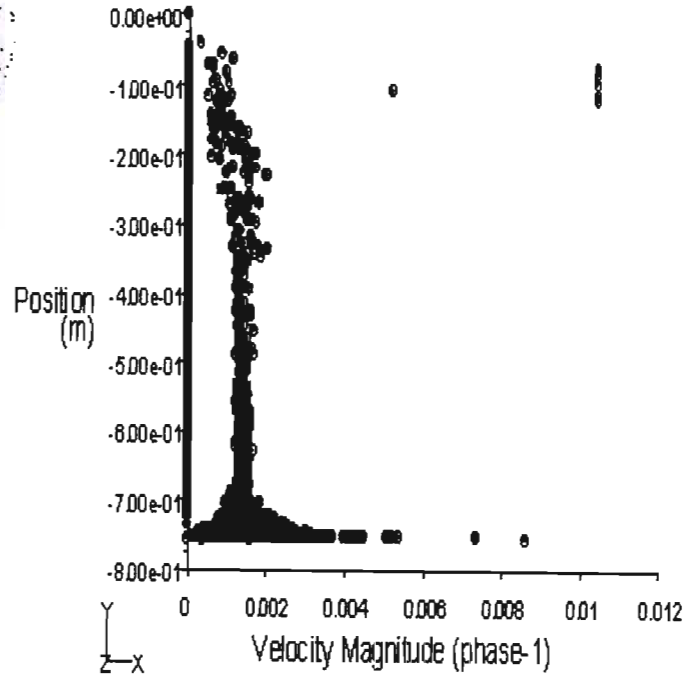

Figure 5.11: Axial Velocity Profile for Plate 2 – 3 l/min

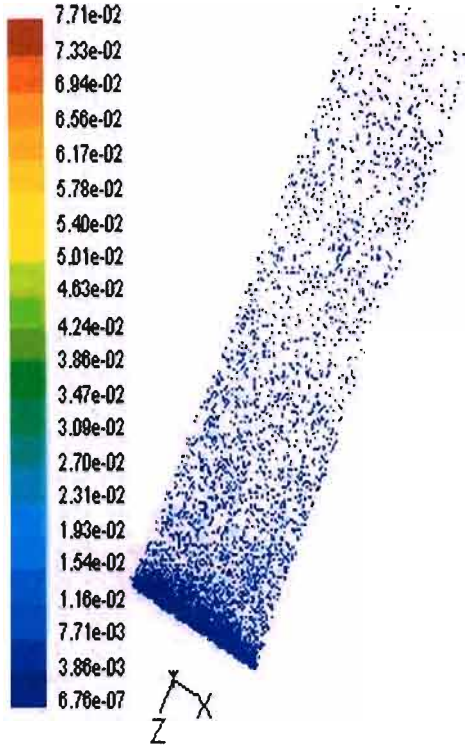

Figure 5.12: Velocity Vector Profile for Plate 2 – 8 l/min

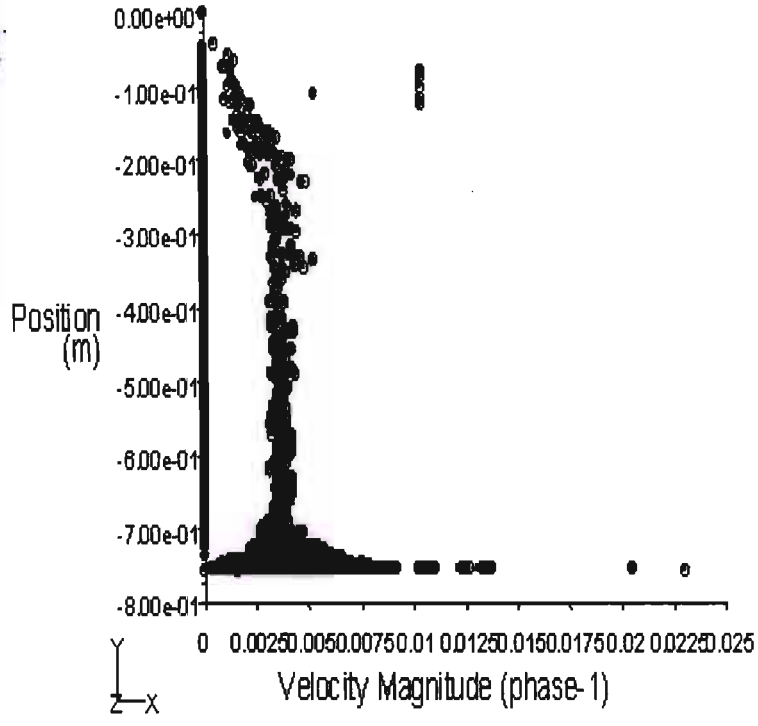

Figure 5.13: Axial Velocity Profile for Plate 2 – 8 l/min

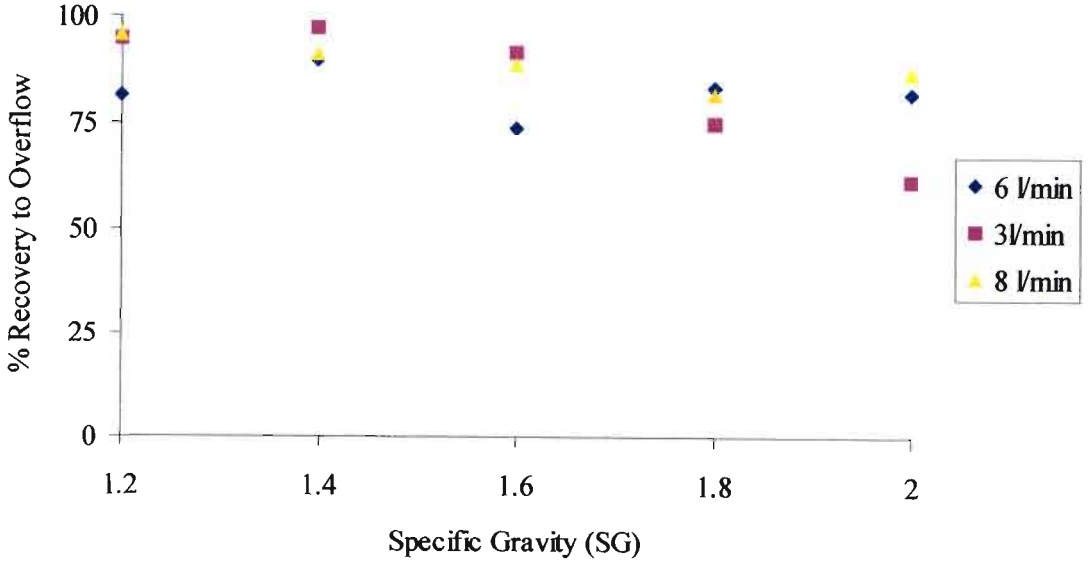

Figure 5.14: Partition Curves for Plate 2

The Mixture Model was used for the simulations of Plate 2 due to the divergence experienced using the Eulerian Model. The vector profile for Plate 2 as seen in Figure 5.8, showed a more stable profile compared with Plate 1. The columns distributor region is more uniform; however many clear spaces exist in the bed region, which indicated the presence of dead zones. This would result in the entrainment of large low-density particles. As the result of the low liquid phase velocity in certain regions of the TBS column, minimal diffusion would occur. This would hinder the creation of the interstitial passages for the high-density particle movements resulting in a tightly packed bed. The distributor pressure drop through the Plate 2 at 6 l/min is extremely high when compared with the simulated results, with a decrease in velocity from 0.017 m/s to approximately 0.004 m/s. A reduction of more than three times the set point velocity, which would be inefficient during operation.

The axial velocity profiles represented by Figures 5.9, 5.11 and 5.13 display a stable flow pattern however due to the low plate open area (22%), which created a high pressure-drop. Plate 2 would not be feasible on a large-scale process, evident from Table 5.1.

The partition curves for Plate 2 reveal that the Ep values have improved; however, the effective separation density is higher. Both plates indicate that the lower flow rate resulted in a more efficient process comparatively. The Ep for Runs 1, 2 and 3 of Plate 2 are 0.23, 0.26 and 0.35 respectively. The D_{50} values are 2.32, 2.08 and 2.15 respectively. The partition curves did not agree with the Fluent plots, which suggested a high pressure-drop and low velocity due to the reduced open area. A lower velocity would have lowered the cut-point and sharpened the gradient of Figure 5.14.

5.4. Results from Plate 3

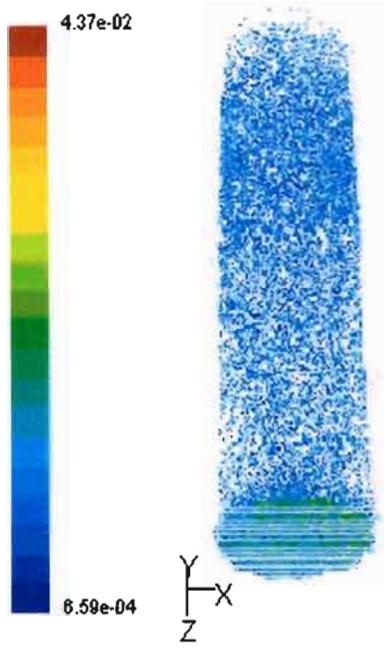

Figure 5.15: Velocity Vector Profile for Plate 3 – 6 l/min

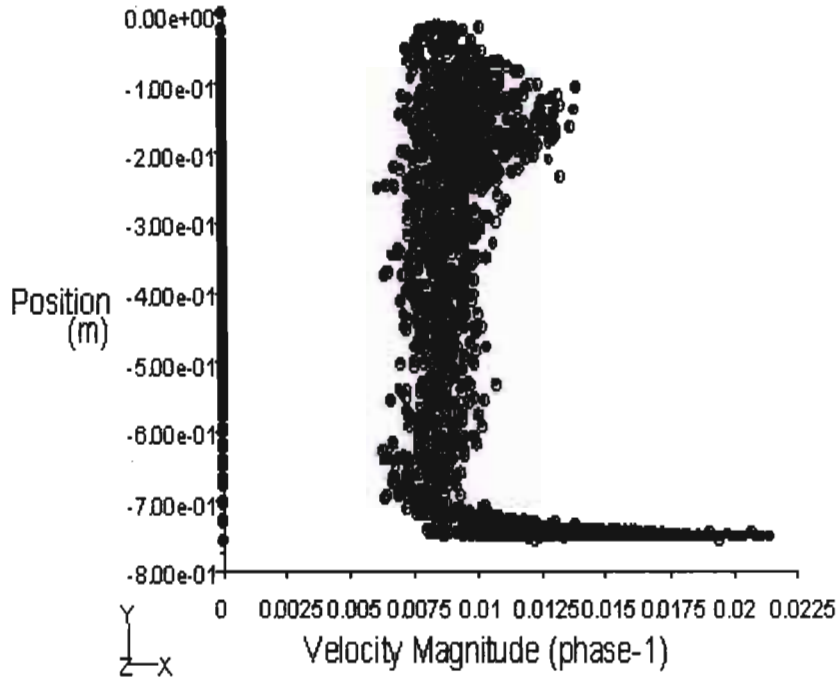

Figure 5.16: Axial Velocity Profile for Plate 3 – 6 l/min

Figure 5.17: Velocity Vector Profile for Plate 3 – 3 l/min

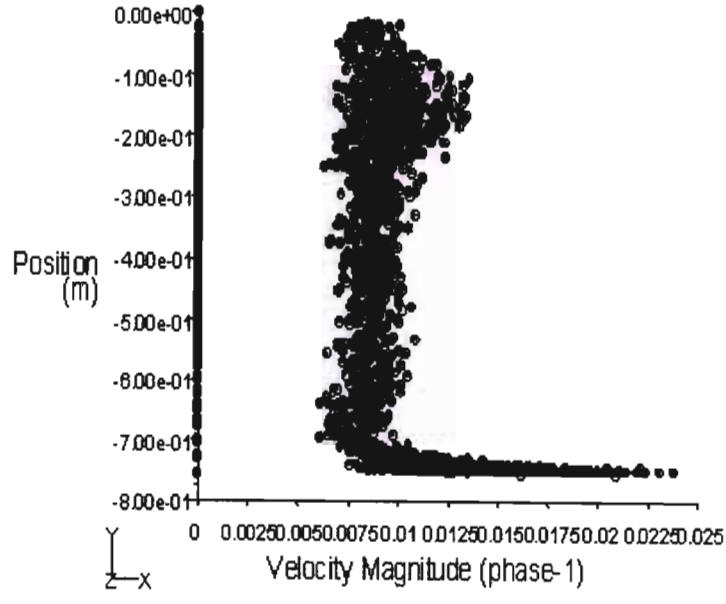

Figure 5.18: Axial Velocity Profile for Plate 3 – 3 l/min

Figure 5.19: Velocity Vector Profile for Plate 3 – 8 l/min

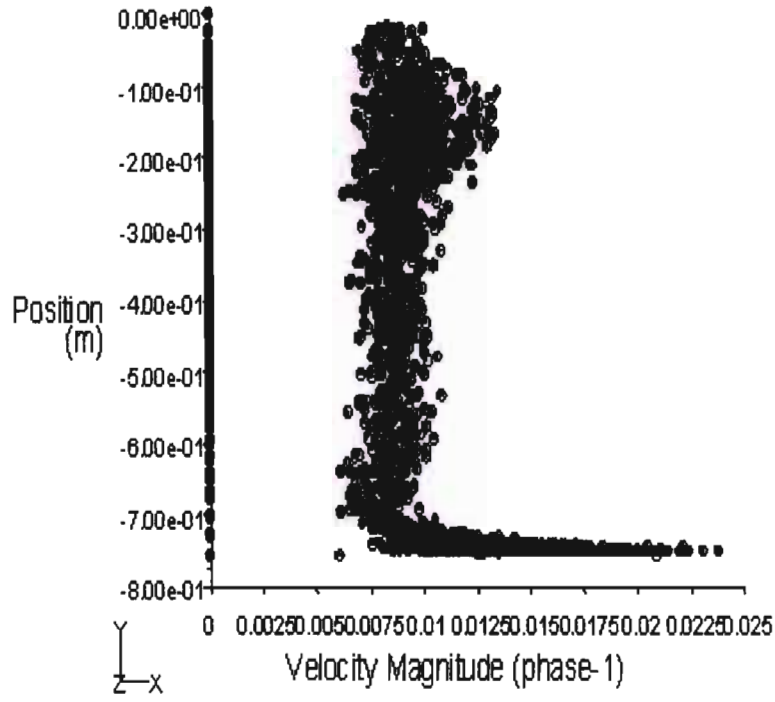

Figure 5.20: Axial Velocity Profile for Plate 3 – 8 l/min

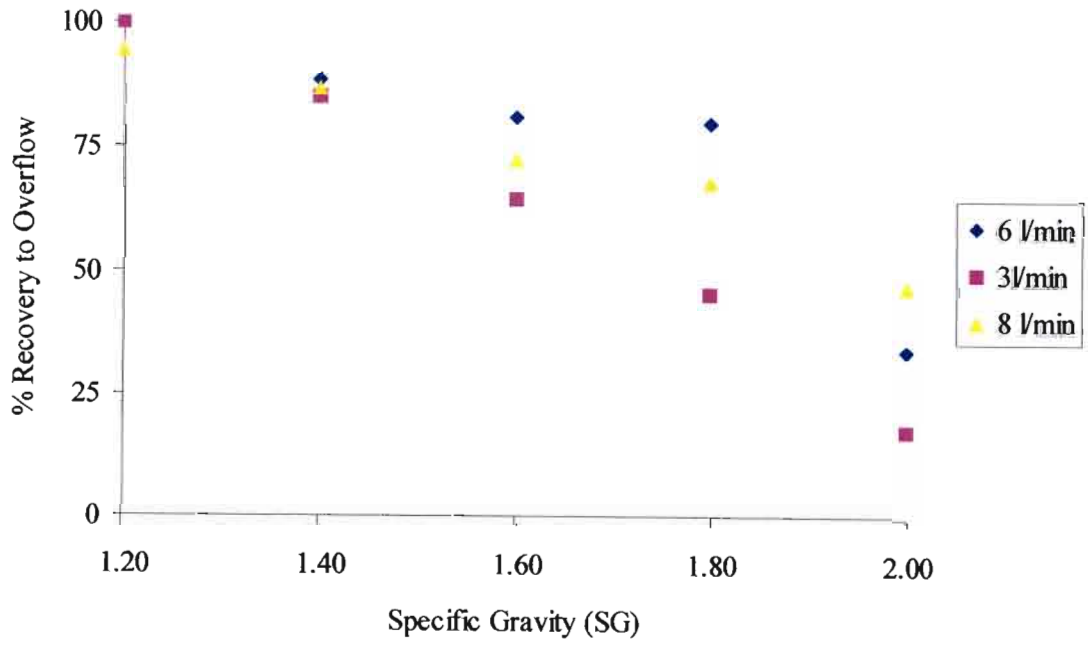

Figure 5.21: Partition Curves for Plate 3

The profiles simulated for Plate 3 at 6 l/min indicate that the pressure-drop is significantly lower than the previous plate. The teeter-water velocity was set at 0.0089 m/s for Run 1. From Figure 5.16, the axial velocity magnitude was between 0.0075 and 0.01 m/s. The set point is within the simulation range, suggesting that the pressure drop percentage decrease was in the range of 18.7 to 12.3 % respectively. The vector profile is evenly distributed, especially at the top of the column. The region close to the plate (-7e-01 to -8e-01 m) on Figure 5.16 shows that the distributor flow pattern is intermediate. The maximum velocity near the plate is below turbulence (< 0.023 m/s). It is also noticeable that the feed region (0m to 0.3m) did not show a decline in the column velocity resulting in a smooth profile throughout.

Figures 5.18 and 5.20 show an average velocity magnitude identical to Figure 5.16. The flow rates were changed and saved accordingly for each run, however it seemed that since the simulations of Runs 2 and 3 were performed after obtaining the solution convergence for Run1, the profiles did not indicate the velocity magnitude adjustment on their respective graphs. From the ease of simulation, convergence and the trend of the current profiles, it would be justifiable to suggest that the Figures 5.18 and 5.20 would only differ in velocity magnitude and not disrupt the even flow distribution evident in Figure 5.16.

The partition curves (Fig. 5.21) show a much-improved trend compared to Plates 1 and 2. As from the previous plots, the lower teeter-water velocity results in an improvement of the separation efficiency. The Ep values are, 0.19, 0.25 and 0.29 for the respective runs, with D_{50} values of 1.9, 1.74 and 1.96 respectively. The product cut improved due to a more stable flow pattern; with minimum feed and wall disturbances together with a reduced pressure drop effect.

5.5. Results from Plate 4

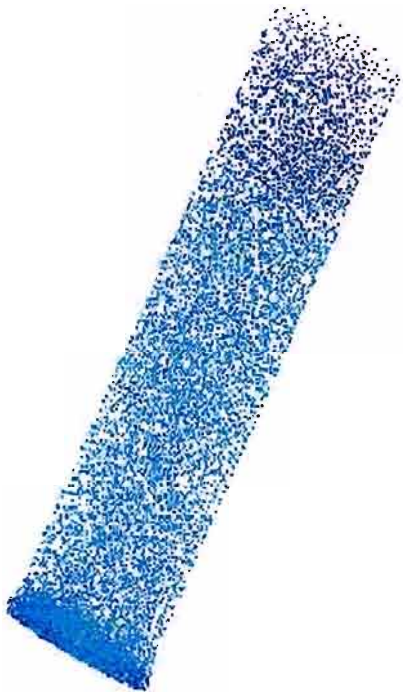

Figure 5.22: Velocity Vector Profile for Plate 4 – 6 l/min

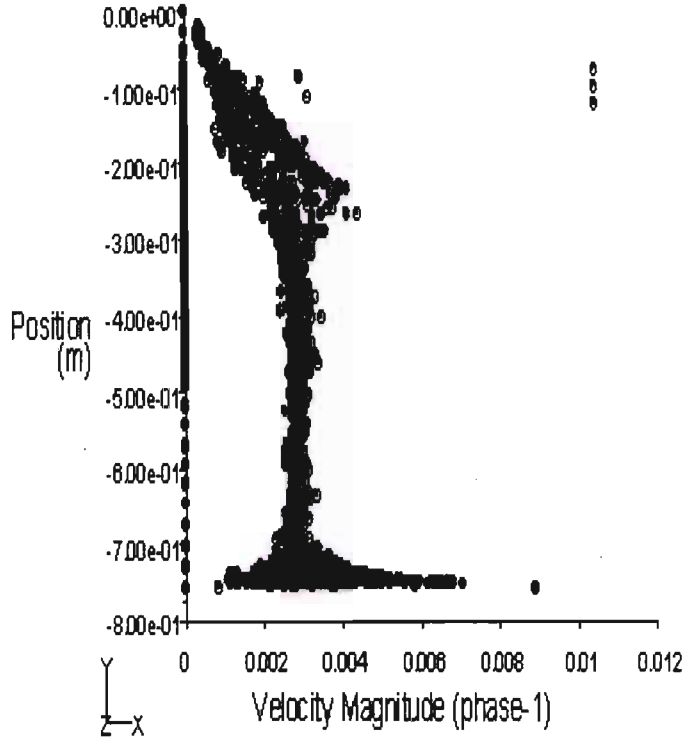

Figure 5.23: Axial Velocity Profile for Plate 4 – 6 l/min

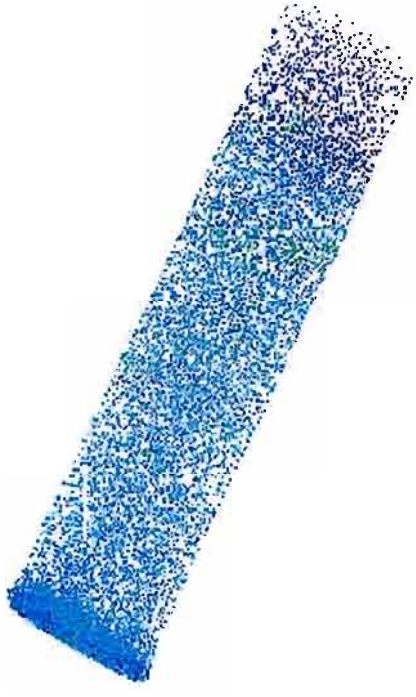

Figure 5.24: Velocity Vector Profile for Plate 4 – 3 l/min

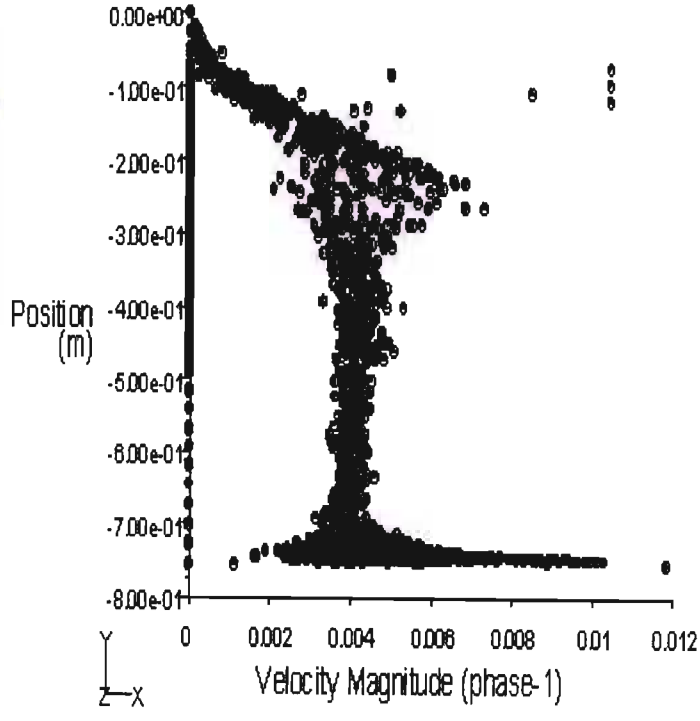

Figure 5.25: Axial Velocity Profile for Plate 4 – 3 l/min

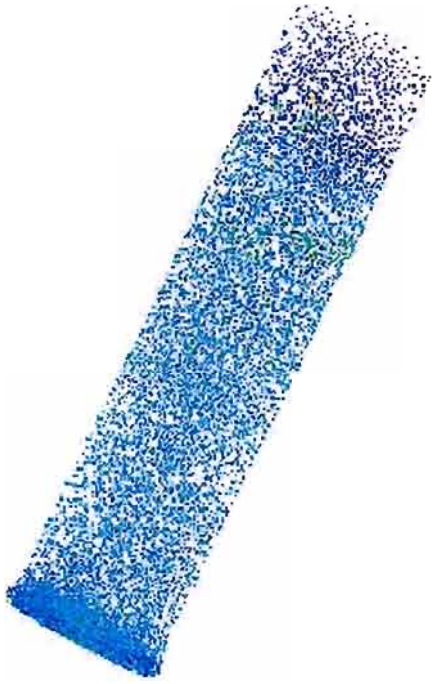

Figure 5.26: Velocity Vector Profile for Plate 4 – 8 l/min

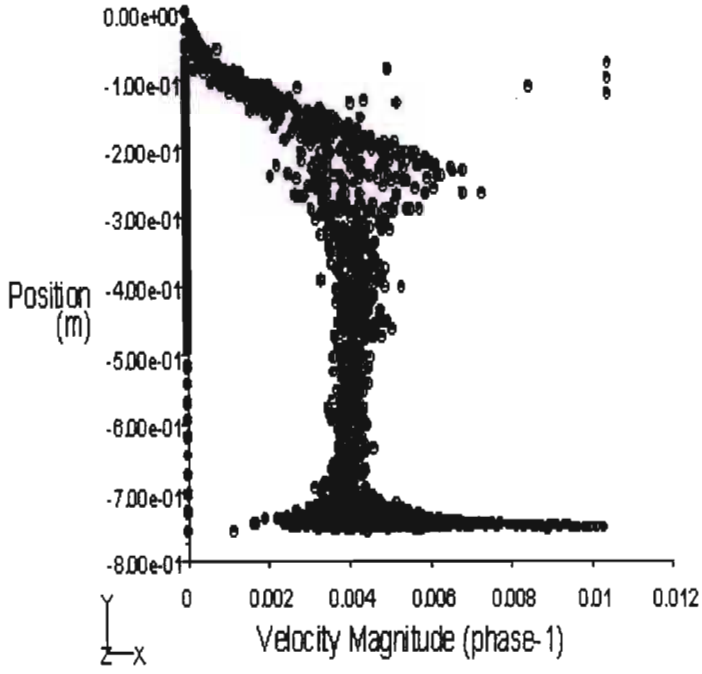

Figure 5.27: Axial Velocity Profile for Plate 4 – 8 l/min

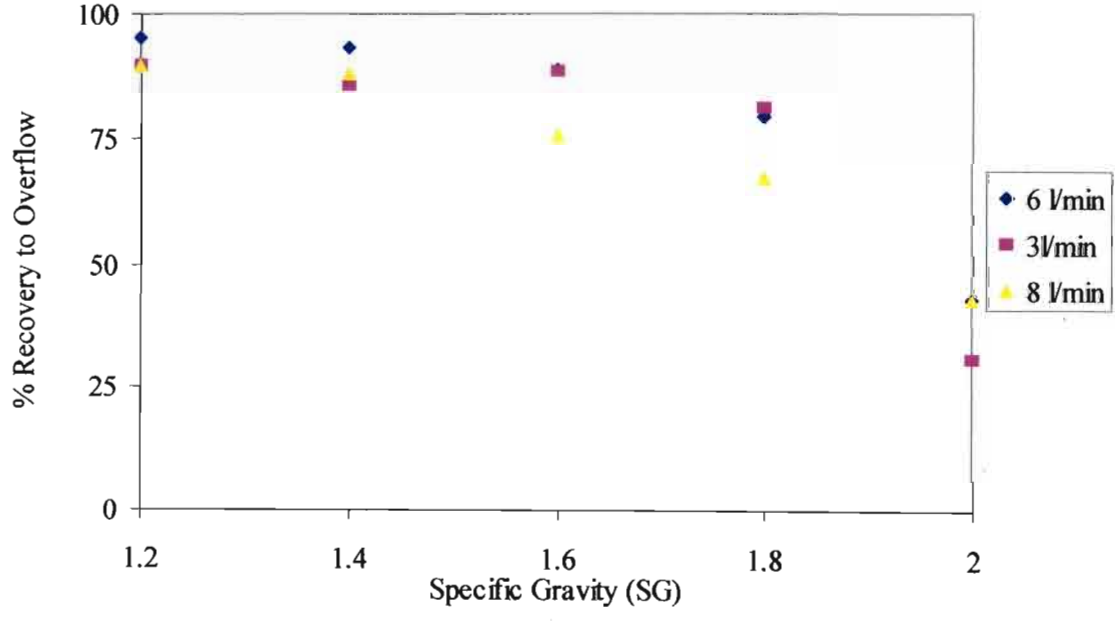

Figure 5.28: Partition Curves for Plate 4

Plate 1, 2 and 3 were designed based on the comparison of the maximum, minimum and intermediate aperture size. The square arrangement of Plate 1 was compared to the circular aperture arrangement of Plates 2 and 3. The pressure-drop and velocity relationship was considered uniformly throughout the plate. The design of plates 4 to 7 were geared towards the reduction of the dead zones and wall effects, by modifying the pressure-drop profile. The pressure drop was related to the hole density and percentage open area of the plate. In Plate 4, 10mm diameter holes were drilled on the outer portion of the plate and 20mm diameter holes were drilled in a circular arrangement towards the centre. The profiles shown in Figures 5.22 and 5.23 at 6 l/min are similar to the Plate 2 profiles. There is a significant reduction in the turbulence near the plate in the range of 0.001 to 0.007 m/s. The flow conditions near the plate are laminar, therefore the diffusion effects has been reduced. The variation in velocity magnitude for Run 1 was 0.0032 m/s compared with the set point value of 0.0088 m/s, a percentage change of approximately 63.8%.

The velocity magnitude is more accurate at 3 l/min. The average velocity magnitude is approximately 0.004 m/s, which is almost identical to the set point velocity of 0.0042 m/s. This is expected since as the flow rate decreases, the pressure resistance on the plate also decreases.

At the high flow rate of Run 3 – 8 l/min, Plate 4 experienced a high teeter-water velocity. Due to the high pressure-drop effect and hole density, a velocity reduction of 64.4% was noted. A velocity reduction was expected at the centre of the plate and a velocity increase was expected on the boundary sections due to the smaller aperture size. The flow profile in Figure 5.26 was even, however the velocity fluctuations did not make it a feasible option.

The partition curves in Figure 5.28 showed Ep values of 0.14, 0.12 and 0.29 respectively with D_{50} values of 1.96, 1.96 and 1.98 for each TBS run. The error separation is lower than Plate 3 however; the effective separation density remains higher. The recovery of the 2.0 SG particles has decreased. This shows some agreement with the Fluent simulations suggesting that at 6 and 8 l/min, the plate experiences a high pressure resistance and the recovery of the high density material decreases. At 3 l/min it experiences a very low resistance resulting in a better partition curve for that run.

5.6. Results from Plate 5

Figure 5.29: Velocity Vector Profile for Plate 5 – 6 l/min

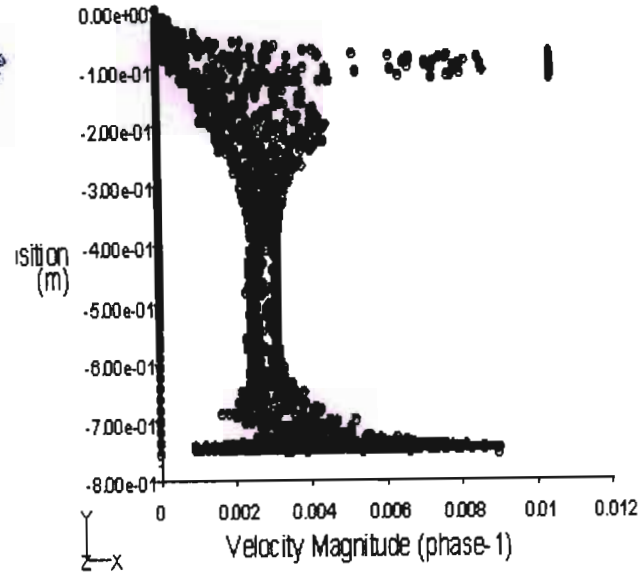

Figure 5.30: Axial Velocity Profile for Plate 5 – 6 l/min

Figure 5.31: Velocity Vector Profile for Plate 5 – 3 l/min

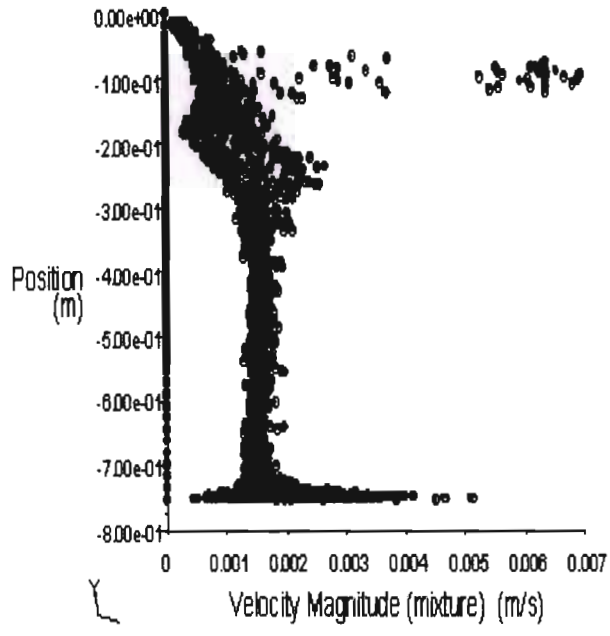

Figure 5.32: Axial Velocity Profile for Plate 5 – 3 l/min

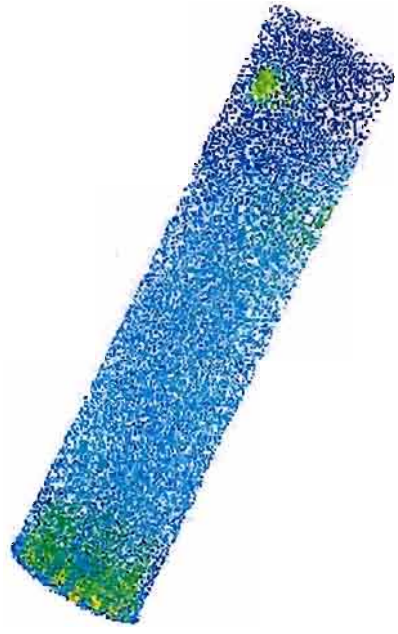

Figure 5.33: Velocity Vector Profile for Plate 5 – 8 l/min

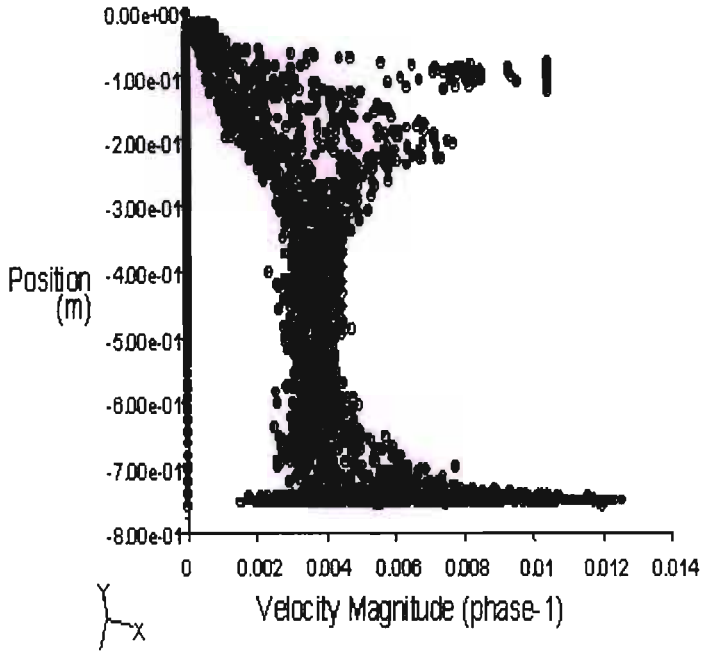

Figure 5.34: Axial Velocity Profile for Plate 5 – 8 l/min

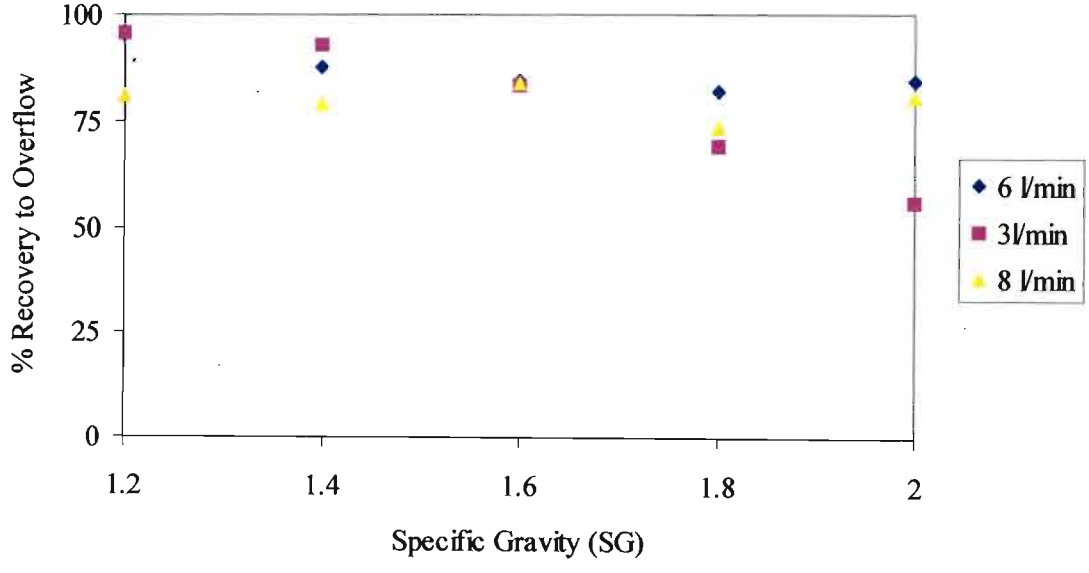

Figure 5.35: Partition Curves for Plate 5

Plate 5 was designed with the large 20mm apertures on the outer portion of the plate and with the 10mm apertures on the inner section. This would result in lower velocities on the outer section and higher velocities at the centre of the unit during high flow rates. The design was based on the reduction of the column wall effects and creating interstitial passages through the bed for large high-density transport. The simulations did not converge using the Eulerian model; therefore the Mixture model was used to obtain these profiles.

It is clearly visible from the simulated results that the dead zones have been reduced, however there is a 65.5% velocity reduction. This could be as result of the distributor plate pressure drop or due to the increased feed disturbances noted in Figure 5.30, since the plate had a large fractional open area of 0.44. Unlike with Plate 4, it is noted with Figures 5.31, instead of it resulting in a higher velocities at the centre, it caused an increased resistance of 66.5%. The velocity magnitude range for Run 3 near the plate is 0.002 – 0.013 m/s. The disturbances at the high flow rate existed near the upper section of the column near the feed, and in the distributor region, however the flow profile is steady throughout the bed section. The yellow vectors present near the plate indicate the high flow circulation patterns and disturbances in that region.

Plates 4 and 5 had been designed very similarly. The only difference was the arrangement of the apertures between the inner and outer sections of the plates. Both the simulations and the experimental runs indicate that Plate 4 would be a better option between the two. The Ep and D_{50} values are significantly lower for the Plate 4 configuration. The Ep values for Plate 5 from Figure 5.35 are 0.24, 0.32 and 0.28 respectively and the D_{50} values are 2.16, 2.04 and 2.24 respectively. Plate 5 operated inefficiently at low velocities since the particle movements were restricted. This creates a more packed bed, thus resulting in a higher cut.

5.7. Results from Plate 6

Figure 5.36: Velocity Vector Profile for Plate 6 – 6 l/min

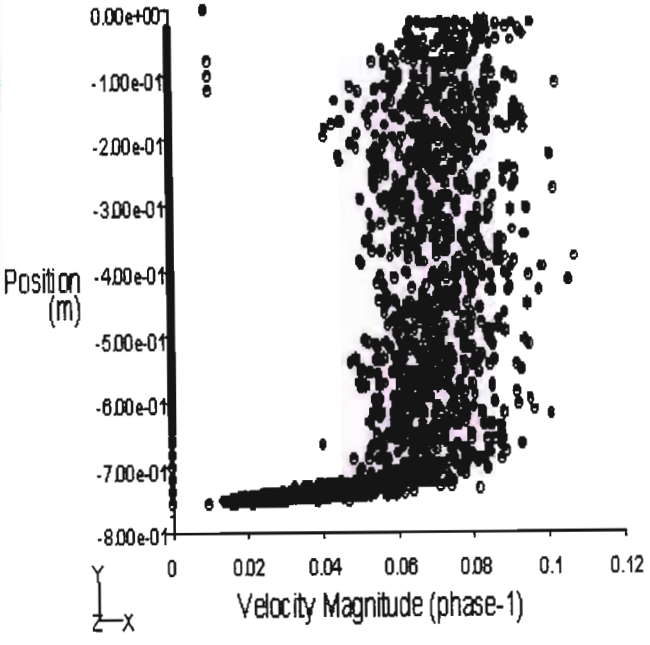

Figure 5.37: Axial Velocity Profile for Plate 6 – 6 l/min

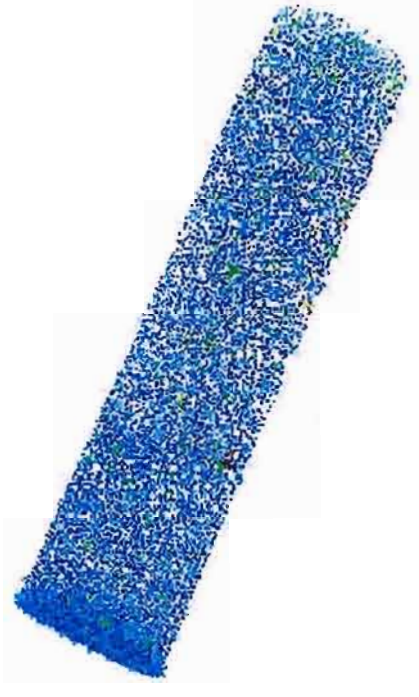

Figure 5.38: Velocity Vector Profile for Plate 6 – 3 l/min

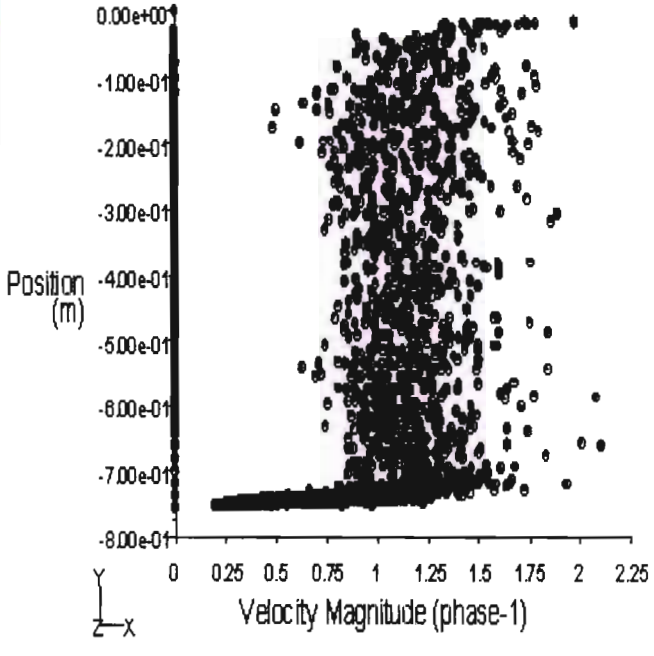

Figure 5.39: Axial Velocity Profile for Plate 6 – 3 l/min

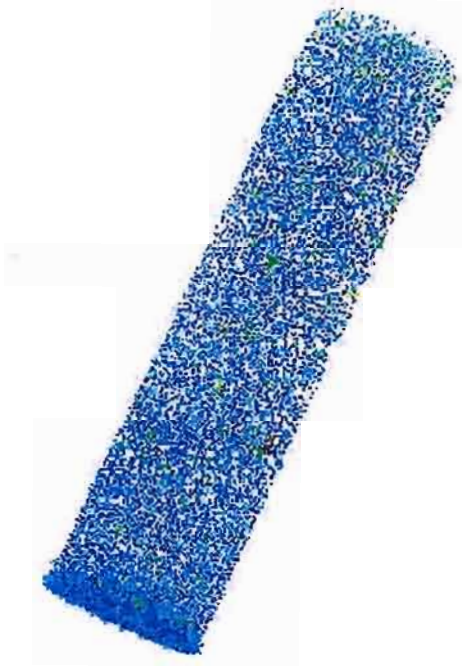

Figure 5.40: Velocity Vector Profile for Plate 6 – 8 l/min

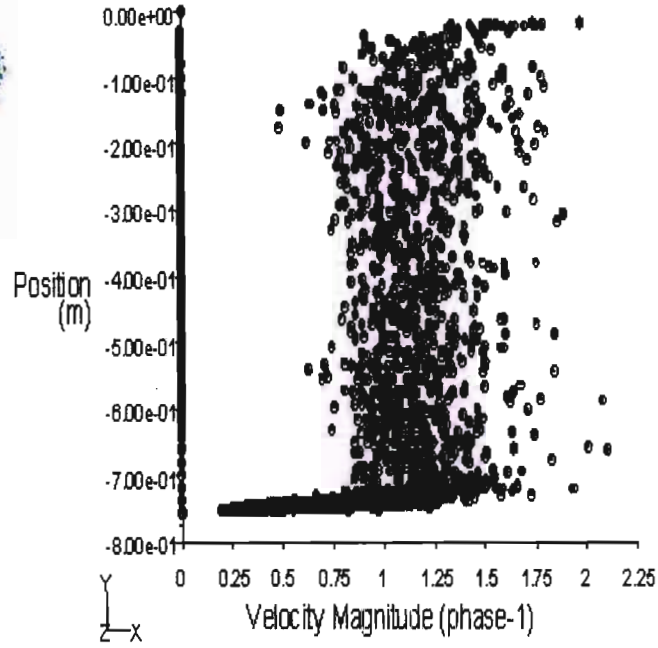

Figure 5.41: Axial Velocity Profile for Plate 6 – 8 l/min

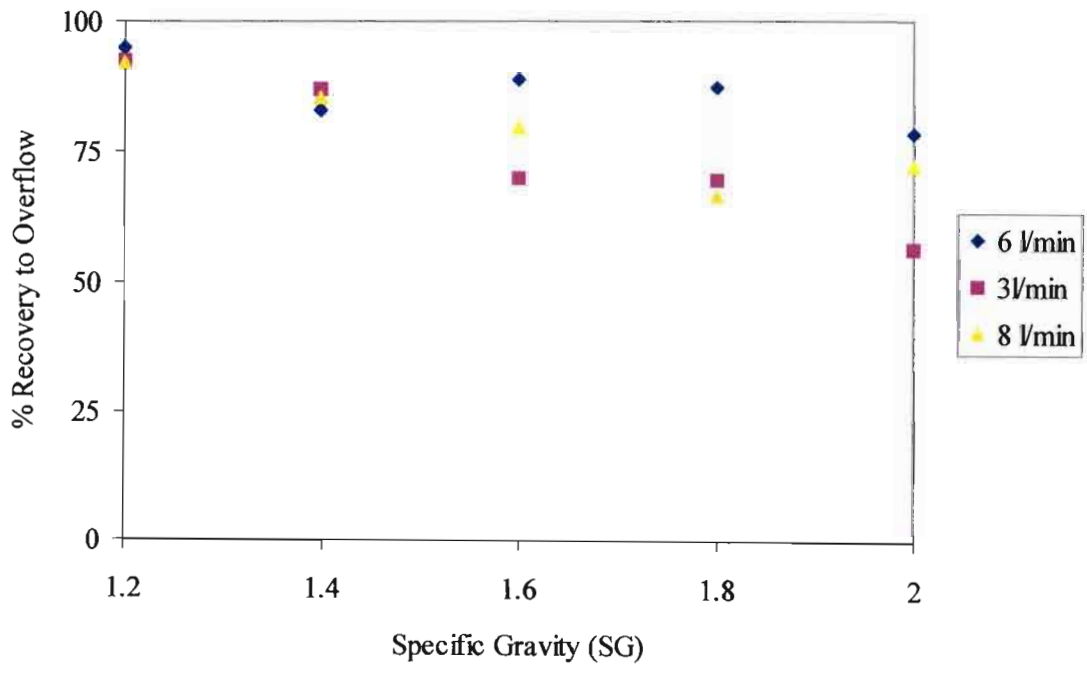

Figure 5.42: Partition Curves for Plate 6

Plate 6 investigated the use of 10mm outer apertures and 5mm inner apertures. The results indicate the presence of extreme wall effects and turbulent mixing. In Figure 5.36, several yellow coloured velocity vectors are present throughout the column. The axial velocity profile has a scattered pattern with the velocity magnitude range between 0.06 – 0.08 m/s, which is excessively higher than the set point of 0.0098 m/s for Run 1.

Figure 5.39 and 5.41 indicate turbulence throughout the TBS column although the velocity set point was specified in the intermediate flow regime. The profiles are all scattered with wall effects and turbulent circulative patterns. This plate is definitely unfavourable since it results in a high degree of disturbances.

The cut point densities of Plate 6 are noticeably higher than Plate 5. This is due to the reduction of the aperture size resulting in a higher velocity at the centre of the plate, thus increasing the recovery of high-density material. Plate 6 has extremely turbulent circulation patterns and eddies. This is due to the velocity jets created by the 5mm apertures. The Ep values are 0.33, 0.34 and 0.39 respectively for each run. The D_{50} values are 2.2, 2.08 and 2.28 respectively. The velocity created through the apertures causes disturbances throughout the bed resulting in excessive wall and column effects. The partition curves and the Fluent simulations justifies the poor hydrodynamic qualities of Plate 6.

5.8. Results from Plate 7

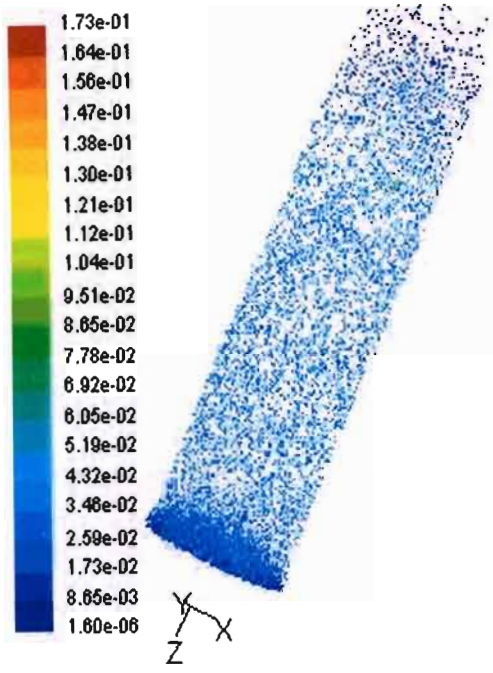

Figure 5.43: Velocity Vector Profile for Plate 7 – 6 l/min

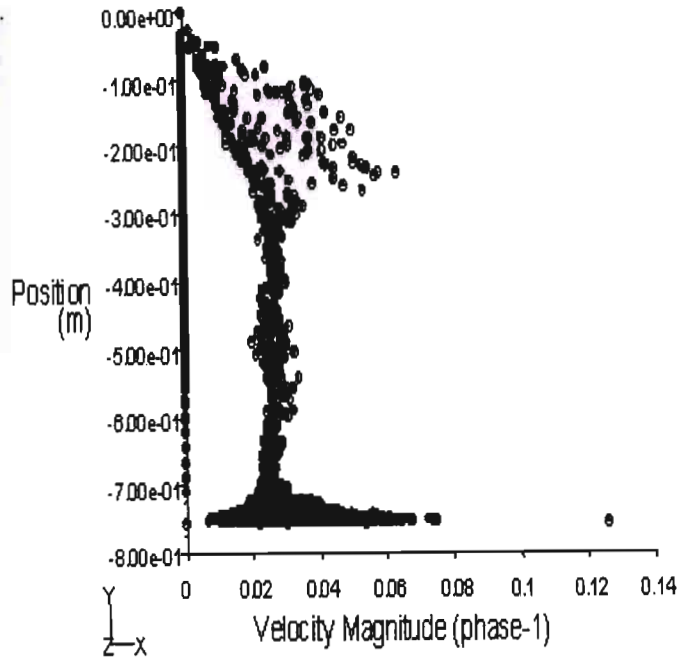

Figure 5.44: Axial Velocity Profile for Plate 7 – 6 l/min

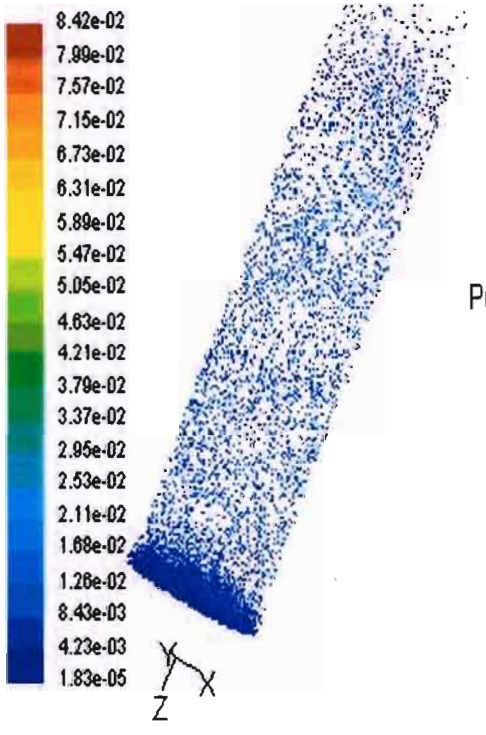

Figure 5.45: Velocity Vector Profile for Plate 7 – 3 l/min

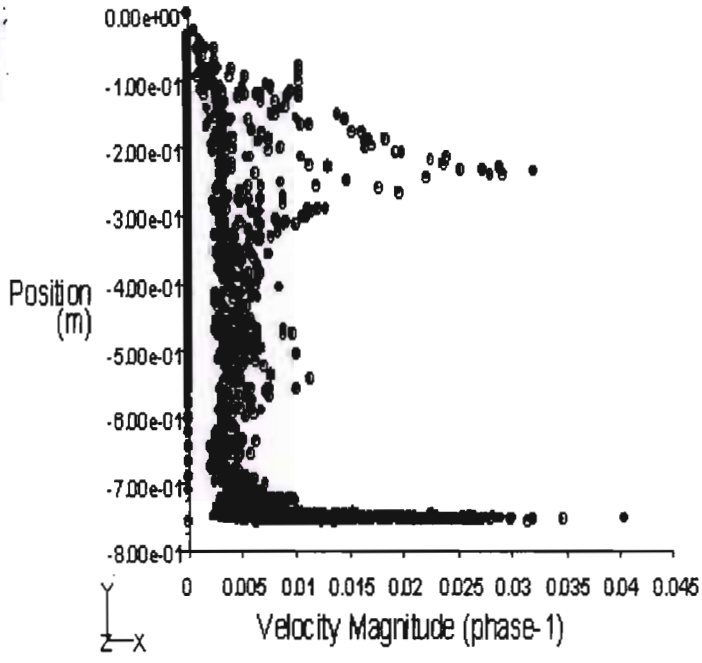

Figure 5.46: Axial Velocity Profile for Plate 7 – 3 l/min

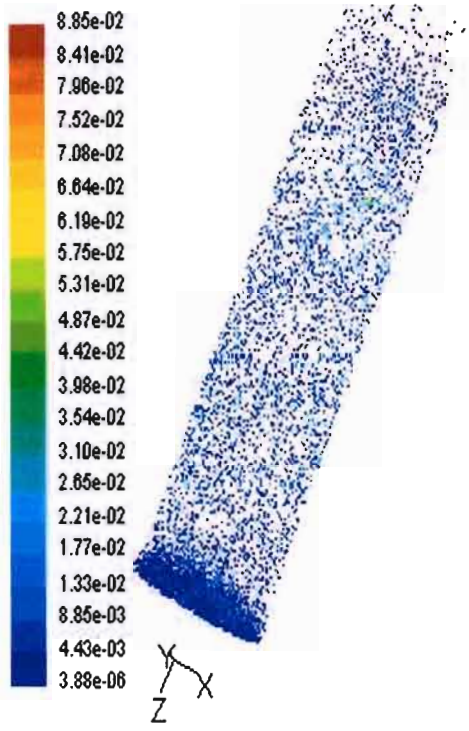

Figure 5.47: Velocity Vector Profile for Plate 7 – 8 l/min

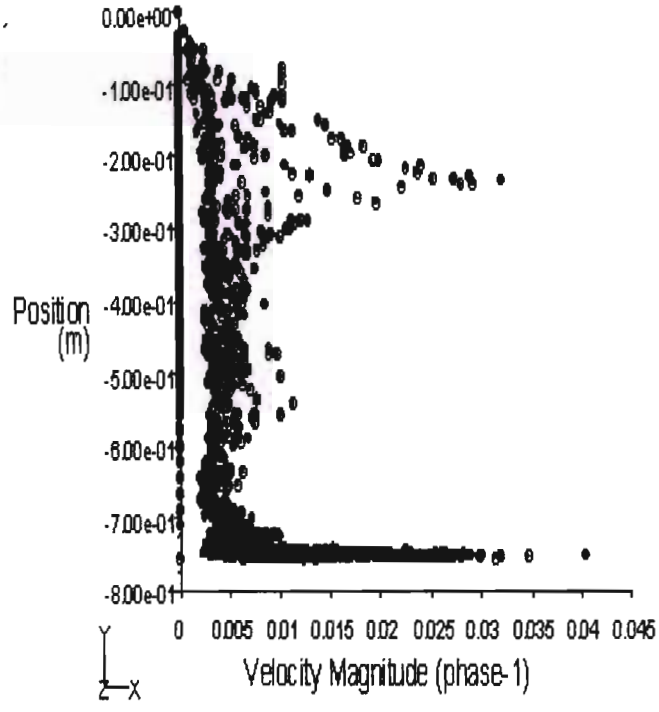

Figure 5.48: Axial Velocity Profile for Plate 7 – 8 l/min

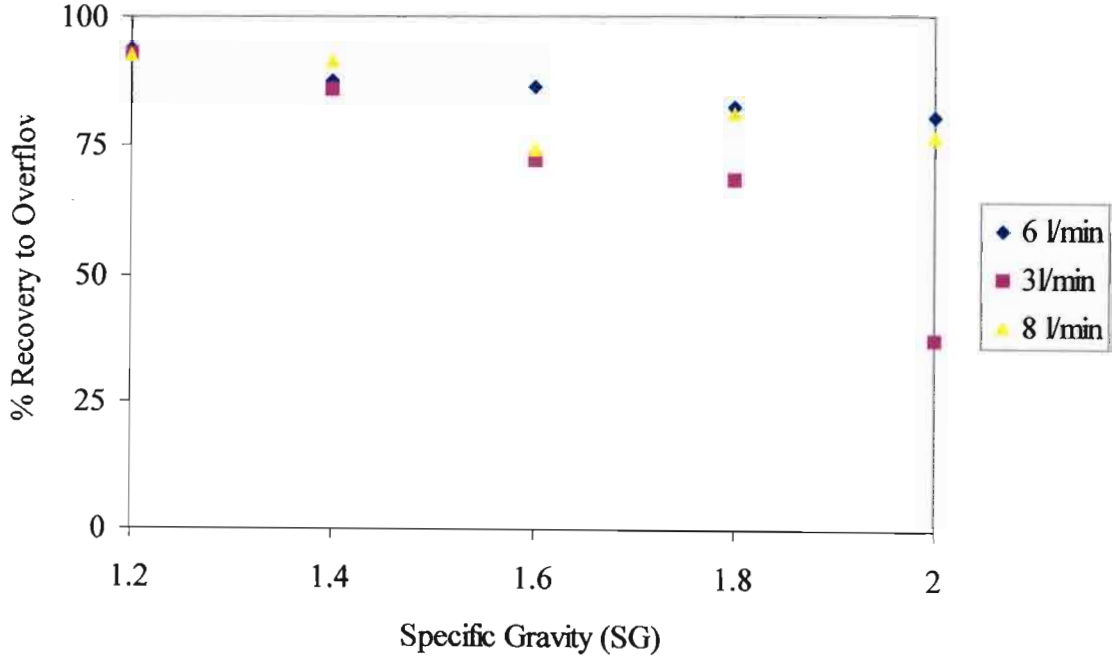

Figure 5.49: Partition Curves for Plate 7

The aperture configuration in Plate 7 was alternated with 5mm and 10mm diameters in order to observe the variation of the Plate 6 design. Figures 5.43 and 5.44 show the profiles at 6 l/min. The velocity through the column is stable, however a low pressure-drop is noted with an average velocity magnitude of 0.02 m/s. Similar results are noted for the profiles at 3 l/min. The teeter-water velocity through the plate is 0.0063 m/s. This is within the velocity magnitude range of 0.0005-0.01m/s. The distributor region experiences turbulence for all three runs thus the coal particles would experience an increased mixing effect, which could affect density segregation through the column.

The Ep values for Plate 7 are 0.45, 0.26 and 0.35 respectively. The D_{50} values are 2.3, 1.86 and 2.28 respectively. Plate 7 is also not feasible for industrial use on the TBS. The aperture arrangement results in unstable velocity profiles. The alternate arrangement of large and small apertures creates the turbulent conditions. The plate would only perform well under low flow conditions since the high velocity jets at high teeter-water flow rates causes an uneven effect in the bed similar to Plates 5 and 6.

5.9. Partition Curve Comparisons

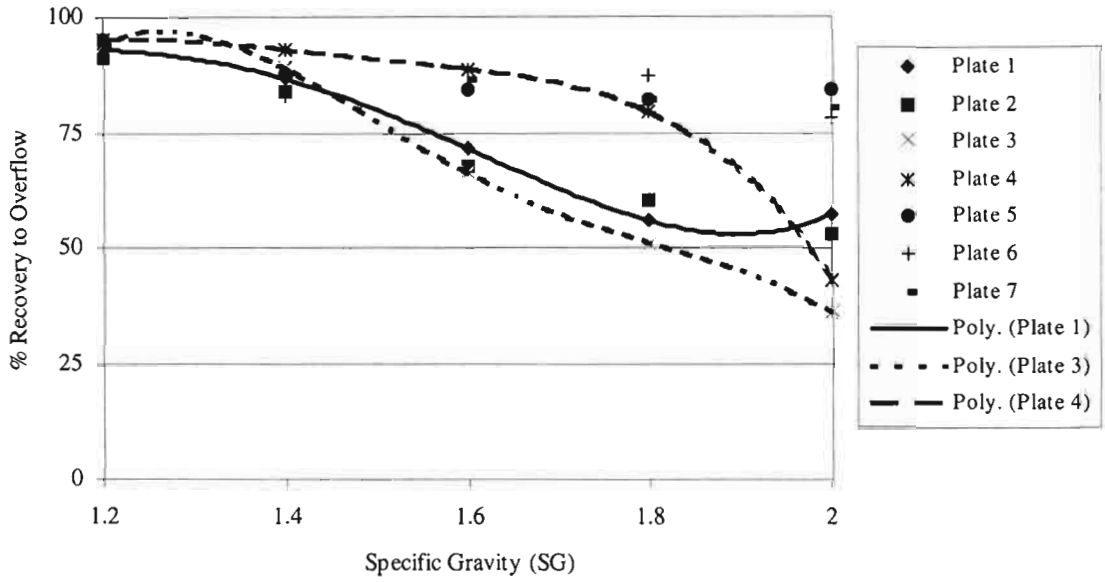

Figure 5.50: Partition Curve Comparison for each Distributor Plate – 6 l/min

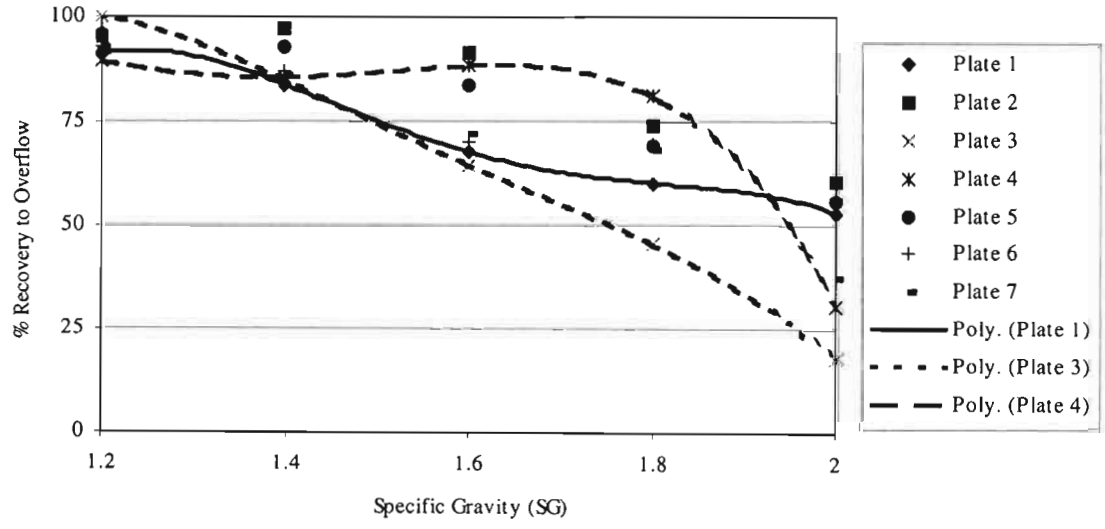

Figure 5.51: Partition Curve Comparison for each Distributor Plate – 3 l/min

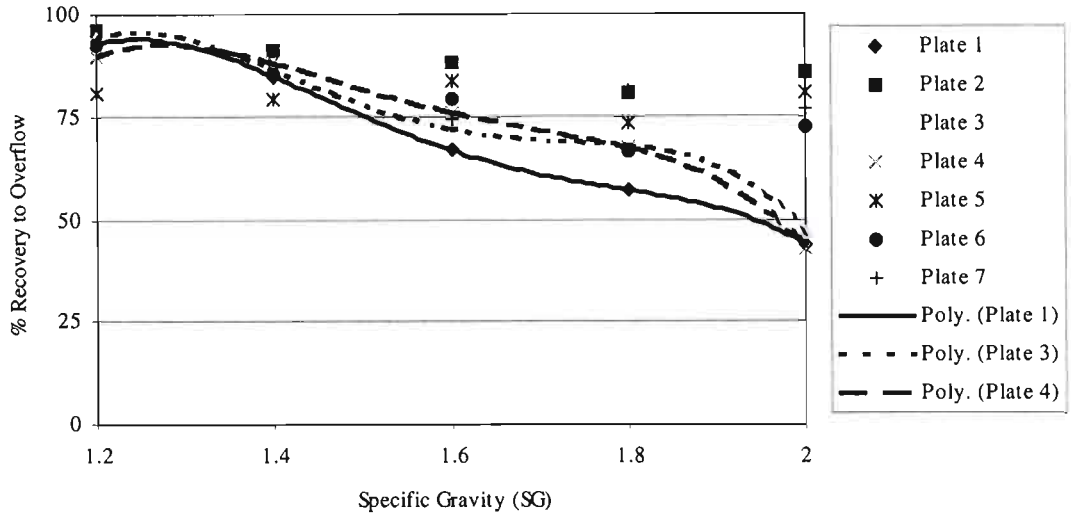

Figure 5.52: Partition Curve Comparison for each Distributor Plate – 8 l/min

The Partition curves were plotted on the same system of axes for each plate at the three set point flow rates in order to determine the best plate from the experimental work performed on the TBS. This is observed in Figure 5.50, 5.51 and 5.52 respectively. The simulated results were only presented for Plates 1, 3 and 4 since their profiles were most promising compared to Plates 2, 5, 6 and 7, which exhibited many turbulent regions and dead zones in the flow regime at the test conditions. All three profiles above suggest that Plates 1, 3 and 4 could be used on an industrial scale units, however from the Ep, D_{50} data and the careful interpretation of the Fluent simulations, it is concluded that at all three flow rates, Plate 3 has the best aperture and geometric configuration.

5.10. Pressure-Drop Comparisons

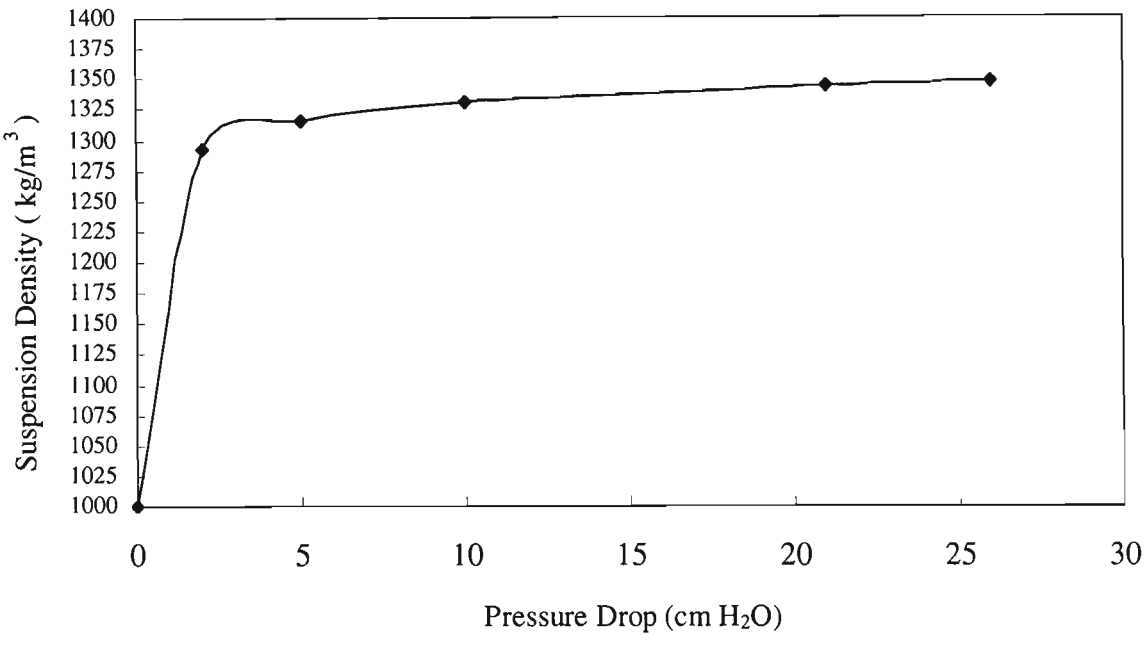

Figure 5.53: Pressure Drop vs Suspension Density in Teeter Bed

The pressure-drop was recorded across the teeter bed for each run. This was performed in order to determine the suspension density change with time. Fig 5.53 represented a typical profile of the density variation through the bed. An average bed density of 1350 kg/m^3 was used to calculate the particle slip velocities from Asif's model (1997) to make the theoretical comparisons with the Fluent simulations. Additional graphs for each run are contained in Appendix C.

5.11. Repeat Run Comparisons

All experimental runs were performed twice in order to confirm the validity of the results. From the comparisons of the repeat run plots in Appendix C, it is evident that the results are similar.

5.12. Tracer and Sink-Float Comparisons

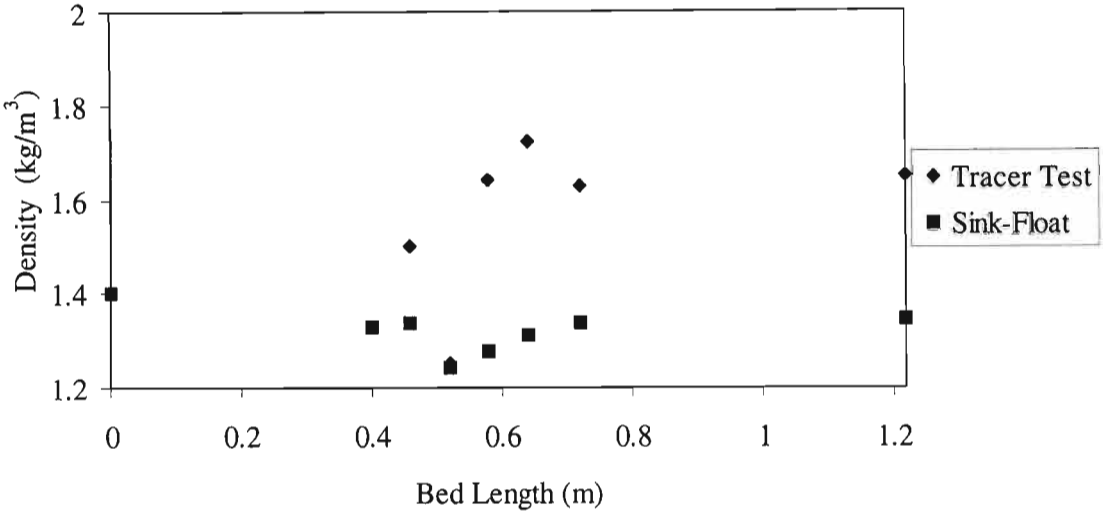

Figure 5.54: Comparison of Tracer & Sink-Float Profiles through the TBS

Two methods of density tests were performed in order to obtain the density profile through the bed. From Fig. 5.54 it is evident that tracer and sink-float results differed considerably. The sink-float method was used to plot the partition curves since the tracers tests are visibly inaccurate. The main factors which resulted in this inaccuracy of the tracer tests, were the tracer losses, the use of a limited amount of tracers and the cubic shape of the tracers did not describe the coal particle size, especially for the coarse size fraction.

5.13. Gidaspow and Syamlal O' Brien Model Comparisons

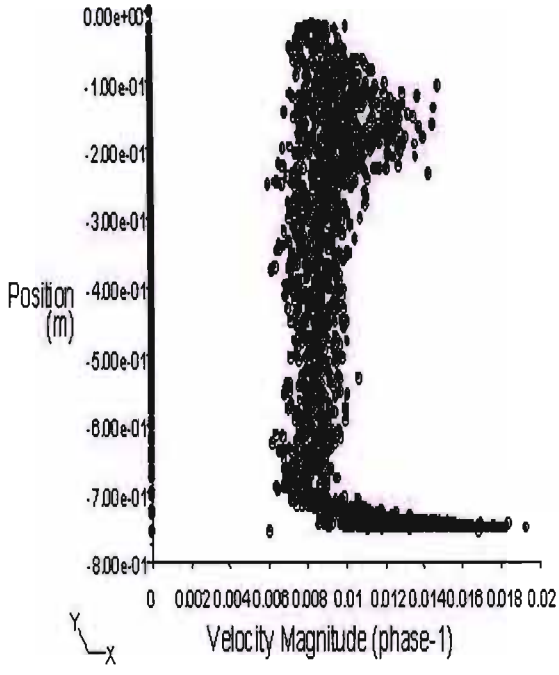

Figure 5.55: Axial Velocity Profile for Plate 3 – 3 l/min Syamlal O' Brien Model

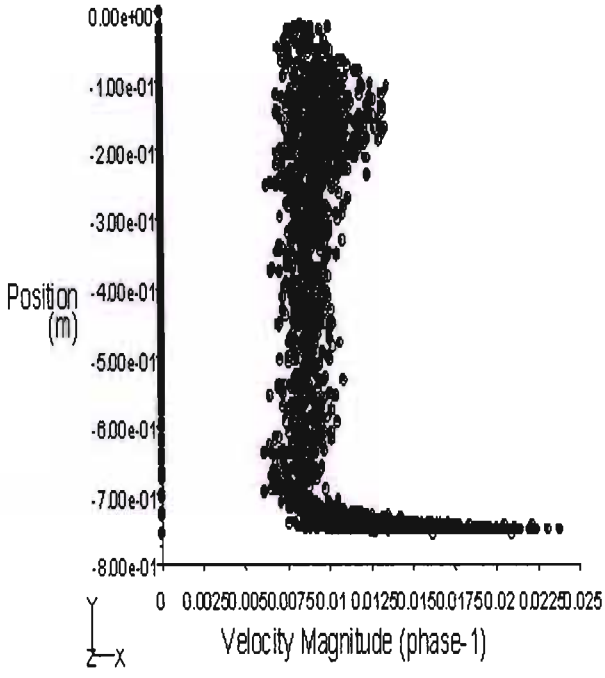

Figure 5.56: Axial Velocity Profile for Plate 3 – 3 l/min Gidaspow Model

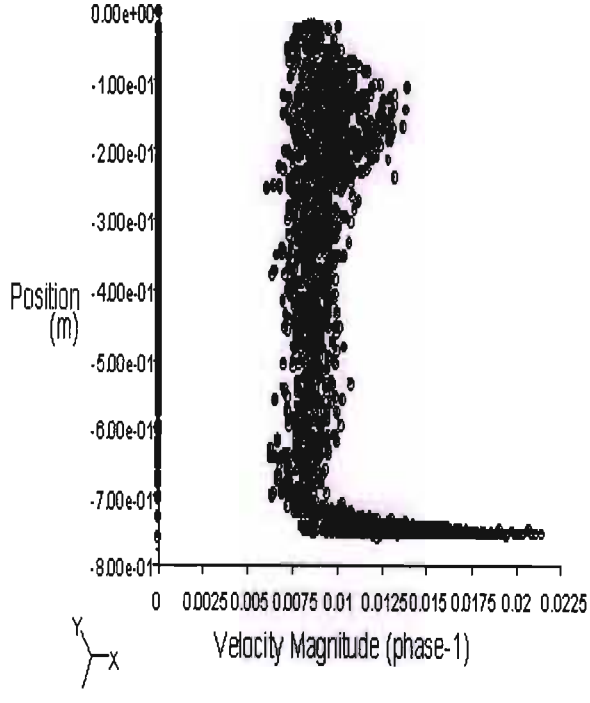

Figure 5.57: Axial Velocity Profile for Plate 3 – 6 l/min Syamlal O' Brien Model

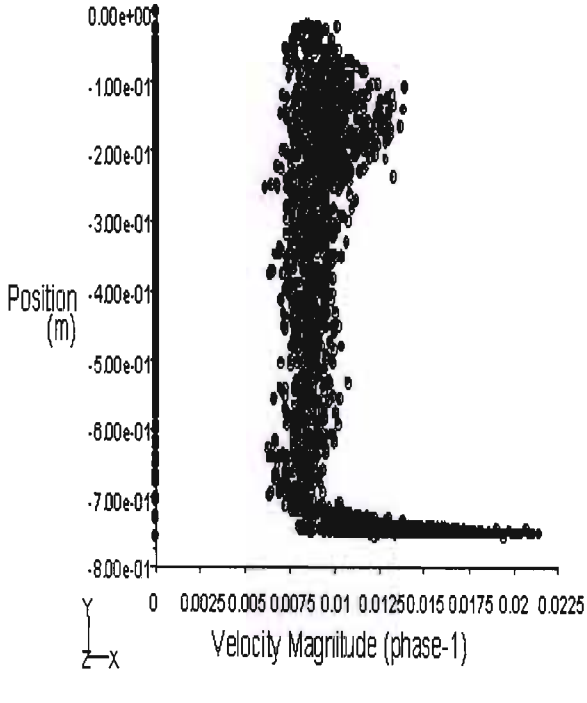

Figure 5.58: Axial Velocity Profile for Plate 3 – 6 l/min Gidaspow Model

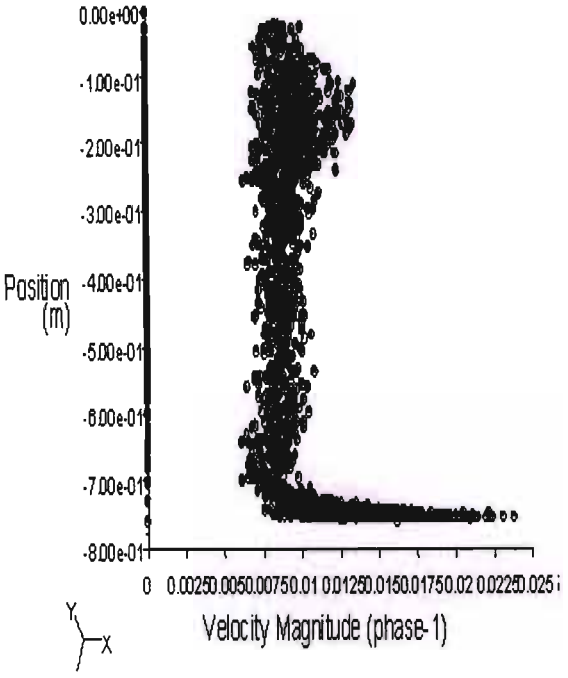

Figure 5.59: Axial Velocity Profile for Plate 3 – 8 l/min Syamlal O' Brien Model

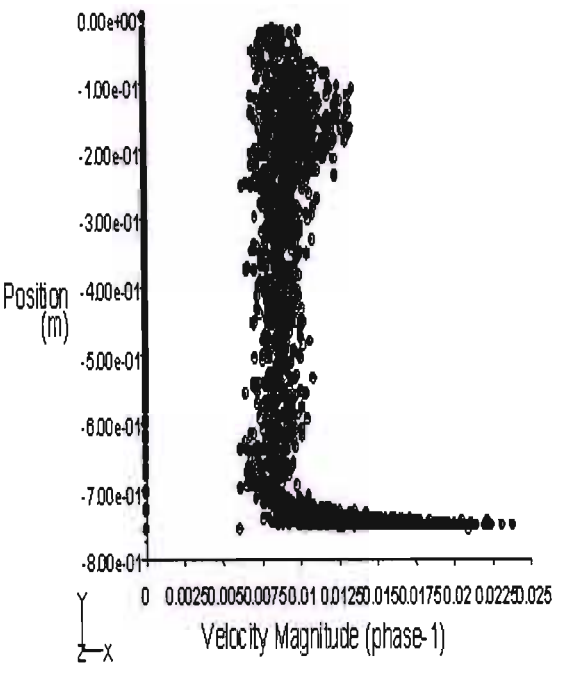

Figure 5.60: Axial Velocity Profile for Plate 3 – 8 l/min Gidaspow Model

Two drag coefficient models were tested in the Fluent simulations, the Gidaspow and Syamlal O' Brien Model. The Gidaspow model was recommended for dense fluidised bed systems. The Fluent User Manual specified that the Syamlal O' Brien model used a higher minimum liquid phase velocity when calculating the solid-liquid drag coefficient. Simulations were performed using both the models for Plate 3. The results indicate no significant change to the flow profiles of the axial velocity magnitudes. Figures 5.55, 5.57 and 5.59 were obtained using the Syamlal O' Brien Model. Figures 5.56, 5.58 and 5.60 for Plate 3 were simulated using the Gidaspow model. No differences are noted in the profile comparisons, therefore for this system, the choice of the drag law did not seem significant.

5.14. Eulerian Muliphase Profile Comparisons

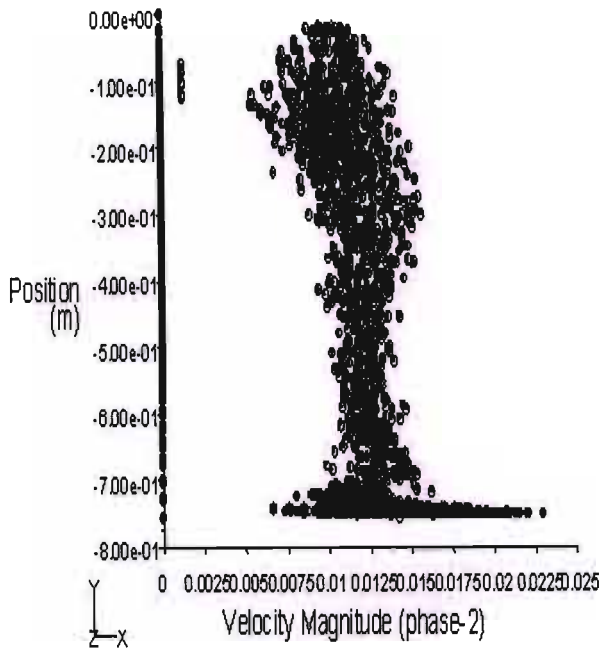

Figure 5.61: Axial Velocity Profile for Phase 2 – 1.2 SG

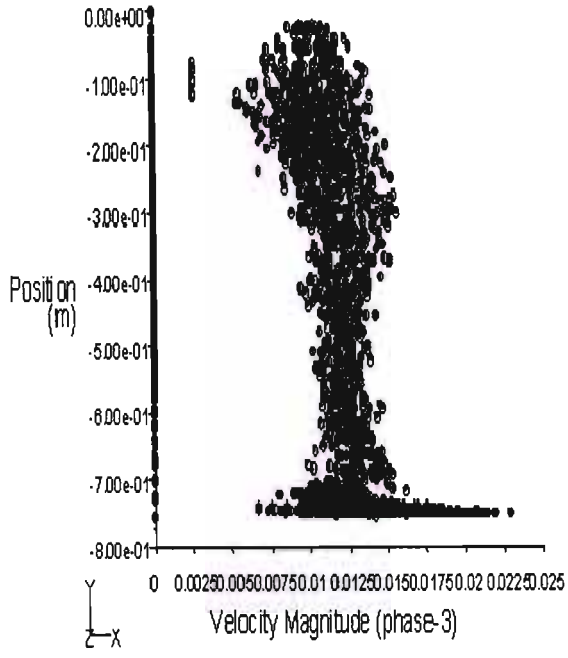

Figure 5.62: Axial Velocity Profile for Phase 3 – 1.4 SG

Particle Density (kg/m^3)	1400	1600	1800	2000
Particle Size (mm)	u_i (m/s)	u_i (m/s)	u_i (m/s)	u_i (m/s)
5.0	2.929E-02	1.035E-01	1.417E-01	1.649E-01
2.0	1.148E-02	4.799E-02	6.855E-02	8.139E-02
1.5	7.352E-03	3.474E-02	5.116E-02	6.165E-02
1.0	3.095E-03	1.954E-02	3.092E-02	3.858E-02
0.9	2.328E-03	1.633E-02	2.653E-02	3.352E-02
0.8	1.636E-03	1.313E-02	2.207E-02	2.835E-02
0.7	1.047E-03	1.003E-02	1.761E-02	2.311E-02
0.6	5.879E-04	7.124E-03	1.327E-02	1.790E-02
0.5	2.750E-04	4.570E-03	9.207E-03	1.290E-02
0.4	1.002E-04	2.538E-03	5.681E-03	8.375E-03
0.3	2.671E-05	1.158E-03	2.963E-03	4.658E-03
0.2	5.177E-06	4.063E-04	1.205E-03	2.036E-03
0.1	7.202E-07	8.891E-05	2.953E-04	5.266E-04
0.05	1.643E-07	2.241E-05	7.632E-05	1.377E-04

Table 5.3: Minimum Fluidisation Velocity (u_{mf}) as a function particle density

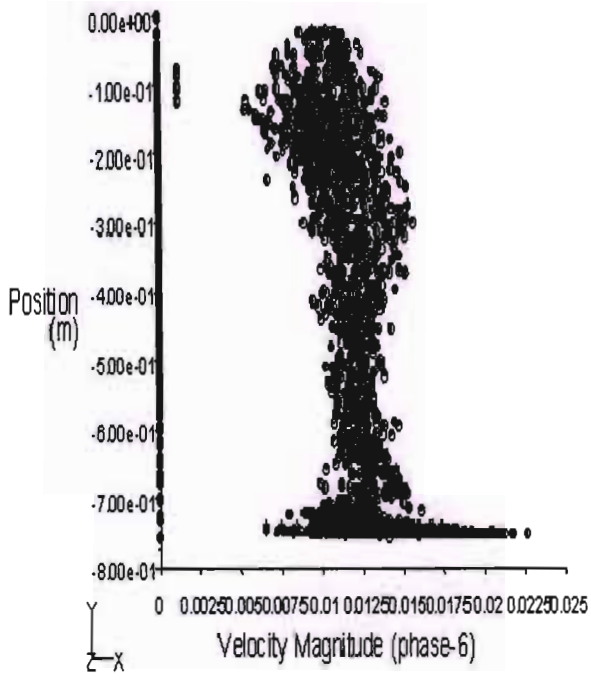

Figure 5.63: Axial Velocity Profile for Phase 6 – 2.0 SG

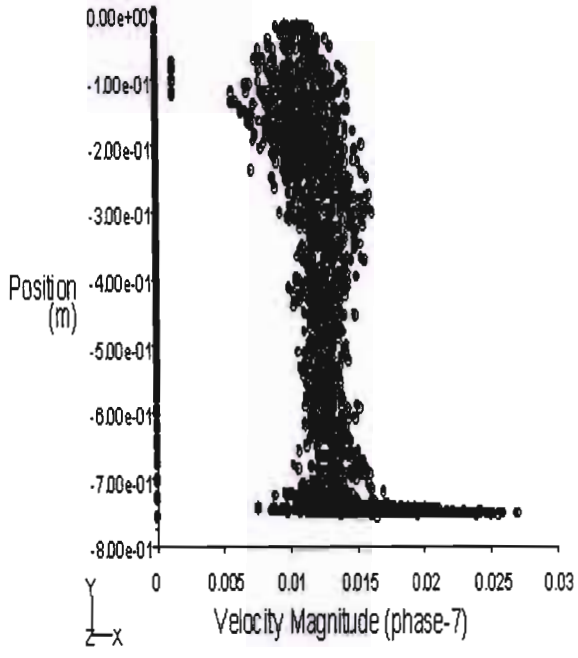

Figure 5.64: Axial Velocity Profile for Phase 7 – 1.2 SG

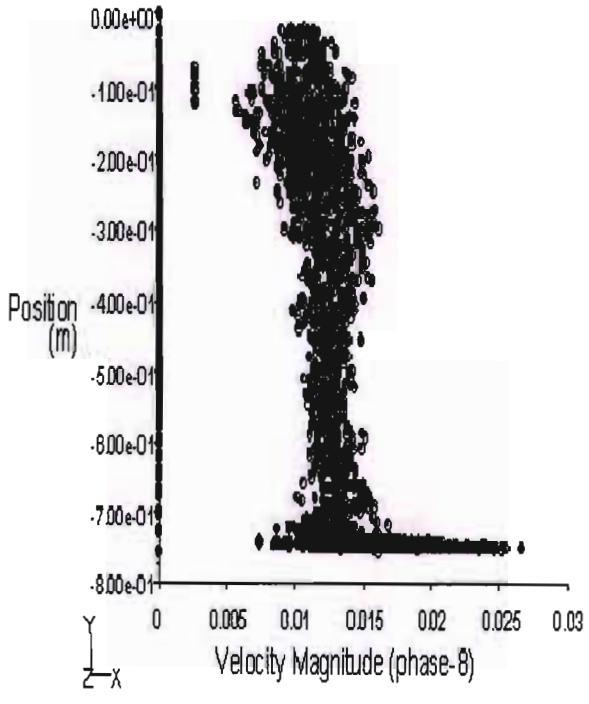

Figure 5.65: Axial Velocity Profile for Phase 8 – 1.4 SG

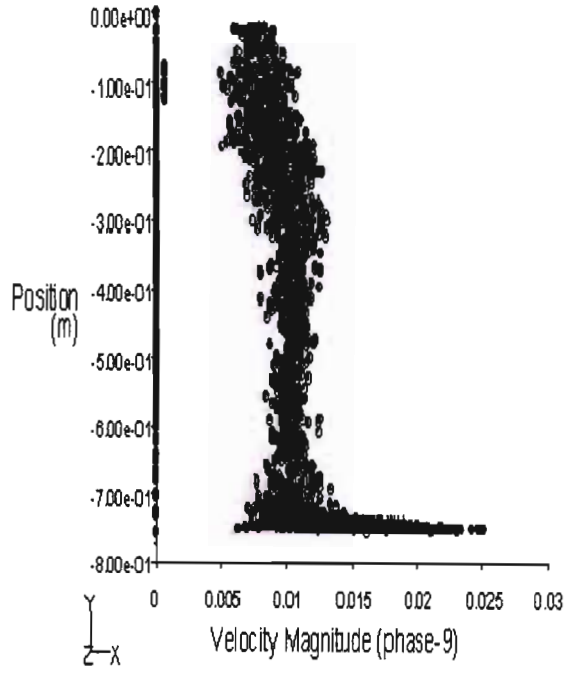

Figure 5.66: Axial Velocity Profile for Phase 9 – 1.6 SG

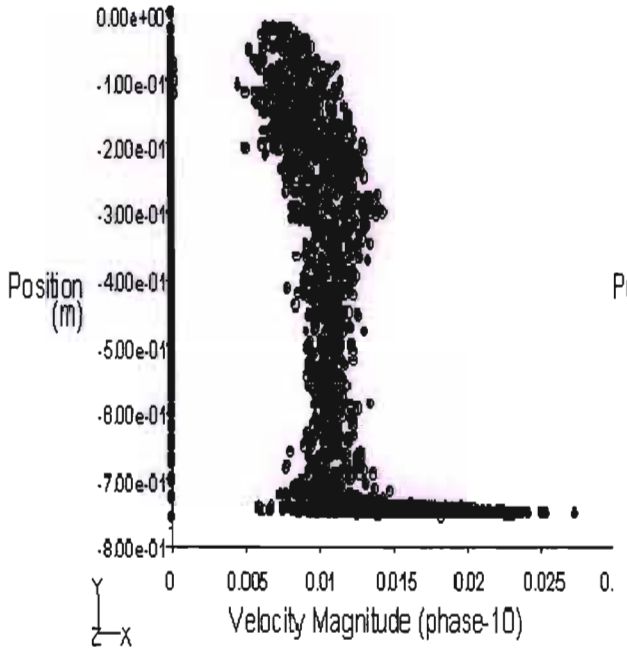

Figure 5.67: Axial Velocity Profile for Phase 10 – 1.8 SG

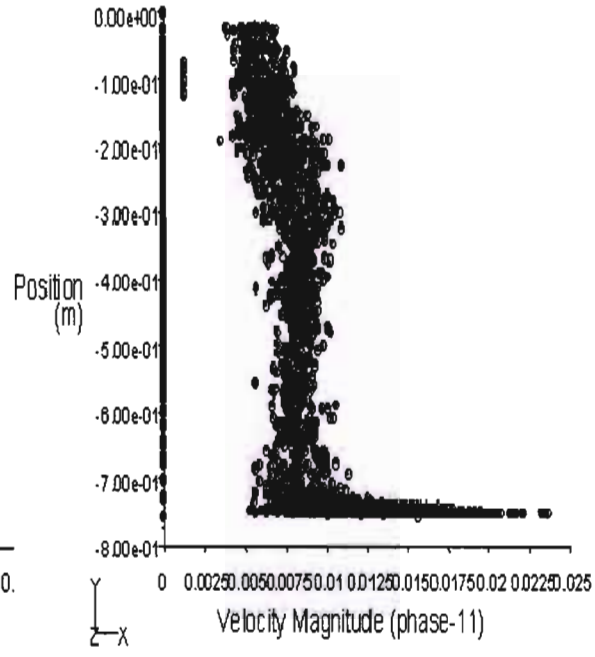

Figure 5.68: Axial Velocity Profile for Phase 11 – 2.0 SG

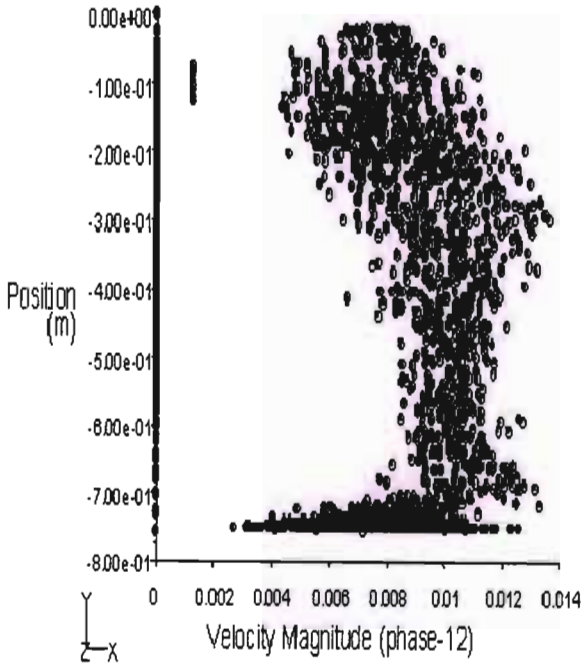

Figure 5.69: Axial Velocity Profile for Phase 12 – 1.2 SG

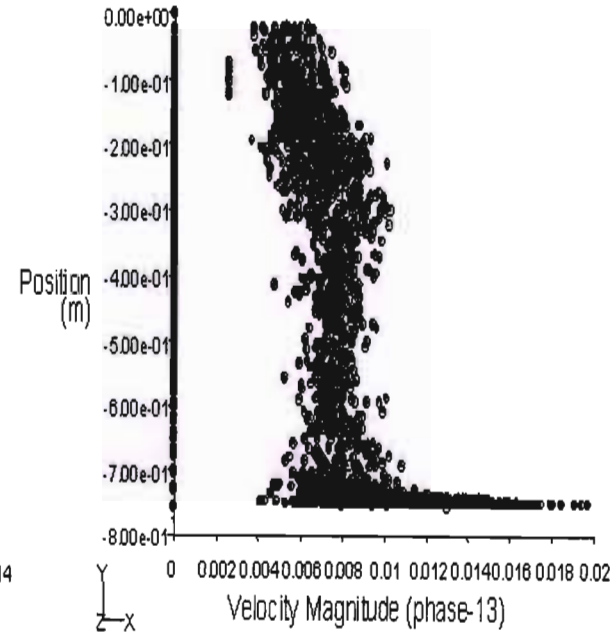

Figure 5.70: Axial Velocity Profile for Phase 13 – 1.4 SG

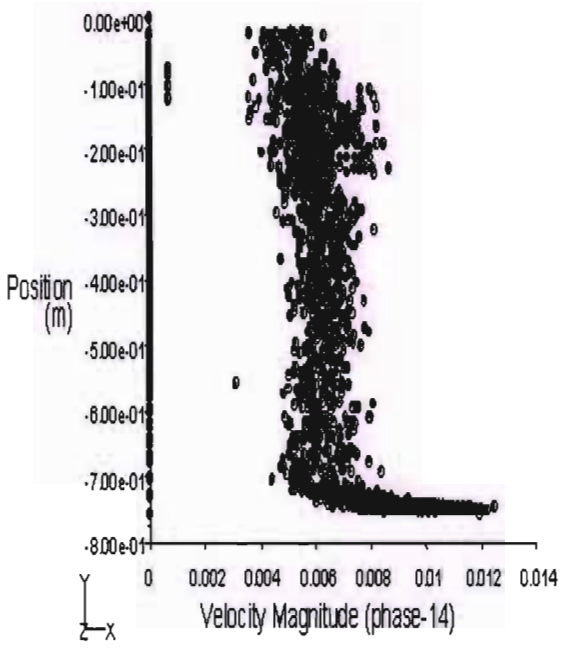

Figure 5.71: Axial Velocity Profile for Phase 14 – 1.6 SG

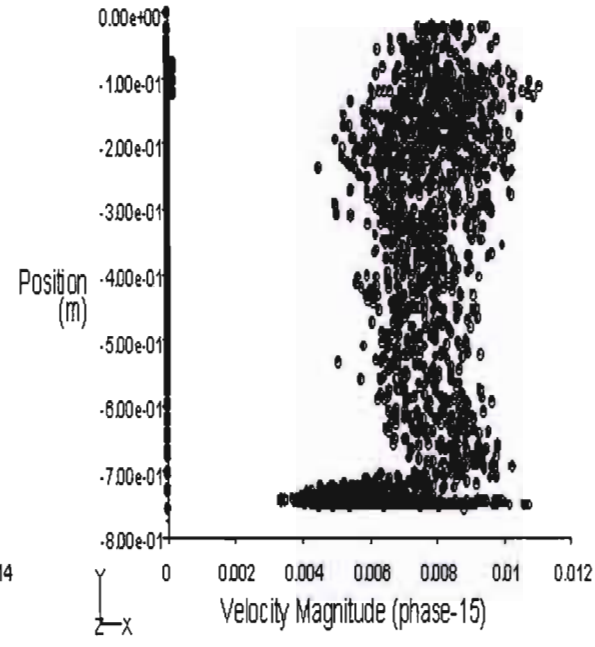

Figure 5.72: Axial Velocity Profile for Phase 15 – 1.8 SG

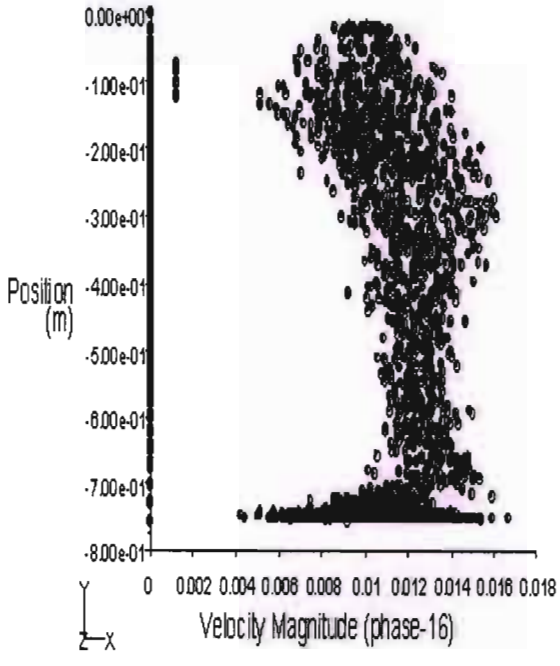

Figure 5.73: Axial Velocity Profile for Phase 16 – 2.0 SG

As explained in Chapter 4, 16 phases were considered in the simulations. The 15 solid phases were considered as three equal size fractions of 5, 2 and 0.8mm particles, each with a SG range of 1.2-2.0 in a 0.2 interval. Coal 1-5 was specified as the 5mm particles, Coal 6-11 was specified as the 2mm size fraction and Coal 12-16 was considered as the 0.8mm size fraction for Plates 2, 3, 4, 5 and 7. The opposite configuration was used in the specifications of Plate 1. The significance of the size fractions and density fractions are observed when interpreting the phase velocity profiles represented below and in Appendix C.

The Mixture Model is not as useful as the Eulerian Model since it only predicted the liquid phase velocity and the mixture velocity profile. The secondary phase profiles are significant as they reflected the particles behaviour and velocity profiles within the column. Since the Eulerian Model only converged for Plates 1, 3 and 4, only those secondary phase profiles were available for the discussion. Due to volume of profiles generated ie. 15 secondary phase profiles per run, with 3 runs per plate, 135 profiles were obtained from the simulations of these three plates.

The discussion is based on the particle behaviour in Plate 3 at 6 l/min since this plate is observed to have the best hydrodynamic conditions, observed from the liquid phase velocity vectors and axial velocity magnitudes. The additional graphs have been placed in Appendix C for observation.

Phases 7 to 11 (Fig 5.64-5.68) represent the 2mm particles of an increasing SG of 1.2 to 2.0. These profiles show a slightly higher range indicating the effect of the settling velocity variation with particle size, with the smaller particles having lower settling rates. It is evident that the velocity magnitude phase range is due to the particle settling velocities and the effect of the upward water flow. This indicates the importance of the distributor plates and their hydrodynamic profiles to the particle interactions in the bed. The 5mm particle profiles have higher settling velocities thus reducing the overall velocity magnitude seen in Figures 5.59 to 5.63. From Figures 5.64 to 5.68, the velocity range is between 0.01 and 0.015 m/s.

Figures 5.69 to 5.73 represent the profiles of the 0.8mm particles. The theoretical settling range is between 0.0016 and 0.028 m/s. The velocity magnitude range from the simulations, indicate that the average range lies between 0.006 and 0.01 m/s. This agrees with the theoretical range when one considers the effect of the 0.012 m/s upward flow. The secondary phase profiles provide a detailed illustration of the individual particle flow profiles and this is significant when describing the particle segregation in the bed. Plate 4 profiles in Appendix C displays the effect of particle segregation more clearly than the current profiles.

CHAPTER 6: FURTHER DISCUSSION

6.1. Fluent Simulations and Profiles

The Fluent simulations were useful in attaining the hydrodynamic flow profiles through the TBS column for the seven distributor configurations considered. The simulation specifications were based on the proportion of the tracer particles in the feed material. The teeter-water and feed water flows were based on the experimental work conducted. The Eulerian Multiphase model was useful in obtaining the individual phase velocities of the particles settling through the column.

The axial velocity vectors and velocity magnitude through the unit proved significant in the assessment of the teeter bed hydrodynamics. The comparisons of these profiles indicated that the hole density and percentage open area of the plate were the most important variables in the distributor plate design. The colourful vector contours illustrated the dead zones, the wall effects and the velocity variations around specific regions and served as a visual method to assess hydrodynamics, rather than assessing the actual mathematical modelling achieved by the segregated solver. Plates 3 and 4 had the most stable distributor regions from these comparisons. Plate 6 experienced a large amount of turbulence near the distributor region, due to the choice of smaller apertures at the centre of the plate, which created high velocity jets evident from the random vector arrangements.

The plots of the axial velocity magnitudes were most significant. They served two purposes. It provided a detailed view of the flow profile through the column, the disturbances at the feed and the distributor zone. It also illustrated the velocity range, which was a useful comparison with the theoretical data. In general, it was noted that Plate 3 had the most stable flow throughout the column. The velocity vector and axial velocity magnitude profiles were even, stable and steady with negligible feed disturbances and with minimal distributor pressure drop effects. In terms of diffusion and classification, Plate 3 provided ideal conditions for classification by density segregation and significantly reduced the mixing effect. It was generally noted the Plates 1, 3

and 4 had a lower hole density and thus performed more efficiently compared to the other plates in the simulations. Plate 3 had a percentage open area of 32.4% and a hole density of 0.413.

6.2. Tracer Tests

The tracer tests provided some evidence of the particle classification in the unit. The cubic tracers were not ideal for the investigation since the coal particles were irregularly sized, granular shaped particles. The cubic tracers were more representative in the lower size range as the finer particles were more cubic. The tracer results varied significantly due to the number of particles used. Although for every experiment conducted the tracer count was usually between 150 – 175 tracers, the ratio of tracer particles to coal particles was extremely low from a visual basis.

The Perspex windows were inserted in order to track the tracer movements and calculate the average settling rates, however due to the high concentration of coal, the dark colour in the column and the lack of a significant number of tracers, this was aborted. However, from various papers on plant efficiency tests, it was evident that tracers play a significant role and if a significant budget were available for tracers alone, due to high tracer costs, the tracer investigation would prove worthwhile.

From the comparisons of the tracer profiles and the sink-float bed profiles, it was evident that the tracer tests were invalid. The tracers indicated an average bed density above 1.6 SG whereas the sink float tests consistently indicated that it was below 1.4 SG.

6.3. Partition Curves

The D_{50} and Ep values were generally much higher for this investigation compared to the literature data available for the TBS, in regard to its separation capabilities. It must be noted that the project investigation considered the fine coal separation in a broad size and density range. Since the cut-point and Ep are a function of the particle size range, the larger the particle size range, the larger were these parameters. The determination of the best plate was still possible

since Plate 3 still displayed the lowest Ep and D_{50} compared to the other plate configurations. The partition curves were also useful in observing the importance of the particle slip velocities on separation. It was noted that the recovery of high-density material was more significant for higher flow rates. Tables 6.1 and 6.2 provide a summary of the Ep values and cut points (D_{50}) for each plate.

Flow (l/min)	1	2	3	4	5	6	7
3	0.37	0.26	0.25	0.115	0.32	0.34	0.26
6	0.45	0.225	0.19	0.135	0.24	0.33	0.45
8	0.53	0.35	0.29	0.29	0.28	0.39	0.35

Table 6.1: Summary of the Ep values for Plates 1-7

Flow (l/min)	1	2	3	4	5	6	7
3	1.92	2.08	1.74	1.96	2.04	2.08	1.86
6	1.98	2.32	1.9	1.96	2.16	2.16	2.3
8	2.06	2.15	1.96	1.96	1.98	2.24	2.28

Table 6.2: Summary of the D_{50} values for Plates 1-7

The TBS is capable of Ep's as low as 0.07 and cuts of 1.38 SG. The only possible explanation for the major variation in these parameters was the feed size range of –2mm + 0.038mm. This large size variation together with large density difference caused these inefficiencies. The lack of proper density control could have also been a factor. From the concentration criterion, the ratio of particle size for separation was 2:1, so the screening of the feed into small fraction would have improved separation, however this would be expensive and impractical for industrial purposes. Screening of the feed in this case would not have been beneficial to the hydrodynamic investigation that was performed on the TBS, since it was essential to note the effect of size and density of coal particles on the circulation patterns in the bed.

6.4. Comparisons

Various comparison graphs were plotted from the experimental work to determine the consistency of the results. The results from the comparisons of the repeat experimental TBS runs at all three teeter-water flow rates were very consistent. These profiles were all comparable at each flow rate so it could be concluded that any experimental error was not due to the operation of the unit, but rather on the specified feed quality required for this hydrodynamic investigation. The additional graphs for each repeat run were compiled in Appendix C since the general trend could be noted from just a single plot.

The pressure drop was recorded for each run during the experiments. Using the Ergun equation, the bed voidage was calculated using the Goal Seek Method in Microsoft Excel. The teeter-water velocity was used as the superficial velocity in this equation. The mean particle size was obtained from the Rosin-Rammler Average Particle Diameter in Chapter 4. The suspension densities were calculated and plotted against time to obtain the various profiles for each run. These profiles were all consistent with each other. The partition curves were plotted on the same system of axes. All three plots revealed that Plate 3 was the most efficient of the configurations designed.

6.5. Distributor Plates

The seven distributor configurations designed for the investigation provided a thorough investigation of the hydrodynamic behavoiur of the TBS. The plates were designed with a minimum thickness of 5mm, so the pressure drops across the apertures were negligible. A square and circular geometric arrangement was considered. When using large apertures the square arrangement created large dead zones in the corner sections of the plate, which resulted in dead zones throughout the bed. This was visible in the Plate 1 velocity vector profile.

The circular arrangement provides a more even flow pattern, which definitely reduced wall effects as long as the aperture size was consistent throughout the plate. The use of variable sized apertures on the inner section or towards the centre of the plates seemed to be an innovative idea, however the results were not satisfactory, since Plates 5, 6 and 7 had more turbulent

effects and circulative patterns. The reduction of the aperture size at the centre of these plates resulted in high velocity throughputs since the fractional open area of the plate was fairly constant for these plates resulting in a minimal pressure drop effect and just high velocity streams. The velocity vectors illustrated movement at 45° angles from the centre resulting in sideways mixing, thus increasing the radial distributions across the column and therefore resulting in enhanced wall effects. The Plate 4 configuration was beneficial. It had larger apertures towards the centre, with smaller apertures on the boundary. This was an effective method of reducing the dead zones and wall effects.

Plate 3 was based on the general showerhead design. The perforations were in a circular arrangement and the crux of the configuration was obtaining the correct open plate area and aperture diameter to promote even liquid flow with a minimum pressure drop effect. Literature on liquid distribution plates, were vague at most times regarding the actual plate design methodology. Using the little information available, together with practical ideas and innovative designs of other distribution mechanisms, the plate configurations were developed. All the different scenarios or worst case conditions were considered, and a proposed configuration was designed to remedy the different TBS problems such as the dead zones, turbulence, wall effects and pressure drop issues which have been explained in detail. From the investigations, Plate 3 was found to be the most successful when tested experimentally, however its industrial application will determine its true worth.

6.6. CFD in Industrial Application

The CFD package, Fluent 6.1 was a vital part of the investigation. The geometry of the unit could be intricately drawn to consider each aspect of the unit. The program was very user friendly with regard to specifications and boundary conditions. The information gathered on the hydrodynamics and fundamental particle interactions within the TBS was useful for optimization. The inputs for the model are very general since they only require the feed densities and the feed and teeter-water velocities. This makes the current model very useful since it can be used to predict the separation for several different ores using the TBS by just modifying the current inputs. The geometry can be altered quickly to observe if any modifications to the unit bring about improvements to the hydrodynamic behaviour.

The CFD work was not run concurrently with the experimental work. It was completed in advance and compared to the experimental findings. It would be even more useful when run concurrently, since a real time comparison would be available and new configurations and changes to other operating parameters may be tested to obtain optimum results.

In general, CFD is definitely a useful tool for industrial scale-up of units. It has been useful for most gravity concentration devices and for optimising hydrocyclones. It provided significant information on the effect of distributor configurations on the hydrodynamic behaviour of the TBS, in an attempt to improve the fine coal separation mechanism.

CHAPTER 7: CONCLUSION

The objective of the research work was to investigate the hydrodynamic behaviour and fundamental particle interactions in a TBS by testing various distributor plate configuration designs. The lab scale unit was successfully designed with seven distributor plate configurations considered. The investigations involved the use of the CFD package Fluent 6.1 to observe the flow patterns within the column.

The results obtained from the simulations indicated that Plate 3 had the best configuration. The Eulerian Multiphase model for granular solids was successful in determining the best distributor plate configuration based on the hydrodynamic flow pattern modelling. The simulations illustrated the comparisons of the plate velocity vectors and axial velocity profiles for the unit. The simulations revealed that Plate 3 had the most the stable flow pattern, with an even teeter-water flow profile throughout the column, minimum wall and turbulent effects and a low distributor pressure drop.

The experimental work was performed at three set point flow rates. Tracers were used to investigate the particle interactions within the unit. At the low flow rate of 3 l/min, it was evident that density segregation was favoured however the large high-density material tended to accumulate in the bed. The tracer bed profile was inaccurate compared to the sink-float bed profile due to an inadequate number of tracers.

Partition curves were plotted for all the runs. It resulted in high D_{50} and Ep values. This was due to the large size range (– 2mm + 0.038mm) of the feed material due to the project objective and due to the lack of density control. A large size range was used in order to investigate the particle and density interaction in the bed due to hindered settling and segregation.

Comparisons of the partition curves indicated that Plate 3 had the best D_{50} of 1.74 SG at 3 l/min, although Plate 4 had lower Ep values. Fine coal recovery was achieved below 0.1mm however this was not tested using a high mass fraction of fine material in the feed, which may have a greater effect on the suspension viscosity.

The CFD simulations and experimental work both confirmed that Plate 3 had the best distributor configuration. It had an open area of 32.4% and a hole density of 0.413. Plate 3 may be beneficial to an industrial scale unit based on the research conducted.

The simulations do not directly predict the improvements of the unit by computing new Ep and D_{50} values, lower than previous tests. They suggest the best conditions required for the operation of the unit, which would lead to these improved separation efficiencies and lower cut-point densities. The experimental work conformed that CFD simulations were accurate. The stable flow pattern and even upward teeter-water velocity profiles of Plate 3 suggest that the unit can be optimized to separate a broad size and density range of coal particles.

The capability of the unit as a fine coal separator can be extended to other ores and applications. The feed inputs in the Fluent model are the only governing parameters and can be modified to account for other material properties, densities, the particle size range and feed inputs and teeter-water velocities. The unit geometry and feed input velocities can be modified to observe the hydrodynamic behaviour within the TBS.

The CFD simulations were an extremely useful tool in this investigation and industry would benefit from implementing CFD on units when performing optimization tests to improve the efficiency. It would be a more cost effective approach of testing new modifications on these units using simulation packages before incurring the high fixed costs, which result during the implementation process. Design errors could also be reduced since simulations can be performed on large-scale geometry if higher computer processor speeds are available.

CHAPTER 8: RECOMMENDATIONS

The following recommendations were considered beneficial in improving the TBS operation:

- A PID controller with a calibrated density probe connected to the underflow exit valve would help to maintain the desired cut point density.

- A rotameter on the feed water tank would maintain a constant feed water flow rate. A PID controller on the teeter-water upward flow and on the feed water would also help maintain all the set points and would definitely improve the efficiency and cut point density.

- Methods such as Laser Doppler Velocimetry (LDV) and other optical methods could be used to determine the experimental particle velocities within the TBS in order to compare to theoretical data and the Fluent phase velocities. The current investigation was based on the partition curves and theoretical data only. A real time method obtaining the actual particle slip velocities in the TBS would provide a more detailed comparison with the multiphase simulated profiles at each set point flow rate and help to improve the simulation package even further.

- Screening of the feed material would improve the Ep and D_{50} values however may be impractical depending on the size fraction and cut point desired.

- The use of a large quantity of tracers would be more beneficial to the research. Magnetic tracers could be used and recovered using a magnetic separator. This could result in the use of fine tracers, which could be used with the feed to gain a better understanding of fundamental fine particle interactions with regard to segregation and classification.

- The shape of the tracers could be more irregular and granular rather than cubic. This would be more representative and tracer partition curve would be more reliable.

- The Fluent model for the TBS is a general model since it can be extended to other ores besides coal. The inputs can be easily adjusted to account for the different material conditions and flow conditions.

- The TBS grid geometry near the feed entry can be modified to account for baffle plate. This was present on the laboratory scale unit for the experimental work however it was not tested in the Fluent simulations. This comparison with the current profiles would determine if the baffle plate has a significant effect in reducing the feed water disturbances near the overflow.

- The simulations are useful at providing a visual description of the hydrodynamic behaviour allowing for the detection of turbulent zones, dead zones and wall effects to obtain the most stable flow patterns within the unit.

- CFD simulations can be used by industry for optimising various units and reducing undesired costs due to design errors and scale-up problems.

REFERENCES

Al-Dibouni M.R., and Garside, J., Particle Mixing and Classification in Liquid Fluidised Beds, Transactions of the Institution of Chemical Engineers, Vol 57, 1979, pp 94-103.

Asif, M., Kalogerakis, N., Behie, L.A., Distributor effects in Liquid Fluidized Beds of Low-Density Particles, American Institute of Chemical Engineers Journal, Vol.37, No.12, December 1991, pp 1825-1832.

Asif, M., Kalogerakis, N., Behie, L.A., Hydrodynamics of Liquid Fluidized Beds including the Distributor region., Chemical Engineering Science, Vol. 47, No 15/16, 1992, pp 4155-4166.

Asif, M., Modelling of Multi-Solid Liquid Fluidized Bed, Chemical Engineering Technology, Vol. 20, 1997, pp 485-490.

Barnea, E. and Mizrahi, J., A Generalised Approach to the Fluid Dynamics of Particulate Systems, Part 1, Chemical Engineering Journal, Vol. 5, 1973, pp.171-189.

Bird, R.B; Stewart, W.E; Lightfoot, E.N, Transport Phenomena, John Wiley & Sons, New York, 1960, pp. 56-61.

Brauer, H. and Thiele, H., Bewegung von Partikel-schwarmen, Chem.-Ing.-Tech., Vol 45, No.3, 1973, pp 909-912.

Carsky, M., Some Hydrodynamic Considerations for Design and Operation of Fluidized-Bed Units, Industrial Fluidization South Africa, 2002, pp.163-176.

Craddock, M. and Hand, P., Hydrosizer / TBS Separator, QVA Process Technologies (PTY) Ltd, 2002.

Couderc, J.P. and Angelino, H., Chim. Ind., Genie Chim, Vol. 103, pp.225, 1970.

Couderc, J.-P., Incipient Fluidization and Particulate Systems, Fluidization 2nd Edition, Institut du Gene Chimique, Chemin de la Loge, Toulouse, France, 1985.

Davidson, J.F., Clift, R. and Harrison, D., Fluidization 2nd Edition, Academic Press Inc. (London) Ltd, 1985.

DeVaney, F.D. and Shelton, S.M., Properties of suspension media for float-and-sink concentration, Report of Investigations 3469, U.S. Bureau of Mines, 1939.

Drummond, R., Nicol, S. and Swanson, A., Teetered bed separators – The Australian Experience. XIV International Coal Preparation Congress and Exhibition, South African Institute of Mining & Metallurgy, 2002.

Dutta, B.K., Bhattacharya, S., Chaudhury, S.K. and Barman, B., Mixing and Segregation in a liquid Fluidised Bed of Particles with different size and density. The Canadian Journal of Chemical Engineering, Vol. 66, August 1988, pp 676-680.

Ergun,S., Fluid Flow through packed Columns, Chem. Engng Prog. Vol.48, pp 89-94, 1952.

Eriez Manufacturing Co, Crossflow Separator, 2003 Eriez Magnetics, http://www.eriez.com.

Eriez Manufacturing Co, Hydrofloat Separator, 2003 Eriez Magnetics, http://www.eriez.com.

FLUENT 6.1 User's guide, Lebanon NH, Fluent Inc, (2003).

Foscolo, P.U., Gibilaro, L.G. and Waldram, S.P., A Unified Model for Particulate Expansion of Fluidised beds and flow in fixed porous media. Chemical Engineering Science, Vol. 38, No. 8, 1983, pp.1251-1260.

Galvin, K.P., Pratten, S. and Nguyentranlam, G., A generalized empirical description for particle slip velocities in liquid fluidized beds. Chemical Engineering Science, 54, 1999, pp 1045-1052.

Galvin, K.P.,Pratten, S.J., Nicol, S.K., Dense medium Separation using a Teetered bed separator. Minerals Engineering Vol 12, Issue 9, September 1999.

Galvin, K.P., Pratten, S. and Nguyentranlam, G., Letters to the Executive Editors, Comments on "A generalized empirical description for particle slip velocities in liquid fluidized beds", Chemical Engineering Science, Vol. 55, 2000, pp 1945-1947.

Nguyentranlam, G. and Galvin, K.P., Particle classification in the reflux classifier. Mineral Engineering, Vol 14, No. 9, 2001, pp 1081-1091.

Galvin, K.P., Nguyentranlam, G., Influence of parallel inclined plates in a liquid fluidized bed system. Chemical Engineering Science, 57, 2002, pp 1231-1234.

Galvin, K.P., Dorodchi, E., Callen, A.M., Lambert, N., Pratten, S.J., Pilot trial of the reflux classifier. Minerals Engineering, Vol 15, 2002, pp 19-25.

Galvin, K.P., Callen, A.M., Lambert, N., Pratten, S.J., Lui, J., Influence of a jigging action on the gravity separation achieved in a teetered bed separator. Minerals Engineering, 15, 2002, pp 1199-1202

Gibilaro, L.G., Felice, D.I., Waldram, S.P. and Foscolo, P.U., A Predictive Model for the Equilibrium Composition and Inversion of Binary-Solid Liquid Fluidised Beds, Chemical Engineering Science, Vol. 41, No. 2, 1986, pp. 379-387.

Handley, D., Doraisamy, A., Butcher, K.L. and Franklin, N.L., Transt. Inst. Chem. Eng., Vol. 44, 1966, pp. 260.

Hassett, N.J., Br. Chem. Eng., Vol. 6, 1961, pp. 777.

Hyde, D.A., Williams, K.P., Morris, A.N. and Yexley, P.M., The beneficiation of fine coal using the hydrosizer, Mine & Quarry, March, 1998, pp. 50 -53

Honaker, R.Q. and Mondal, K., Dynamic modelling of fine coal separations in a hindered-bed classifier, Coal Preparation, Vol.21, No.2, 2000, pp.211-232.

Horsfall, D.W., Coal Preparation and Usages, Vol. II, 1993, Chapters 14-20.

Joshi, J.B., Solid-Liquid Fluidised Beds, Chem. Eng. Res. Des., Vol. 61, May 1983, pp. 151-161.

Juma, A.K.A. and Richardson, J.F., Segregation and Mixing in Liquid Fluidised Beds, Chemical Engineering Science, Vol. 38, 1983, pp 955-967.

Kennedy, S.C. and Bretton, R.H., Axial Dispersion of Spheres Fluidised with Liquids, AIChE J., Vol. 12, 1966, pp 24-30.

Khan, A.R. and Richardson, J.F., Pressure gradient and friction factor for sedimentation and sedimentation and fluidisation of uniform spheres in liquids, Chemical Engineering Science, Vol. 45, 1990, pp. 255-265.

Kim, B.H., Kilma, M.S. and Cho, H., Modelling of hindered-settling column separations, Innovations in fine coal density separation, In Advances in Gravity Concentration, ed. By Honaker, R.Q and Forrest W.R., SME, Littleton, CO., 2003, pp. 115-124.

Kohmuench, J.N., Improving Efficiencies in water based separators using mathematical analysis tools. Dissertation, Blacksburg, Virginia, 2000.

Kunii, D. and Levenspiel, O., Fluidization Engineering, 1969, pp.88-90. Wiley. New York

Lee, C.H., Modelling of Batch Hindered Settling, PhD Dissertation, Pennsylvania State University, 1989.

Littler, A, Sand Processing, Product Optimization and Waste Treatment – Part 3 Classification, Quarry Management, November 1987, pp 41-48.

Lockett, M.J. and Al-Habbooby, H.M., Relative particle velocities in two-species settling, Powder Technology, Vol. 10, 1974, pp. 67-71.

Low, G.S. and Bhattacharya, S.N., On the Study of Maximum Solids Concentration in Suspension Rheology, The Twelfth Australian Chemical Engineering Conference, Melbourne, Australia, August 26-29, 1984, Paper 23b, pp. 805-812.

Masliyah, J.H., Hindered settling in a multi-species particle system. Chemical Engineering Science, Vol. 34, 1979, pp1166-1168.

McGeary, R.K., Mechanical Packing of Spherical Particles, Journal of American Ceramic Society, Vol. 44, No.10, 1961, pp.513-522.

Nicol, S., A Case Study in the Implementation of Novel Technology: Teetered bed separators, The Australian Coal Review, Oct. 1998, pp. 31-34.

Oliver, D.R., The Sedimentation of suspensions of closely sized spherical particles, Chemical Engineering Science, Vol. 15, 1961, pp .230-242.

Partwardhan, V.S, Tien, C., Sedimentation and liquid fluidization of solid particles of different sizes and densities, Chemical Engineering Science, Vol. 40, No.7, 1985, pp 1051-1060.

Peng, F.F., Xia, Y. and Gu, Z., Performance of hindered settling bed density separator in fine coal cleaning circuit. SME 2004 Annual Meeting and Exhibit, Denver, Colorado, February 23-25.

Richardson, J.F. and Zaki, W.N., Sedimentation and Fluidisation: Part I. Transactions of the Institution of Chemical Engineers, 1954, Vol.32, pp 35-53.

Smith, T.N., The Sedimentation of Particles having a Dispersion of Sizes, Transactions of the Institution of Chemical Engineers, Vol. 44, 1966, pp. 153-157.

Swanson, V.F. Free and hindered settling. Minerals & Metallurgical Processing, November 1989, pp 190-196.

Sudduth, R.D., A New Method to Predict the Maximum Packing Fraction and the Viscosity of Solutions with a Size Distribution of Suspended Particles, Journal of Applied Polymer Science, Vol. 48, 1993, pp. 37-55.

Wills, B.A, Mineral Processing Technology, 3rd Edtion, Pergamon Press, 1985, pp 260-265.

Zigrang, D.J. and Sylvester, N.D., An Explicit Equation for Particle Settling Velocities in Solid-Liquid Systems. AIChe. Journal, Vol. 27, No.6, 1981, pp. 1043-1044.

Zimmel, Y., Generalised buoyancy forces in dispersions, Journal of Applied Physics, Vol. 68, 1990, pp. 2007-2012.

APPENDIX A: ADDITIONAL THEORY & EXPERIMENTAL PROCEDURES

APPENDIX A: ADDITIONAL THEORY AND EXPERIMENTAL PROCEDURES

A1.Eulerian Model Equations

A1.1 Volume Fractions

In the multiphase model in Fluent, the volume fractions represent the space occupied by each phase. This concept is known as phase volume fractions and is denoted as α_q. The conservation of mass and momentum are solved individually for each phase. Equations (A1) to (A14) have been extracted from the Fluent 6.1 User Manual for Eulerian Multiphase Models. These equations form the basis for the Euler method of simulation.

The volume of phase q, V_q is defined as

$$V_q = \int_V \alpha_q dV \tag{A1}$$

Where

$$\sum_{q=1}^{n} \alpha_q = 1 \tag{A2}$$

The effective density contribution of phase q is

$$\hat{\rho}_q = \alpha_q \rho_q \tag{A3}$$

Where ρ_q is the physical density of phase q.

A1.2 Conservation of Mass

The conservation equations defined by Fluent are shown below:

The continuity of phase q is

$$\frac{\partial}{\partial t}(\alpha_q \rho_q) + \nabla.\left(\alpha_q \rho_q \vec{v}_q\right) = \sum_{p=1}^{n} \dot{m}_{pq} \tag{A4}$$

Where $\vec{v}_q$ is the velocity of phase q, $\dot{m}_{pq}$ is the mass transfer from the pth to qth phase.

From the mass conservation the following are obtained:

$$\dot{m}_{pq} = -\dot{m}_{qp} \tag{A5}$$

and

$$\dot{m}_{pp} = 0 \tag{A6}$$

A1.3. Conservation of Momentum

The momentum balance of q yields

$$\frac{\partial}{\partial t}\left(\alpha_q \rho_q \vec{v}_q\right) + \nabla.\left(\alpha_q \rho_q \vec{v}_q \vec{v}_q\right) = -\alpha_q \nabla._p + \nabla.\overline{\overline{\tau}}_q + \sum_{p=1}^{n}\left(\vec{R}_{pq} + \dot{m}_{pq}\vec{v}_{pq}\right) + \alpha_q \rho_q\left(\vec{F}_q + \vec{F}_{lift,q} + \vec{F}_{vm,q}\right) \tag{A7}$$

Where $\overline{\overline{\tau}}_q$ is the qth stress-strain tensor.

$$\overline{\overline{\tau}}_q = \alpha_q \mu_q\left(\nabla \vec{v}_q + \nabla \vec{v}_q^{\,T}\right) + \alpha_q\left(\lambda_q - \frac{2}{3}\mu_q\right)\nabla.\vec{v}_q\,\overline{\overline{I}} \tag{A8}$$

Here μ_q and λ_q are the shear and bulk viscosity of phase q, $\vec{F}_q$ is an external body force, $\vec{F}_{lift,q}$ is a lift force, $\vec{F}_{vm,q}$ is a virtual mass force, $\vec{R}_{pq}$ is an interaction force between phases, and p is the pressure shared by all phases. $\vec{v}_{pq}$ is the interphase velocity, defined as follows. If $\dot{m}_{pq} > 0$ (ie., phase p mass is being transferred to phase q), $\vec{v}_{pq} = \vec{v}_p$; if $\dot{m}_{pq} < 0$ (ie., phase q mass is being transferred to phase p), $\vec{v}_{pq} = \vec{v}_q$; and $\vec{v}_{pq} = \vec{v}_{qp}$.

Fluent uses the following interaction terms:

$$\sum_{p=1}^{n} \vec{R}_{pq} = \sum_{p=1}^{n} k_{pq}(\vec{v}_p - \vec{v}_q) \tag{A9}$$

Where K_{pq} ($=K_{qp}$) is the interphase momentum exchange coefficient.

A1.4. Virtual Mass Force

Fluent includes a virtual mass force effect for multiphase flow. This occurs when the secondary phase q accelerates in relation to the primary phase p. The inertia of the primary phase mass encountered by the accelerating particle, exerts a virtual mass force on the particle.

$$F_{vm} = 0.5\alpha_p \rho_q \left(\frac{d_q v_q}{dt} - \frac{d_p v_p}{dt}\right) \tag{A10}$$

The term dq/dt denotes the phase material time derivative in the form

$$\frac{d_q(\phi)}{dt} = \frac{\partial(\phi)}{\partial t} + (\vec{v}_q . \nabla)\phi \tag{A11}$$

The virtual mass force, F_{vm} will be added to the right hand side of the momentum equations for both phases ($F_{vm,\,q} = - F_{vm,\,p}$). The virtual mass affect was neglected since it is only significant if

the secondary phase has a much lower density than the primary phase. In the TBS, the coal particles are of a higher density compared to water.

A1.5. Equations Solved by Fluent

The equations for fluid-fluid and granular multiphase flow are presented below for an n^{th} phase flow. These equations were selected in Fluent to solve the various flow parameters.

A1.5.1Continuity Equation:

The volume fraction of each phase is calculated using the Continuity Equation below:

$$\frac{\partial}{\partial t}(\alpha_q) + \nabla.(\alpha_q \vec{v_q}) = \frac{1}{\rho_q}\left(\sum_{p=1}^{n} \dot{m}_{pq} - \alpha_q \frac{d_q \rho_q}{dt}\right) \tag{A12}$$

A1.5.2. Fluid-Fluid Momentum Equations:

The conservation of momentum for fluid phase q is:

$$\frac{\partial}{\partial t}\left(\alpha_q \rho_q \vec{v}_q\right) + \nabla.\left(\alpha_q \rho_q \vec{v}_q \vec{v}_q\right) = -\alpha_q \nabla p + \nabla.\bar{\bar{\tau}}_q + \alpha_q \rho_q \vec{g} + \alpha_q \rho_q (\vec{F}_q + \vec{F}_{lift,q} + \vec{F}_{vm,q}) + \sum_{p=1}^{n} (K_{pq}(\vec{v}_p - \vec{v}_q) + \dot{m}_{pq} \vec{v}_{pq}) \tag{A13}$$

Where g is the acceleration due to gravity, $F_{q,}$, $F_{lift,\,q}$, $F_{vm,\,q}$ are defined above.

A1.5.3. Fluid-Solid Momentum Equations:

Fluent uses a multi grid granular model to describe flow behaviour for a fluid-solid mixture. Particle-particle collisions normally attributed to the particle random motion is used to model the solid phase stresses. The kinetic energy, which is caused by the velocity fluctuations, is used to determine the viscosity, stresses and pressure of the solid phase. The fluid momentum remains the same. The solid momentum equation for the s^{th} solid phase is:

$$\frac{\partial}{\partial t}\left(\alpha_s \rho_s \vec{v}_s\right)+\nabla.\left(\alpha_s \rho_s \vec{v}_s \vec{v}_s\right)=-\alpha_s \nabla p-\nabla p_s+\nabla.\bar{\bar{\tau}}_s+\alpha_s \rho_s \vec{g}+\alpha_s \rho_s(\vec{F}_s+\vec{F}_{lift,s}+\vec{F}_{vm,s})+ \tag{A14}$$

$$\sum_{l=1}^{n}(K_{ls}(\vec{v}_l-\vec{v}_s)+\dot{m}_{ls}\vec{v}_{ls})$$

Where p_s is the s^{th} solid pressure, $K_{ls} = K_{sl}$ is the momentum exchange coefficient, between the fluid or solid phase l, and the solid phase s, N is the total number of phases and F_q, F_{vm} and $F_{lift,\,q}$ are as defined above.

A2. EXPERIMENTAL PROCEDURES

A2.1. TBS Experimental Procedure

The operating procedure for the TBS is shown below for Plate 1 at 6 l/min:

- The coal sample was weighed out and the constant head feed tank was filled with water.
- A 5g sample of the feed was kept aside and the feed solid density was determined using the density bottle method.
- The underflow valve was closed and teeter water flow rate was set for Run 1 using the rotameter to 6 l/min from the calibration graph.
- Once water overflowed from the TBS, the coal feed was added continuously.
- Overflow samples were not analysed during start-up, as the unit behaves as an elutriator initially, separating on particle size only. The overflow samples were collected in one 125 litre and three 75 litre drums.
- Once a density gradient was created, (i.e. the presence of the teeter bed was noted – five minutes), the density tracers were periodically added, every four to five minutes. The tracers were divided into 3 equal batches to obtain a more accurate density distribution. The pressure drop was monitored using a manometer. The TBS was operated in a semi-batch mode with a continuous feed and overflow. The underflow valve was closed during the run. All material below the distributor plate was classified as the underflow samples.
- A stopwatch was used to determine the feed coal, water and overflow rates. Once the feed coal was depleted the run was terminated. Each run would take between twenty to thirty-five minutes to complete.
- At the end of the run, the underflow valve was opened very slowly to allow all the water present within the TBS to drain out.

- The unit was dis-assembled by removing the bolted metal rods. Using a thin sheet of plastic, the sections of the bed were removed.

- The sections were initially wet screened using the Vibrating Screen Shaker and a 4mm screen to collect the 5mm tracers in each section. This procedure was modified to account for the 0.8, 1.5 and 2mm tracers, which would have been difficult to retrieve using the wet screening method.

- Thereafter, the five sections, including the tops, overflow and underflow were dried in the oven overnight at 105^0 C.

- The dry samples were then screened using a 1mm aperture screen and a base plate. The 5mm, 2mm and 1.5mm tracers were remained on the screen and were removed accordingly. The 0.8mm tracers were recovered from the base plate. This was used recorded for each sample and tracer distributions graphs were plotted.

- Once all the tracers were removed, the sections were riffled to obtain 100 to 150 g samples. These samples were collected and labelled accordingly for the heavy liquid tests.

- The following procedure was performed for Runs 2 and 3 at 3 and 8 l/min respectively for each plate. The procedures for the heavy liquids tests and density bottle method are explained below.

A2.2. Experimental Procedure for the Laboratory Heavy Liquid Tests

Laboratory testing may be performed on ores in order to assess the suitability of heavy medium separation on the crushed material and to determine the economic separating density (Wills, 1985).

Liquids covering a range of densities in incremental steps are prepared, and the representative sample of crushed ore is introduced into the liquid of highest density (Wills, 1985). The floats product is removed and washed and placed in the liquid of next lower density, whose float product is then transferred to the next lower density and so on. The sinks product is finally drained, washed and dried, and then weighed, together with the final floats product, to give the density distribution of the sample by weight (Wills, 1985).

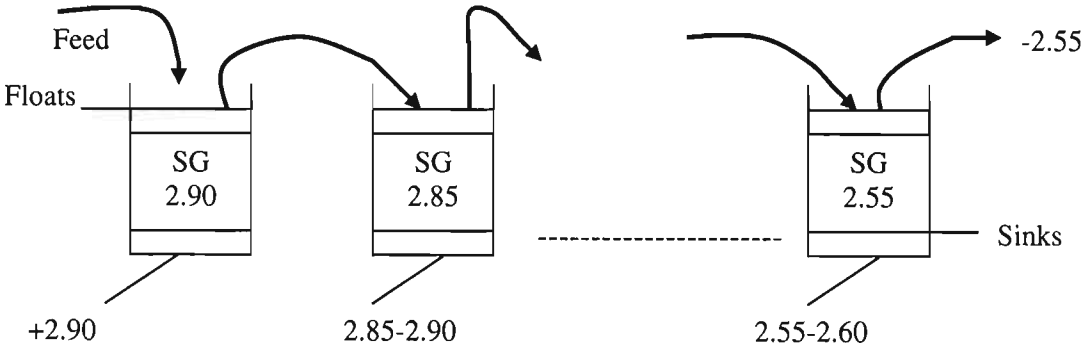

Figure A1: Heavy liquid testing (Wills, 1985)

The Heavy liquid testing or sink-float analysis as it commonly known, was performed using tetrabromoethane (TBE) as the heavy liquid and diluted with acetone to obtain the specific density solutions

The equations (A15-A27) were derived to obtain the correct standard solution densities. The volume change of mixing was also tested using the equations derived below to determine if the standard solutions were of the correct density.

From the overall mass balance:

$$m_t = m_1 + m_2 \tag{A15}$$

Where m_t is the total mass of the solution (g), m_1 is the mass of TBE (g) and m_2 is the mass of acetone (g).

Since $$m = \rho V \tag{A16}$$

Where ρ is the mixture volume (g/cm^3) and V is the volume (cm^3).

Eqn. (A15) becomes:

$$\rho_m \mathrm{V_m} = V_1\rho_1 + V_2\rho_2 \tag{A17}$$

Where subscript m, is the mixture, 1 denotes TBE and 2 denotes acetone.

Dividing by $\mathrm{V_m}$:

$$\rho_m = \frac{V_1}{V_m}\rho_1 + \frac{V_2}{V_m}\rho_2 \tag{A18}$$

And from the definition of volume fractions in a binary system:

$$\frac{V_1}{V_m} = 1 - \frac{V_2}{V_m} \tag{A19}$$

Eqn. (A17) becomes:

$$\rho_m = \frac{V_1}{V_m}(\rho_1 - \rho_2) + \rho_2 \tag{A20}$$

In terms of V_1:

$$V_1 = V_m \frac{(\rho_m - \rho_2)}{(\rho_1 - \rho_2)} \tag{A21}$$

Testing for the Volume change of mixing

From Eqn. (A16):

$$V_m = \frac{m_m}{\rho_m} \tag{A22}$$

Substituting Eqn (A1) into (A22):

$$V_m = \frac{m_1 + m_2}{\rho_m} \tag{A23}$$

And since

$$m = \frac{n}{MW} \tag{A24}$$

Where n is the number of moles and MW is the molecular weight (g/mol)

Eqn (A22) becomes:

$$V_m = \frac{n_1 MW_1 + n_2 MW_2}{\rho_m} \tag{A25}$$

Since

$$C = \frac{n}{V} \tag{A26}$$

Where C is the concentration of the solution (mol/cm^3)

Eqn (A25) becomes:

$$V_m = \frac{C_1 V_1 MW_1 + C_2 V_2 MW_2}{\rho_m} \tag{A27}$$

Using Eqn.(A21) and assuming V_m to be 60ml, V_1 and V_2 were obtained. Eqn. (A27) was then solved and the mixture volume, V_m was found to be 59.93 ml. The percentage error between the assumed and calculated mixture volume, due to volume change of mixing was only 0.1%. Therefore the density of the standard solutions would be fairly accurate for the heavy liquid tests.

ρ_1	2.963 g/cm^3
ρ_2	0.7899 g/cm^3
MW_1	345.65 g/cm^3
MW_2	58.08 g/cm^3

Table A1: Properties of the TBE and Acetone

ρ_m (g/cm^3)	V_1 (ml)	V_2 (ml)
1.2	22.6	97.4
1.4	33.7	86.3
1.6	44.7	75.3
1.8	55.8	64.2
2	66.8	53.2

Table A2. Standard solutions for each SG for a mixture volume of 120ml

A2.2.1. Sink-Float Experimental Procedure

- The volumes of TBE and acetone were mixed according to the ratios shown above for each specific gravity solution of 120ml using a burette, which allowed measurement to the first decimal place improving the solution accuracy

- The solutions stored in flasks and shaken well before used for each run to ensure that the density of the solution was homogenous.

- 40 vials were labeled with the relevant solution SG ranging from 1.2 – 2.0 since the TBS consisted of the overflow, tops, five sections of the bed and the underflow region. This resulted in 8 sets of samples per run, with 5 SGs' per sample resulting in 40 vials in a batch.

- 5g-coal sub-samples were obtained for each region (overflow, tops, etc) by performing a size distribution on the large samples obtained from the experimental runs on the TBS. The highest size fractions were chosen and riffled to approximately 5g for the sink-float analysis.

- Small portions of the sub-samples were added to the 2.0 SG (highest SG range) vial with a spatula, in order to allow the particles to mix well (3 minutes) and reduce entrainment.

- The floats from the vial are then collected, rinsed with acetone to wash off any excess solution on the particles. These are then transferred to the 1.8 SG vial. This process was repeated until the 1.2 SG vial.

- The vials are then decanted to remove the specific gravity solution. The coal was then washed with acetone to remove any TBE on the particles. The vials were then left to air dry under the fume hood overnight.

- The samples were then weighed and placed in crucibles and placed in the furnace at 850°C for 3 hours.

- The residues were then cooled and weighed. The ash content could then be determined by the difference in the initial sample mass.

A2.3. Density-Bottle Experimental Procedure

The density bottle method was used to determine the average density of the feed material. This was used to calculate the average velocity of the coal particles entering the unit with the feed and in the Ergun Equation for the calculation of the voidage and thus the bed suspension density.

The experimental procedure outlined below was obtained from Wills (1985).

- Distilled water was added to the density bottle.
- The mass of the density bottle with distilled water was measured.
- The dry coal samples were weighed and added to the density bottle.
- The bottle was then filled to the brim with water, shaken and allowed to settle for a while.
- Once there were no air bubbles present, the mass of the bottle + water + solids was recorded.

The specific gravity of the solids (SG_s) was calculated using the following method.

$$SG_s = \frac{(\ mass\ of\ dry\ coal\ )}{[\{(\ mass\ of\ bottle + water\ ) - (\ mass\ of\ bottle + water + coal\ )\} + mass\ of\ dry\ coal\ ]} \qquad \text{(A28)}$$

APPENDIX B: TABLES & RAW DATA

APPENDIX B: TABLES & RAW DATA

Aperture Size (μm)	Mass of Screen (g)	Sample + Screen (g)	Sample (g)	% Retained	% Cumulative Passing
1700	403.1	459.1	56.0	34.59	65.41
1400	398.2	444.6	46.4	28.66	36.75
1000	356.2	376.0	19.8	12.23	24.52
710	314.9	333.9	19.0	11.74	12.79
300	457.6	469.5	11.9	7.35	5.44
106	272.0	278.4	6.4	3.95	1.48
38	259.7	262.0	2.3	1.42	0.06
-38	428	428.1	0.1	0.06	0.00
Total			161.9		

Table B1: Feed Size Distribution

d	Y_d
Size (μm)	Cumulative Passing
1700	0.654
1400	0.368
1000	0.245
710	0.128
300	0.054
106	0.015
38	0.0006
0	0

Table B2: The Rosin -Rammler Diameter Distribution Method

Runs	1	2	3	4	5	6
Mass of coal (g)	11.03	1.47	2.92	2.10	3.40	3.07
Mass of jar + water (g)	80.05	80.04	79.78	79.74	80.06	80.05
Mass of jar +water +coal (g)	83.78	80.53	80.78	80.49	81.22	81.00
Specific Gravity (g/cm^3)	1.51	1.50	1.52	1.57	1.52	1.45
Average SG	1.51	g/cm^3				

Table B3: The Density Bottle Method

Runs	Mass of crucible (g)	Mass of Coal (g)	Mass of Crucible + Coal Before (g)	Mass of Crucible + Coal After (g)	Difference (g)	Moisture Content (%)
1	25.69	2.51	28.20	28.10	0.10	4.17
2	8.22	2.73	10.95	10.84	0.11	4.07
3	8.79	2.78	11.57	11.46	0.11	3.97
4	8.56	3.08	11.64	11.52	0.12	3.83
5	8.51	2.82	11.34	11.23	0.11	3.80

Table B4: Moisture Content

SG	Coal (kg)	Mass Frac.	Coal (kg)	Volume (m3)	Vol. frac	Fluent Name	Flow (m/s)	(Vol. Frac)/3
2	1.40	0.23	6.19	0.00	0.06	Phases 6 / 11 / 16	0.00	0.02
1.8	0.23	0.04	1.04	0.00	0.01	Phases 5 / 10 / 15	0.00	0.00
1.6	0.77	0.13	3.43	0.00	0.04	Phases 4 / 9 / 14	0.00	0.01
1.4	2.59	0.43	11.50	0.01	0.16	Phases 3 / 8 / 13	0.00	0.05
1.2	1.09	0.18	4.84	0.00	0.08	Phases 2 / 7 / 12	0.00	0.03
1				0.03	0.65	Phase 1	0.01	
Total	6.09	1.00		0.05	1.00			

Table B5: Fluent Simulation Velocity and Vol. Frac Input Data

Rotameter Reading	Time (s)	Volume (l)	Flowrate (l/min)
2	35	0.98	1.67
5	23	1.02	2.66
10	13.6	1.00	4.41
15	9.5	1.00	6.32
20	7.3	1.03	8.42
25	5.3	1.00	11.32

Table B6: Teeter-water Calibration Data

Time elapsed (min)	Volume (l)	Time Taken (s)	Flowrate (l/min)
0	1.00	33.5	1.79
4	1.00	34.0	1.78
8	1.00	36.3	1.65
12	1.00	37.7	1.59
16	1.00	40.6	1.48
20	1.00	43.3	1.39
24	1.00	46.7	1.29
28	1.00	52.0	1.15

Table B7: Feed Water Calibration

Time	20	min
Feed Coal	18.48	kg
Density (Average)	1510.3	kg/m^3
Coal Flow	0.61	l/min
Water Remaining in unit	11.90	kg
Feed Water Flow	2.08	l/min
Teeter Water Flow	6	l/min

Table B8: Flow Data for Run 1, Plate1

SG	Vials Mass before (g)	Mass After (g)	Crucibles before (g)	Crucibles after (g)	Mass of Coal (g)	Mass frac.	Coal Comb. (g)	Ash (g)	% Comb
2	14.14	14.03	20.86	20.82	0.11	1.75	0.048	42.58	57.42
1.8	14.53	14.30	20.83	20.73	0.23	3.54	0.10	44.00	55.99
1.6	16.61	14.76	20.89	20.36	1.85	28.69	0.52	28.31	71.69
1.4	16.35	14.02	21.68	21.37	2.33	36.09	0.31	13.24	86.76
1.2	15.23	14.02	20.66	20.58	1.21	18.78	0.09	7.046	92.95
Total					5.73				

Table B9: Sink-Float Data for Run1, Plate1

Time	25	min
Feed Coal	20.21	kg
Density (Average)	1510	kg/m^3
Coal Flow	0.51	l/min
Water Remaining in unit	11.05	kg
Feed Water Flow	1.98	l/min
Teeter Water Flow	3	l/min

Table B10: Flow Data for Run 2,Plate 1

SG	Vials Mass before (g)	Mass After (g)	Crucibles before (g)	Crucibles after (g)	Mass of Coal (g)	Mass frac.	Coal Comb. (g)	Ash (g)	% Comb
2	14.09	14.03	20.39	20.36	0.07	1.05	0.03	46.98	53.02
1.8	14.27	14.03	21.47	21.37	0.23	3.62	0.09	39.67	60.33
1.6	15.54	14.76	20.82	20.58	0.77	11.98	0.25	32.22	67.78
1.4	16.91	14.32	20.98	20.56	2.59	40.16	0.42	16.22	83.78
1.2	16.46	14.03	21.03	20.82	2.43	37.69	0.22	8.88	91.12
					6.09				

Table B11: Sink-Float Data for Run2, Plate1

Time	22	min
Feed Coal	17.23	kg
Density (Average)	1510.3	kg/m^3
Coal Flow	0.52	l/min
Water Remaining in unit	10.89	kg
Feed Water Flow	2.64	l/min
Teeter Water Flow	8	l/min

Table B12: Flow Data for Run 3,Plate 1

SG	Vials Mass before (g)	Mass After (g)	Crucibles before (g)	Crucibles after (g)	Mass of Coal (g)	Mass frac.	Coal Comb. (g)	Ash (g)	% Comb
2	12.48	12.27	20.94	20.82	0.21	3.30	0.12	56.12	43.88
1.8	12.54	12.32	20.65	20.56	0.22	3.45	0.10	42.95	57.05
1.6	13.26	12.53	20.82	20.58	0.73	11.29	0.24	33.21	66.79
1.4	15.64	12.28	21.88	21.37	3.36	52.07	0.51	15.08	84.92
1.2	11.34	9.79	20.48	20.36	1.55	24.01	0.11	7.23	92.77
Total					6.07				

Table B13: Sink-Float Data for Run3, Plate1

Time	20	min
Feed Coal	15.48	kg
Density (Average)	1510.3	kg/m^3
Coal Flow	0.51	l/min
Water Remaining in unit	11.90	kg
Feed Water Flow	2.48	l/min
Teeter Water Flow	6	l/min

Table B14: Flow Data for Run 1,Plate 2

Time (min)	Manometer Readings (cm)		Head (cm)	Offset (cm)	P (Pa)	f(e)=0	e	Bed Density (kg/m^3)
0	41.0	60.0	19.0	19.0	1863.9			1000.0
5	39.5	66.5	27.0	8.0	784.8	-0.00031	0.523	1240.7
9	36.4	64.2	27.8	8.8	863.2	-0.00033	0.52	1246.2
14	33.2	67.3	34.1	15.1	1481.3	-0.00046	0.46	1276.1
20	30.0	71.0	41.0	22.0	2158.2	-0.00059	0.42	1296.1

Table B15: Pressure-Drop Data for Run 1,Plate 2

Density Range (SG)	1.2	1.3	1.4	1.5	1.6	1.8	2	No. of tracers	Average SG
Overflow									
5mm	5								
2mm			2						
1.5mm			1	1			1		
Total	5	0	3	1	0	0	1	10	1.37
Tops SG	1.2	1.3	1.4	1.5	1.6	1.8	2		
5mm	2		7	5		4	4		
2mm			5	7		3	5		
1.5mm			3			3	1		
Total	2	0	15	12	0	10	10	49	1.62
Sect 5 SG	1.2	1.3	1.4	1.5	1.6	1.8	2		
5mm	2		3	1		8	2		
2mm			2	1		3	6		
1.5mm							1		
Total	2	0	5	2	0	11	9	29	1.73
Sect 4 SG	1.2	1.3	1.4	1.5	1.6	1.8	2		
5mm			1		1		2		
2mm			2	1			1		
1.5mm			1			1	2		
Total	0	0	4	1	1	1	5	12	1.71
Sect 3 SG	1.2	1.3	1.4	1.5	1.6	1.8	2		
5mm	1		5		5	4	2		
2mm			2	2		3			
1.5mm			1	1		1			
Total	1	0	8	3	5	8	2	27	1.60
Sect 2 SG	1.2	1.3	1.4	1.5	1.6	1.8	2		
5mm			1		2	3	5		
2mm			2	2		3			
1.5mm						2	1		
Total	0	0	3	2	2	8	6	21	1.75
Sect 1 SG	1.2	1.3	1.4	1.5	1.6	1.8	2		
5mm		none							
2mm									
1.5mm									
Total	0	0	0	0	0	0	0	0	0
Underflow SG	1.2	1.3	1.4	1.5	1.6	1.8	2		
5mm		none							
2mm									
1.5mm									
Total	0	0	0	0	0	0	0	0	0

Table B16: Density Tracer Data for Run 1,Plate 2

SG	Vials Mass before (g)	Mass After (g)	Crucibles before (g)	Crucibles after (g)	Mass of Coal (g)	Mass frac.	Coal Comb. (g)	Ash (g)	% Ash	Av. Density	% Comb
2	9.62	9.42	31.35	31.19	0.20	0.06	0.16	0.04	18.87	0.12	81.13
1.8	9.48	9.38	33.52	33.45	0.09	0.03	0.08	0.02	17.41	0.05	82.59
1.6	9.61	9.37	33.91	33.74	0.24	0.07	0.18	0.06	26.73	0.11	73.27
1.4	11.55	9.85	33.21	31.69	1.70	0.50	1.52	0.18	10.37	0.69	89.63
1.2	10.66	9.47	34.56	33.59	1.19	0.35	0.97	0.22	18.33	0.42	81.67
Total					3.42					1.39	

Table B17: Sink-Float Data for Run1, Plate2

Sections	Column Length (m)	Sink-Float SG	Tracer SG
Overflow	0.00	1.39	1.37
Tops	0.40	1.37	1.62
Sect 5	0.46	1.47	1.73
Sect 4	0.52	1.43	1.71
Sect 3	0.58	1.43	1.60
Sect 2	0.64	1.39	0.00
Sect 1	0.72	1.43	1.75
Underflow	1.22	1.42	0.00

Table B18: Sink-Float and Tracer Bed Profile Data for Run1, Plate2

Time	18	min
Feed Coal	13.15	kg
Density (Average)	1510.3	kg/m3
Coal Flow	0.48	l/min
Water Remaining in unit	9.73	kg
Feed Water Flow	2.08	l/min
Teeter Water Flow	3	l/min

Table B19: Flow Data for Run 2,Plate 2

Time (min)	Manometer Readings (cm)		Head (cm)	Offset (cm)	P (Pa)	f(e)=0	e	Bed Density (kg/m^3)
0	42.0	59.0	17.0	17.0	1667.7			1000
6	41.4	59.5	18.1	1.1	107.9	-0.00023	0.69	1158.3
12	40.0	61.0	21.0	4.0	392.4	-0.00043	0.56	1226.8
18	35.3	66.0	30.7	13.7	1344.0	-0.00091	0.43	1291.2

Table B20: Pressure-Drop Data for Run 2,Plate 2

SG	Vials Mass before (g)	Mass After (g)	Crucible before (g)	Crucible after (g)	Mass of Coal (g)	Mass frac.	Coal Comb. (g)	Ash (g)	% Ash	Av. Density	% Comb
2	9.62	9.44	35.11	35.01	0.18	0.08	0.11	0.07	39.43	0.17	60.57
1.8	9.49	9.36	34.86	34.76	0.13	0.06	0.010	0.03	25.77	0.11	74.23
1.6	9.51	9.41	34.47	34.38	0.10	0.04	0.09	0.01	8.79	0.07	91.22
1.4	10.63	9.55	35.66	34.61	1.08	0.50	1.05	0.03	2.96	0.70	97.04
1.2	9.94	9.25	32.35	31.70	0.69	0.32	0.65	0.03	5.00	0.38	94.99
Total					2.17					1.43	

Table B21: Sink-Float Data for Run2, Plate2

Sections	Column Length (m)	Sink-Float SG	Tracer SG
Overflow	0.00	1.43	1.40
Tops	0.40	1.41	1.61
Sect 5	0.46	1.40	1.52
Sect 4	0.52	1.41	1.74
Sect 3	0.58	1.42	1.68
Sect 2	0.64	1.39	1.69
Sect 1	0.72	1.34	1.90
Underflow	1.22	1.32	1.80

Table B22: Sink-Float and Tracer Bed Profile Data for Run2, Plate2

SG Range	1.2	1.3	1.4	1.5	1.6	1.8	2	No.of tracers	Avg SG
Overflow									
5mm									
2mm									
1.5mm			1						
Total	0	0	1	0	0	0	0	1	1.40
Tops	1.2	1.3	1.4	1.5	1.6	1.8	2		
5mm	4		5		4	4	3		
2mm			4	6		3	4		
1.5mm			2	2		2	1		
Total	4	0	11	8	4	9	8	44	1.61
Sect 5	1.2	1.3	1.4	1.5	1.6	1.8	2		
5mm	3		4		2	3	1		
2mm			1			1			
1.5mm			2						
Total	3	0	7	0	2	4	1	17	1.52
Sect 4	1.2	1.3	1.4	1.5	1.6	1.8	2		
5mm	1		1		4	5	4		
2mm			1	2		3	3		
1.5mm						1			
Total	1	0	2	2	4	9	7	25	1.74
Sect 3	1.2	1.3	1.4	1.5	1.6	1.8	2		
5mm	2		4	2		6	5		
2mm			7	2		3	4		
1.5mm				1		3	2		
Total	2	0	11	5	0	12	11	41	1.68
Sect 2	1.2	1.3	1.4	1.5	1.6	1.8	2		
5mm			3		2	1	2		
2mm				3		1	1		
1.5mm			1				2		
Total	0	0	4	3	2	2	5	16	1.68
Sect 1	1.2	1.3	1.4	1.5	1.6	1.8	2		
5mm									
2mm						1	1		
1.5mm									
Total	0	0	0	0	0	1	1	2	1.90
Underflow	1.2	1.3	1.4	1.5	1.6	1.8	2		
5mm									
2mm							1		
1.5mm			1				1		
Total	0	0	1	0	0	0	2	3	1.80

Table B23: Density Tracer Data for Run 2,Plate 2

Time	18	min
Feed Coal	13.85	kg
Density (Average)	1510.3	kg/m3
Coal Flow	0.51	l/min
Water Remaining in unit	12.59	kg
Feed Water Flow	2.84	l/min
Teeter Water Flow	8	l/min

Table B24: Flow Data for Run3, Plate 2

Time (min)	Manometer Readings (cm)		Head (cm)	Offset (cm)	P (Pa)	f(e)=0	e	Bed Density (kg/m^3)
0	40.8	60.2	19.4	19.4	1903.1			1000.0
4	40.0	61.2	21.2	1.8	176.6	-0.0002	0.74	1132.5
8	39.4	61.5	22.1	2.7	264.9	-0.0003	0.69	1156.3
13	37.0	63.0	26.0	6.6	647.5	-0.0006	0.59	1210.5
18	33	68.0	35.0	15.6	1530.4	0.0000	0.49	1261.5

Table B25: Pressure-Drop Data for Run 3,Plate 2

SG	Vials Mass before (g)	Mass After (g)	Crucibles before (g)	Crucibles after (g)	Mass of Coal (g)	Mass frac.	Coal Comb. (g)	Ash (g)	% Ash	Av. Density	% Comb
2	9.71	9.35	24.38	24.07	0.36	0.08	0.31	0.05	14.18	0.17	85.82
1.8	9.40	9.32	22.73	22.67	0.07	0.02	0.06	0.01	19.01	0.03	80.99
1.6	9.82	9.38	37.60	37.21	0.44	0.10	0.39	0.05	11.74	0.16	88.26
1.4	11.678	9.30	57.87	55.71	2.38	0.55	2.16	0.22	9.11	0.77	90.89
1.2	10.49	9.40	14.05	13.00	1.09	0.25	1.04	0.05	4.10	0.30	95.90
					4.34					1.43	

Table B26: Sink-Float Data for Run3, Plate 2

Sections	Column Length (m)	Sink-Float SG	Tracer SG
Overflow	0.0	1.43	1.38
Tops	0.40	1.34	1.37
Sect 5	0.46	1.40	1.49
Sect 4	0.52	1.41	1.60
Sect 3	0.58	1.41	1.68
Sect 2	0.64	1.43	1.74
Sect 1	0.72	1.42	1.76
Underflow	1.22	1.48	0.00

Table B27: Sink-Float and Tracer Bed Profile Data for Run3, Plate2

SG Range	1.2	1.3	1.4	1.5	1.6	1.8	2	No. of tracers	Avg SG
Overflow									
5mm	1								
2mm			2						
1.5mm			1	1					
Total	1	0	3	1	0	0	0	5	1.38
Tops	1.2	1.3	1.4	1.5	1.6	1.8	2		
5mm	7								
2mm			4	2					
1.5mm			2	1			1		
Total	7	0	6	3	0	0	1	17	1.37
Sect 5	1.2	1.3	1.4	1.5	1.6	1.8	2		
5mm									
2mm			4	2					
1.5mm			2	1			1		
Total	0	0	6	3	0	0	1	10	1.49
Sect 4	1.2	1.3	1.4	1.5	1.6	1.8	2		
5mm	1		3	3		3	1		
2mm			2	3		1	2		
1.5mm			1			1			
Total	1	0	6	6	0	5	3	21	1.60
Sect 3	1.2	1.3	1.4	1.5	1.6	1.8	2		
5mm	1		7		7	8	4		
2mm			3	3		5	2		
1.5mm				1		5	1		
Total	1	0	10	4	7	18	7	47	1.68
Sect 2	1.2	1.3	1.4	1.5	1.6	1.8	2		
5mm			2		2	2	4		
2mm				2		2			
1.5mm						2			
Total	0	0	2	2	2	6	4	16	1.74
Sect 1	1.2	1.3	1.4	1.5	1.6	1.8	2		
5mm			5		2	6	6		
2mm			1	3		3	5		
1.5mm						2	1		
Total	0	0	6	3	2	11	12	34	1.76
Underflow	1.2	1.3	1.4	1.5	1.6	1.8	2		
5mm	none								
2mm									
1.5mm									
Total	0	0	0	0	0	0	0	0	

Table B28: Density Tracer Data for Run 3,Plate 2

Time	27	min
Feed Coal	15.91	kg
Density (Average)	1510.3	kg/m^3
Coal Flow	0.39	l/min
Water Remaining in unit	9.29	kg
Feed Water Flow	2.45	l/min
Teeter Water flow	6	l/min

Table B29: Flow Data for Run 1,Plate 3

Time (min)	Manometer Readings (cm)		Head (cm)	Offset (cm)	P (Pa)	f(e)=0	e	Bed Density (kg/m^3)
0	34.0	69.0	35.0	35.0	3433.5			1000.0
5	33.0	69.0	36.0	1.0	98.1	-3.00E-05	0.72	1141.4
10	33.0	69.5	36.5	1.5	147.2	-3.32E-05	0.68	1162.9
20	33.0	70.5	37.5	2.5	245.3	-3.99E-05	0.63	1191.0
27	33.0	71.0	38.0	3.0	294.3	-4.21E-05	0.61	1201.1

Table B30: Pressure-Drop Data for Run 1,Plate 3

SG	Vials Mass before (g)	Mass After (g)	Crucibles before (g)	Crucibles after (g)	Mass of Coal (g)	Mass frac.	Coal Comb. (g)	Ash (g)	% Ash	Av. Density	% Comb
2	13.44	13.14	20.85	20.75	0.29	0.03	0.11	0.19	64.07	0.06	35.93
1.8	12.58	12.48	20.47	20.41	0.10	0.01	0.05	0.05	48.98	0.02	51.02
1.6	15.22	14.33	21.71	21.12	0.89	0.09	0.59	0.30	33.55	0.15	66.45
1.4	20.48	14.37	23.69	21.41	6.11	0.63	2.28	3.83	62.69	0.88	89.00
1.2	14.60	12.28	29.59	27.43	2.32	0.24	2.16	0.16	6.743	0.29	94.00
					9.71					1.40	100.00

Table B31: Sink-Float Data for Run1, Plate3

Sections	Column Length (m)	Sink-Float SG	Tracer SG
Overflow	0.0	1.40	1.80
Tops	0.40	1.42	1.60
Sect 5	0.46	1.42	1.65
Sect 4	0.52	1.42	1.45
Sect 3	0.58	1.41	0.00
Sect 2	0.64	1.37	1.58
Sect 1	0.72	1.35	1.76
Underflow	1.22	1.53	1.80

Table B32: Sink-Float and Tracer Bed Profile Data for Run1, Plate3

SG Range	1.2	1.4	1.6	1.8	2	No. of tracers	Avg SG
Overflow							
5mm							
2mm		1			1		
1.5mm					1		
Total	0	1	0	0	2	3	1.80
Top	1.2	1.4	1.6	1.8	2		
5mm	3	3	3	3	3		
2mm							
1.5mm							
Total	3	3	3	3	3	15	1.60
Sect 5	1.2	1.4	1.6	1.8	2		
5mm	3	3	2	3	3		
2mm	1	1		2	2		
1.5mm				1	1		
Total	4	4	2	6	6	22	1.65
Sect 4	1.2	1.4	1.6	1.8	2		
5mm							
2mm	2		1	1			
1.5mm							
Total	2	0	1	1	0	4	1.45
Sect 3	1.2	1.4	1.6	1.8	2		
5mm							
2mm							
1.5mm							
Total	0	0	0	0	0	0	0.00
Sect 2	1.2	1.4	1.6	1.8	2		
5mm	4	2	1	1			
2mm		2	1	2	2		
1.5mm		1		2	1		
Total	4	5	2	5	3	19	1.58
Sect 1	1.2	1.4	1.6	1.8	2		
5mm		1	2	2	1		
2mm		1		1	2		
1.5mm					1		
Total	0	2	2	3	4	11	1.76
Underflow	1.2	1.4	1.6	1.8	2		
5mm		1	1	1	3		
2mm							
1.5mm							
Total	0	1	1	1	3	6	1.80

Table B33: Density Tracer Data for Run1, Plate 3

Time	37	min
Feed Coal	19.01	kg
Density (Average)	1510.3	kg/m3
Coal Flow	0.34	l/min
Water Remaining in unit	7.22	kg
Feed Water Flow	2.01	l/min
Teeter water flow	3	l/min

Table B34: Flow Data for Run 2,Plate 3

Time (min)	Manometer Readings (cm)		Head (cm)	Offset (cm)	P (Pa)	f(e)=0	e	Bed Density (kg/m^3)
0	40.0	63.8	23.8	23.8	2334.8			1000.0
8	39.5	64.0	24.5	0.7	68.7	-0.00047	0.72	1143.1
17	38.5	64.5	26.0	2.2	215.8	-0.00076	0.61	1200.7
26	37.8	65.4	27.6	3.8	372.8	-0.000030	0.55	1229.3
32	37.0	66.0	29.0	5.2	510.1	-0.000031	0.52	1245.8

Table B35: Pressure-Drop Data for Run 2,Plate 3

SG	Vials Mass before (g)	Mass After (g)	Crucibles before (g)	Crucibles after (g)	Mass of Coal (g)	Mass frac.	Coal Comb. (g)	Ash (g)	% Ash	Av. Density	% Comb
2	9.47	9.42	22.69	22.68	0.05	0.01	0.01	0.04	82.18	0.02	17.82
1.8	9.45	9.38	20.67	20.64	0.08	0.02	0.03	0.04	54.36	0.03	45.64
1.6	9.78	9.36	24.47	24.20	0.42	0.09	0.27	0.15	35.40	0.14	64.60
1.4	12.26	9.56	29.53	27.23	2.70	0.55	2.30	0.41	15.08	0.76	84.92
1.2	11.17	9.46	14.66	13.09	1.70	0.34	1.56	0.14	0.00	0.41	100.00
					4.95					1.36	

Table B36: Sink-Float Data for Run2, Plate3

Sections	Column Length (m)	Sink-Float SG	Tracer SG
Overflow	0.00	1.36	1.61
Tops	0.40	1.35	1.68
Sect 5	0.46	1.34	0.00
Sect 4	0.52	1.34	0.00
Sect 3	0.58	1.38	0.00
Sect 2	0.64	1.35	1.73
Sect 1	0.72	1.43	1.87
Underflow	1.22	1.37	2.00

Table B37: Sink-Float and Tracer Bed Profile Data for Run2, Plate3

SG Range		1.2	1.4	1.6	1.8	2	No. of Tracers	Average SG
Overflow	5mm	4	5	4	4	3		
	2mm	2	6	0	4	3		
Total		6	11	4	8	8	37	1.61
Tops	5mm	2	3	5	4	5		
	2mm	1	2	1	5	5		
Total		9	16	10	17	24	76	1.68
Sect 2	2mm		1			1		
	0.8mm			1				
Total		10	19	12	22	43	106	1.73
Sect 1	5mm	4	4	4	4	4		
	2mm		1	1		2		
Total		4	5	5	4	49	67	1.87
Underflow	2mm					1		2.00

Table B38: Density Tracer Data for Run 2,Plate 3

Time	19	min
Feed Coal	15.28	kg
Density (Average)	1510.3	kg/m^3
Coal Flow	0.53	l/min
Water Remaining in unit	10.62	kg
Feed Water Flow	2.45	l/min
Teeter Water Flow	8	l/min

Table B39: Flow Data for Run3, Plate 3

Time (min)	Manometer Readings (cm)		Head (cm)	Offset (cm)	P (Pa)	f(e)=0	e	Bed Density (kg/m^3)
0	41.0	62.3	21.3	21.3	2089.5			1000.0
4	40.3	63.1	22.8	1.5	147.2	-0.0002	0.71	1148.0
8	39.4	64.3	24.9	3.6	353.2	-0.0003	0.61	1198.0
12	37.1	66.0	28.9	7.6	745.6	-0.0004	0.53	1241.0
19	33.0	70.0	37.0	15.7	1540.2	-0.0006	0.45	1281.0

Table B40: Pressure-Drop Data for Run 3,Plate 3

SG Range	1.2	1.4	1.6	1.8	2	No. of Tracers	Average SG
Sect 5							
5mm	1	1	1	1	1		
2mm		2		2	2		
Total	1	3	1	3	3	11	1.67
Sect 4	1.2	1.4	1.6	1.8	2		
5mm		3	3	1	2		
2mm		1		3	3		
Total	0	4	3	4	5	16	1.73
Sect 3	1.2	1.4	1.6	1.8	2		
5mm			0	1	1		
2mm			1	1			
0.8mm				1			
Total	0	0	1	3	1	5	1.80
Sect 2	1.2	1.4	1.6	1.8	2		
5mm	1	2	1	1			
2mm		3		3	4		
0.8mm				1			
Total	1	5	1	5	4	16	1.68
Sect 1	1.2	1.4	1.6	1.8	2		
5mm	2		2	7	3		
2mm		5	1	1	2		
0.8mm				2	2		
Total	2	5	3	10	7	27	1.71
Tops	1.2	1.4	1.6	1.8	2		
5mm	4						
2mm	1	4					
0.8mm				2	2		
Total	5	4	0	2	2	13	1.48
Product	1.2	1.4	1.6	1.8	2		
2mm	1	1	1	1	1		
0.8mm	3	4	1	2	2		
Total	4	5	2	3	3	17	1.55
Underflow	1.2	1.4	1.6	1.8	2		
5mm		1		3	5		
2mm		1		1			
Total	0	2	0	4	5	11	1.82

Table B41: Density Tracer Data for Run 3,Plate 3

SG	Vials Mass before (g)	Mass After (g)	Crucibles before (g)	Crucibles after (g)	Mass of Coal (g)	Mass frac.	Coal Comb. (g)	Ash (g)	% Ash	Av. Density	% Comb
2	35.90	35.86	31.55	31.53	0.04	0.01	0.02	0.02	53.33	0.02	46.66
1.8	50.02	49.98	33.44	33.41	0.04	0.00	0.03	0.01	32.08	0.02	67.92
1.6	22.70	22.44	35.00	34.81	0.26	0.06	0.19	0.07	28.02	0.10	71.97
1.4	16.54	14.29	35.69	33.74	2.25	0.57	1.95	0.30	13.43	0.79	86.57
1.2	22.78	21.39	35.09	33.78	1.40	0.35	1.31	0.08	5.78	0.42	94.21
Total					3.99					1.35	

Table B42: Sink-Float Data for Run3, Plate3

Sections	Column Length (m)	Sink-Float SG	Tracer SG
Overflow	0.00	1.35	1.55
Tops	0.40	1.35	1.48
Sect 5	0.46	1.45	1.67
Sect 4	0.52	1.38	1.73
Sect 3	0.58	1.38	1.80
Sect 2	0.64	1.39	1.68
Sect 1	0.72	1.36	1.71
Underflow	1.22	1.42	1.82

Table B43: Sink-Float and Tracer Bed Profile Data for Run3, Plate3

Time	23	min
Feed Coal	16.83	kg
Density (Average)	1510.3	kg/m^3
Coal Flow	0.48	l/min
Water Remaining in unit	9.64	kg
Feed Water Flow	2.60	l/min
Teeter water flow	6	l/min

Table B44: Flow Data for Run 1,Plate 4

Time (min)	Manometer Readings (cm)		Head (cm)	Offset (cm)	P (Pa)	f(e)=0	e	Bed Density (kg/m^3)
0	41.6	61.7	20.1	20.1	1971.8			1000.0
5	44.7	65.0	20.3	0.2	19.6	-0.0003	0.84	1082.7
10	42.3	66.3	24.0	3.9	382.6	-0.0001	0.56	1225.8
15	37.4	68.2	30.8	10.7	1049.6	-0.0001	0.45	1279.0
22	33.1	69.4	36.3	16.2	1589.2	-0.0001	0.41	1299.8

Table B45: Pressure-Drop Data for Run 1,Plate 4

SG Range	1.2	1.4	1.6	1.8	2	No. of tracers	Avg SG
Sect 5							
5mm	1	4		4	2		
2mm	2	1		1	2		
0.8mm		1		1			
Total	3	6	0	6	4	19	1.62
Sect 4	1.2	1.4	1.6	1.8	2		
5mm		1					
2mm	1			1	1		
0.8mm		1			1		
Total	1	2	0	1	2	6	1.63
Sect 3	1.2	1.4	1.6	1.8	2		
5mm	1	1					
2mm		1					
Total	1	2	0	0	0	3	1.33
Sect 2	1.2	1.4	1.6	1.8	2		
5mm	1	3	3	4	1		
2mm		5		1	3		
Total	1	8	3	5	4	21	1.63
Sect 1	1.2	1.4	1.6	1.8	2		
5mm	1	1	2		2		
2mm		1	1	2			
Total	1	2	3	2	2	10	1.64
Tops	1.2	1.4	1.6	1.8	2		
5mm	4	1	3	2	3		
2mm	5	3	0	2	1		
Total	9	4	3	4	4	24	1.52
Product	1.2	1.4	1.6	1.8	2		
5mm							
2mm	1						
Total	1	0	0	0	0	1	1.20
Underflow	1.2	1.4	1.6	1.8	2		
5mm	3	6	6	9	8		
2mm	2	5		3	6		
Total	5	11	6	12	14	48	1.68

Table B46: Density Tracer Data for Run 1, Plate 4

SG	Vials Mass before (g)	Mass After (g)	Crucibles before (g)	Crucibles after (g)	Mass of Coal (g)	Mass frac.	Coal Comb. (g)	Ash (g)	% Ash	Av. Density	% Comb
2	9.63	9.46	20.56	20.48	0.17	0.13	0.07	0.10	57.08	0.26	42.92
1.8	9.58	9.41	27.48	27.35	0.17	0.13	0.13	0.03	20.48	0.23	79.52
1.6	9.33	9.22	20.76	20.67	0.10	0.08	0.09	0.01	11.15	0.12	88.85
1.4	9.84	9.36	21.35	20.91	0.48	0.36	0.45	0.03	6.99	0.50	93.01
1.2	9.72	9.32	21.01	20.62	0.41	0.31	0.39	0.02	4.97	0.37	95.03
Total					1.33					1.48	

Table B47: Sink-Float Data for Run1, Plate4

Sections	Column Length (m)	Sink-Float SG	Tracer SG
Overflow	0.00	1.48	1.20
Tops	0.40	1.35	1.52
Sect 5	0.46	1.33	1.62
Sect 4	0.52	1.33	1.63
Sect 3	0.58	1.41	1.33
Sect 2	0.64	1.41	1.63
Sect 1	0.72	1.42	1.64
Underflow	1.22	1.42	1.68

Table B48: Sink-Float and Tracer Bed Profile Data for Run1, Plate4

Time	28.4	min
Feed Coal	15.59	kg
Density (Average)	1510.3	kg/m^3
Coal Flow	0.36	l/min
Water Remaining in unit	7.595	kg
Feed Water Flow	2.33	l/min
Teeter water flow	3	l/min

Table B49: Flow Data for Run 2,Plate 4

Time (min)	Manometer Readings (cm)		Head (cm)	Offset (cm)	P (Pa)	f(e)=0	e	Bed Density (kg/m^3)
0	41.0	62.0	21.0	21.0	2060.1			1000.0
7.1	42.2	64.9	22.7	1.7	166.8	-0.0003	0.63	1190.5
14.5	36.8	66.0	29.2	8.2	804.4	0.0001	0.47	1271.8
22.1	32.7	70.0	37.3	16.3	1599.0	0.0002	0.40	1305.6
28.4	30.1	72.4	42.3	21.3	2089.5	0.0002	0.38	1318.1

Table B50: Pressure-Drop Data for Run 2,Plate 4

SG Range	1.2	1.4	1.6	1.8	2	No. of tracers	Avg SG
Sect 5							
5mm							
2mm							
0.8mm							
Total	0	0	0	0	0	0	0.00
Sect 4	1.2	1.4	1.6	1.8	2		
5mm							
2mm				1	1		
0.8mm							
Total	0	0	0	1	1	2	1.90
Sect 3	1.2	1.4	1.6	1.8	2		
5mm	4	5	4	3	4		
2mm		3		4	3		
Total	4	8	4	7	0	30	1.63
Sect 2	1.2	1.4	1.6	1.8	2		
5mm		1		3	1		
2mm		3		1			
Total	0	4	0	4	1	9	1.64
Sect 1	1.2	1.4	1.6	1.8	2		
5mm					1		
2mm							
Total	0	0	0	0	1	1	2.00
Tops	1.2	1.4	1.6	1.8	2		
5mm	3	6	4	7	6		
2mm		5		2	5		
Total	3	11	4	9	11	38	1.67
Product	1.2	1.4	1.6	1.8	2		
5mm							
2mm			2				
Total	0	0	2	0	0	2	1.60
Underflow	1.2	1.4	1.6	1.8	2		
5mm	4	5	5	6	4		
2mm		5		5	5		
Total	4	10	5	11	9	39	1.66

Table B51: Density Tracer Data for Run 2,Plate4

SG	Vials Mass before (g)	Mass After (g)	Crucibles before (g)	Crucibles after (g)	Mass of Coal (g)	Mass frac.	Coal Comb. (g)	Ash (g)	% Ash	Av. Density	% Comb
2	9.58	9.43	31.83	31.79	0.15	0.13	0.05	0.10	69.34	0.27	30.66
1.8	9.54	9.39	34.75	34.63	0.15	0.13	0.12	0.03	18.88	0.24	81.12
1.6	9.61	9.39	31.74	31.54	0.22	0.20	0.19	0.03	11.75	0.32	88.25
1.4	9.74	9.58	33.55	33.42	0.16	0.15	0.14	0.02	14.43	0.20	85.57
1.2	9.91	9.48	33.87	33.48	0.43	0.39	0.39	0.05	10.57	0.47	89.43
Total					1.11					1.50	

Table B52: Sink-Float Data for Run2, Plate4

Sections	Column Length (m)	Sink-Float SG	Tracer SG
Overflow	0.00	1.50	1.60
Tops	0.40	1.43	1.67
Sect 5	0.46	1.46	0.00
Sect 4	0.52	1.41	1.90
Sect 3	0.58	1.41	1.63
Sect 2	0.64	1.32	1.64
Sect 1	0.72	1.37	2.00
Underflow	1.22	1.37	1.66

Table B53: Sink-Float and Tracer Bed Profile Data for Run2, Plate4

Time	18	min
Feed Coal	13.76	kg
Density (Average)	1510.3	kg/m^3
Coal Flow	0.51	l/min
Water Remaining in unit	10.30	kg
Feed Water Flow	2.34	l/min
Teeter water flow	8	l/min

Table B54: Flow Data for Run 3,Plate 4

Time (min)	Manometer Readings (cm)		Head (cm)	Offset (cm)	P (Pa)	f(e)=0	e	Bed Density (kg/m^3)
0	41.0	61.0	20.0	20.0	1962.0			1000.0
3.4	42.1	63.5	21.4	1.4	137.3	-0.0003	0.69	1160.5
7.5	40.5	64.0	23.5	3.5	343.4	-0.0005	0.59	1210.8
12	37.0	65.0	28.0	8.0	784.8	-0.0009	0.50	1256.3
18	33.0	69.0	36.0	16	1569.6	0.0000	0.43	1292.6

Table B55: Pressure-Drop Data for Run 3,Plate 4

SG Range	1.2	1.4	1.6	1.8	2	No. of tracers	Avg SG
Sect 5							
5mm	2						
2mm		2					
0.8mm							
Total	2	2	0	0	0	4	1.30
Sect 4	1.2	1.4	1.6	1.8	2		
5mm	2		1				
2mm		1					
0.8mm							
Total	2	1	1	0	0	4	1.35
Sect 3	1.2	1.4	1.6	1.8	2		
5mm	1	2	1	3	1		
2mm		2		3	4		
Total	1	4	1	6	5	17	1.72
Sect 2	1.2	1.4	1.6	1.8	2		
5mm		3	3	4	2		
2mm		2		1	2		
Total	0	5	3	5	4	17	1.69
Sect 1	1.2	1.4	1.6	1.8	2		
5mm	1	3	3	2	4		
2mm		2		2	2		
Total	1	5	3	4	6	19	1.69
Tops	1.2	1.4	1.6	1.8	2		
5mm	1						
2mm		1					
Total	1	1	0	0	0	2	1.30
Product	1.2	1.4	1.6	1.8	2		
5mm							
2mm							
Total	0	0	0	0	0	0	0.00
Underflow	1.2	1.4	1.6	1.8	2		
5mm	3	9	6	10	9		
2mm		6	1	6	5		
Total	3	15	7	16	14	55	1.68

Table B56: Density Tracer Data for Run 3,Plate 4

SG	Vials Mass before (g)	Mass After (g)	Crucibles before (g)	Crucibles after (g)	Mass of Coal (g)	Mass frac.	Coal Comb. (g)	Ash (g)	% Ash	Av. Density	% Comb
2	9.77	9.46	33.69	33.56	0.31	0.22	0.13	0.17	56.99	0.44	43.01
1.8	9.46	9.35	33.56	33.48	0.11	0.08	0.08	0.04	32.59	0.14	67.41
1.6	9.49	9.41	35.09	35.04	0.07	0.053	0.06	0.02	24.01	0.08	75.99
1.4	10.02	9.51	32.20	31.75	0.51	0.37	0.45	0.06	11.87	0.52	88.13
1.2	9.69	9.31	31.91	31.57	0.38	0.28	0.34	0.04	10.52	0.33	89.48
Total					1.38					1.51	

Table B57: Sink-Float Data for Run3, Plate4

Sections	Column Length (m)	Sink-Float SG	Tracer SG
Overflow	0.00	1.51	1.30
Tops	0.40	1.40	1.35
Sect 5	0.46	1.35	1.72
Sect 4	0.52	1.35	1.69
Sect 3	0.58	1.39	1.69
Sect 2	0.64	1.38	1.30
Sect 1	0.72	1.38	0.00
Underflow	1.22	1.43	1.68

Table B58: Sink-Float and Tracer Bed Profile Data for Run3, Plate4

Time	22	min
Feed Coal	15.93	kg
Density (Average)	1510.3	kg/m^3
Coal Flow	0.48	l/min
Water Remaining in unit	10.30	kg
Feed Water Flow	1.99	l/min
Teeter water flow	6	l/min

Table B59: Flow Data for Run 1,Plate 5

Time (min)	Manometer Readings (cm)		Head (cm)	Offset (cm)	P (Pa)	f(e)=0	e	Bed Density (kg/m^3)
0	40.8	61.5	20.7	20.7	2030.7			1000.0
5	44.0	66.0	22.0	1.3	127.5	-0.00087	0.67	1166.0
10	44.0	67.0	23.0	2.3	225.6	-0.000041	0.62	1196.0
15	39.3	68.2	28.9	8.2	804.4	-0.000078	0.48	1264.2
22	34.0	71.0	37.0	16.3	1599.0	-0.00012	0.41	1299.1

Table B60: Pressure-Drop Data for Run 1,Plate 5

SG Range	1.2	1.3	1.4	1.5	1.6	1.8	2	No. of tracers	Avg SG
Sect 5									
5mm									
2mm									
1.5mm									
Total	0	0	0	0	0	0	0	0	0.00
Sect 4	1.2	1.3	1.4	1.5	1.6	1.8	2		
5mm									
2mm									
1.5mm									
Total	0	0	0	0	0	0	0	0	0.00
Sect 3	1.2	1.3	1.4	1.5	1.6	1.8	2		
5mm	2		6		3	6	4		
2mm			3	4		5	5		
1.5mm									
Total	2	0	9	4	3	11	9	38	1.67
Sect 2	1.2	1.3	1.4	1.5	1.6	1.8	2		
5mm	1				3				
2mm						1			
1.5mm							1		
Total	1	0	0	0	3	1	1	6	1.63
Sect 1	1.2	1.3	1.4	1.5	1.6	1.8	2		
5mm	2				4	4	5		
2mm			2			2	4		
1.5mm									
Total	2	0	2	0	4	6	9	23	1.76
Tops	1.2	1.3	1.4	1.5	1.6	1.8	2		
5mm	4		6		5	6	5		
2mm	1		10	5		2	4		
1.5mm			2	3		5	4		
Total	5	0	18	8	5	13	13	62	1.62
Product	1.2	1.3	1.4	1.5	1.6	1.8	2		
5mm									
2mm		10		1					
1.5mm		7	5	1		1	1		
Total	0	17	5	2	0	1	1	26	1.38
Underflow	1.2	1.3	1.4	1.5	1.6	1.8	2		
5mm			2		1	3	2		
2mm				1		4	1		
1.5mm				2		1	3		
Total	0	0	2	3	1	8	6	20	1.77

Table B61: Density Tracer Data for Run 1,Plate 5

SG	Vials Mass before (g)	Mass After (g)	Crucibles before (g)	Crucibles after (g)	Mass of Coal (g)	Mass frac.	Coal Comb. (g)	Ash (g)	% Ash	Av. Density	% Comb
2	9.58	9.35	22.75	22.55	0.23	0.09	0.19	0.04	15.82	0.18	84.18
1.8	9.53	9.33	24.19	24.02	0.20	0.08	0.1674	0.04	18.02	0.14	81.98
1.6	9.55	9.39	55.59	55.45	0.16	0.06	0.14	0.03	15.62	0.10	84.38
1.4	10.45	9.27	38.31	37.28	1.17	0.46	1.03	0.15	12.37	0.64	87.63
1.2	10.17	9.37	13.78	13.01	0.81	0.31	0.77	0.04	4.69	0.38	95.31
Total					2.57					1.44	

Table B62: Sink-Float Data for Run1, Plate5

Sections	Column Length (m)	Sink-Float SG	Tracer SG
Overflow	0.00	1.44	0.00
Tops	0.40	1.37	0.00
Sect 5	0.46	1.43	1.67
Sect 4	0.52	1.43	1.63
Sect 3	0.58	1.39	1.76
Sect 2	0.64	1.37	1.62
Sect 1	0.72	1.36	1.38
Underflow	1.22	1.37	1.77

Table B63: Sink-Float and Tracer Bed Profile Data for Run1, Plate5

Time	31	min
Feed Coal	15.40	kg
Density (Average)	1510.3	kg/m^3
Coal Flow	0.33	l/min
Water Remaining in unit	8.22	kg
Feed Water Flow	2.49	l/min
Teeter water flow	3	l/min

Table B64: Flow Data for Run 2,Plate 5

Time (min)	Manometer Readings (cm)		Head (cm)	Offset (cm)	P (Pa)	f(e)=0	e	Bed Density (kg/m^3)
0	41.0	61.0	20.0	20.0	1962.0			1000.0
8	42.2	63.0	20.8	0.8	78.5	-0.0001	0.70	1152.6
16	37.5	64.6	27.1	7.1	696.5	-0.0001	0.48	1264.2
23	33.0	69.0	36.0	16.0	1569.6	-0.0001	0.40	1304.4
31	30.0	71.5	41.5	21.5	2109.2	-0.0001	0.38	1318.3

Table B65: Pressure-Drop Data for Run 2,Plate 5

SG Range	1.2	1.3	1.4	1.5	1.6	1.8	2	No. of tracers	Avg SG
Sect 5									
5mm									
2mm									
1.5mm			1						
Total	0	0	1	0	0	0	0	1	1.40
Sect 4	1.2	1.3	1.4	1.5	1.6	1.8	2		
5mm									
2mm						1			
1.5mm		1							
Total	0	1	0	0	0	1	0	2	1.55
Sect 3	1.2	1.3	1.4	1.5	1.6	1.8	2		
5mm	1		2		3	3	5		
2mm			1	4		3	3		
1.5mm		2	1	2		3	2		
Total	1	2	4	6	3	9	10	35	1.70
Sect 2	1.2	1.3	1.4	1.5	1.6	1.8	2		
5mm	2		4		2	3			
2mm			4				2		
1.5mm			2	4		1	4		
Total	2	0	10	4	2	4	6	28	1.60
Sect 1	1.2	1.3	1.4	1.5	1.6	1.8	2		
5mm	3		6		5	4	4		
2mm			4	3		2	4		
1.5mm			1	4		4	4		
Total	3	0	11	7	5	10	12	48	1.66
Tops	1.2	1.3	1.4	1.5	1.6	1.8	2		
5mm	4		5		4	7	5		
2mm			4	6		6			
1.5mm			4	6		6	4		
Total	4	0	13	12	4	19	9	61	1.63
Product	1.2	1.3	1.4	1.5	1.6	1.8	2		
5mm	none								
2mm									
1.5mm									
Total	0	0	0	0	0	0	0	0	0.00
Underflow									
5mm							2	2	
2mm				1	2				
1.5mm			2						
Total	0	0	2	1	2	0	2	7	1.64

Table B66: Density Tracer Data for Run 2,Plate 5

SG	Vials Mass before (g)	Mass After (g)	Crucibles before (g)	Crucibles after (g)	Mass of Coal (g)	Mass frac.	Coal Comb. (g)	Ash (g)	% Ash	Av. Density	% Comb
2	9.62	9.45	22.69	22.60	0.17	0.04	0.09	0.07	44.06	0.08	55.94
1.8	9.71	9.46	24.24	24.07	0.26	0.06	0.18	0.08	30.86	0.10	69.14
1.6	10.12	9.30	56.23	55.55	0.82	0.18	0.69	0.14	16.38	0.30	83.62
1.4	11.63	9.41	39.35	37.28	2.22	0.50	2.07	0.16	7.03	0.70	92.97
1.2	10.31	9.31	13.98	13.03	0.99	0.22	0.95	0.04	4.45	0.27	95.55
					4.46					1.45	

Table B67: Sink-Float Data for Run2, Plate5

Sections	Column Length (m)	Sink-Float SG	Tracer SG
Overflow	0.00	1.45	1.40
Tops	0.40	1.34	1.55
Sect 5	0.46	1.38	1.69
Sect 4	0.52	1.39	1.60
Sect 3	0.58	1.37	1.66
Sect 2	0.64	1.35	1.63
Sect 1	0.72	1.40	0.00
Underflow	1.22	1.39	1.64

Table B68: Sink-Float and Tracer Bed Profile Data for Run2, Plate5

Time	19	min
Feed Coal	14.60	kg
Density (Average)	1510.3	kg/m^3
Coal Flow	0.51	l/min
Water Remaining in unit	10.53	kg
Feed Water Flow	2.87	l/min
Teeter water flow	8	l/min

Table B69: Flow Data for Run 3,Plate 5

Time (min)	Manometer Readings (cm)		Head (cm)	Offset (cm)	P (Pa)	f(e)=0	e	Bed Density (kg/m^3)
0	41.0	61.0	20.0	20.0	1962.0			1000.0
4	43.0	63.1	20.1	0.1	9.8	-0.0006	0.91	1048.3
9	44.0	65.2	21.2	1.2	117.7	-0.0002	0.70	1151.7
13	41.6	67.3	25.7	5.7	559.2	-0.0006	0.53	1237.4
19	30.6	65.4	34.8	14.8	1451.9	0.0000	0.44	1288.3

Table B70: Pressure-Drop Data for Run 3,Plate 5

SG Range	1.2	1.3	1.4	1.5	1.6	1.8	2	No. of tracers	Avg SG
Overflow									
5	1								
2									
1.5		3	2	1					
Total	1	3	2	1	0	0	0	7	1.34
Tops	1.2	1.3	1.4	1.5	1.6	1.8			
5	4								
2			2						
1.5			2	6					
Total	4	0	4	6	0	0	0	14	1.39
Sect 1	1.2	1.3	1.4	1.5	1.6	1.8			
5			6		6	4	3		
2			4	4		3	2		
1.5			1	5		4	3		
Total	0	0	11	9	6	11	8	45	1.65
Sect 2	1.2	1.3	1.4	1.5	1.6	1.8			
5	4						1		
2			2	1		1			
1.5				2		1	3		
Total	4	0	2	3	0	2	4	15	1.58
Sect 3	1.2	1.3	1.4	1.5	1.6	1.8			
5			2		2	2	3		
2				1		1	2		
1.5							1		
Total	0	0	2	1	2	3	6	14	1.78
Sect 4	1.2	1.3	1.4	1.5	1.6	1.8			
5	1								
2			2	1			1		
1.5			2	4		5	1		
Total	1	0	4	5	0	5	2	17	1.61
Sect 5	1.2	1.3	1.4	1.5	1.6	1.8			
5	1								
2			2	1			1		
1.5									
Total	1	0	2	1	0	0	1	5	1.50
Underflow	1.2	1.3	1.4	1.5	1.6	1.8			
5			4		3	9	6		
2			1			7	6		
1.5			1			3	4		
Total	0	0	6	0	3	19	16	44	1.80

Table B71: Density Tracer Data for Run 3,Plate 5

SG	Vials Mass before (g)	Mass After (g)	Crucibles before (g)	Crucibles after (g)	Mass of Coal (g)	Mass frac.	Coal Comb. (g)	Ash (g)	% Ash	Av. Density	% Comb
2	9.50	9.42	22.59	22.53	0.08	0.02	0.06	0.02	19.30	0.04	80.70
1.8	9.46	9.36	24.07	23.99	0.10	0.03	0.07	0.03	26.73	0.05	73.27
1.6	9.65	9.47	37.36	37.21	0.17	0.05	0.15	0.03	16.32	0.08	83.68
1.4	11.17	9.53	56.97	55.67	1.64	0.45	1.30	0.34	20.73	0.62	79.27
1.2	10.93	9.25	14.67	13.31	1.68	0.46	1.36	0.32	19.19	0.55	80.81
Total					3.67					1.34	

Table B72: Sink-Float Data for Run3, Plate5

Sections	Column Length (m)	Sink-Float SG	Tracer SG
Overflow	0.00	1.34	1.34
Tops	0.40	1.46	1.39
Sect 5	0.46	1.34	1.65
Sect 4	0.52	1.38	1.58
Sect 3	0.58	1.38	1.78
Sect 2	0.64	1.41	1.61
Sect 1	0.72	1.37	1.50
Underflow	1.22	1.38	1.80

Table B73: Sink-Float and Tracer Bed Profile Data for Run3, Plate5

Time	21	min
Feed Coal	14.50	kg
Density (Average)	1510.3	kg/m^3
Coal Flow	0.46	l/min
Water Remaining in unit	9.45	kg
Feed Water Flow	2.92	l/min
Teeter water flow	6	l/min

Table B74: Flow Data for Run 1,Plate 6

Time (min)	Manometer Readings (cm)		Head (cm)	Offset (cm)	P (Pa)	f(e)=0	e	Bed Density (kg/m^3)
0	41.0	60.5	19.5	19.5	1913.0			1000
5	42.0	61.7	19.7	0.2	19.6	-0.0002	0.85	1077.7
11	41.5	63.8	22.3	2.8	274.7	-0.0005	0.60	1204.5
16	37.0	65.0	28.0	8.5	833.9	0.0000	0.48	1264.3
21	34.0	68.0	34.0	14.5	1422.5	0.0000	0.43	1291.8

Table B75: Pressure-Drop Data for Run 1,Plate 6

SG Range	1.2	1.3	1.4	1.5	1.6	1.8	2	No. of tracers	Avg SG
Overflow									
5									
2									
1.5		3							
Total	0	3	0	0	0	0	0	3	1.30
Tops	1.2	1.3	1.4	1.5	1.6	1.8	2		
5	4		2		2	1	2		
2	1		3	2			5		
1.5			2	4		2	1		
Total	5	0	7	6	2	3	8	31	1.59
Sect 1	1.2	1.3	1.4	1.5	1.6	1.8	2		
5	1		3		4	4	5		
2			3	4		5	4		
1.5			2	4		1	4		
Total	1	0	8	8	4	10	13	44	1.70
Sect 2	1.2	1.3	1.4	1.5	1.6	1.8	2		
5	1		2		3	5	1		
2	1		5	3		2			
1.5			2	3		4	2		
Total	2	0	9	6	3	11	3	34	1.61
Sect 3	1.2	1.3	1.4	1.5	1.6	1.8	2		
5	1								
2			1						
1.5			1						
Total	1	0	2	0	0	0	0	3	1.33
Sect 4	1.2	1.3	1.4	1.5	1.6	1.8	2		
5	2				1				
2			1				2		
1.5									
Total	2	0	1	0	1	0	2	6	1.57
Sect 5	1.2	1.3	1.4	1.5	1.6	1.8	2		
5	1		2		2	5	3		
2			1	2		2			
1.5			1	3		2	1		
Total	1	0	4	5	2	9	4	25	1.67
Underflow	1.2	1.3	1.4	1.5	1.6	1.8	2		
5			7		2	4	4		
2	1					2	3		
1.5						1	2		
Total	1	0	7	0	2	7	9	26	1.72

Table B76: Density Tracer Data for Run 1,Plate 6

SG	Vials Mass before (g)	Mass After (g)	Crucibles before (g)	Crucibles after (g)	Mass of Coal (g)	Mass frac.	Coal Comb. (g)	Ash (g)	% Ash	Av. Density	% Comb
2	9.43	9.36	24.04	23.98	0.07	0.02	0.06	0.02	21.67	0.03	78.33
1.8	9.58	9.39	22.71	22.54	0.19	0.04	0.17	0.02	12.72	0.08	87.28
1.6	9.58	9.28	37.43	37.16	0.30	0.07	0.27	0.03	11.16	0.11	88.84
1.4	12.08	9.27	58.11	55.77	2.81	0.64	2.34	0.47	16.82	0.89	83.18
1.2	10.41	9.36	14.04	13.05	1.04	0.24	0.99	0.05	5.13	0.28	94.87
Total					4.41					1.39	

Table B77: Sink-Float Data for Run1, Plate6

Sections	Column Length (m)	Sink-Float SG	Tracer SG
Overflow	0.00	1.39	1.30
Tops	0.40	1.32	1.59
Sect 5	0.46	1.41	1.70
Sect 4	0.52	1.38	1.61
Sect 3	0.58	1.37	1.33
Sect 2	0.64	1.39	1.57
Sect 1	0.72	1.40	1.67
Underflow	1.22	1.42	1.72

Table B78: Sink-Float and Tracer Bed Profile Data for Run1, Plate6

Time	25	min
Feed Coal	17.92	kg
Density (Average)	1510.3	kg/m^3
Coal Flow	0.48	l/min
Water Remaining in unit	7.30	kg
Feed Water Flow	2.05	l/min
Teeter water flow	3	l/min

Table B79: Flow Data for Run 2,Plate 6

Time (min)	Manometer Readings (cm)		Head (cm)	Offset (cm)	P (Pa)	f(e)=0	e	Bed Density (kg/m^3)
0	41.0	61.0	20.0	20.0	1962.0			1000.0
7	40.8	60.9	20.1	0.1	9.8	-0.0010	0.86	1072.2
13	36.2	65.6	29.4	9.4	922.1	-0.0003	0.46	1278.0
21	32.0	70.0	38.0	18.0	1765.8	-0.0005	0.39	1309.6
25	30.0	71.0	41.0	21.0	2060.1	-0.0005	0.38	1316.8

Table B80: Pressure-Drop Data for Run 2,Plate 6

SG Range	1.2	1.3	1.4	1.5	1.6	1.8	2	No. of tracers	Avg SG
Overflow									
5	2		6		2	1	1		
2			4	2		1	1		
1.5			1	3		1	1		
Total	2	0	11	5	2	3	3	26	1.53
Tops	1.2	1.3	1.4	1.5	1.6	1.8	2		
5	2		1		3	6	4		
2			2	4		2	4		
1.5			2	5			3		
Total	2	0	5	9	3	8	11	38	1.69
Sect 5	1.2	1.3	1.4	1.5	1.6	1.8	2		
5	3		4		5	5	4		
2			3	3		2	5		
1.5				3		3	1		
Total	3	0	7	6	5	10	10	41	1.67
Sect 4	1.2	1.3	1.4	1.5	1.6	1.8	2		
5			none						
2									
1.5									
Total	0	0	0	0	0	0	0	0	0.00
Sect 3	1.2	1.3	1.4	1.5	1.6	1.8	2		
5									
2									
1.5				1					
Total	0	0	0	1	0	0	0	1	1.50
Sect 2	1.2	1.3	1.4	1.5	1.6	1.8	2		
5	1								
2			1						
1.5				1					
Total	1	0	1	1	0	0	0	3	1.37
Sect 1	1.2	1.3	1.4	1.5	1.6	1.8	2		
5	2		6		3	6	6		
2			5	4		4	4		
1.5			2			4	5		
Total	2	0	13	4	3	14	15	51	1.70
Underflow	1.2	1.3	1.4	1.5	1.6	1.8	2		
5					1	1			
2									
1.5						1			
Total	0	0	0	0	1	2	0	3	1.73

Table B81: Density Tracer Data for Run 2,Plate 6

SG	Vials Mass before (g)	Mass After (g)	Crucibles before (g)	Crucibles after (g)	Mass of Coal (g)	Mass frac.	Coal Comb. (g)	Ash (g)	% Ash	Av. Density	% Comb
2	9.46	9.4203	24.00	23.98	0.04	0.01	0.02	0.03	43.38	0.02	56.62
1.8	9.47	9.3832	55.28	55.22	0.09	0.02	0.06	0.03	30.34	0.03	69.66
1.6	9.75	9.3686	37.50	37.23	0.38	0.08	0.27	0.11	30.05	0.12	69.96
1.4	12.12	9.5626	25.17	22.87	2.64	0.54	2.29	0.34	13.00	0.75	87.00
1.2	11.24	9.48	14.75	13.12	1.76	0.36	1.63	0.13	7.42	0.43	92.58
Total					4.91					1.35	

Table B82: Sink-Float Data for Run2, Plate6

Sections	Column Length (m)	Sink-Float SG	Tracer SG
Overflow	0.0	1.35	1.53
Tops	0.40	1.43	1.69
Sect 5	0.46	1.37	1.67
Sect 4	0.52	1.41	0.00
Sect 3	0.58	1.39	1.50
Sect 2	0.64	1.37	1.37
Sect 1	0.72	1.41	1.70
Underflow	1.22	1.38	1.73

Table B83: Sink-Float and Tracer Bed Profile Data for Run2, Plate6

Time	18	min
Feed Coal	12.49	kg
Density (Average)	1510.3	kg/m^3
Coal Flow	0.46	l/min
Water Remaining in unit	10.71	kg
Feed Water Flow	2.35	l/min
Teeter water flow	8	l/min

Table B84: Flow Data for Run 3,Plate 6

Time (min)	Manometer Readings (cm)		Head (cm)	Offset (cm)	P (Pa)	f(e)=0	e	Bed Density (kg/m^3)
0	41.0	61.0	20.0	20.0	1962.0			1000.0
4	41.2	61.5	20.3	0.3	29.4	-0.0006	0.83	1082.0
8	39.4	62.6	23.2	3.2	313.9	0.0000	0.60	1201.8
12	36.5	65.0	28.5	8.5	833.9	-0.0001	0.50	1256.3
18	32.8	69.0	36.2	16.2	1589.2	-0.0001	0.43	1290.4

Table B85: Pressure-Drop Data for Run 3,Plate 6

SG Range	1.2	1.3	1.4	1.5	1.6	1.8	2	No. of tracers	Avg SG
Overflow									
5									
2									
1.5			1						
Total	0	0	1	0	0	0	0	1	1.40
Tops	1.2	1.3	1.4	1.5	1.6	1.8	2		
5									
2		1		1					
1.5			3	1					
Total	0	1	3	2	0	0	0	6	1.42
Sect 5	1.2	1.3	1.4	1.5	1.6	1.8	2		
5	4								
2		1							
1.5		1	2	1					
Total	4	2	2	1	0	0	0	9	1.30
Sect 4	1.2	1.3	1.4	1.5	1.6	1.8	2		
5	2								
2			1						
1.5			1						
Total	2	0	2	0	0	0	0	4	1.30
Sect 3	1.2	1.3	1.4	1.5	1.6	1.8	2		
5									
2			2						
1.5				1					
Total	0	0	2	1	0	0	0	3	1.43
Sect 2	1.2	1.3	1.4	1.5	1.6	1.8	2		
5					2	3	2		
2			2			3			
1.5			1	2		1			
Total	0	0	3	2	2	7	2	16	1.69
Sect 1	1.2	1.3	1.4	1.5	1.6	1.8	2		
5	1		6		3	8	4		
2			3	3		3	5		
1.5				3		2	4		
Total	1	0	9	6	3	13	13	45	1.71
Underflow	1.2	1.3	1.4	1.5	1.6	1.8	2		
5	3		11		8	8	9		
2			5	6		4	9		
1.5				4		3	7		
Total	3	0	16	10	8	15	25	77	1.70

Table B86: Density Tracer Data for Run 3,Plate 6

SG	Vials Mass before (g)	Mass After (g)	Crucibles before (g)	Crucibles after (g)	Mass of Coal (g)	Mass frac.	Coal Comb. (g)	Ash (g)	% Ash	Av. Density	% Comb
2	9.65	9.41	22.74	22.57	0.24	0.06	0.17	0.07	27.77	0.11	72.23
1.8	9.70	9.43	55.19	55.00	0.27	0.06	0.18	0.09	33.38	0.11	66.62
1.6	9.90	9.24	37.78	37.25	0.66	0.15	0.52	0.14	20.48	0.24	79.52
1.4	11.49	9.37	25.09	23.28	2.12	0.49	1.81	0.31	14.74	0.69	85.26
1.2	10.31	9.29	14.01	13.07	1.01	0.24	0.94	0.08	7.57	0.28	92.43
Total					4.30					1.43	

Table B87: Sink-Float Data for Run3, Plate6

Sections	Column Length (m)	Sink-Float SG	Tracer SG
Overflow	0.00	1.43	1.40
Tops	0.40	1.36	1.42
Sect 5	0.46	1.41	1.30
Sect 4	0.52	1.31	1.30
Sect 3	0.58	1.35	1.43
Sect 2	0.64	1.40	1.69
Sect 1	0.72	1.41	1.71
Underflow	1.22	1.41	1.70

Table B88: Sink-Float and Tracer Bed Profile Data for Run3, Plate6

Time	20	min
Feed Coal	13.36	kg
Density (Average)	1510.3	kg/m^3
Coal Flow	0.44	l/min
Water Remaining in unit	10.90	kg
Feed Water Flow	2.20	l/min
Teeter water flow	6	l/min

Table B89: Flow Data for Run 1,Plate 7

Time (min)	Manometer Readings (cm)		Head (cm)	Offset (cm)	P (Pa)	f(e)=0	e	Bed Density (kg/m^3)
0	40.0	62.0	22.0	22.0	2158.2			1000.0
6	36.0	66.0	30.0	8.0	784.8	-0.0001	0.50	1254.1
11	33.4	68.0	34.6	12.6	1236.1	-0.0001	0.45	1278.4
15	30.8	71.0	40.2	18.2	1785.4	-0.0001	0.42	1297.3
20	29.5	71.8	42.3	20.3	1991.4	-0.0001	0.41	1302.8

Table B90: Pressure-Drop Data for Run 1,Plate 7

SG Range	1.2	1.3	1.4	1.5	1.6	1.8	2	No. of tracers	Avg SG
Overflow									
5									
2									
1.5			1						
Total	0	0	1	0	0	0	0	1	1.40
Tops	1.2	1.3	1.4	1.5	1.6	1.8	2		
5	2								
2									
1.5			2						
Total	2	0	2	0	0	0	0	4	1.30
Sect 5	1.2	1.3	1.4	1.5	1.6	1.8	2		
5	3		4		1	2	2		
2	1		4	2		1	4		
1.5			5	2		2	2		
Total	4	0	13	4	1	5	8	35	1.59
Sect 4	1.2	1.3	1.4	1.5	1.6	1.8	2		
5			2		3	3	1		
2				3		1	1		
1.5						2	2		
Total	0	0	2	3	3	6	4	18	1.72
Sect 3	1.2	1.3	1.4	1.5	1.6	1.8	2		
5	1					1	2		
2			1			1			
1.5						1			
Total	1	0	1	0	0	3	2	7	1.71
Sect 2	1.2	1.3	1.4	1.5	1.6	1.8	2		
5	2		3		2	3	1		
2			4	2		1	3		
1.5				2		2	4		
Total	2	0	7	4	2	6	8	29	1.66
Sect 1	1.2	1.3	1.4	1.5	1.6	1.8	2		
5			3		4	8	8		
2				5		3	5		
1.5				3		3	3		
Total	0	0	3	8	4	14	16	45	1.77
Underflow	1.2	1.3	1.4	1.5	1.6	1.8	2		
5	2		5		4	2	1		
2			4	2		1	2		
1.5				3		1	1		
Total	2	0	9	5	4	4	4	28	1.58

Table B91: Density Tracer Data for Run 1, Plate 7

SG	Vials Mass before (g)	Mass After (g)	Crucibles before (g)	Crucibles after (g)	Mass of Coal (g)	Mass frac.	Coal Comb. (g)	Ash (g)	% Ash	Av. Density	% Comb
2	9.47	9.41	20.79	20.74	0.06	0.02	0.05	0.01	19.39	0.03	80.61
1.8	9.40	9.35	54.85	54.81	0.05	0.01	0.04	0.01	17.63	0.03	82.37
1.6	9.56	9.42	37.25	37.13	0.14	0.04	0.12	0.02	13.53	0.06	86.47
1.4	11.60	9.50	24.63	22.78	2.10	0.55	1.84	0.26	12.26	0.77	87.74
1.2	10.74	9.27	14.47	13.09	1.47	0.38	1.38	0.09	6.10	0.46	93.90
Total					3.82					1.35	

Table B92: Sink-Float Data for Run1, Plate7

Sections	Column Length (m)	Sink-Float SG	Tracer SG
Overflow	0.00	1.35	1.40
Tops	0.40	1.35	1.30
Sect 5	0.46	1.33	1.59
Sect 4	0.52	1.35	1.72
Sect 3	0.58	1.38	1.71
Sect 2	0.64	1.36	1.66
Sect 1	0.72	1.39	1.77
Underflow	1.22	1.37	1.58

Table B93: Sink-Float and Tracer Bed Profile Data for Run1, Plate7

Time	22	min
Feed Coal	18.37	kg
Density (Average)	1510.3	kg/m^3
Coal Flow	0.55	l/min
Water Remaining in unit	8.16	kg
Feed Water Flow	2.10	l/min
Teeter water flow	3	l/min

Table B94: Flow Data for Run 2,Plate 7

Time (min)	Manometer Readings (cm)		Head (cm)	Offset (cm)	P (Pa)	f(e)=0	e	Bed Density (kg/m^3)
0	39.6	62.2	22.6	22.6	2217.1			1000.0
6	40.0	65.3	25.3	2.7	264.9	-0.0009	0.59	1211.0
12	39.0	68.0	29.0	6.4	627.8	0.0000	0.50	1256.3
18	36.0	72.0	36.0	13.4	1314.5	-0.0001	0.42	1293.7
22	33.0	71.0	38.0	15.4	1510.7	-0.0001	0.41	1300.5

Table B95: Pressure-Drop Data for Run 2,Plate 7

SG Range	1.2	1.3	1.4	1.5	1.6	1.8	2	No. of tracers	Avg SG
Overflow									
5	4		3		1				
2			1			1	1		
1.5			1			1			
Total	4	0	5	0	1	2	1	13	1.46
Tops	1.2	1.3	1.4	1.5	1.6	1.8	2		
5	1		2		3	7	5		
2			4		3	1	2		
1.5			3	1		2			
Total	1	0	9	1	6	10	7	34	1.67
Sect 5	1.2	1.3	1.4	1.5	1.6	1.8	2		
5	1		6		4	6	5		
2			4	5		6	4		
1.5				1		3	3		
Total	1	0	10	6	4	15	12	48	1.70
Sect 4	1.2	1.3	1.4	1.5	1.6	1.8	2		
5					1				
2									
1.5									
Total	0	0	0	0	1	0	0	1	1.60
Sect 3	1.2	1.3	1.4	1.5	1.6	1.8	2		
5									
2						1			
1.5							1		
Total	0	0	0	0	0	1	1	2	1.90
Sect 2	1.2	1.3	1.4	1.5	1.6	1.8	2		
5	4		5		5	5	4		
2			5	3		6	4		
1.5			2			6	2		
Total	4	0	12	3	5	17	10	51	1.66
Sect 1	1.2	1.3	1.4	1.5	1.6	1.8	2		
5			1			1	1		
2									
1.5							1		
Total	0	0	1	0	0	1	2	4	1.80
Underflow	1.2	1.3	1.4	1.5	1.6	1.8	2		
5									
2									
1.5									
Total	0	0	0	0	0	0	0	0	0.00

Table B96: Density Tracer Data for Run 2,Plate 7

SG	Vials Mass before (g)	Mass After (g)	Crucibles before (g)	Crucibles after (g)	Mass of Coal (g)	Mass frac.	Coal Comb. (g)	Ash (g)	% Ash	Av. Density	% Comb
2	9.38	9.34	22.57	22.56	0.04	0.01	0.01	0.03	62.56	0.02	37.44
1.8	9.34	9.25	54.74	54.68	0.08	0.02	0.06	0.03	31.55	0.03	68.45
1.6	9.60	9.38	37.32	37.16	0.21	0.05	0.16	0.06	27.71	0.07	72.29
1.4	11.53	9.25	23.01	21.05	2.28	0.49	1.96	0.32	13.90	0.69	86.10
1.2	11.35	9.35	15.01	13.15	2.00	0.43	1.89	0.14	7.082	0.52	92.92
Total					4.61					1.33	

Table B97: Sink-Float Data for Run2, Plate7

Sections	Column Length (m)	Sink-Float SG	Tracer SG
Overflow	0.00	1.33	1.46
Tops	0.40	1.36	1.67
Sect 5	0.46	1.39	1.70
Sect 4	0.52	1.36	1.60
Sect 3	0.58	1.41	1.90
Sect 2	0.64	1.43	1.66
Sect 1	0.72	1.36	1.80
Underflow	1.22	1.38	0.00

Table B98: Sink-Float and Tracer Bed Profile Data for Run2, Plate7

Time	16	min
Feed Coal	13.91	kg
Density (Average)	1510.3	kg/m^3
Coal Flow	0.58	l/min
Water Remaining in unit	10.25	kg
Feed Water Flow	2.36	l/min
Teeter water flow	8	l/min

Table B99: Flow Data for Run 3,Plate 7

Time (min)	Manometer Readings (cm)		Head (cm)	Offset (cm)	P (Pa)	f(e)=0	e	Bed Density (kg/m^3)
0	39.6	62.2	22.6	22.6	2217.1			1000.0
3	38.2	63.0	24.8	2.2	215.8	-0.0004	0.67	1167.3
7	37.6	65.9	28.3	5.7	559.2	-0.0007	0.56	1222.5
10	35.0	69.3	34.3	11.7	1147.8	0.0000	0.48	1263.3
16	29.4	73.2	43.8	21.2	2079.7	0.0000	0.42	1295.1

Table B100: Pressure-Drop Data for Run 3,Plate 7

SG Range	1.2	1.3	1.4	1.5	1.6	1.8	2	No. of tracers	Avg SG
Overflow									
5			2	1					
2									
1.5									
Total	0	0	2	1	0	0	0	3	1.43
Tops	1.2	1.3	1.4	1.5	1.6	1.8	2		
5									
2									
1.5			3						
Total	0	0	3	0	0	0	0	3	1.40
Sect 5	1.2	1.3	1.4	1.5	1.6	1.8	2		
5									
2			2						
1.5									
Total	0	0	2	0	0	0	0	2	1.40
Sect 4	1.2	1.3	1.4	1.5	1.6	1.8	2		
5	2								
2			2						
1.5				1					
Total	2	0	2	1	0	0	0	5	1.34
Sect 3	1.2	1.3	1.4	1.5	1.6	1.8	2		
5	2		1		1	2	1		
2			4				2		
1.5			3	3			1		
Total	2	0	8	3	1	2	4	20	1.57
Sect 2	1.2	1.3	1.4	1.5	1.6	1.8	2		
5	2		3		2	2	3		
2			1	1		1	2		
1.5						4			
Total	2	0	4	1	2	7	5	21	1.68
Sect 1	1.2	1.3	1.4	1.5	1.6	1.8	2		
5	2		7		2	5	3		
2			1	4		2	2		
1.5				1		2	1		
Total	2	0	8	5	2	9	6	32	1.64
Underflow	1.2	1.3	1.4	1.5	1.6	1.8	2		
5	2		6		8	10	8		
2			3	9		6	9		
1.5			3	3		6	5		
Total	2	0	12	12	8	22	22	78	1.71

Table B101. Density Tracer Data for Run 3,Plate 7

SG	Vials Mass before (g)	Mass After (g)	Crucibles before (g)	Crucibles after (g)	Mass of Coal (g)	Mass frac.	Coal Comb. (g)	Ash (g)	% Ash	Av. Density	% Comb
2	9.74	9.33	21.10	20.79	0.41	0.13	0.31	0.10	23.35	0.26	76.65
1.8	9.37	9.29	22.61	22.55	0.08	0.03	0.07	0.02	18.58	0.05	81.42
1.6	9.31	9.30	37.12	37.10	0.02	0.01	0.01	0.004	25.64	0.01	74.36
1.4	11.29	9.33	56.57	54.78	1.96	0.61	1.79	0.17	8.69	0.86	91.31
1.2	10.07	9.34	13.73	13.06	0.73	0.23	0.68	0.05	7.29	0.28	92.71
Total					3.20					1.46	

Table B102: Sink-Float Data for Run3, Plate7

Sections	Column Length (m)	Sink-Float SG	Tracer SG
Overflow	0.00	1.46	1.43
Tops	0.40	1.39	1.40
Sect 5	0.46	1.31	1.40
Sect 4	0.52	1.34	1.34
Sect 3	0.58	1.38	1.57
Sect 2	0.64	1.39	1.68
Sect 1	0.72	1.40	1.64
Underflow	1.22	1.39	1.71

Table B103: Sink-Float and Tracer Bed Profile Data for Run3, Plate7

Time	19	min
Feed Coal	14.13	kg
Density (Average)	1510.3	kg/m^3
Coal Flow	0.49	l/min
Water Remaining in unit	9.72	kg
Feed Water Flow	2.79	l/min
Teeter water flow	6	l/min

Table B104: Flow Data for Run 1,Plate 1a

Time (min)	Manometer Readings (cm)		Head (cm)	Offset (cm)	P (Pa)	f(e)=0	e	Bed Density (kg/m^3)
0	39.8	61.0	21.2	21.2	2079.7			1000.0
5	42.2	64.0	21.8	0.6	58.9	-0.0001	0.75	1127.4
10	40.0	67.7	27.7	6.5	637.7	-0.0004	0.51	1252.1
15	35.6	65.2	29.6	8.4	824.0	-0.0005	0.48	1265.6
19	33.0	76.2	43.2	22	2158.2	-0.0009	0.39	1313.7

Table B105: Pressure-Drop Data for Run 1,Plate 1a

SG Range	1.2	1.3	1.4	1.5	1.6	1.8	2	No. of tracers	Avg SG
Overflow									
5	none								
2									
1.5									
Total	0	0	0	0	0	0	0	0	0.00
Tops	1.2	1.3	1.4	1.5	1.6	1.8	2		
5	2								
2			1						
1.5									
Total	2	0	1	0	0	0	0	3	1.27
Sect 5	1.2	1.3	1.4	1.5	1.6	1.8	2		
5	3		3			3	2		
2			2	2		2	2		
1.5									
Total	3	0	5	2	0	5	4	19	1.61
Sect 4	1.2	1.3	1.4	1.5	1.6	1.8	2		
5			3		5	4	2		
2			2			1	1		
1.5									
Total	0	0	5	0	5	5	3	18	1.67
Sect 3	1.2	1.3	1.4	1.5	1.6	1.8	2		
5	1								
2			2						
1.5						1			
Total	1	0	2	0	0	1	0	4	1.45
Sect 2	1.2	1.3	1.4	1.5	1.6	1.8	2		
5					1				
2			1			1			
1.5						1			
Total	0	0	1	0	1	2	0	4	1.65
Sect 1	1.2	1.3	1.4	1.5	1.6	1.8	2		
5	2		6		3	3	3		
2			2			3	3		
1.5									
Total	2	0	8	0	3	6	6	25	1.65
Underflow	1.2	1.3	1.4	1.5	1.6	1.8	2		
5	2		5		5	9	8		
2			3	9		4	2		
1.5			3	1		2			
Total	2	0	11	10	5	15	10	53	1.66

Table B106: Density Tracer Data for Run 1,Plate 1a

SG	Vials Mass before (g)	Mass After (g)	Crucibles before (g)	Crucibles after (g)	Mass of Coal (g)	Mass frac.	Coal Comb. (g)	Ash (g)	% Ash	Av. Density	% Comb
2	9.57	9.42	20.89	20.77	0.15	0.03	0.12	0.02	16.00	0.05	84.00
1.8	9.50	9.37	54.55	54.44	0.12	0.02	0.11	0.01	8.76	0.04	91.24
1.6	9.59	9.37	37.32	37.12	0.22	0.04	0.21	0.02	8.21	0.07	91.79
1.4	12.57	9.56	25.54	22.86	3.01	0.54	2.68	0.33	10.96	0.75	89.04
1.2	11.59	9.47	15.14	13.16	2.12	0.38	1.97	0.15	6.93	0.45	93.07
Total					5.62					1.36	

Table B107: Sink-Float Data for Run1, Plate1a

Sections	Column Length (m)	Sink-Float SG	Tracer SG
Overflow	0.00	1.36	0.00
Tops	0.40	1.36	1.27
Sect 5	0.46	1.33	1.61
Sect 4	0.52	1.30	1.67
Sect 3	0.58	1.32	1.45
Sect 2	0.64	1.39	1.65
Sect 1	0.72	1.38	1.65
Underflow	1.22	1.40	1.66

Table B108: Sink-Float and Tracer Bed Profile Data for Run1, Plate1a

Time	18	min
Feed Coal	15.88	kg
Density (Average)	1510.3	kg/m^3
Coal Flow	0.58	l/min
Water Remaining in unit	7.47	kg
Feed Water Flow	2.04	l/min
Teeter Water Flow	3	l/min

Table B109: Flow Data for Run 2,Plate 1a

Time (min)	Manometer Readings (cm)		Head (cm)	Offset (cm)	P (Pa)	f(e)=0	e	Bed Density (kg/m^3)
0	40.8	60.3	19.5	19.5	1913.0			1000.0
6	31.5	69.0	37.5	18.0	1765.8	0.0001	0.39	1310.0
12	29.8	71.0	41.2	21.7	2128.8	0.0001	0.38	1318.7
18	28.0	72.3	44.3	24.8	2432.9	0.0002	0.36	1324.8

Table B110: Pressure-Drop Data for Run 2,Plate 1a

SG Range	1.2	1.3	1.4	1.5	1.6	1.8	2	No. of tracers	Avg SG
Overflow									
5	none								
2									
1.5									
Total	0	0	0	0	0	0	0	0	0.00
Tops	1.2	1.3	1.4	1.5	1.6	1.8	2		
5	4		6		5	6	6		
2			3	1		3	3		
1.5						2			
Total	4	0	9	1	5	11	9	39	1.66
Sect 5	1.2	1.3	1.4	1.5	1.6	1.8	2		
5									
2			1						
1.5									
Total	0	0	1	0	0	0	0	1	1.40
Sect 4	1.2	1.3	1.4	1.5	1.6	1.8	2		
5									
2							1		
1.5									
Total	0	0	0	0	0	0	1	1	2.00
Sect 3	1.2	1.3	1.4	1.5	1.6	1.8	2		
5	1								
2			2				1		
1.5						1			
Total	1	0	2	0	0	1	1	5	1.56
Sect 2	1.2	1.3	1.4	1.5	1.6	1.8	2		
5	1		5		4	5	4		
2			1	4		4	3		
1.5			2						
Total	1	0	8	4	4	9	7	33	1.67
Sect 1	1.2	1.3	1.4	1.5	1.6	1.8	2		
5	3		3		3	6	2		
2			4	4		3	3		
1.5			1				1		
Total	3	0	8	4	3	9	6	33	1.63
Underflow	1.2	1.3	1.4	1.5	1.6	1.8	2		
5	1		3		2	2	3		
2				4		1	1		
1.5						3	1		
Total	1	0	3	4	2	6	5	21	1.69

Table B111: Density Tracer Data for Run 2,Plate 1a

SG	Vials Mass before (g)	Mass After (g)	Crucibles before (g)	Crucibles after (g)	Mass of Coal (g)	Mass frac.	Coal Comb. (g)	Ash (g)	% Ash	Av. Density	% Comb
2	10.27	10.17	20.87	20.78	0.10	0.02	0.09	0.01	13.05	0.04	86.95
1.8	10.42	10.29	54.45	54.34	0.14	0.03	0.11	0.02	17.82	0.05	82.18
1.6	10.48	10.26	37.31	37.13	0.22	0.04	0.18	0.03	15.92	0.07	84.08
1.4	12.10	10.34	24.29	22.75	1.76	0.35	1.54	0.22	12.46	0.49	87.54
1.2	12.75	9.91	15.87	13.26	2.84	0.56	2.61	0.23	8.06	0.68	91.94
Total					5.06					1.33	

Table B112: Sink-Float Data for Run2, Plate1a

Sections	Column Length (m)	Sink-Float SG	Tracer SG
Overflow	0.00	1.33	0.00
Tops	0.40	1.34	1.66
Sect 5	0.46	1.31	1.40
Sect 4	0.52	1.42	2.00
Sect 3	0.58	1.40	1.56
Sect 2	0.64	1.38	1.67
Sect 1	0.72	1.36	1.63
Underflow	1.22	1.38	1.69

Table B113: Sink-Float and Tracer Bed Profile Data for Run2, Plate1a

Time	17	min
Feed Coal	12.41	kg
Density (Average)	1510.3	kg/m^3
Coal Flow	0.48	l/min
Water Remaining in unit	10.81	kg
Feed Water Flow	2.21	l/min
Teeter water flow	8	l/min

Table B114: Flow Data for Run 3,Plate 1a

Time (min)	Manometer Readings (cm)		Head (cm)	Offset (cm)	P (Pa)	f(e)=0	e	Bed Density (kg/m^3)
0	40.4	60.4	20.0	20.0	1962.0			1000.0
4	38.0	62.0	24.0	4.0	392.4	-0.0006	0.57	1218.0
8	37.3	65.1	27.8	7.8	765.2	-0.0009	0.50	1254.7
12	34.0	66.2	32.2	12.2	1196.8	0.0000	0.45	1278.5
16	30.1	70.0	39.9	19.9	1952.2	0.0000	0.41	1303.3

Table B115: Pressure-Drop Data for Run 3,1a

SG Range	1.2	1.3	1.4	1.5	1.6	1.8	2	No. of tracers	Avg SG
Overflow									
5	none								
2									
1.5									
Total	0	0	0	0	0	0	0	0	0.00
Tops	1.2	1.3	1.4	1.5	1.6	1.8	2		
5	none								
2									
1.5									
Total	0	0	0	0	0	0	0	0	0.00
Sect 5	1.2	1.3	1.4	1.5	1.6	1.8	2		
5	1								
2									
1.5						1			
Total	1	0	0	0	0	1	0	2	1.50
Sect 4	1.2	1.3	1.4	1.5	1.6	1.8	2		
5	3								
2			1						
1.5									
Total	3	0	1	0	0	0	0	4	1.25
Sect 3	1.2	1.3	1.4	1.5	1.6	1.8	2		
5	1		3		3	3	3		
2			2	1		3			
1.5				1					
Total	1	0	5	2	3	6	3	20	1.64
Sect 2	1.2	1.3	1.4	1.5	1.6	1.8	2		
5			3		2	4	4		
2			2	2		2	3		
1.5				1		2			
Total	0	0	5	3	2	8	7	25	1.72
Sect 1	1.2	1.3	1.4	1.5	1.6	1.8	2		
5	1		1		2	3	2		
2			2	4		2			
1.5			2			1	1		
Total	1	0	5	4	2	6	3	21	1.63
Underflow	1.2	1.3	1.4	1.5	1.6	1.8	2		
5	4		10		7	9	9		
2			5	5		5	6		
1.5			4				1		
Total	4	0	19	5	7	14	16	65	1.65

Table B116: Density Tracer Data for Run 3,Plate 1a

SG	Vials Mass before (g)	Mass After (g)	Crucibles before (g)	Crucibles after (g)	Mass of Coal (g)	Mass frac.	Coal Comb. (g)	Ash (g)	% Ash	Av. Density	% Comb
2	9.64	9.44	20.95	20.78	0.20	0.04	0.17	0.03	15.05	0.07	84.95
1.8	9.79	9.40	54.60	54.28	0.38	0.07	0.32	0.06	16.34	0.13	83.66
1.6	9.66	9.36	37.39	37.12	0.30	0.05	0.27	0.03	9.54	0.08	90.46
1.4	12.61	9.29	25.85	23.19	3.33	0.57	2.66	0.67	20.03	0.80	79.97
1.2	10.91	9.32	14.63	13.22	1.59	0.28	1.41	0.19	11.59	0.33	88.41
Total					5.80					1.41	

Table B117: Sink-Float Data for Run3, Plate1a

Sections	Column Length (m)	Sink-Float SG	Tracer SG
Overflow	0.00	1.41	0.00
Tops	0.40	1.33	0.00
Sect 5	0.46	1.34	1.50
Sect 4	0.52	1.24	1.25
Sect 3	0.58	1.28	1.64
Sect 2	0.64	1.31	1.72
Sect 1	0.72	1.34	1.63
Underflow	1.22	1.35	1.65

Table B118: Sink-Float and Tracer Bed Profile Data for Run3, Plate1a

Time	14	min
Feed Coal	9.61	kg
Density (Average)	1510.3	kg/m^3
Coal Flow	0.46	l/min
Water Remaining in unit	12.70	kg
Feed Water Flow	2.42	l/min
Teeter water flow	6	l/min

Table B119: Flow Data for Run 1,Plate 2a

Time (min)	Manometer Readings (cm)		Head (cm)	Offset (cm)	P (Pa)	f(e)=0	e	Bed Density (kg/m^3)
0	40.0	61.0	21.0	21.0	2060.1			1000.0
5	39.4	62.7	23.3	2.3	225.6	-0.0007	0.67	1168.4
9	36.0	66.1	30.1	9.1	892.7	0.0000	0.51	1248.0
14	32.1	71.8	39.7	18.7	1834.5	0.0000	0.44	1287.6

Table B120: Pressure-Drop Data for Run 1,Plate 2a

SG Range	1.2	1.3	1.4	1.5	1.6	1.8	2	No. of tracers	Avg SG
Overflow									
5	none								
2									
1.5									
Total	0	0	0	0	0	0	0	0	0.00
Tops	1.2	1.3	1.4	1.5	1.6	1.8	2		
5	3		2						
2			5						
1.5			5						
Total	3	0	12	0	0	0	0	15	1.36
Sect 5	1.2	1.3	1.4	1.5	1.6	1.8	2		
5	3		5		4	6	5		
2			2	2		3			
1.5				3		1			
Total	3	0	7	5	4	10	5	34	1.63
Sect 4	1.2	1.3	1.4	1.5	1.6	1.8	2		
5	1		4		6	5	3		
2			2			3	3		
1.5				1		2			
Total	1	0	6	1	6	10	6	30	1.69
Sect 3	1.2	1.3	1.4	1.5	1.6	1.8	2		
5	3		3		2	3	5		
2			2	7		2	2		
1.5			3	1		1			
Total	3	0	8	8	2	6	7	34	1.61
Sect 2	1.2	1.3	1.4	1.5	1.6	1.8	2		
5			3		2	5	2		
2			1	2			3		
1.5									
Total	0	0	4	2	2	5	5	18	1.71
Sect 1	1.2	1.3	1.4	1.5	1.6	1.8	2		
5									
2							1		
1.5									
Total	0	0	0	0	0	0	1	1	2.00
Underflow	1.2	1.3	1.4	1.5	1.6	1.8	2		
5	none								
2									
1.5									
Total	0	0	0	0	0	0	0	0	0.00

Table B121: Density Tracer Data for Run 1,Plate 2a

SG	Vials Mass before (g)	Mass After (g)	Crucibles before (g)	Crucibles after (g)	Mass of Coal (g)	Mass frac.	Coal Comb. (g)	Ash (g)	% Ash	Av. Density	% Comb
2	9.38	9.34	22.57	22.56	0.04	0.01	0.02	0.03	62.56	0.02	37.44
1.8	9.34	9.25	54.74	54.68	0.08	0.02	0.06	0.03	31.55	0.03	68.45
1.6	9.60	9.38	37.32	37.16	0.21	0.05	0.16	0.06	27.71	0.07	72.29
1.4	11.53	9.25	23.01	21.05	2.28	0.49	1.96	0.32	13.90	0.69	86.10
1.2	11.35	9.35	15.01	13.15	2.00	0.43	1.86	0.14	7.08	0.52	92.92
Total					4.61					1.33	

Table B122: Sink-Float Data for Run1, Plate2a

Sections	Column Length (m)	Sink-Float SG	Tracer SG
Overflow	0.00	1.33	1.46
Tops	0.40	1.36	1.67
Sect 5	0.46	1.39	1.70
Sect 4	0.52	1.36	1.60
Sect 3	0.58	1.41	1.90
Sect 2	0.64	1.43	1.66
Sect 1	0.72	1.36	1.80
Underflow	1.22	1.38	0.00

Table B123: Sink-Float and Tracer Bed Profile Data for Run1, Plate2a

Time	18	min
Feed Coal	13.19	kg
Density (Average)	1510.3	kg/m^3
Coal Flow	0.49	l/min
Water Remaining in unit	10.55	kg
Feed Water Flow	1.91	l/min
Teeter water flow	3	l/min

Table B124: Flow Data for Run 2,Plate 2a

Time (min)	Manometer Readings (cm)		Head (cm)	Offset (cm)	P (Pa)	f(e)=0	e	Bed Density (kg/m^3)
0	40.2	60.8	20.6	20.6	2020.9			1000.0
7	36.9	58.2	21.3	0.7	68.7	-0.0002	0.73	1135.8
14	34.0	63.1	29.1	8.5	833.9	-0.0007	0.48	1266.8
18	31.0	65.7	34.7	14.1	1383.2	-0.0009	0.43	1292.6

Table B125: Pressure-Drop Data for Run 2,Plate 2a

SG Range	1.2	1.3	1.4	1.5	1.6	1.8	2	No. of tracers	Avg SG
Overflow									
5	3		4		2	1			
2			4			1			
1.5			3						
Total	3	0	11	0	2	2	0	18	1.43
Tops	1.2	1.3	1.4	1.5	1.6	1.8	2		
5	3		8		7	11	10		
2			3	6		2	4		
1.5			2	3		1			
Total	3	0	13	9	7	14	14	60	1.66
Sect 5	1.2	1.3	1.4	1.5	1.6	1.8	2		
5						1			
2			1	1		1	1		
1.5									
Total	0	0	1	1	0	2	1	5	1.70
Sect 4	1.2	1.3	1.4	1.5	1.6	1.8	2		
5									
2						1			
1.5							1		
Total	0	0	0	0	0	1	1	2	1.90
Sect 3	1.2	1.3	1.4	1.5	1.6	1.8	2		
5									
2			1			1			
1.5							1		
Total	0	0	1	0	0	1	1	3	1.73
Sect 2	1.2	1.3	1.4	1.5	1.6	1.8	2		
5	2		5		5	2	2		
2			1	2		2	1		
1.5			1			2			
Total	2	0	7	2	5	6	3	25	1.60
Sect 1	1.2	1.3	1.4	1.5	1.6	1.8	2		
5	2					4	3		
2			1	1		1	2		
1.5									
Total	2	0	1	1	0	5	5	14	1.74
Underflow	1.2	1.3	1.4	1.5	1.6	1.8	2		
5	none								
2									
1.5									
Total									

Table B126: Density Tracer Data for Run 2,Plate 2a

SG	Vials Mass before (g)	Mass After (g)	Crucibles before (g)	Crucibles after (g)	Mass of Coal (g)	Mass frac.	Coal Comb. (g)	Ash (g)	% Ash	Av. Density	% Comb
2	9.38	9.27	22.59	22.54	0.11	0.02	0.05	0.06	56.01	0.04	43.99
1.8	9.38	9.31	54.18	54.14	0.07	0.01	0.04	0.03	41.76	0.02	58.25
1.6	9.38	9.29	37.17	37.09	0.08	0.02	0.08	0.01	8.00	0.03	92.00
1.4	11.42	9.30	22.88	20.89	2.12	0.40	1.99	0.13	6.13	0.56	93.87
1.2	12.21	9.29	15.96	13.48	2.92	0.55	2.49	0.43	14.86	0.66	85.14
Total					5.30					1.31	

Table B127: Sink-Float Data for Run2, Plate2a

Sections	Column Length (m)	Sink-Float SG	Tracer SG
Overflow	0.00	1.31	1.43
Tops	0.40	1.96	1.66
Sect 5	0.46	1.33	1.70
Sect 4	0.52	1.38	1.90
Sect 3	0.58	1.38	1.73
Sect 2	0.64	1.30	1.60
Sect 1	0.72	1.38	1.74
Underflow	1.22	1.33	0.00

Table B128: Sink-Float and Tracer Bed Profile Data for Run2, Plate2a

Time	12	min
Feed Coal	9.85	kg
Density (Average)	1510.3	kg/m^3
Coal Flow	0.54	l/min
Water Remaining in unit	13.34	kg
Feed Water Flow	2.56	l/min
Teeter water flow	8	l/min

Table B129: Flow Data for Run 3,Plate 2a

Time (min)	Manometer Readings (cm)		Head (cm)	Offset (cm)	P (Pa)	f(e)=0	e	Bed Density (kg/m^3)
0	39.8	60.9	21.1	21.1	2069.9			1000.0
6	42.3	66.8	24.5	3.4	333.5	-0.0005	0.67	1170.2
9	36.0	69.0	33.0	11.9	1167.4	0.0000	0.52	1245.8
12	29.5	71.0	41.5	20.4	2001.2	0.0000	0.46	1276.7

Table B130: Pressure-Drop Data for Run 3,Plate 2a

SG Range	1.2	1.3	1.4	1.5	1.6	1.8	2	No. of tracers	Avg SG
Overflow									
5									
2									
1.5				1					
Total	0	0	0	1	0	0	0	1	1.50
Tops	1.2	1.3	1.4	1.5	1.6	1.8	2		
5			6						
2			1						
1.5			2						
Total	0	0	9	0	0	0	0	9	1.40
Sect 5	1.2	1.3	1.4	1.5	1.6	1.8	2		
5			1						
2			2						
1.5									
Total	0	0	3	0	0	0	0	3	1.40
Sect 4	1.2	1.3	1.4	1.5	1.6	1.8	2		
5	1		3		6	4	1		
2			1	3		3	4		
1.5						2			
Total	1	0	4	3	6	9	5	28	1.68
Sect 3	1.2	1.3	1.4	1.5	1.6	1.8	2		
5	2		4			5	5		
2			4	2		1			
1.5						2			
Total	2	0	8	2	0	8	5	25	1.64
Sect 2	1.2	1.3	1.4	1.5	1.6	1.8	2		
5			3			1	4		
2			1	1			1		
1.5			2			1			
Total	0	0	6	1	0	2	5	14	1.68
Sect 1	1.2	1.3	1.4	1.5	1.6	1.8	2		
5	1		6		8	9	5		
2			3	6		2	2		
1.5				1		3	1		
Total	1	0	9	7	8	14	8	47	1.67
Underflow	1.2	1.3	1.4	1.5	1.6	1.8	2		
5									
2									
1.5						1			
Total	0	0	0	0	0	1	0	1	1.80

Table B131: Density Tracer Data for Run 3,Plate 2a

SG	Vials Mass before (g)	Mass After (g)	Crucibles before (g)	Crucibles after (g)	Mass of Coal (g)	Mass frac.	Coal Comb. (g)	Ash (g)	% Ash	Av. Density	% Comb
2	9.68	9.44	22.73	22.54	0.25	0.06	0.19	0.06	23.21	0.11	76.79
1.8	9.59	9.49	54.02	53.93	0.10	0.02	0.09	0.01	10.11	0.04	89.89
1.6	9.70	9.38	37.40	37.10	0.32	0.07	0.30	0.02	7.11	0.12	92.89
1.4	10.58	9.58	21.77	20.86	1.00	0.23	0.91	0.10	9.48	0.32	90.52
1.2	12.24	9.51	15.78	13.56	2.73	0.62	2.22	0.51	18.71	0.75	81.29
Total					4.40					1.34	

Table B132: Sink-Float Data for Run3, Plate2a

Sections	Column Length (m)	Sink-Float SG	Tracer SG
Overflow	0.00	1.34	1.50
Tops	0.40	1.31	1.40
Sect 5	0.46	1.35	1.40
Sect 4	0.52	1.38	1.68
Sect 3	0.58	1.45	1.64
Sect 2	0.64	1.49	1.68
Sect 1	0.72	1.47	1.67
Underflow	1.22	1.30	1.80

Table B133: Sink-Float and Tracer Bed Profile Data for Run3, Plate2a

Time	18	min
Feed Coal	14.44	kg
Density (Average)	1510.3	kg/m^3
Coal Flow	0.53	l/min
Water Remaining in unit	9.32	kg
Feed Water Flow	2.36	l/min
Teeter water flow	6	l/min

Table B134: Flow Data for Run 1,Plate 3a

Time (min)	Manometer Readings (cm)		Head (cm)	Offset (cm)	P (Pa)	f(e)=0	e	Bed Density (kg/m^3)
0	39.8	60.8	21.0	21.0	2060.1			1000.0
5	38.0	61.3	23.3	2.3	225.6	0.0000	0.64	1186.4
9	37.4	62.0	24.6	3.6	353.2	0.0000	0.59	1211.3
13	33.6	64.0	30.4	9.4	922.1	-0.0001	0.48	1264.1
18	30.5	67.2	36.7	15.7	1540.2	-0.0001	0.43	1290.9

Table B135: Pressure-Drop Data for Run 1,Plate 3a

SG Range	1.2	1.3	1.4	1.5	1.6	1.8	2	No. of tracers	Avg SG
Overflow									
5									
2	7		1						
1.5	7		2	2					
Total	14	0	3	2	0	0	0	19	1.26
Tops	1.2	1.3	1.4	1.5	1.6	1.8	2		
5	2								
2			3	3		1			
1.5			1				3		
Total	2	0	4	3	0	1	3	13	1.56
Sect 5	1.2	1.3	1.4	1.5	1.6	1.8	2		
5	4		2	1		2			
2			1	4		2	2		
1.5			1				3		
Total	4	0	4	5	0	4	5	22	1.60
Sect 4	1.2	1.3	1.4	1.5	1.6	1.8	2		
5			3	2	3	5	5		
2	2		2			4	3		
1.5			1	1			2		
Total	2	0	6	3	3	9	10	33	1.71
Sect 3	1.2	1.3	1.4	1.5	1.6	1.8	2		
5				1	1				
2			3			1	1		
1.5			1				1		
Total	0	0	4	1	1	1	2	9	1.61
Sect 2	1.2	1.3	1.4	1.5	1.6	1.8	2		
5			2	3	5	3	3		
2			2	2		3			
1.5				1		2			
Total	0	0	4	6	5	8	3	26	1.65
Sect 1	1.2	1.3	1.4	1.5	1.6	1.8	2		
5	1		6	4	2	3	4		
2			7	2		5	3		
1.5				1		1	3		
Total	1	0	13	7	2	9	10	42	1.65
Underflow	1.2	1.3	1.4	1.5	1.6	1.8	2		
5	2		4		2	6	3		
2			3	6		5	3		
1.5			3	1		4	1		
Total	2	0	10	7	2	15	7	43	1.65

Table B136: Density Tracer Data for Run 1,Plate 3a

SG	Vials Mass before (g)	Mass After (g)	Crucibles before (g)	Crucibles after (g)	Mass of Coal (g)	Mass frac.	Coal Comb. (g)	Ash (g)	% Ash	Av. Density	% Comb
2	9.64	9.44	22.73	22.62	0.20	0.05	0.11	0.09	45.28	0.09	54.72
1.8	9.59	9.49	54.02	53.94	0.10	0.02	0.07	0.02	23.88	0.04	76.12
1.6	9.70	9.38	37.40	37.13	0.32	0.07	0.27	0.05	16.42	0.12	83.58
1.4	10.58	9.58	21.77	20.86	1.00	0.23	0.91	0.10	9.48	0.32	90.52
1.2	12.24	9.51	15.78	13.56	2.73	0.63	2.22	0.51	18.71	0.75	81.29
Total					4.35					1.32	

Table B137: Sink-Float Data for Run1, Plate3a

Sections	Column Length (m)	Sink-Float SG	Tracer SG
Overflow	0.00	1.32	1.26
Tops	0.40	1.31	1.56
Sect 5	0.46	1.35	1.60
Sect 4	0.52	1.38	1.71
Sect 3	0.58	1.37	1.61
Sect 2	0.64	1.37	1.65
Sect 1	0.72	1.37	1.65
Underflow	1.22	1.39	1.65

Table B138: Sink-Float and Tracer Bed Profile Data for Run1, Plate3a

Time	18	min
Feed Coal	14.47	kg
Density (Average)	1510.3	kg/m^3
Coal Flow	0.53	l/min
Water Remaining in unit	9.87	kg
Feed Water Flow	2.04	l/min
Teeter water flow	3	l/min

Table B139: Flow Data for Run 2,Plate 3a

Time (min)	Manometer Readings (cm)		Head (cm)	Offset (cm)	P (Pa)	f(e)=0	e	Bed Density (kg/m^3)
0	40.0	61.0	21.0	21.0	2060.1			1000.0
6	39.0	63.0	24.0	3.0	294.3	-0.0009	0.58	1217.0
12	37.0	67.5	30.5	9.5	932.0	0.0000	0.46	1276.9
18	33.0	71.9	38.9	17.9	1756.0	-0.0001	0.40	1308.0

Table B140: Pressure-Drop Data for Run 2,Plate 3a

SG Range	1.2	1.3	1.4	1.5	1.6	1.8	2	No. of tracers	Avg SG
Overflow									
5									
2	4								
1.5	2		4	1					
Total	6	0	4	1	0	0	0	11	1.30
Tops	1.2	1.3	1.4	1.5	1.6	1.8	2		
5	2		5	2	7	4	4		
2			5	3		4	3		
1.5			5	3		3	1		
Total	2	0	15	8	7	11	8	51	1.62
Sect 5	1.2	1.3	1.4	1.5	1.6	1.8	2		
5				1		4			
2						1	1		
1.5			1			1			
Total	0	0	1	1	0	6	1	9	1.74
Sect 4	1.2	1.3	1.4	1.5	1.6	1.8	2		
5									
2			1						
1.5						1			
Total	0	0	1	0	0	1	0	2	1.60
Sect 3	1.2	1.3	1.4	1.5	1.6	1.8	2		
5	3		6		3	6	5		
2			5		3	4	4		
1.5				2					
Total	3	0	11	2	6	10	9	41	1.65
Sect 2	1.2	1.3	1.4	1.5	1.6	1.8	2		
5									
2			1	1			1		
1.5				1		3	1		
Total	0	0	1	2	0	3	2	8	1.73
Sect 1	1.2	1.3	1.4	1.5	1.6	1.8	2		
5	3		6	2	5	7	6		
2			11	7		14	5		
1.5			3			3	2		
Total	3	0	20	9	5	24	13	74	1.65
Underflow	1.2	1.3	1.4	1.5	1.6	1.8	2		
5	1								
2	4								
1.5			2	1					
Total	5	0	2	1	0	0	0	8	1.29

Table B141: Density Tracer Data for Run 2,Plate 3a

SG	Vials Mass before (g)	Mass After (g)	Crucibles before (g)	Crucibles after (g)	Mass of Coal (g)	Mass frac.	Coal Comb. (g)	Ash (g)	% Ash	Av. Density	% Comb
2	9.50	9.37	20.89	20.8386	0.13	0.025	0.0553	0.078	57.82	0.05	42.18
1.8	9.66	9.50	37.16	37.1163	0.08	0.02	0.0485	0.035	42.06	0.03	57.94
1.6	10.07	9.60	54.3341	54.0200	0.47	0.08	0.3141	0.15	32.80	0.14	67.20
1.4	12.33	9.50	25.3149	22.9216	2.83	0.53	2.3933	0.43	15.34	0.74	84.66
1.2	11.12	9.334	14.8474	13.1925	1.78	0.34	1.6549	0.14	7.54	0.40	92.46
Total					5.29					1.36	

Table B142: Sink-Float Data for Run2, Plate3a

Sections	Column Length (m)	Sink-Float SG	Tracer SG
Overflow	0.00	1.36	1.30
Tops	0.40	0.00	1.62
Sect 5	0.46	1.39	1.74
Sect 4	0.52	1.34	1.60
Sect 3	0.58	1.39	1.65
Sect 2	0.64	1.35	1.73
Sect 1	0.72	1.36	1.65
Underflow	1.22	2.04	1.29

Table B143: Sink-Float and Tracer Bed Profile Data for Run2, Plate3a

Time	16	min
Feed Coal	11.62	kg
Density (Average)	1510.3	kg/m^3
Coal Flow	0.48	l/min
Water Remaining in unit	10.15	kg
Feed Water Flow	2.82	l/min
Teeter water flow	8	l/min

Table B144: Flow Data for Run3,Plate 3a

Time (min)	Manometer Readings (cm)		Head (cm)	Offset (cm)	P (Pa)	f(e)=0	e	Bed Density (kg/m^3)
0	40.5	60.2	19.7	19.7	1932.6			1000.0
4	38.0	62.0	24.0	4.3.0	421.8	-0.0003	0.59	1208.3
8	35.0	63.5	28.5	8.8	863.3	-0.0005	0.51	1249.3
12	33.2	67.0	33.8	14.1	1383.2	-0.0007	0.46	1275.3
16	31.0	69.3	38.3	18.6	1824.7	-0.0008	0.43	1290.0

Table B145: Pressure-Drop Data for Run 3,Plate 3a

SG Range	1.2	1.3	1.4	1.5	1.6	1.8	2	No. of tracers	Avg SG
Overflow									
5									
2	7								
1.5	4		4	1		1	1		
Total	11	0	4	1	0	1	1	18	1.34
Tops	1.2	1.3	1.4	1.5	1.6	1.8	2		
5									
2	1		10	6					
1.5			3	5					
Total	1	0	13	11	0	0	0	25	1.44
Sect 5	1.2	1.3	1.4	1.5	1.6	1.8	2		
5	4								
2			4			1			
1.5				2					
Total	4	0	4	2	0	1	0	11	1.38
Sect 4	1.2	1.3	1.4	1.5	1.6	1.8	2		
5	2				1				
2			4	1		3			
1.5			1				1		
Total	2	0	5	1	1	3	1	13	1.53
Sect 3	1.2	1.3	1.4	1.5	1.6	1.8	2		
5			1	2					
2			1	1		4			
1.5			1	1		1	1		
Total	0	0	3	4	0	5	1	13	1.63
Sect 2	1.2	1.3	1.4	1.5	1.6	1.8	2		
5	1		4	1	1	2	2		
2			1	1		4			
1.5			1	1		1	1		
Total	1	0	6	3	1	7	3	21	1.63
Sect 1	1.2	1.3	1.4	1.5	1.6	1.8	2		
5			1	1	2	6	1		
2				4		3	3		
1.5				1			2		
Total	0	0	1	6	2	9	6	24	1.74
Underflow	1.2	1.3	1.4	1.5	1.6	1.8	2		
5	3		11	5	10	11	12		
2			3		5	9	9		
1.5			3			6	5		
Total	3	0	17	5	15	26	26	92	1.71

Table B146: Density Tracer Data for Run 3,Plate 3a

SG	Vials Mass before (g)	Mass After (g)	Crucibles before (g)	Crucibles after (g)	Mass of Coal (g)	Mass frac.	Coal Comb. (g)	Ash (g)	% Ash	Av. Density	% Comb
2	9.67	9.60	20.90	20.88	0.07	0.02	0.022	0.05	69.05	0.03	30.95
1.8	9.58	9.40	53.99	53.86	0.19	0.041	0.12	0.06	33.80	0.06	66.20
1.6	9.69	9.57	37.19	37.10	0.12	0.025	0.088	0.03	24.44	0.04	75.56
1.4	11.43	9.62	24.25	22.72	1.80	0.38	1.53	0.27	15.05	0.55	84.95
1.2	11.94	9.48	15.55	13.65	2.45	0.53	1.90	0.56	22.65	0.64	77.34
Total					4.63					1.32	

Table B147: Sink-Float Data for Run3, Plate3a

Sections	Column Length (m)	Sink-Float SG	Tracer SG
Overflow	0.00	1.32	1.34
Tops	0.40	1.23	1.44
Sect 5	0.46	1.25	1.38
Sect 4	0.52	1.31	1.53
Sect 3	0.58	1.36	1.63
Sect 2	0.64	1.38	1.63
Sect 1	0.72	1.40	1.74
Underflow	1.22	1.43	1.71

Table B148: Sink-Float and Tracer Bed Profile Data for Run3, Plate3a

Time	17	min
Feed Coal	14.27	kg
Density (Average)	1510.3	kg/m^3
Coal Flow	0.56	l/min
Water Remaining in unit	9.52	kg
Feed Water Flow	2.04	l/min
Teeter water flow	6	l/min

Table B149: Flow Data for Run 1,Plate 4a

Time (min)	Manometer Readings (cm)		Head (cm)	Offset (cm)	P (Pa)	f(e)=0	e	Bed Density (kg/m^3)
0	40.2	60.3	20.1	20.1	1971.8			1000.0
5	40.0	63.0	23.0	2.9	284.5	-0.0001	0.59	1208.8
9	38.0	64.0	26.0	5.9	578.8	-0.0002	0.52	1247.1
13	34.8	66.9	32.1	12.0	1177.2	-0.0003	0.44	1284.1
17	31.0	69.0	38.0	17.9	1756.0	-0.0004	0.40	1303.9

Table B150: Pressure-Drop Data for Run 1,Plate 4a

SG Range	1.2	1.3	1.4	1.5	1.6	1.8	2	No. of tracers	Avg SG
Overflow									
5									
2			2	1					
1.5	4		1						
Total	4	0	3	1	0	0	0	8	1.31
Tops	1.2	1.3	1.4	1.5	1.6	1.8	2		
5	7								
2			7	1					
1.5			3	3					
Total	7	0	10	4	0	0	0	21	1.35
Sect 5	1.2	1.3	1.4	1.5	1.6	1.8	2		
5			5	1					
2			2	5		5	3		
1.5			1	1		1	1		
Total	0	0	8	7	0	6	4	25	1.62
Sect 4	1.2	1.3	1.4	1.5	1.6	1.8	2		
5	2		3	1	6	6	5		
2			2	1		2	3		
1.5						1			
Total	2	0	5	2	6	9	8	32	1.69
Sect 3	1.2	1.3	1.4	1.5	1.6	1.8	2		
5									
2						1			
1.5					1	1			
Total	0	0	0	0	1	2	0	3	1.73
Sect 2	1.2	1.3	1.4	1.5	1.6	1.8	2		
5			5	2	2	4	1		
2			2	3		6			
1.5			3	1		2			
Total	0	0	10	6	2	12	1	31	1.61
Sect 1	1.2	1.3	1.4	1.5	1.6	1.8	2		
5	1		2	1	2	5	3		
2			3	1		4	3		
1.5			1	1		3	1		
Total	1	0	6	3	2	12	7	31	1.71
Underflow	1.2	1.3	1.4	1.5	1.6	1.8	2		
5			2	2	4	6	6		
2			2	5		4	6		
1.5						4	1		
Total	0	0	4	7	4	14	13	42	1.75

Table B151: Density Tracer Data for Run 1,Plate 4a

SG	Vials Mass before (g)	Mass After (g)	Crucibles before (g)	Crucibles after (g)	Mass of Coal (g)	Mass frac.	Coal Comb. (g)	Ash (g)	% Ash	Av. Density	% Comb
2	9.68	9.44	22.72	22.53	0.24	0.05	0.19	0.04	18.73	0.10	81.27
1.8	9.79	9.41	54.13	53.81	0.38	0.08	0.32	0.06	15.48	0.14	84.52
1.6	9.56	9.36	37.27	37.10	0.20	0.04	0.17	0.03	15.28	0.06	84.72
1.4	10.68	9.24	22.27	21.01	1.44	0.29	1.26	0.18	12.36	0.41	87.64
1.2	11.96	9.29	15.75	13.53	2.67	0.54	2.22	0.46	17.08	0.65	82.92
Total					4.93					1.36	

Table B152: Sink-Float Data for Run1, Plate4a

Sections	Column Length (m)	Sink-Float SG	Tracer SG
Overflow	0.00	1.36	1.31
Tops	0.40	1.27	1.35
Sect 5	0.46	1.35	1.62
Sect 4	0.52	1.37	1.69
Sect 3	0.58	1.37	1.73
Sect 2	0.64	1.37	1.61
Sect 1	0.72	1.36	1.71
Underflow	1.22	1.37	1.75

Table B153: Sink-Float and Tracer Bed Profile Data for Run1, Plate4a

Time	16	min
Feed Coal	14.24	kg
Density (Average)	1510.3	kg/m^3
Coal Flow	0.59	l/min
Water Remaining in unit	8.53	kg
Feed Water Flow	2.15	l/min
Teeter water flow	3	l/min

Table B154: Flow Data for Run 2,Plate 4a

Time (min)	Manometer Readings (cm)		Head (cm)	Offset (cm)	P (Pa)	f(e)=0	e	Bed Density (kg/m^3)
0	41.0	60.0	19.0	19.0	1863.9			1000.0
5	40.0	61.0	21.0	2.0	196.2	0.0003	0.61	1198.4
11	37.8	62.9	25.1	6.1	598.4	0.0001	0.50	1256.5
16	31.0	65.2	34.2	15.2	1491.1	0.0002	0.41	1302.0

Table B155: Pressure-Drop Data for Run 2,Plate 4a

SG Range	1.2	1.3	1.4	1.5	1.6	1.8	2	No. of tracers	Avg SG
Overflow									
5									
2									
1.5	1		1						
Total	1	0	1	0	0	0	0	2	1.30
Tops	1.2	1.3	1.4	1.5	1.6	1.8	2		
5	4		6	1	3	7	6		
2			10	6		6	5		
1.5			2	1		6	2		
Total	4	0	18	8	3	19	13	65	1.65
Sect 5	1.2	1.3	1.4	1.5	1.6	1.8	2		
5							1		
2									
1.5				1		1			
Total	0	0	0	1	0	1	1	3	1.77
Sect 4	1.2	1.3	1.4	1.5	1.6	1.8	2		
5									
2			1						
1.5			2						
Total	0	0	3	0	0	0	0	3	1.40
Sect 3	1.2	1.3	1.4	1.5	1.6	1.8	2		
5	3		4	1	5	8	5		
2			6	3		1	3		
1.5			1			2	1		
Total	3	0	11	4	5	11	9	43	1.65
Sect 2									
5			1	1	1	2			
2			2			2	1		
1.5			1						
Total	0	0	4	1	1	4	1	11	1.63
Sect 1	1.2	1.3	1.4	1.5	1.6	1.8	2		
5						1	1		
2									
1.5				1			1		
Total	0	0	0	1	0	1	2	4	1.83
Underflow	1.2	1.3	1.4	1.5	1.6	1.8	2		
5	2		6	3	4	4	2		
2			2	3		2	2		
1.5			1						
Total	2	0	9	6	4	6	4	31	1.59

Table B156: Density Tracer Data for Run 2,Plate 4a

SG	Vials Mass before (g)	Mass After (g)	Crucibles before (g)	Crucibles after (g)	Mass of Coal (g)	Mass frac.	Coal Comb. (g)	Ash (g)	% Ash	Av. Density	% Comb
2	9.58	9.54	20.86	20.85	0.05	0.01	0.01	0.03	71.37	0.02	28.63
1.8	9.28	9.24	53.74	53.71	0.04	0.01	0.03	0.01	24.16	0.02	75.84
1.6	9.63	9.48	37.25	37.12	0.15	0.04	0.12	0.03	17.12	0.06	82.88
1.4	10.72	9.51	23.65	22.59	1.21	0.29	1.06	0.15	12.06	0.40	87.94
1.2	12.16	9.43	15.80	13.27	2.73	0.65	2.53	0.20	7.22	0.78	92.78
Total					4.18					1.28	

Table B157: Sink-Float Data for Run2, Plate4a

Sections	Column Length (m)	Sink-Float SG	Tracer SG
Overflow	0.0	1.28	1.30
Tops	0.40	1.36	1.65
Sect 5	0.46	1.38	1.77
Sect 4	0.52	1.38	1.40
Sect 3	0.58	1.37	1.65
Sect 2	0.64	1.39	1.63
Sect 1	0.72	1.38	1.83
Underflow	1.22	1.56	1.59

Table B158: Sink-Float and Tracer Bed Profile Data for Run2, Plate4a

Time	16	min
Feed Coal	12.01	kg
Density (Average)	1510.3	kg/m^3
Coal Flow	0.50	l/min
Water Remaining in unit	12.06	kg
Feed Water Flow	2.59	l/min
Teeter water flow	8	l/min

Table B159: Flow Data for Run 3,Plate 4a

Time (min)	Manometer Readings (cm)		Head (cm)	Offset (cm)	P (Pa)	f(e)=0	e	Bed Density (kg/m^3)
0	40.2	60.4	20.2	20.2	1981.6			1000.0
4	39.0	62.0	23.0	2.8.0	274.7	-0.0006	0.61	1198.5
8	38.0	65.1	27.1	6.9	676.9	0.0000	0.51	1248.2
16	33.4	69.0	35.6	15.4	1510.7	0.0000	0.43	1290.7

Table B160: Pressure-Drop Data for Run 3,Plate 4a

SG Range	1.2	1.3	1.4	1.5	1.6	1.8	2	No. of tracers	Avg SG
Overflow									
5	none								
2									
1.5									
Total	0	0	0	0	0	0	0	0	0.00
Tops	1.2	1.3	1.4	1.5	1.6	1.8	2		
5	none								
2									
1.5									
Total	0	0	0	0	0	0	0	0	0.00
Sect 5	1.2	1.3	1.4	1.5	1.6	1.8	2		
5									
2									
1.5	1								
Total	1	0	0	0	0	0	0	1	1.20
Sect 4	1.2	1.3	1.4	1.5	1.6	1.8	2		
5	5								
2			2						
1.5									
Total	5	0	2	0	0	0	0	7	1.26
Sect 3	1.2	1.3	1.4	1.5	1.6	1.8	2		
5	2		4	5	5	7	4		
2			12	6		3	1		
1.5			3			2			
Total	2	0	19	11	5	12	5	54	1.58
Sect 2	1.2	1.3	1.4	1.5	1.6	1.8	2		
5			2			1	2		
2				2		3	1		
1.5			1			1			
Total	0	0	3	2	0	5	3	13	1.71
Sect 1	1.2	1.3	1.4	1.5	1.6	1.8	2		
5	2		2		2	3	1		
2			1	7		1	3		
1.5			1	1		1	1		
Total	2	0	4	8	2	5	5	26	1.62
Underflow	1.2	1.3	1.4	1.5	1.6	1.8	2		
5			9		8	12	8		
2			7	1		11	7		
1.5			1	1		6	2		
Total	0	0	17	2	8	29	17	73	1.72

Table B161: Density Tracer Data for Run 3,Plate 4a

SG	Vials Mass before (g)	Mass After (g)	Crucibles before (g)	Crucibles after (g)	Mass of Coal (g)	Mass frac.	Coal Comb. (g)	Ash (g)	% Ash	Av. Density	% Comb
2	9.55	9.30	21.09	20.98	0.24	0.05	0.11	0.13	53.34	0.10	46.66
1.8	9.42	9.29	37.18	37.09	0.13	0.03	0.10	0.03	25.06	0.05	74.94
1.6	9.69	9.30	53.99	53.68	0.40	0.08	0.32	0.08	20.14	0.13	79.86
1.4	11.91	9.33	25.06	22.86	2.58	0.52	2.20	0.38	14.73	0.73	85.27
1.2	10.89	9.32	14.65	13.23	1.58	0.32	1.42	0.15	9.57	0.38	90.43
Total					4.93					1.39	

Table B162: Sink-Float Data for Run3, Plate4a

Sections	Column Length (m)	Sink-Float SG	Tracer SG
Overflow	0.00	1.39	0.00
Tops	0.40	0.00	0.00
Sect 5	0.46	1.31	1.20
Sect 4	0.52	1.27	1.26
Sect 3	0.58	1.30	1.58
Sect 2	0.64	1.35	1.71
Sect 1	0.72	1.41	1.62
Underflow	1.22	1.37	1.72

Table B163: Sink-Float and Tracer Bed Profile Data for Run3, Plate4a

Time	12	min
Feed Coal	14.28	kg
Density (Average)	1510.3	kg/m^3
Coal Flow	0.79	l/min
Water Remaining in unit	9.64	kg
Feed Water Flow	2.37	l/min
Teeter water flow	6	l/min

Table B164: Flow Data for Run 1,Plate 5a

Time (min)	Manometer Readings (cm)		Head (cm)	Offset (cm)	P (Pa)	f(e)=0	e	Bed Density (kg/m^3)
0	40.1	60.2	20.1	20.1	1971.8			1000.0
4	38.6	62.0	23.4	3.3	323.7	-0.0004	0.58	1215.5
8	37.1	63.0	25.9	5.8	569.0	-0.0005	0.52	1245.9
12	34.0	69.7	35.7	15.6	1530.4	-0.0010	0.42	1297.0

Table B165: Pressure-Drop Data for Run 1,Plate 5a

SG Range	1.2	1.3	1.4	1.5	1.6	1.8	2	No. of tracers	Avg SG
Overflow									
5									
2									
1.5				1					
Total	0	0	0	1	0	0	0	1	1.50
Tops	1.2	1.3	1.4	1.5	1.6	1.8	2		
5	2		3		2	4	4		
2			7	6		3	4		
1.5						1			
Total	2	0	10	6	2	8	8	36	1.64
Sect 5	1.2	1.3	1.4	1.5	1.6	1.8	2		
5			2		1	1	1		
2				1		1			
1.5									
Total	0	0	2	1	1	2	1	7	1.64
Sect 4	1.2	1.3	1.4	1.5	1.6	1.8	2		
5									
2			1						
1.5						1			
Total	0	0	1	0	0	1	0	2	1.60
Sect 3	1.2	1.3	1.4	1.5	1.6	1.8	2		
5	1		1	1		1	1		
2			1			1			
1.5			1						
Total	1	0	3	1	0	2	1	8	1.56
Sect 2	1.2	1.3	1.4	1.5	1.6	1.8	2		
5	1		2	1		2	2		
2			2	1		1			
1.5									
Total	1	0	4	2	0	3	2	12	1.60
Sect 1	1.2	1.3	1.4	1.5	1.6	1.8	2		
5	2		4	4		2	1		
2			1			2	1		
1.5			1			2	1		
Total	2	0	6	4	0	6	3	21	1.60
Underflow	1.2	1.3	1.4	1.5	1.6	1.8	2		
5	5		5	2	9	11	6		
2			6	4		5	5		
1.5			3	1		2	1		
Total	5	0	14	7	9	18	12	65	1.64

Table B166: Density Tracer Data for Run 1,Plate 5a

SG	Vials Mass before (g)	Mass After (g)	Crucibles before (g)	Crucibles after (g)	Mass of Coal (g)	Mass frac.	Coal Comb. (g)	Ash (g)	% Ash	Av. Density	% Comb
2	9.71	9.48	21.11	20.91	0.24	0.05	0.20	0.04	16.87	0.10	83.13
1.8	9.34	9.24	53.65	53.58	0.09	0.02	0.07	0.02	25.08	0.04	74.92
1.6	9.47	9.36	37.16	37.06	0.11	0.02	0.10	0.02	15.18	0.04	84.82
1.4	10.42	9.47	23.43	22.60	0.95	0.20	0.83	0.13	13.26	0.29	86.74
1.2	12.53	9.30	16.27	13.91	3.22	0.70	2.36	0.86	26.70	0.84	73.30
Total					4.61					1.31	

Table B167: Sink-Float Data for Run1, Plate5a

Sections	Column Length (m)	Sink-Float SG	Tracer SG
Overflow	0.00	1.31	1.50
Tops	0.40	1.34	1.64
Sect 5	0.46	1.33	1.64
Sect 4	0.52	1.38	1.60
Sect 3	0.58	1.38	1.56
Sect 2	0.64	1.34	1.60
Sect 1	0.72	1.37	1.60
Underflow	1.22	1.36	1.64

Table B168: Sink-Float and Tracer Bed Profile Data for Run1, Plate5a

Time	15	min
Feed Coal	16.72	kg
Density (Average)	1510.3	kg/m^3
Coal Flow	0.74	l/min
Water Remaining in unit	7.07	kg
Feed Water Flow	2.59	l/min
Teeter water flow	3	l/min

Table B169: Flow Data for Run 2,Plate 5a

Time (min)	Manometer Readings (cm)		Head (cm)	Offset (cm)	P (Pa)	f(e)=0	e	Bed Density (kg/m^3)
0	40.4	60.1	19.7	19.7	1932.6			1000.0
5	39.4	61.5	22.1	2.4	235.4	0.0001	0.59	1207.8
10	37.0	64.0	27.0	7.3	716.1	0.0001	0.48	1265.6
15	32.0	67.9	35.9	16.2	1589.2	0.0003	0.40	1305.0

Table B170: Pressure-Drop Data for Run 2,Plate 5a

SG Range	1.2	1.3	1.4	1.5	1.6	1.8	2	No. of tracers	Avg SG
Overflow									
5									
2									
1.5			1						
Total	0	0	1	0	0	0	0	1	1.40
Tops	1.2	1.3	1.4	1.5	1.6	1.8	2		
5	3		4	5	6	5	2		
2			3	1		2	1		
1.5				1		2	3		
Total	3	0	7	7	6	9	6	38	1.62
Sect 5	1.2	1.3	1.4	1.5	1.6	1.8	2		
5	2								
2			1				2		
1.5			1						
Total	2	0	2	0	0	0	2	6	1.53
Sect 4	1.2	1.3	1.4	1.5	1.6	1.8	2		
5	3		8	2	6	6	10		
2			10	9		7	7		
1.5			3	1		3			
Total	3	0	21	12	6	16	17	75	1.65
Sect 3	1.2	1.3	1.4	1.5	1.6	1.8	2		
5									
2			1						
1.5						2			
Total	0	0	1	0	0	2	0	3	1.67
Sect 2	1.2	1.3	1.4	1.5	1.6	1.8	2		
5									
2						3			
1.5			1						
Total	0	0	1	0	0	3	0	4	1.70
Sect 1	1.2	1.3	1.4	1.5	1.6	1.8	2		
5	2		5	3	2	7	1		
2			1	3		6	2		
1.5			2			1			
Total	2	0	8	6	2	14	3	35	1.63
Underflow	1.2	1.3	1.4	1.5	1.6	1.8	2		
5							2		
2			1			1			
1.5			1						
Total	0	0	2	0	0	1	2	5	1.72

Table B171: Density Tracer Data for Run 2,Plate 5a

SG	Vials Mass before (g)	Mass After (g)	Crucibles before (g)	Crucibles after (g)	Mass of Coal (g)	Mass frac.	Coal Comb. (g)	Ash (g)	% Ash	Av. Density	% Comb
2	9.47	9.40	20.93	20.90	0.06	0.01	0.03	0.03	47.92	0.02	52.08
1.8	9.68	9.67	53.53	53.52	0.01	0.002	0.01	0.002	28.16	0.004	71.84
1.6	9.54	9.42	37.17	37.07	0.13	0.02	0.10	0.03	22.33	0.04	77.67
1.4	12.54	9.53	25.46	22.87	3.01	0.58	2.59	0.42	13.94	0.81	86.06
1.2	11.35	9.38	15.05	13.27	1.96	0.38	1.78	0.18	9.37	0.46	90.63
Total					5.17					1.33	

Table B172: Sink-Float Data for Run2, Plate5a

Sections	Column Length (m)	Sink-Float SG	Tracer SG
Overflow	0.00	1.33	1.40
Tops	0.40	1.39	1.62
Sect 5	0.46	1.42	1.53
Sect 4	0.52	1.38	1.65
Sect 3	0.58	1.39	1.67
Sect 2	0.64	1.37	1.70
Sect 1	0.72	1.39	1.63
Underflow	1.22	1.37	1.72

Table B173: Sink-Float and Tracer Bed Profile Data for Run2, Plate5a

Time	16	min
Feed Coal	14.94	kg
Density (Average)	1510.3	kg/m^3
Coal Flow	0.62	l/min
Water Remaining in unit	9.48	kg
Feed Water Flow	2.07	l/min
Teeter water flow	8	l/min

Table B174: Flow Data for Run 3,Plate 5a

Time (min)	Manometer Readings (cm)		Head (cm)	Offset (cm)	P (Pa)	f(e)=0	e	Bed Density (kg/m^3)
0	40.1	60.4	20.3	20.3	1991.4			1000.0
4	38.0	60.9	22.9	2.6	255.1	-0.0009	0.61	1197.1
8	37.0	63.2	26.2	5.9	578.8	0.0000	0.52	1242.5
11	32.0	64.0	32	11.7	1147.8	0.0000	0.45	1279.3
16	30.0	68.0	38	17.7	1736.4	0.0000	0.41	1300.4

Table B175: Pressure-Drop Data for Run 3,Plate 5a

SG Range	1.2	1.3	1.4	1.5	1.6	1.8	2	No. of tracers	Avg SG
Overflow									
5	none								
2									
1.5									
Total	0	0	0	0	0	0	0	0	0.00
Tops									
5	6								
2			3						
1.5			3						
Total	6	0	6	0	0	0	0	12	1.30
Sect 5									
5	1		4	1	5	2	2		
2			2	1		2	1		
1.5			1			1	1		
Total	1	0	7	2	5	5	4	24	1.63
Sect 4									
5			1	1	3	3			
2			1	1					
1.5			1						
Total	0	0	3	2	3	3	0	11	1.58
Sect 3									
5	1								
2			2			1			
1.5			2						
Total	1	0	4	0	0	1	0	6	1.43
Sect 2									
5			4	2	1	1			
2			2	6		2	3		
1.5			2						
Total	0	0	8	8	1	3	3	23	1.57
Sect 1									
5	2		5	3	2	8	6		
2			7	1		7	1		
1.5			1			2			
Total	2	0	13	4	2	17	7	45	1.65
Underflow									
5			3	3	3	5	7		
2			2	1		6	4		
1.5			1	1					
Total	0	0	6	5	3	11	11	36	1.74

Table B176: Density Tracer Data for Run 3,Plate 5a

SG	Vials Mass before (g)	Mass After (g)	Crucibles before (g)	Crucibles after (g)	Mass of Coal (g)	Mass frac.	Coal Comb. (g)	Ash (g)	% Ash	Av. Density	% Comb
2	9.63	9.43	21.10	20.94	0.20	0.03	0.16	0.05	22.16	0.07	77.84
1.8	9.70	9.48	22.73	22.56	0.22	0.04	0.17	0.05	24.18	0.07	75.82
1.6	9.50	9.37	37.17	37.06	0.13	0.02	0.11	0.02	14.78	0.04	85.22
1.4	12.86	9.66	56.52	54.05	3.21	0.55	2.47	0.74	22.99	0.77	77.01
1.2	11.56	9.47	15.19	13.44	2.09	0.36	1.74	0.35	16.70	0.43	83.30
Total					5.85					1.38	

Table B177: Sink-Float Data for Run3, Plate5a

Sections	Column Length (m)	Sink-Float SG	Tracer SG
Overflow	0.00	1.38	0.00
Tops	0.40	1.33	1.30
Sect 5	0.46	1.40	1.63
Sect 4	0.52	1.41	1.58
Sect 3	0.58	1.40	1.43
Sect 2	0.64	1.48	1.57
Sect 1	0.72	1.43	1.65
Underflow	1.22	1.43	1.74

Table B178: Sink-Float and Tracer Bed Profile Data for Run3, Plate5a

Time	14	min
Feed Coal	13.23	kg
Density (Average)	1510.3	kg/m^3
Coal Flow	0.63	l/min
Water Remaining in unit	9.88	kg
Feed Water Flow	2.81	l/min
Teeter water flow	6	l/min

Table B179: Flow Data for Run 1,Plate 6a

Time (min)	Manometer Readings (cm)		ΔP	Head (cm)	Offset (cm)	f(e)=0	e	Bed Density (kg/m^3)
0	40.3	60.0	19.7	19.7	1932.6			1000.0
5	38.4	61.0	22.6	2.9	284.5	-0.0005	0.60	1206.4
10	37.7	64.1	26.4	6.7	657.3	-0.0008	0.51	1251.8
14	34.0	69.5	35.5	15.8	1550.0	0.0000	0.42	1296.1

Table B180: Pressure-Drop Data for Run 1,Plate 6a

SG Range	1.2	1.3	1.4	1.5	1.6	1.8	2	No. of tracers	Avg SG
Overflow									
5	none								
2									
1.5									
Total	0	0	0	0	0	0	0	0	0.00
Tops	1.2	1.3	1.4	1.5	1.6	1.8	2		
5	2								
2									
1.5			1						
Total	2	0	1	0	0	0	0	3	1.27
Sect 5	1.2	1.3	1.4	1.5	1.6	1.8	2		
5	1		6	5	2	6	5		
2			6	3		3	1		
1.5			3			1			
Total	1	0	15	8	2	10	6	42	1.60
Sect 4	1.2	1.3	1.4	1.5	1.6	1.8	2		
5									
2									
1.5						1			
Total	0	0	0	0	0	1	0	1	1.80
Sect 3	1.2	1.3	1.4	1.5	1.6	1.8	2		
5	1								
2			1	1					
1.5				1					
Total	1	0	1	2	0	0	0	4	1.40
Sect 2	1.2	1.3	1.4	1.5	1.6	1.8	2		
5	1		4	4	4	5	2		
2			2	1		5	1		
1.5			2						
Total	1	0	8	5	4	10	3	31	1.62
Sect 1	1.2	1.3	1.4	1.5	1.6	1.8	2		
5			2	1		2	3		
2			1			1	1		
1.5						1			
Total	0	0	3	1	0	4	4	12	1.74
Underflow	1.2	1.3	1.4	1.5	1.6	1.8	2		
5	4		5		7	5	5		
2			8	1		5	2		
1.5									
Total	4	0	13	1	7	10	7	42	1.61

Table B181: Density Tracer Data for Run 1,Plate 6a

SG	Vials Mass before (g)	Mass After (g)	Crucibles before (g)	Crucibles after (g)	Mass of Coal (g)	Mass frac.	Coal Comb. (g)	Ash (g)	% Ash	Av. Density	% Comb
2	9.79	9.61	21.08	20.94	0.17	0.03	0.14	0.04	21.22	0.05	78.78
1.8	10.19	9.92	53.58	53.35	0.27	0.04	0.23	0.04	13.90	0.07	86.10
1.6	10.79	10.42	37.42	37.09	0.38	0.06	0.33	0.05	12.32	0.09	87.68
1.4	13.48	10.62	25.35	23.04	2.86	0.43	2.32	0.55	19.10	0.61	80.90
1.2	12.36	9.45	16.01	13.67	2.91	0.44	2.34	0.58	19.79	0.53	80.21
Total					6.59					1.35	

Table B182: Sink-Float Data for Run1, Plate6a

Sections	Column Length (m)	Sink-Float SG	Tracer SG
Overflow	0.00	1.35	0.00
Tops	0.40	1.33	1.27
Sect 5	0.46	1.36	1.60
Sect 4	0.52	1.35	1.80
Sect 3	0.58	1.41	1.40
Sect 2	0.64	1.40	1.62
Sect 1	0.72	1.38	1.74
Underflow	1.22	1.37	1.61

Table B183: Sink-Float and Tracer Bed Profile Data for Run1, Plate6a

Time	17	min
Feed Coal	15.40	kg
Density (Average)	1510.3	kg/m^3
Coal Flow	0.60	l/min
Water Remaining in unit	7.80	kg
Feed Water Flow	2.04	l/min
Teeter water flow	3	l/min

Table B184: Flow Data for Run 2,Plate 6a

Time (min)	Manometer Readings (cm)		Head (cm)	Offset (cm)	P (Pa)	f(e)=0	e	Bed Density (kg/m^3)
0	40.5	60.0	19.5	19.5	1913.0			1000.0
6	39.0	62.0	23.0	3.5	343.4	-0.0002	0.56	1227.0
13	37.5	64.0	26.5	7.0	686.7	-0.0003	0.48	1263.0
17	32.0	69.0	37.0	17.5	1716.8	-0.0005	0.40	1308.3

Table B185: Pressure-Drop Data for Run 2,Plate 6a

SG Range	1.2	1.3	1.4	1.5	1.6	1.8	2	No. of tracers	Avg SG
Overflow									
5	none								
2									
1.5									
Total	0	0	0	0	0	0	0	0	0.00
Tops	1.2	1.3	1.4	1.5	1.6	1.8	2		
5	2		4	3	5	9	5		
2			6			4	2		
1.5			2	1					
Total	2	0	12	4	5	13	7	43	1.64
Sect 5	1.2	1.3	1.4	1.5	1.6	1.8	2		
5			5	1	3	5	4		
2			6	2		6	2		
1.5						4			
Total	0	0	11	3	3	15	6	38	1.68
Sect 4	1.2	1.3	1.4	1.5	1.6	1.8	2		
5	2								
2			4			1			
1.5									
Total	2	0	4	0	0	1	0	7	1.40
Sect 3	1.2	1.3	1.4	1.5	1.6	1.8	2		
5									
2				1			2		
1.5						1			
Total	0	0	0	1	0	1	2	4	1.83
Sect 2	1.2	1.3	1.4	1.5	1.6	1.8	2		
5									
2						1	1		
1.5									
Total	0	0	0	0	0	1	1	2	1.90
Sect 1	1.2	1.3	1.4	1.5	1.6	1.8	2		
5	3		3	2	1	3	2		
2			1	2			2		
1.5						2			
Total	3	0	4	4	1	5	4	21	1.61
Underflow	1.2	1.3	1.4	1.5	1.6	1.8	2		
5	3		5	3	3	2	3		
2			3	5		3	1		
1.5			2	1		2			
Total	3	0	10	9	3	7	4	36	1.57

Table B186: Density Tracer Data for Run 2,Plate 6a

SG	Vials Mass before (g)	Mass After (g)	Crucibles before (g)	Crucibles after (g)	Mass of Coal (g)	Mass frac.	Coal Comb. (g)	Ash (g)	% Ash	Av. Density	% Comb
2	9.83	9.55	22.80	22.63	0.29	0.06	0.17	0.12	40.46	0.12	59.54
1.8	9.57	9.41	53.39	53.28	0.16	0.03	0.11	0.05	29.50	0.06	70.50
1.6	9.73	9.60	37.16	37.06	0.13	0.03	0.10	0.03	24.88	0.04	75.12
1.4	10.96	9.52	22.40	21.16	1.43	0.29	1.24	0.19	13.48	0.41	86.52
1.2	12.38	9.49	16.01	13.31	2.89	0.59	2.69	0.20	6.78	0.71	93.22
Total					4.90					1.34	

Table B187: Sink-Float Data for Run2, Plate6a

Sections	Column Length (m)	Sink-Float SG	Tracer SG
Overflow	0.00	1.34	0.00
Tops	0.40	1.34	1.64
Sect 5	0.46	1.35	1.68
Sect 4	0.52	1.33	1.40
Sect 3	0.58	1.40	1.83
Sect 2	0.64	1.38	1.90
Sect 1	0.72	1.38	1.61
Underflow	1.22	1.38	1.57

Table B188: Sink-Float and Tracer Bed Profile Data for Run2, Plate6a

Time	15	min
Feed Coal	14.45	kg
Density (Average)	1510.3	kg/m^3
Coal Flow	0.64	l/min
Water Remaining in unit	9.39	kg
Feed Water Flow	2.32	l/min
Teeter water flow	8	l/min

Table B189: Flow Data for Run 3,Plate 6a

Time (min)	Manometer Readings (cm)		Head (cm)	Offset (cm)	P (Pa)	f(e)=0	e	Bed Density (kg/m^3)
0	40.8	60.0	19.2	19.2	1883.5			1000.0
4	38.0	61.4	23.4	4.2	412.0	-0.0001	0.57	1217.1
7	37.0	62.0	25.0	5.8	569.0	-0.0001	0.54	1235.2
11	36.2	65.0	28.8	9.6	941.8	-0.0001	0.48	1262.9
15	34.0	70.7	36.7	17.5	1716.8	-0.0002	0.42	1294.4

Table B190: Pressure-Drop Data for Run 3,Plate 6a

SG Range	1.2	1.3	1.4	1.5	1.6	1.8	2	No. of tracers	Avg SG
Overflow									
5	none								
2									
1.5									
Total	0	0	0	0	0	0	0	0	0.00
Tops	1.2	1.3	1.4	1.5	1.6	1.8	2		
5	6								
2									
1.5									
Total	6	0	0	0	0	0	0	6	1.20
Sect 5	1.2	1.3	1.4	1.5	1.6	1.8	2		
5	1		4	2		4	2		
2			4	3		7	4		
1.5			1			3			
Total	1	0	9	5	0	14	6	35	1.67
Sect 4	1.2	1.3	1.4	1.5	1.6	1.8	2		
5	1			1	1	8	3		
2									
1.5									
Total	1	0	0	1	1	8	3	14	1.76
Sect 3	1.2	1.3	1.4	1.5	1.6	1.8	2		
5	1		1						
2			8			2			
1.5						1			
Total	1	0	9	0	0	3	0	13	1.48
Sect 2	1.2	1.3	1.4	1.5	1.6	1.8	2		
5	1		2	1			2		
2			2	2		5	1		
1.5			1			2			
Total	1	0	5	3	0	7	3	19	1.65
Sect 1	1.2	1.3	1.4	1.5	1.6	1.8	2		
5			3		7	6	4		
2						2	2		
1.5			1				1		
Total	0	0	4	0	7	8	7	26	1.74
Underflow	1.2	1.3	1.4	1.5	1.6	1.8	2		
5	1		7	4	1	2	3		
2			1	1		4			
1.5									
Total	1	0	8	5	1	6	3	24	1.60

Table B191: Density Tracer Data for Run 3,Plate 6a

SG	Vials Mass before (g)	Mass After (g)	Crucibles before (g)	Crucibles after (g)	Mass of Coal (g)	Mass frac.	Coal Comb. (g)	Ash (g)	% Ash	Av. Density	% Comb
2	9.61	9.34	21.20	21.03	0.27	0.05	0.17	0.09	35.17	0.11	64.83
1.8	9.44	9.23	53.42	53.28	0.21	0.04	0.14	0.07	33.82	0.08	66.18
1.6	9.48	9.41	37.09	37.03	0.08	0.02	0.06	0.02	25.92	0.03	74.08
1.4	10.74	9.54	23.71	22.66	1.20	0.24	1.05	0.15	12.51	0.33	87.49
1.2	12.71	9.42	16.40	13.59	3.28	0.65	2.81	0.48	14.49	0.78	85.51
Total					5.04					1.33	

Table B192: Sink-Float Data for Run3, Plate6a

Sections	Column Length (m)	Sink-Float SG	Tracer SG
Overflow	0.00	1.33	0.00
Tops	0.40	1.24	1.20
Sect 5	0.46	1.33	1.67
Sect 4	0.52	1.42	1.76
Sect 3	0.58	1.38	1.48
Sect 2	0.64	1.38	1.65
Sect 1	0.72	1.44	1.74
Underflow	1.22	1.36	1.60

Table B193: Sink-Float and Tracer Bed Profile Data for Run3, Plate6a

Time	13	min
Feed Coal	13.00	kg
Density (Average)	1510.3	kg/m^3
Coal Flow	0.66	l/min
Water Remaining in unit	9.96	kg
Feed Water Flow	2.29	l/min
Teeter water flow	6	l/min

Table B194: Flow Data for Run 1,Plate 7a

Time (min)	Manometer Readings (cm)		Head (cm)	Offset (cm)	P (Pa)	f(e)=0	e	Bed Density (kg/m^3)
0	41.0	60.0	19.0	19.0	1863.9			1000.0
5	39.0	62.5	23.5	4.5	441.5	-0.0001	0.56	1222.3
9	37.0	64.0	27.0	8.0	784.8	-0.0001	0.50	1254.1
13	33.0	69.0	36.0	17.0	1667.7	-0.0002	0.42	1293.9

Table B195: Pressure-Drop Data for Run 1,Plate 7a

SG Range	1.2	1.3	1.4	1.5	1.6	1.8	2	No. of tracers	Avg SG
Overflow									
5	none								
2									
1.5									
Total	0	0	0	0	0	0	0	0	0.00
Tops	1.2	1.3	1.4	1.5	1.6	1.8	2		
5	6								
2			1						
1.5			2						
Total	6	0	3	0	0	0	0	9	1.27
Sect 5	1.2	1.3	1.4	1.5	1.6	1.8	2		
5	1		3	2	4	6	4		
2			3	1		1	1		
1.5									
Total	1	0	6	3	4	7	5	26	1.66
Sect 4	1.2	1.3	1.4	1.5	1.6	1.8	2		
5	1		6	1	1	3	1		
2			2	1		2			
1.5						1			
Total	1	0	8	2	1	6	1	19	1.57
Sect 3	1.2	1.3	1.4	1.5	1.6	1.8	2		
5	1		2	2	2	3	4		
2			2	1		6	1		
1.5			1			1			
Total	1	0	5	3	2	10	5	26	1.69
Sect 2	1.2	1.3	1.4	1.5	1.6	1.8	2		
5			1	2		6	2		
2			1			2	1		
1.5									
Total	0	0	2	2	0	8	3	15	1.75
Sect 1	1.2	1.3	1.4	1.5	1.6	1.8	2		
5			5		2	3	2		
2			4	2		6	3		
1.5			1			1	1		
Total	0	0	10	2	2	10	6	30	1.67
Underflow	1.2	1.3	1.4	1.5	1.6	1.8	2		
5					1	2	1		
2			1			1	1		
1.5			1						
Total	0	0	2	0	1	3	2	8	1.73

Table B196: Density Tracer Data for Run 1,Plate 7a

SG	Vials Mass before (g)	Mass After (g)	Crucibles before (g)	Crucibles after (g)	Mass of Coal (g)	Mass frac.	Coal Comb. (g)	Ash (g)	% Ash	Av. Density	% Comb
2	9.67	9.52	22.65	22.53	0.15	0.03	0.12	0.03	18.27	0.07	81.73
1.8	9.84	9.32	53.68	53.23	0.51	0.12	0.44	0.07	13.57	0.21	86.43
1.6	9.45	9.37	37.08	37.02	0.08	0.02	0.06	0.02	24.45	0.03	75.55
1.4	11.47	9.37	23.03	21.22	2.10	0.48	1.81	0.29	13.70	0.67	86.30
1.2	10.89	9.34	14.66	13.36	1.55	0.35	1.30	0.25	15.89	0.42	84.11
Total					4.39					1.40	

Table B197: Sink-Float Data for Run1, Plate7a

Sections	Column Length (m)	Sink-Float SG	Tracer SG
Overflow	0.00	1.40	0.00
Tops	0.40	1.33	1.27
Sect 5	0.46	1.35	1.66
Sect 4	0.52	1.35	1.57
Sect 3	0.58	1.35	1.69
Sect 2	0.64	1.36	1.75
Sect 1	0.72	1.41	1.67
Underflow	1.22	1.41	1.73

Table B198: Sink-Float and Tracer Bed Profile Data for Run1, Plate7a

Time	14	min
Feed Coal	12.57	kg
Density (Average)	1510.3	kg/m^3
Coal Flow	0.60	l/min
Water Remaining in unit	11.40	kg
Feed Water Flow	1.88	l/min
Teeter water flow	3	l/min

Table B199: Flow Data for Run 2,Plate 7a

Time (min)	Manometer Readings (cm)		Head (cm)	Offset (cm)	P (Pa)	f(e)=0	e	Bed Density (kg/m^3)
0	40.6	59.8	19.2	19.2	1883.5			1000.0
5	38.0	60.6	22.6	3.4	333.5	-0.0009	0.62	1192.5
10	37.6	61.7	24.1	4.9	480.7	0.0000	0.58	1213.7
14	35.8	67.0	31.2	12	1177.2	0.0000	0.48	1264.7

Table B200: Pressure-Drop Data for Run 2,Plate 7a

SG Range	1.2	1.3	1.4	1.5	1.6	1.8	2	No. of tracers	Avg SG
Overflow									
5	none								
2									
1.5									
Total	0	0	0	0	0	0	0	0	0.00
Tops	1.2	1.3	1.4	1.5	1.6	1.8	2		
5	2		4	3	4	1	2		
2			8	6		2	1		
1.5			1						
Total	2	0	13	9	4	3	3	34	1.53
Sect 5	1.2	1.3	1.4	1.5	1.6	1.8	2		
5			1		1	5	1		
2			3	4			1		
1.5			1						
Total	0	0	5	4	1	5	2	17	1.62
Sect 4	1.2	1.3	1.4	1.5	1.6	1.8	2		
5	3		5		2	2	4		
2			4			3	4		
1.5			2			2	1		
Total	3	0	11	0	2	7	9	32	1.65
Sect 3	1.2	1.3	1.4	1.5	1.6	1.8	2		
5	1			1					
2			2	1		1			
1.5									
Total	1	0	2	2	0	1	0	6	1.47
Sect 2	1.2	1.3	1.4	1.5	1.6	1.8	2		
5									
2						1			
1.5									
Total	0	0	0	0	0	1	0	1	1.80
Sect 1	1.2	1.3	1.4	1.5	1.6	1.8	2		
5									
2						1			
1.5			1			1			
Total	0	0	1	0	0	2	0	3	1.67
Underflow	1.2	1.3	1.4	1.5	1.6	1.8	2		
5	4		7	5	5	11	7		
2			3			6	3		
1.5				1		1			
Total	4	0	10	6	5	18	10	53	1.66

Table B201: Density Tracer Data for Run 2,Plate 7a

SG	Vials Mass before (g)	Mass After (g)	Crucibles before (g)	Crucibles after (g)	Mass of Coal (g)	Mass frac.	Coal Comb. (g)	Ash (g)	% Ash	Av. Density	% Comb
2	9.84	9.65	22.69	22.62	0.19	0.04	0.08	0.11	60.04	0.07	39.96
1.8	9.44	9.31	53.25	53.16	0.13	0.02	0.09	0.04	29.73	0.04	70.27
1.6	9.67	9.40	37.27	37.07	0.28	0.05	0.20	0.07	26.04	0.08	73.96
1.4	9.89	9.40	21.44	21.02	0.49	0.09	0.43	0.06	12.28	0.13	87.73
1.2	13.64	9.37	17.39	13.53	4.27	0.80	3.86	0.41	9.55	0.96	90.45
Total					5.36					1.28	

Table B202: Sink-Float Data for Run2, Plate7a

Sections	Column Length (m)	Sink-Float SG	Tracer SG
Overflow	0.00	1.28	0.00
Tops	0.40	1.37	1.53
Sect 5	0.46	1.37	1.62
Sect 4	0.52	1.36	1.65
Sect 3	0.58	1.39	1.47
Sect 2	0.64	1.47	1.80
Sect 1	0.72	1.34	1.67
Underflow	1.22	1.38	1.66

Table B203: Sink-Float and Tracer Bed Profile Data for Run2, Plate7a

Time	13	min
Feed Coal	6.83	kg
Density (Average)	1510.3	kg/m^3
Coal Flow	0.35	l/min
Water Remaining in unit	11.12	kg
Feed Water Flow	2.75	l/min
Teeter water flow	8	l/min

Table B204: Flow Data for Run 3Plate 7a

Time (min)	Manometer Readings (cm)		Head (cm)	Offset (cm)	P (Pa)	f(e)=0	e	Bed Density (kg/m^3)
0	40.6	60.0	19.4	19.4	1903.1			1000.0
3	39.0	60.5	21.5	2.1	206.0	-0.0003	0.61	1197.7
7	38.0	62.0	24.0	4.6	451.3	-0.0005	0.53	1239.0
10	35.5	63.6	28.1	8.7	853.5	-0.0007	0.47	1272.1
13	33.2	69.0	35.8	16.4	1608.8	0.0000	0.41	1303.6

Table B205: Pressure-Drop Data for Run 3,Plate 7a

SG Range	1.2	1.3	1.4	1.5	1.6	1.8	2	No. of tracers	Avg SG
Overflow									
5	none								
2									
1.5									
Total	0	0	0	0	0	0	0	0	0.00
Tops	1.2	1.3	1.4	1.5	1.6	1.8	2		
5	none								
2									
1.5									
Total	0	0	0	0	0	0	0	0	0.00
Sect 5	1.2	1.3	1.4	1.5	1.6	1.8	2		
5	1								
2									
1.5									
Total	1	0	0	0	0	0	0	1	1.20
Sect 4	1.2	1.3	1.4	1.5	1.6	1.8	2		
5	5		4			1	1		
2									
1.5									
Total	5	0	4	0	0	1	1	11	1.40
Sect 3	1.2	1.3	1.4	1.5	1.6	1.8	2		
5	2		4	3	4	2	3		
2			2	2		1			
1.5									
Total	2	0	6	5	4	3	3	23	1.57
Sect 2	1.2	1.3	1.4	1.5	1.6	1.8	2		
5			2			2			
2			2			3			
1.5						1			
Total	0	0	4	0	0	6	0	10	1.64
Sect 1	1.2	1.3	1.4	1.5	1.6	1.8	2		
5			5	4	1	4	3		
2			5			8	2		
1.5						2			
Total	0	0	10	4	1	14	5	34	1.67
Underflow	1.2	1.3	1.4	1.5	1.6	1.8	2		
5	4		2		5	12	7		
2			7	2		8	1		
1.5			1			3	2		
Total	4	0	10	2	5	23	10	54	1.69

Table B206: Density Tracer Data for Run3, late 7a

SG	Vials Mass before (g)	Mass After (g)	Crucibles before (g)	Crucibles after (g)	Mass of Coal (g)	Mass frac.	Coal Comb. (g)	Ash (g)	% Ash	Av. Density	% Comb
2	9.74	9.34	22.93	22.64	0.41	0.05	0.29	0.12	28.83	0.11	71.17
1.8	10.07	9.56	53.54	53.18	0.51	0.07	0.36	0.15	29.19	0.12	70.81
1.6	9.77	9.43	37.34	37.06	0.35	0.05	0.28	0.06	17.69	0.07	82.31
1.4	12.61	9.49	24.07	21.47	3.11	0.41	2.59	0.52	16.64	0.58	83.36
1.2	12.53	9.38	16.28	13.46	3.15	0.42	2.82	0.32	10.30	0.50	89.70
Total					7.53					1.38	

Table B207: Sink-Float Data for Run3, Plate7a

Sections	Column Length (m)	Sink-Float SG	Tracer SG
Overflow	0.00	1.38	1.20
Tops	0.40	1.34	1.20
Sect 5	0.46	1.40	1.20
Sect 4	0.52	1.26	1.40
Sect 3	0.58	1.35	1.57
Sect 2	0.64	1.37	1.64
Sect 1	0.72	1.38	1.67
Underflow	1.22	1.39	1.69

Table B208: Sink-Float and Tracer Bed Profile Data for Run3, Plate7a

APPENDIX C: ADDITIONAL EXPERIMENTAL RESULTS & GRAPHS

APPENDIX C: ADDITIONAL EXPERIMENTAL RESULTS & GRAPHS

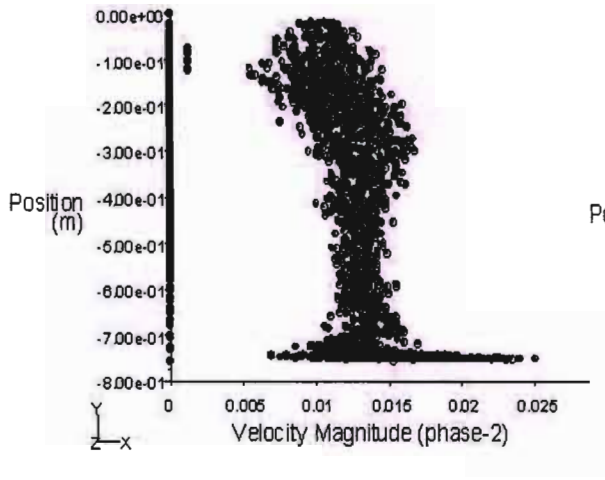

Figure C1: Phase2 Velocity Profile at 3l/min – Plate3. 1.2 SG

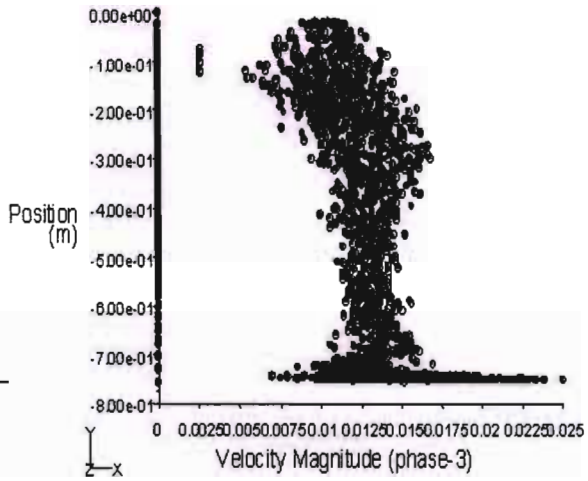

Figure C2: Phase3 Velocity Profile at 3l/min – Plate3. 1.4 SG

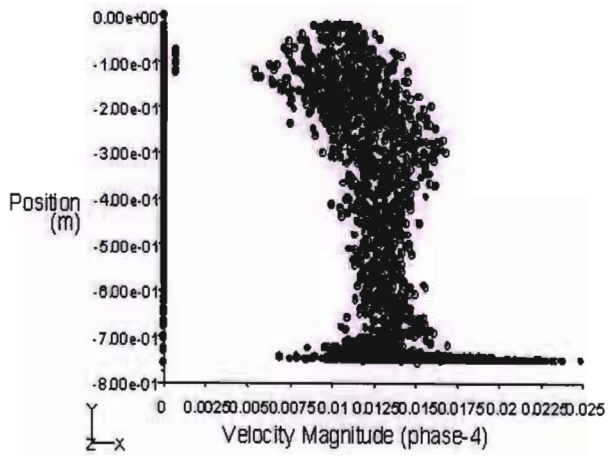

Figure C3: Phase4 Velocity Profile at 3l/min – Plate3.1.6 SG

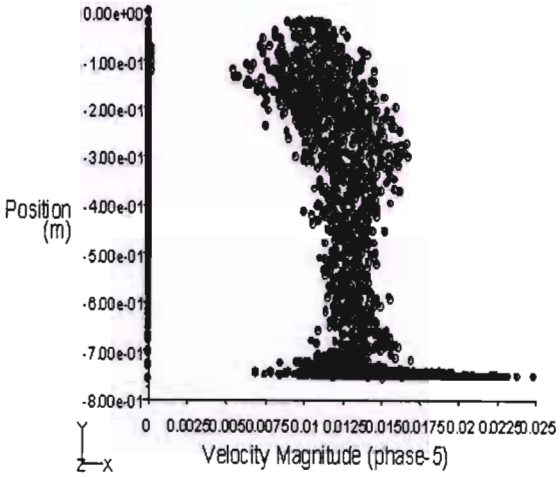

Figure C4: Phase5 Velocity Profile at 3l/min – Plate3. 1.8 SG

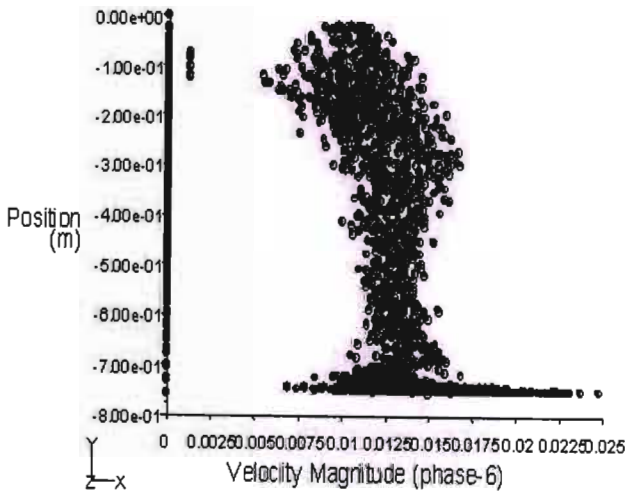

Figure C5: Phase6 Velocity Profile at 3l/min – Plate3. 2.0 SG

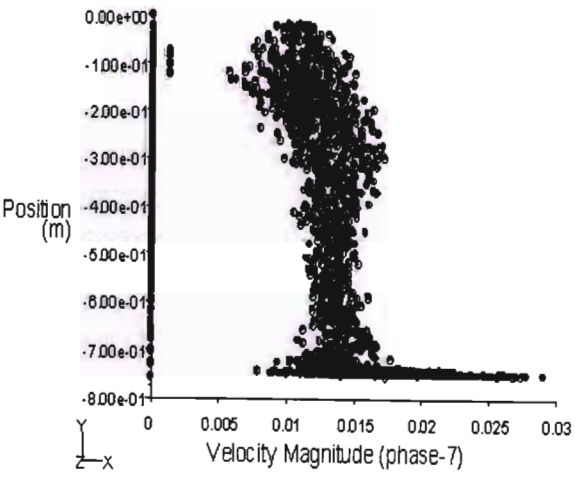

Figure C6: Phase7 Velocity Profile at 3l/min – Plate3. 1.2 SG

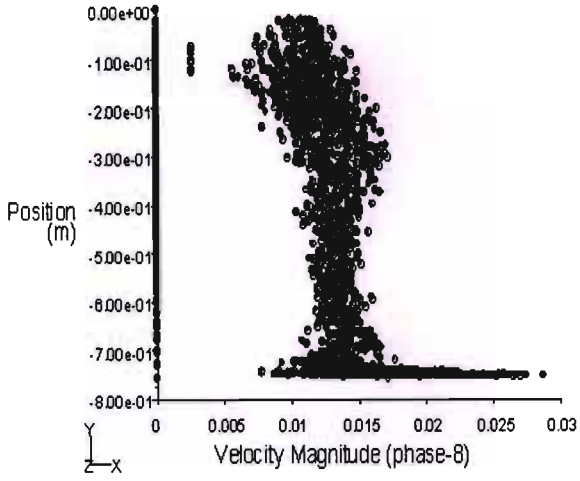

Figure C7: Phase8 Velocity Profile at 3l/min – Plate3. 1.4 SG

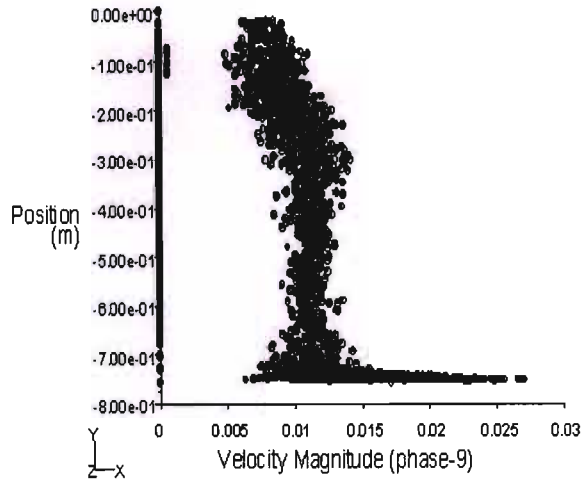

Figure C8: Phase9 Velocity Profile at 3l/min – Plate3. 1.6 SG

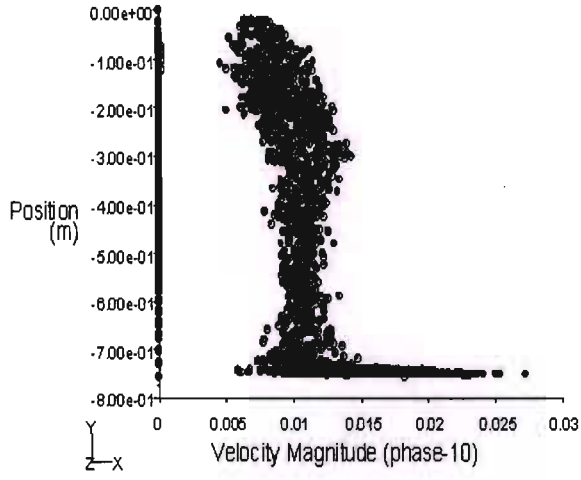

Figure C9: Phase10 Velocity Profile at 3l/min – Plate3. 1.8 SG

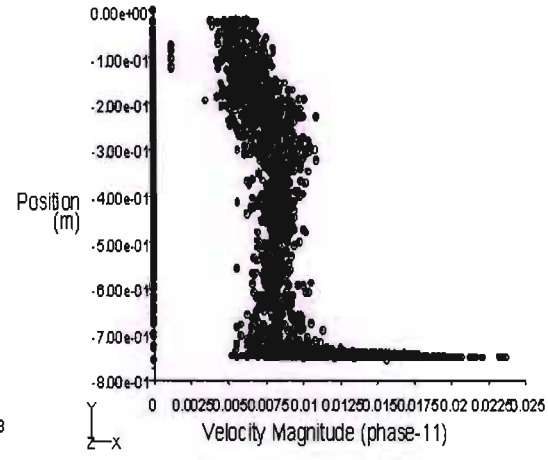

Figure C10: Phase11 Velocity Profile at 3l/min –Plate3. 2.0 SG

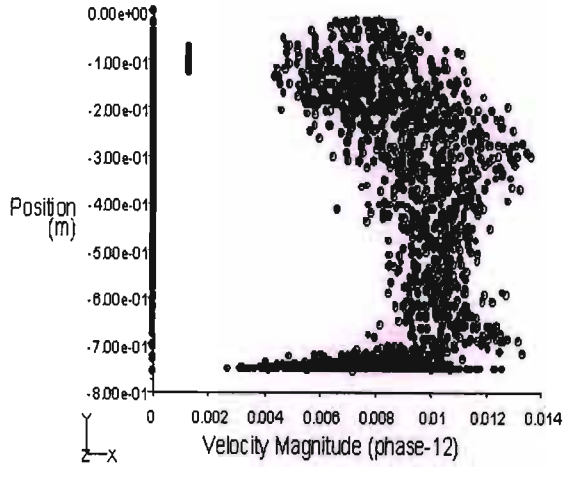

Figure C11: Phase12 Velocity Profile at 3l/min – Plate3. 1.2 SG

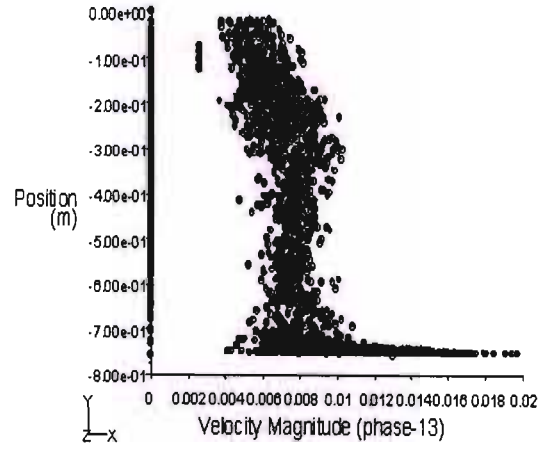

Figure C12: Phase13 Velocity Profile at 3l/min – Plate3. 1.4 SG

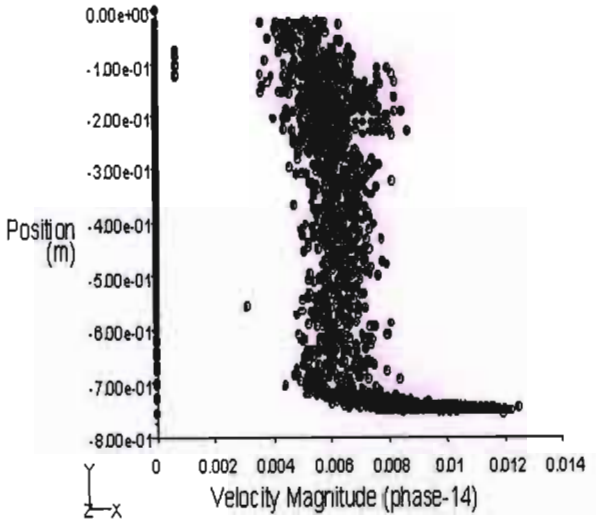

Figure C13: Phase14 Velocity Profile at 3l/min – Plate3. 1.6 SG

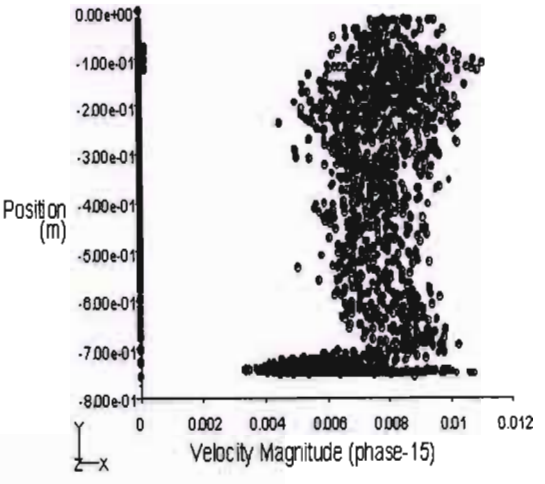

Figure C14: Phase15 Velocity Profile at 3l/min –Plate3. 1.8 SG

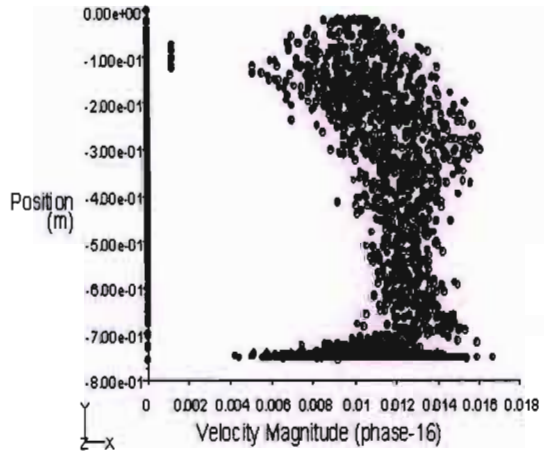

Figure C15: Phase16 Velocity Profile at 3l/min –Plate3. 2.0 SG

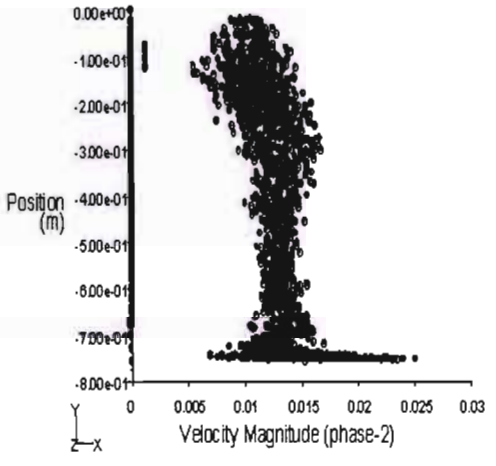

Figure C16: Phase2 Velocity Profile at 8l/min – Plate3. 1.2 SG

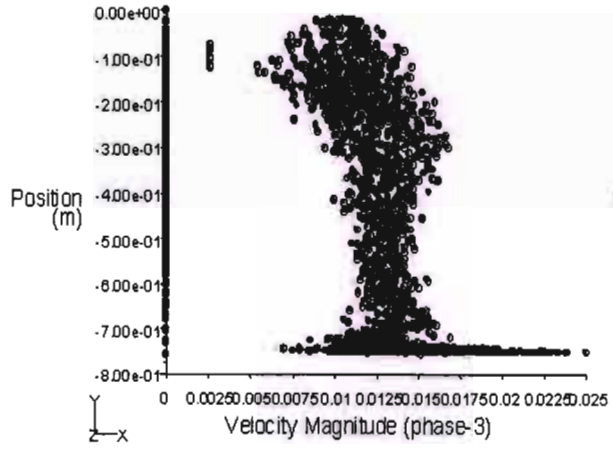

Figure C17: Phase3 Velocity Profile at 8l/min – Plate3. 1.4 SG

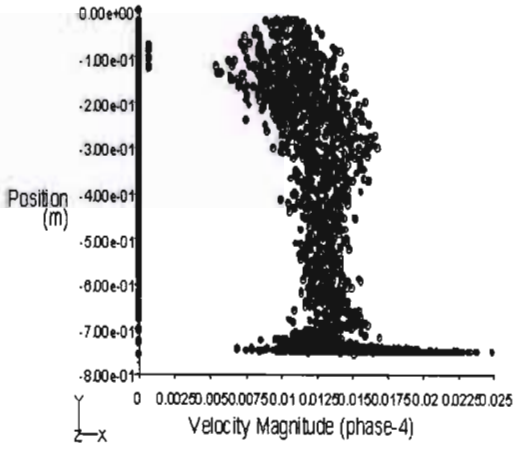

Figure C18: Phase4 Velocity Profile at 8l/min –Plate3. 1.6 SG

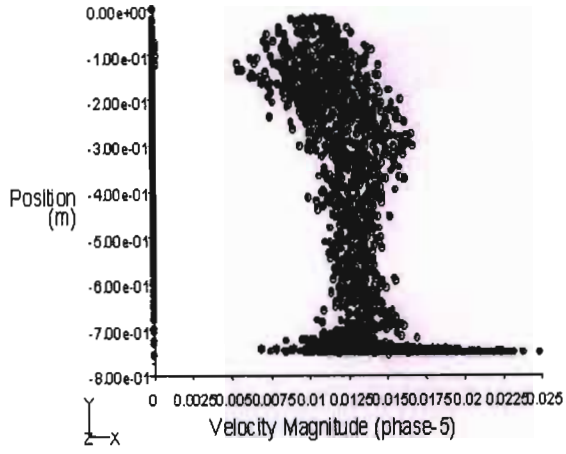

Figure C19: Phase5 Velocity Profile at 8l/min – Plate3. 1.8 SG

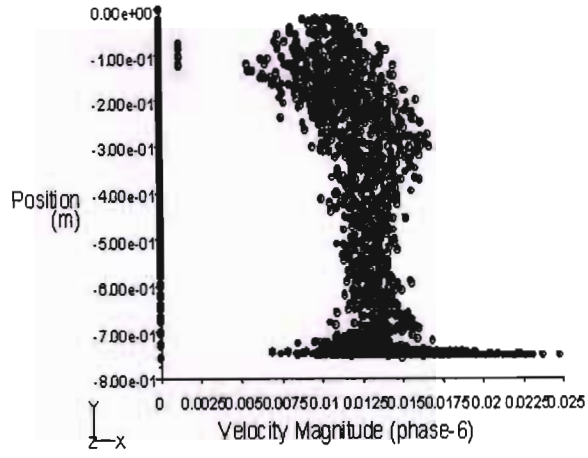

Figure C20: Phase6 Velocity Profile at 8l/min – Plate3. 2.0 SG

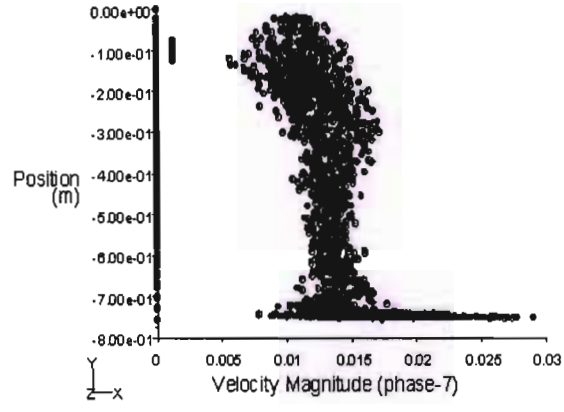

Figure C21: Phase7 Velocity Profile at 8l/min –Plate3. 1.2 SG

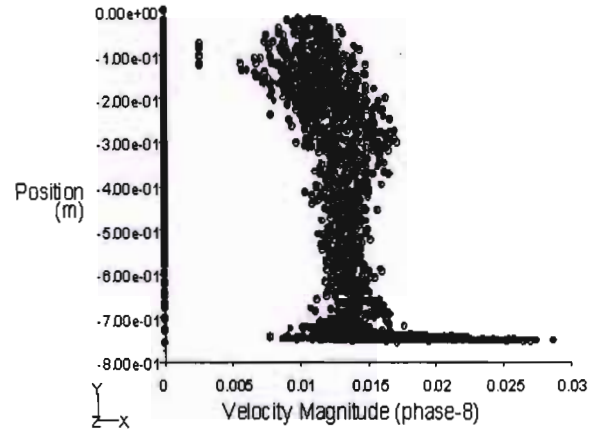

Figure C22: Phase8 Velocity Profile at 8l/min – Plate3. 1.4 SG

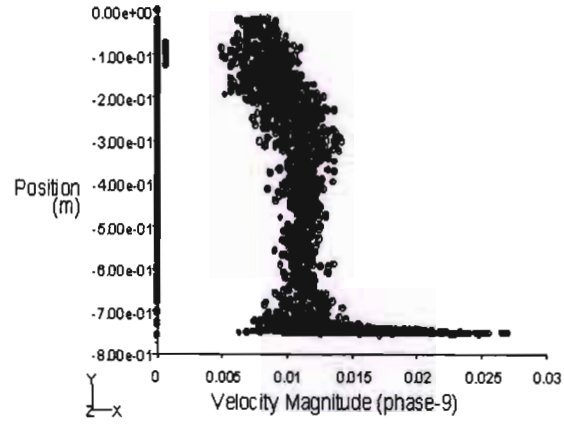

Figure C23: Phase9 Velocity Profile at 8l/min – Plate3. 1.6 SG

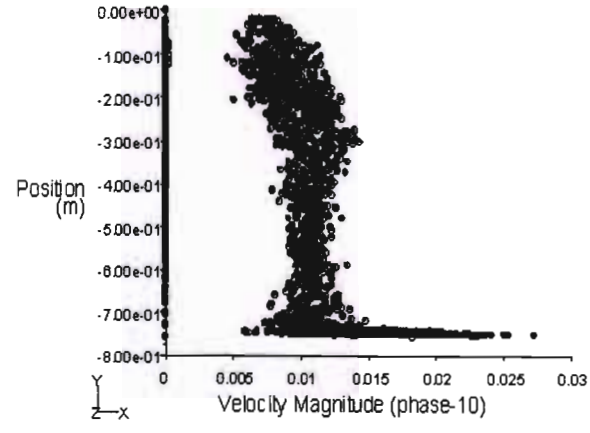

Figure C24: Phase10 Velocity Profile at 8l/min – Plate3. 1.8 SG

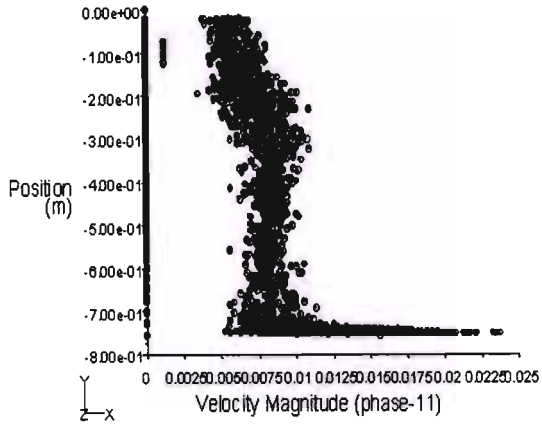

Figure C25: Phase11 Velocity Profile at 8l/min –Plate3. 2.0 SG

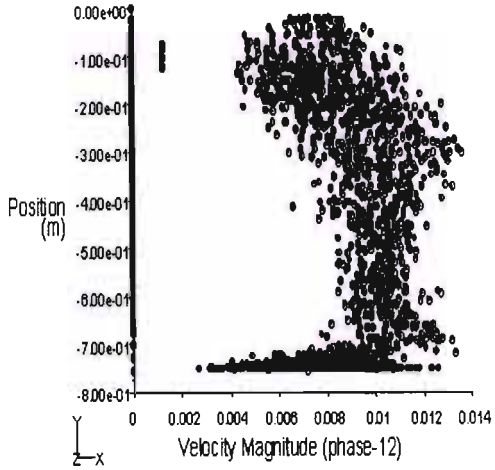

Figure C26: Phase12 Velocity Profile at 8l/min – Plate3. 1.2 SG

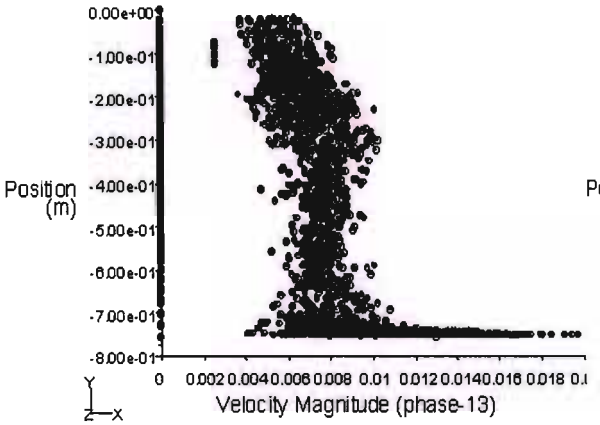

Figure C27: Phase13 Velocity Profile at 8l/min – Plate3. 1.4 SG

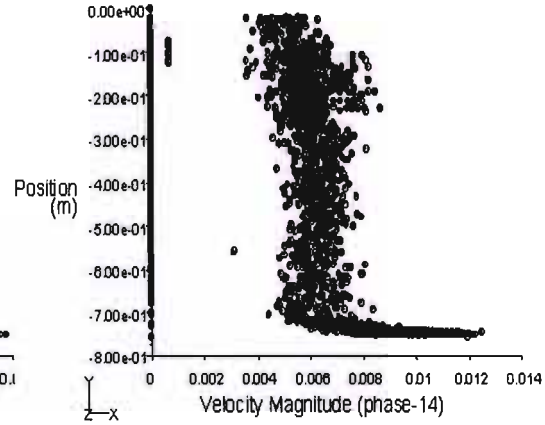

Figure C28: Phase14 Velocity Profile at 8l/min – Plate3. 1.6 SG

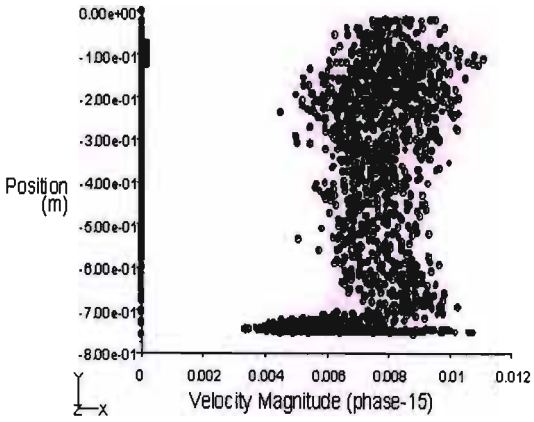

Figure C29: Phase15 Velocity Profile at 8l/min –Plate3. 1.8 SG

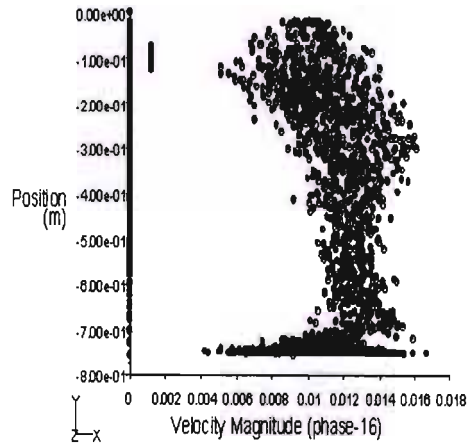

Figure C30: Phase16 Velocity Profile at 8l/min – Plate3. 2.0 SG

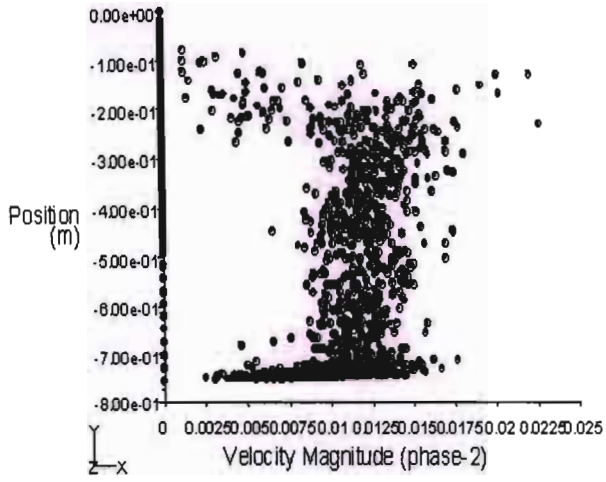

Figure C31: Phase2 Velocity Profile at 3l/min – Plate4. 1.2 SG

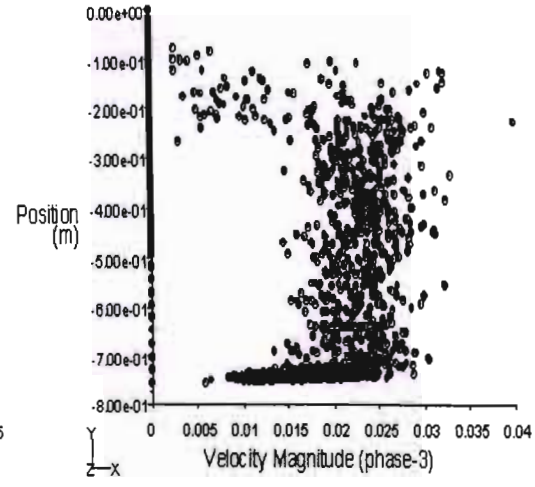

Figure C32: Phase3 Velocity Profile at 3l/min – Plate4. 1.4 SG

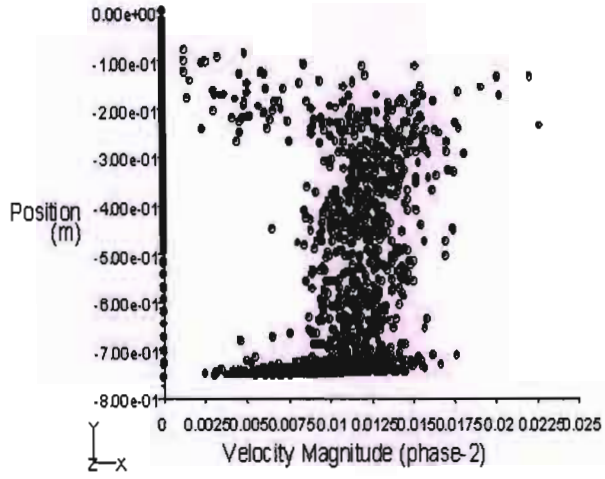

Figure C31: Phase2 Velocity Profile at 3l/min – Plate4. 1.2 SG

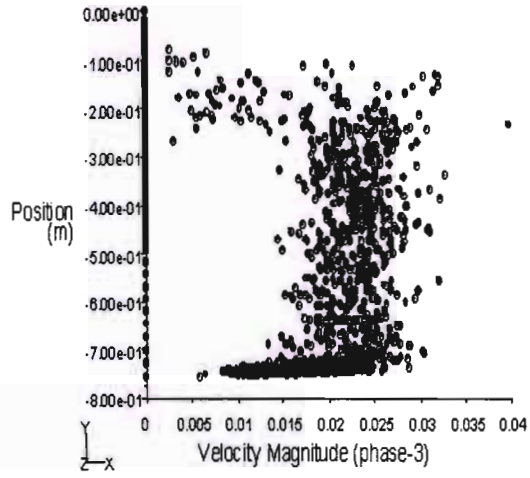

Figure C32: Phase3 Velocity Profile at 3l/min – Plate4. 1.4 SG

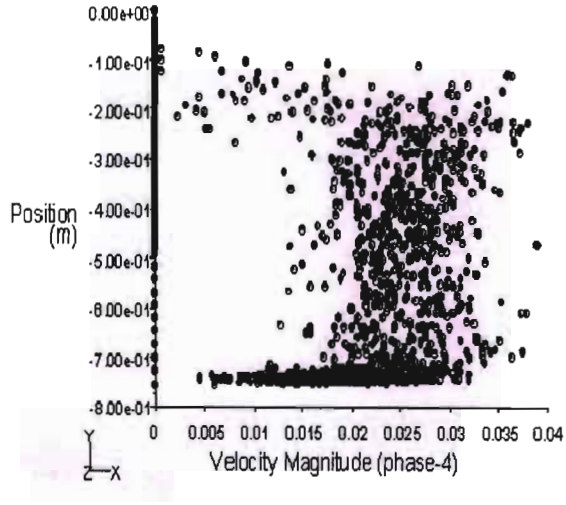

Figure C33: Phase4 Velocity Profile at 3l/min – Plate4. 1.6 SG

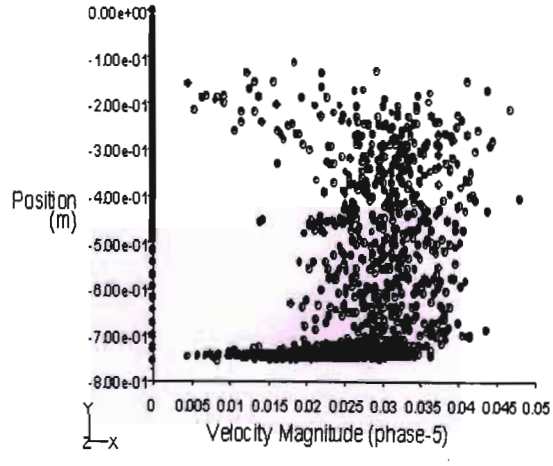

Figure C34: Phase5 Velocity Profile at 3l/min – Plate4. 1.8 SG

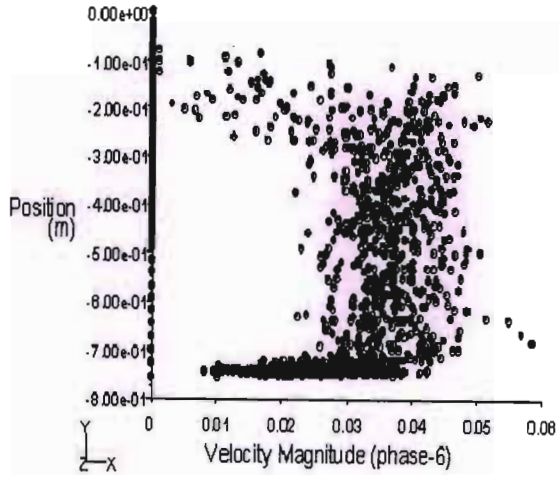

Figure C35: Phase6 Velocity Profile at 3l/min – Plate4. 2.0 SG

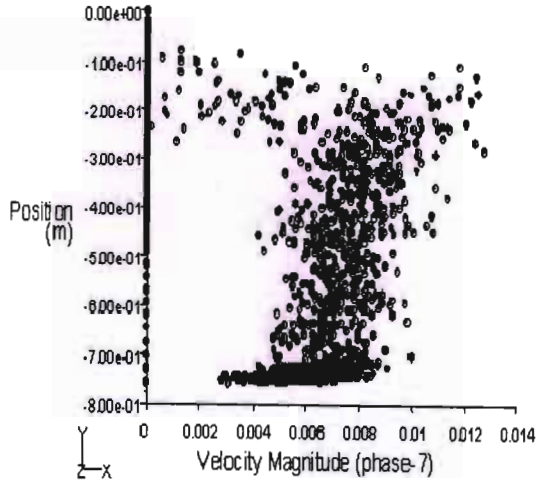

Figure C36: Phase7 Velocity Profile at 3l/min – Plate4. 1.2 SG

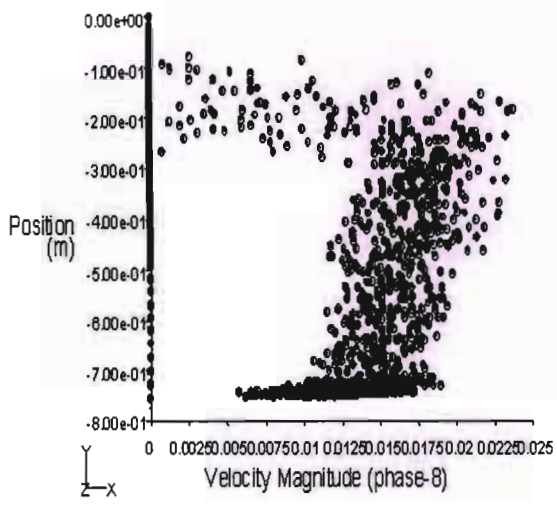

Figure C37: Phase8 Velocity Profile at 3l/min – Plate4. 1.4 SG

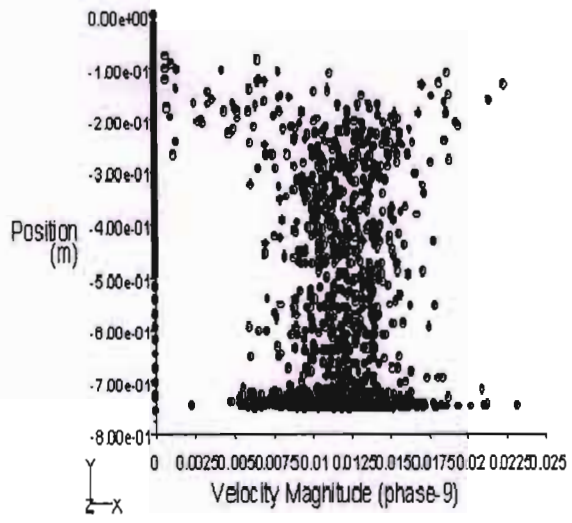

Figure C38: Phase9 Velocity Profile at 3l/min – Plate4. 1.6 SG

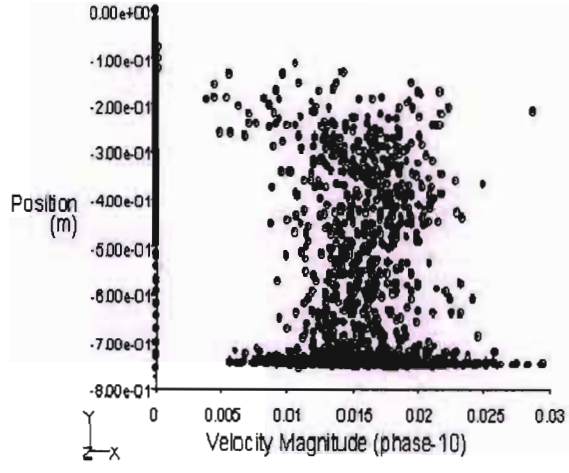

Figure C39: Phase10 Velocity Profile at 3l/min – Plate4. 1.8 SG

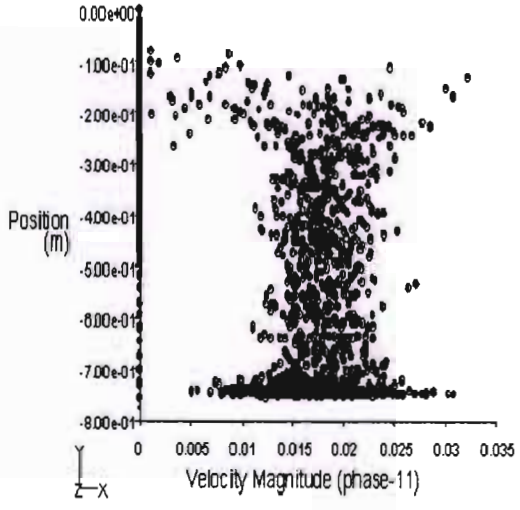

Figure C40: Phase11 Velocity Profile at 3l/min – Plate4. 2.0 SG

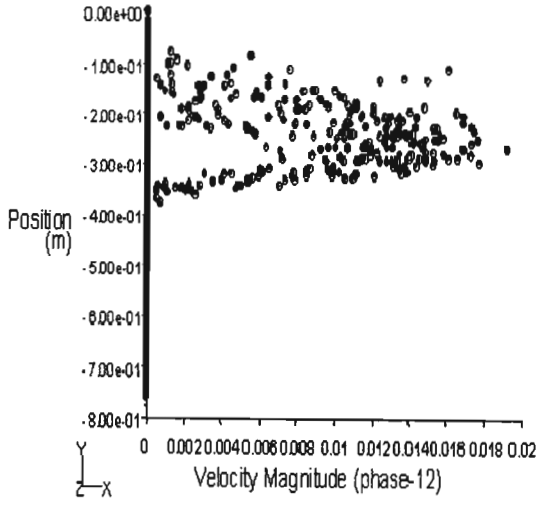

Figure C41: Phase12 Velocity Profile at 3l/min – Plate4. 1.2 SG

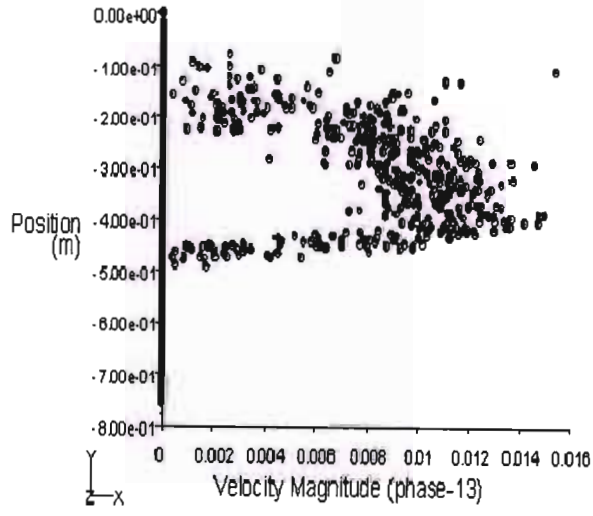

Figure C42: Phase13 Velocity Profile at 3l/min – Plate4. 1.4 SG

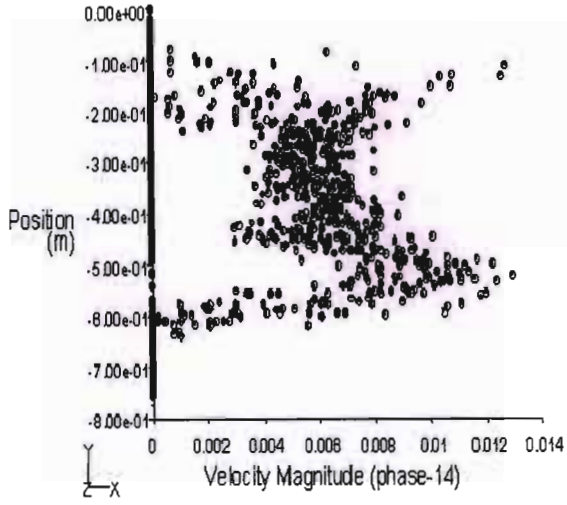

Figure C43: Phase14 Velocity Profile at 3l/min – Plate4. 1.6 SG

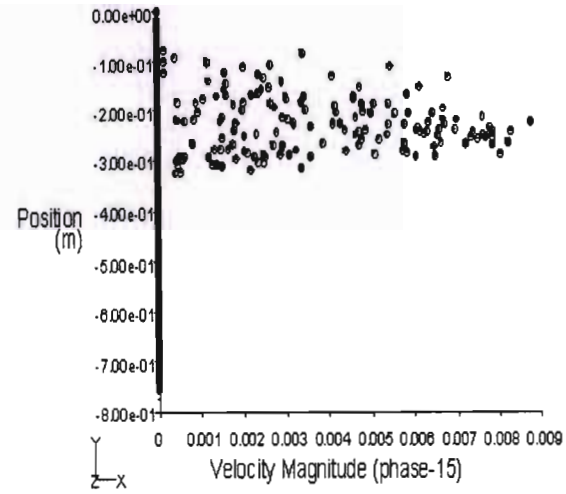

Figure C44: Phase15 Velocity Profile at 3l/min – Plate4. 1.8 SG

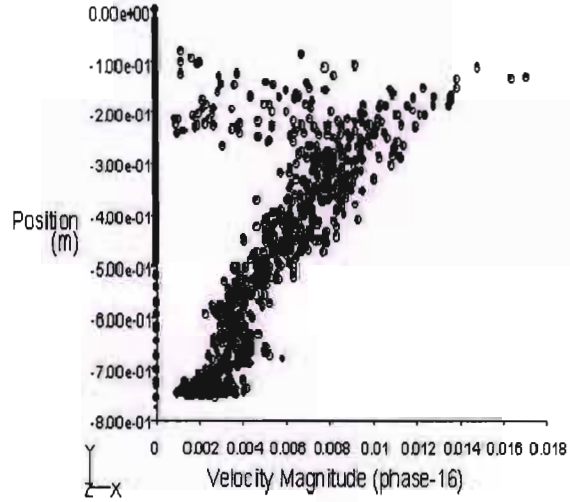

Figure C45: Phase16 Velocity Profile at 3l/min – Plate4. 2.0 SG

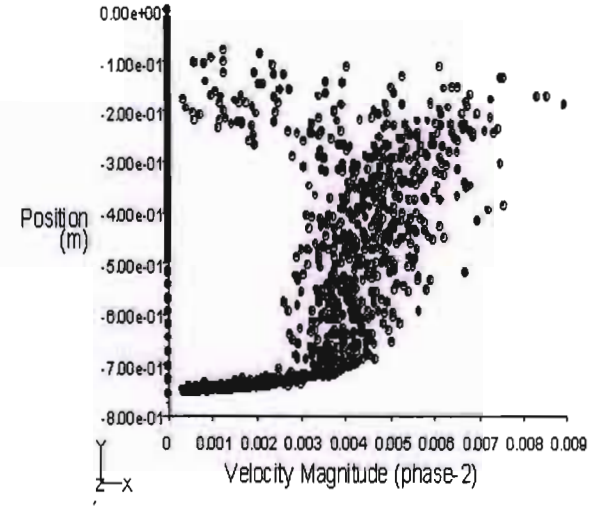

Figure C46: Phase2 Velocity Profile at 6l/min – Plate4. 1.2 SG

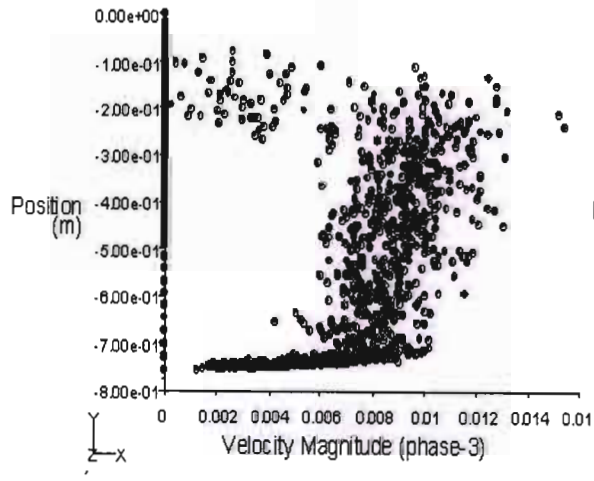

Figure C47: Phase3 Velocity Profile at 6l/min – Plate4. 1.4 SG

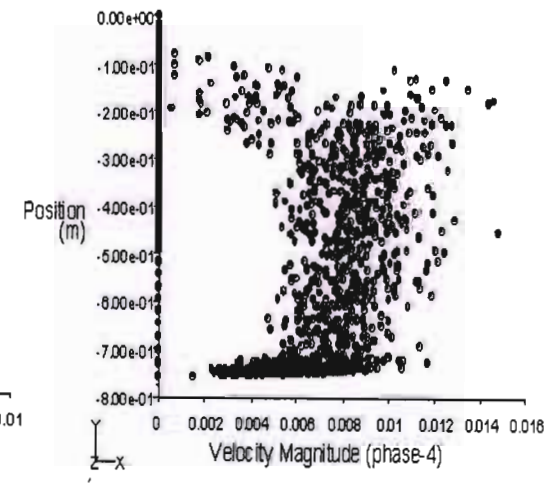

Figure C48: Phase4 Velocity Profile at 6l/min – Plate4. 1.6 SG

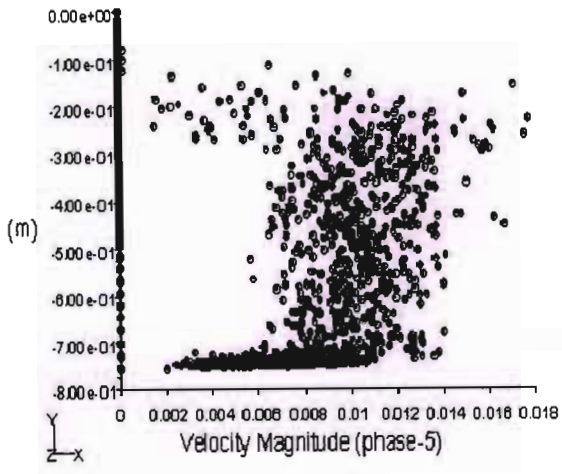

Figure C49: Phase5 Velocity Profile at 6l/min – Plate4. 1.8 SG

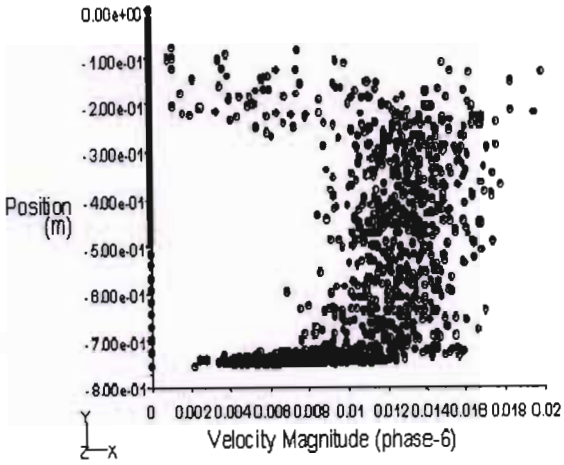

Figure C50: Phase6 Velocity Profile at 6l/min – Plate4. 2.0 SG

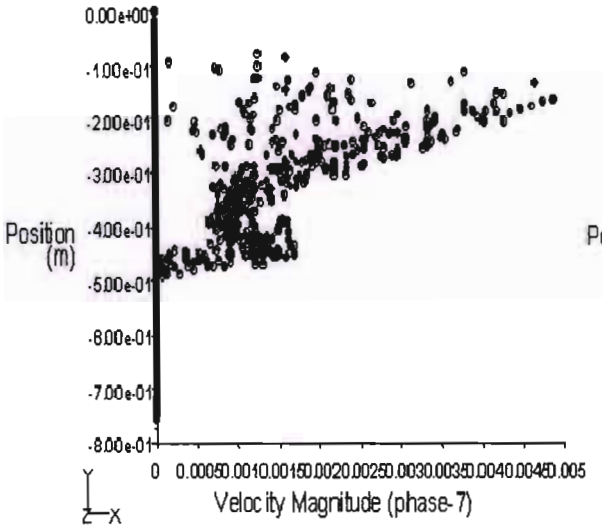

Figure C51: Phase7 Velocity Profile at 6l/min – Plate4. 1.2 SG

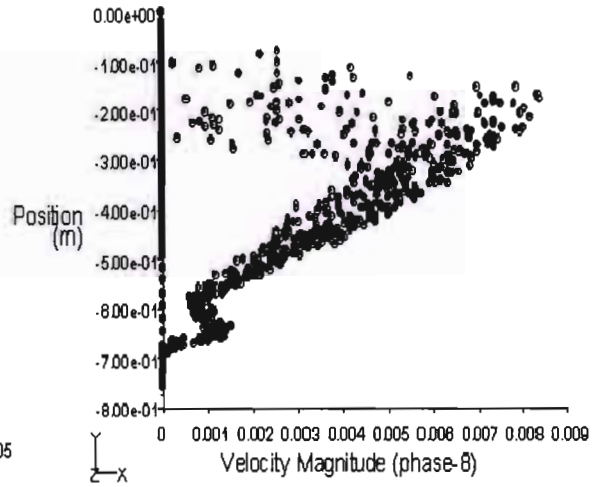

Figure C52: Phase8 Velocity Profile at 6l/min – Plate4. 1.4 SG

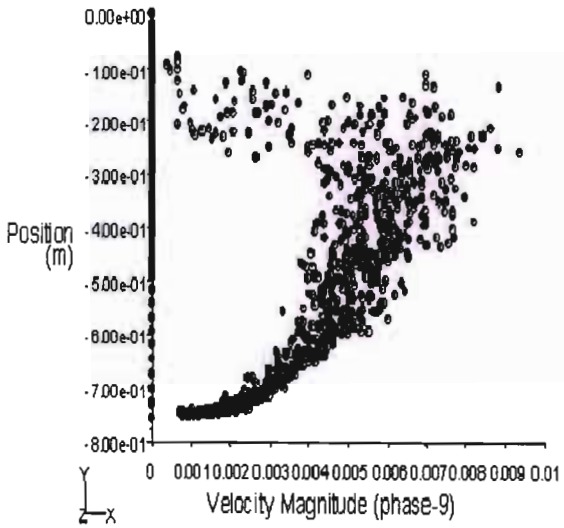

Figure C53: Phase9 Velocity Profile at 6l/min – Plate4. 1.6 SG

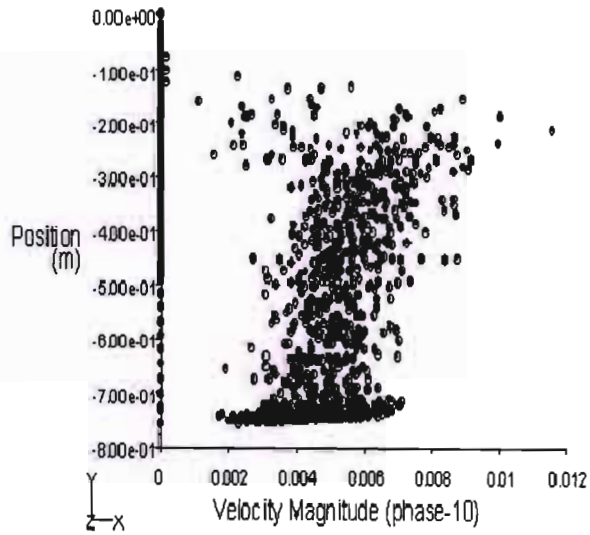

Figure C54: Phase10 Velocity Profile at 6l/min – Plate4. 1.8 SG

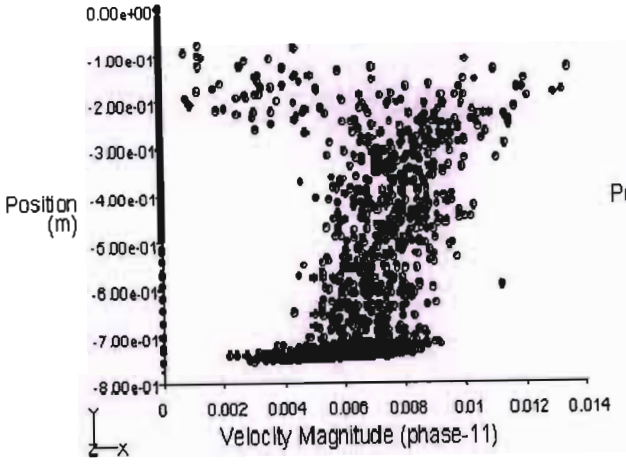

Figure C55: Phase11. Velocity Profile at 6l/min – Plate4. 2.0 SG

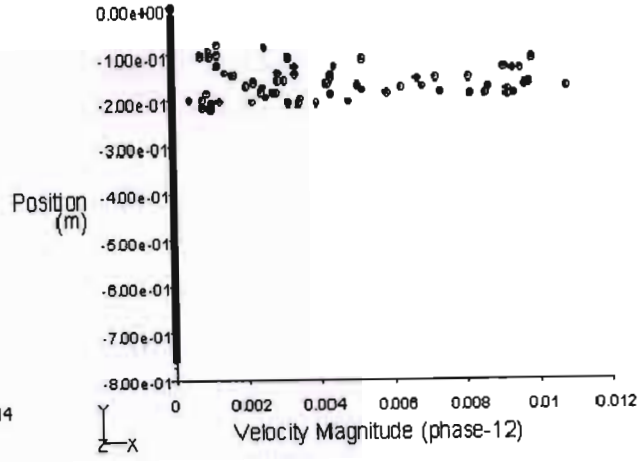

Figure C56: Phase12. Velocity Profile at 6l/min – Plate4. 1.2 SG

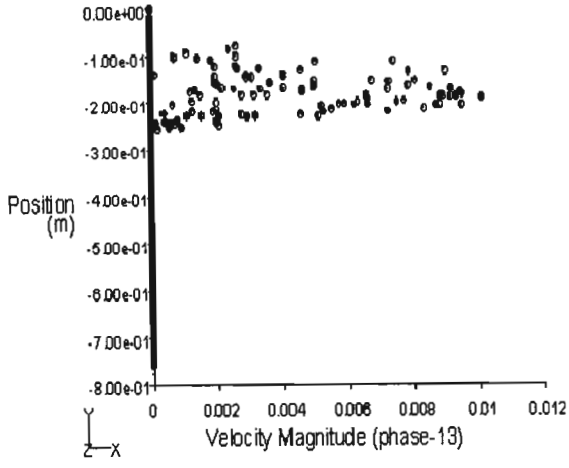

Figure C57: Phase13. Velocity Profile at 6l/min – Plate4. 1.4 SG

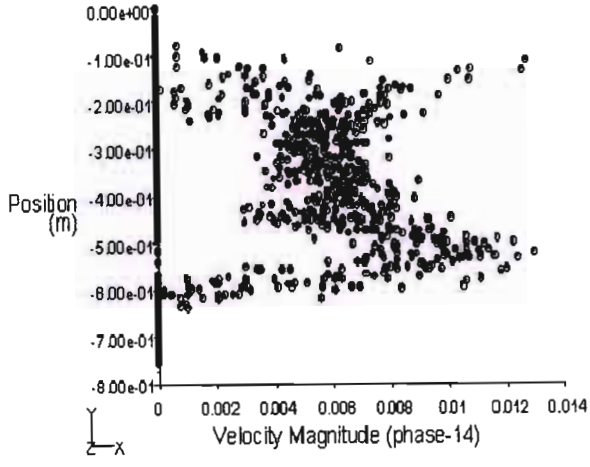

Figure C58: Phase14. Velocity Profile at 6l/min – Plate4. 1.6 SG

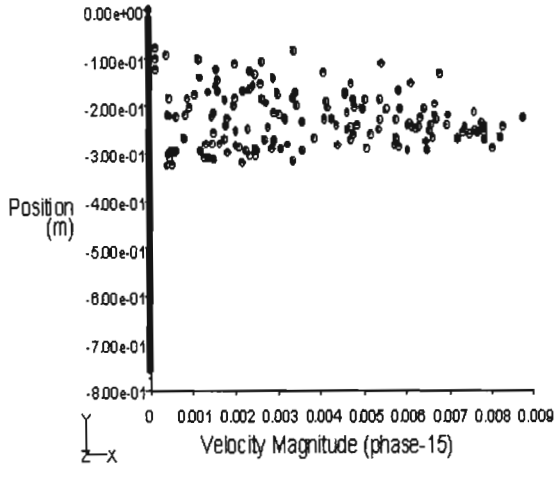

Figure C59: Phase15. Velocity Profile at 6l/min – Plate4. 1.8 SG

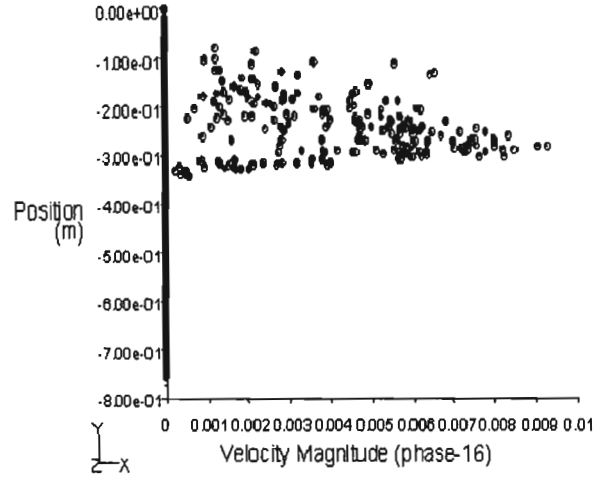

Figure C60: Phase16. Velocity Profile at 6l/min – Plate4. 2.0 SG

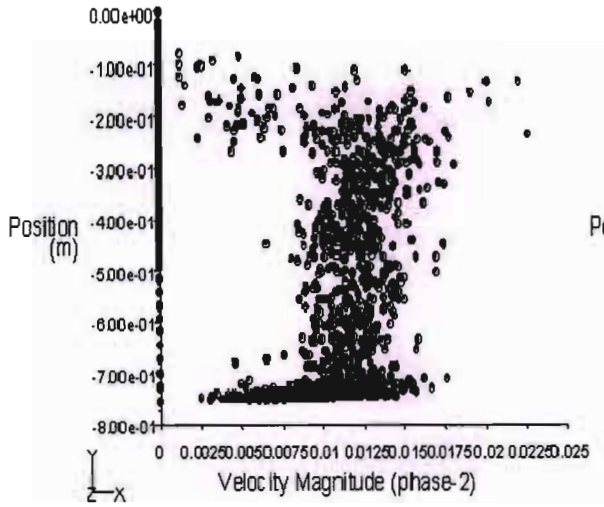

Figure C61: Phase2. Velocity Profile at 8l/min – Plate4. 1.2 SG

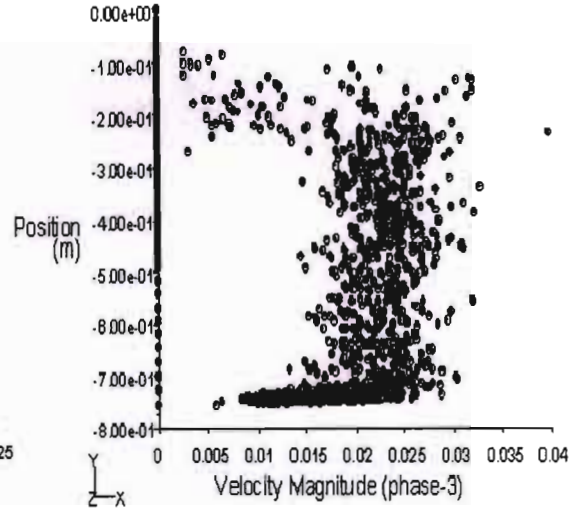

Figure C62: Phase3. Velocity Profile at 8l/min – Plate4. 1.4 SG

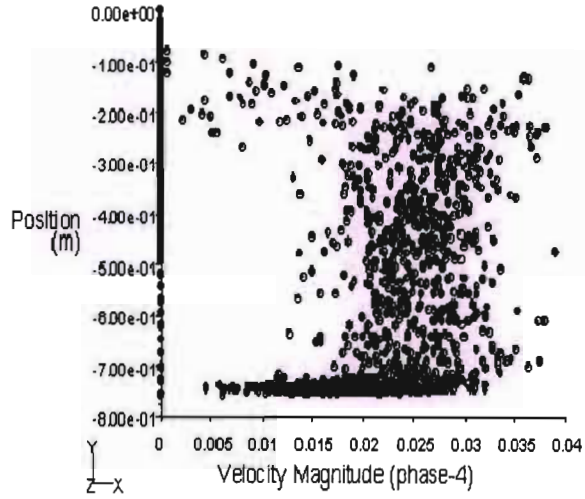

Figure C63: Phase4. Velocity Profile at 8l/min – Plate4. 1.6 SG

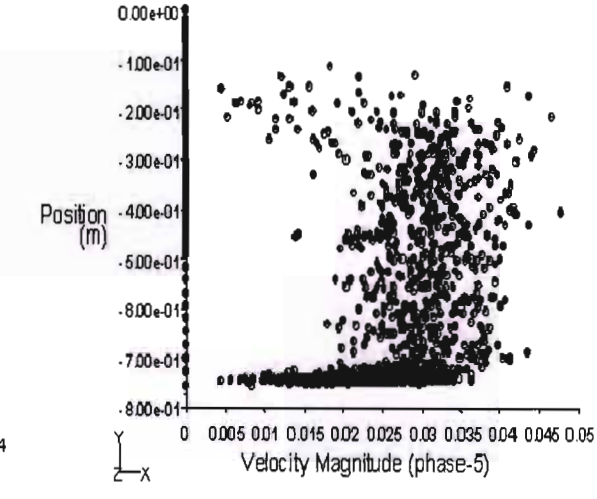

Figure C64: Phase5. Velocity Profile at 8l/min – Plate4. 1.8 SG

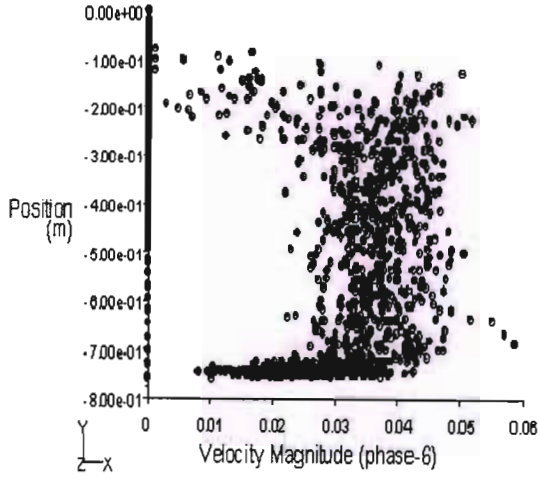

Figure C65: Phase6. Velocity Profile at 8l/min – Plate4. 2.0 SG

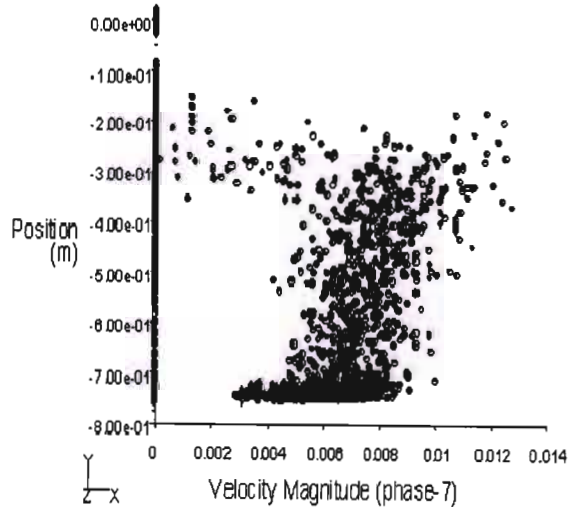

Figure C66: Phase7. Velocity Profile at 8l/min – Plate4. 1.2 SG

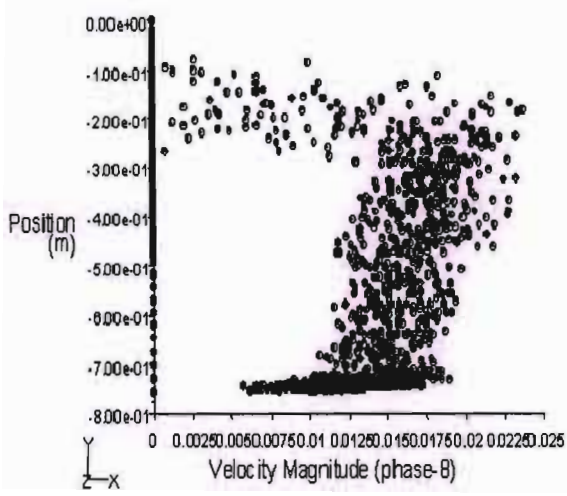

Figure C67: Phase8. Velocity Profile at 8l/min – Plate4. 1.4 SG

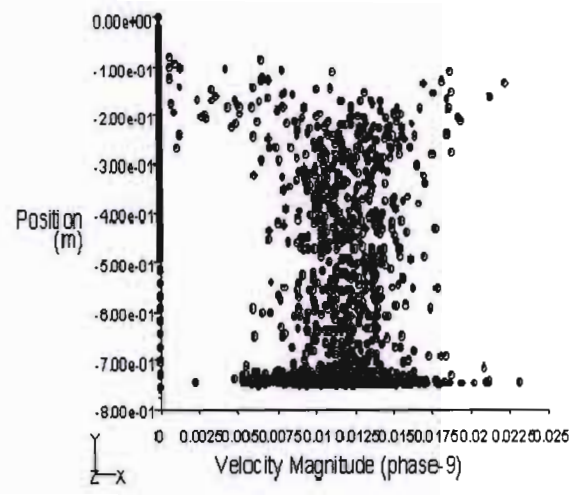

Figure C68: Phase9. Velocity Profile at 8l/min – Plate4. 1.6 SG

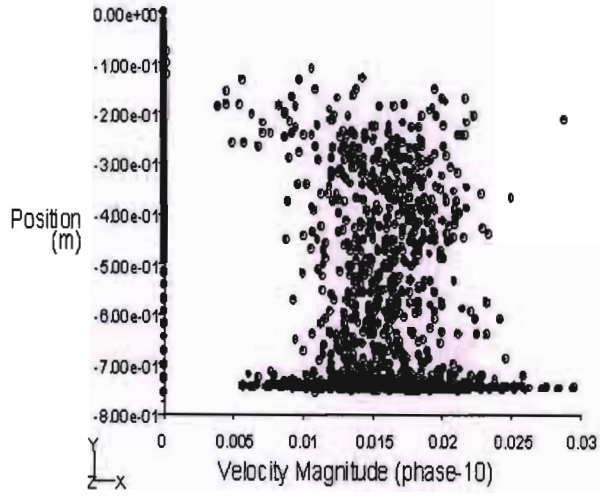

Figure C69.: Phase10. Velocity Profile at 8l/min – Plate4. 1.8 SG

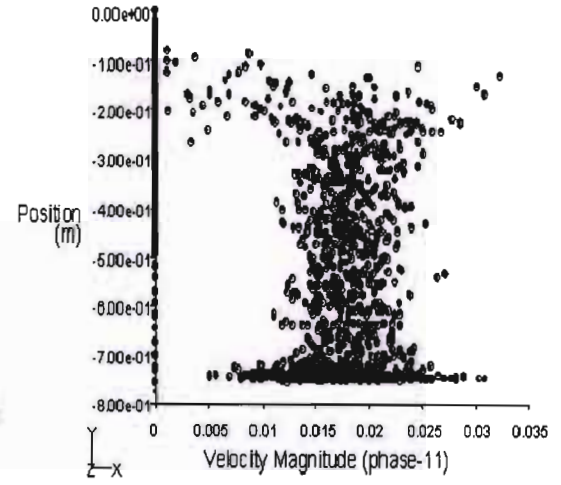

Figure C70: Phase11. Velocity Profile at 8l/min – Plate4. 2.0 SG

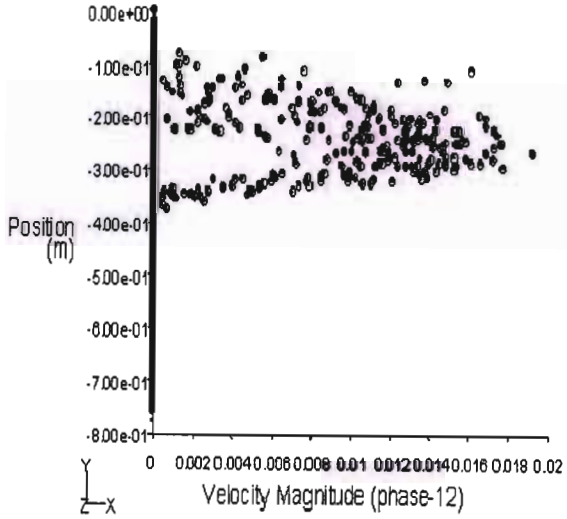

Figure C71: Phase12 Velocity Profile at 8l/min – Plate4. 1.2 SG

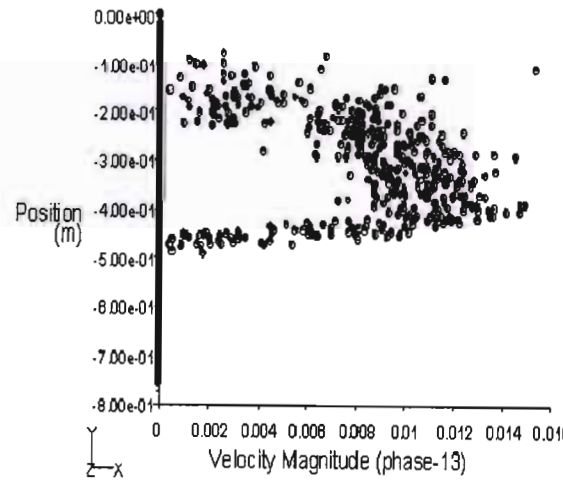

Figure C72: Phase13. Velocity Profile at 8l/min – Plate4. 1.4 SG

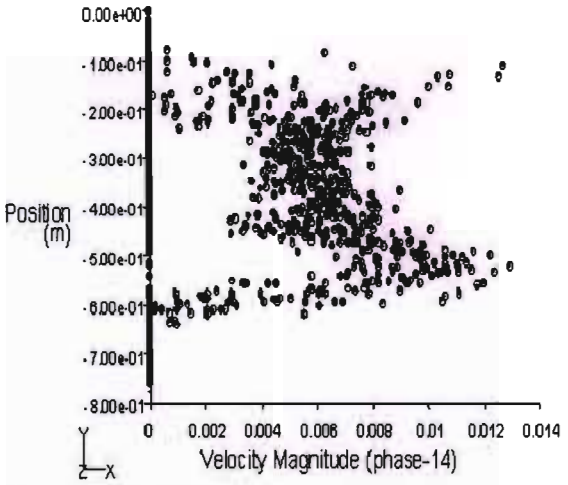

Figure C73: Phase14. Velocity Profile at 8l/min – Plate4. 1.6 SG

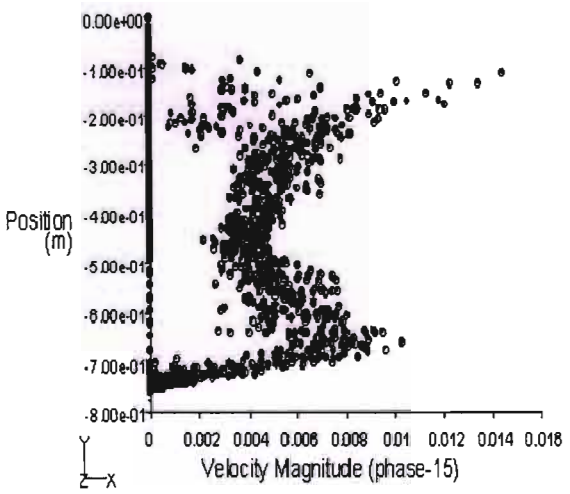

Figure C74: Phase15. Velocity Profile at 8l/min – Plate4. 1.8 SG

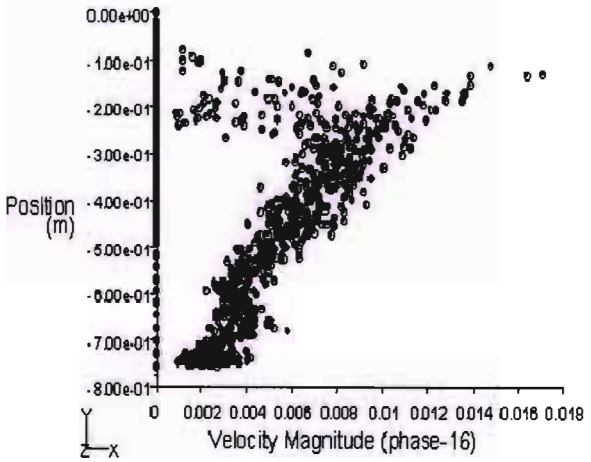

Figure C75: Phase16. Velocity Profile at 8l/min – Plate4. 2.0 SG

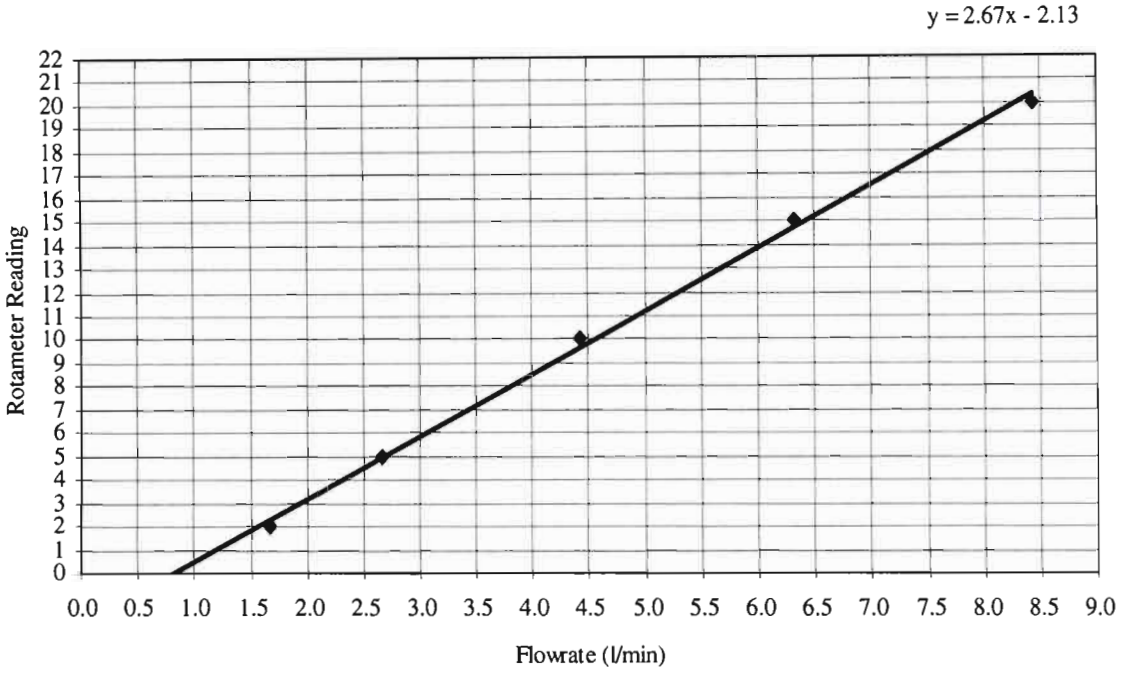

Figure C76: Teeter-water Calibration Graph for Rotameter

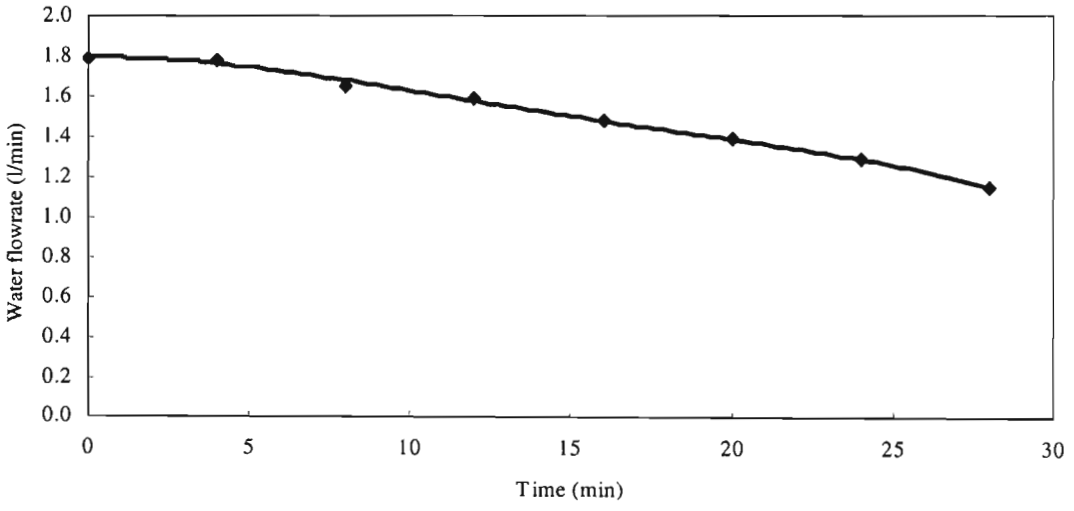

Figure C77: Effect of the Feed Water flow without a Constant Head Tank

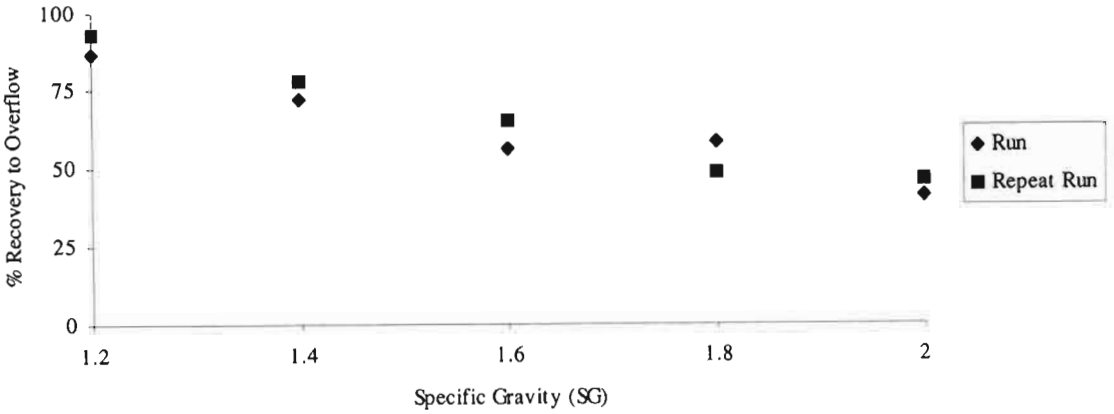

Figure C78: Partition Curve Comparisons for Plate 1 - 6 l/min

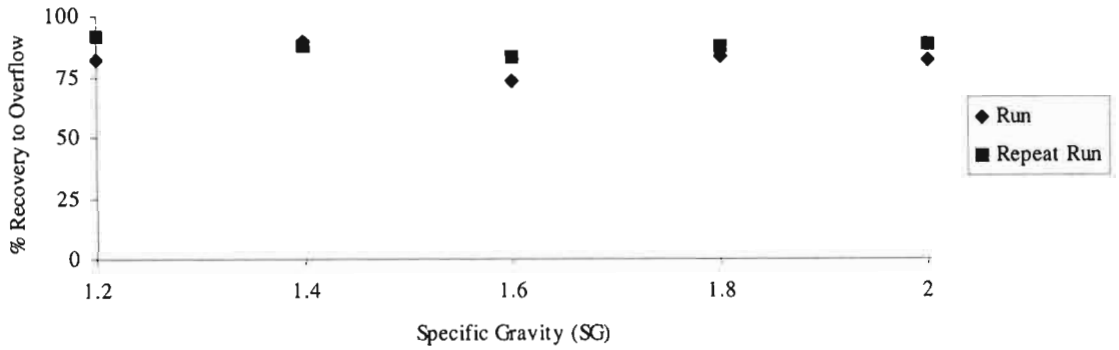

Figure C79: Partition Curve Comparisons for Plate 2 - 6 l/min

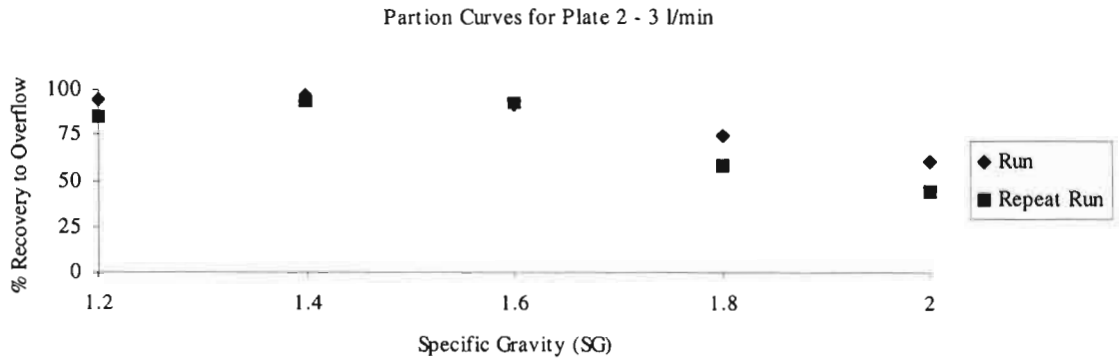

Figure C80: Partition Curve Comparisons for Plate 2 - 3 l/min

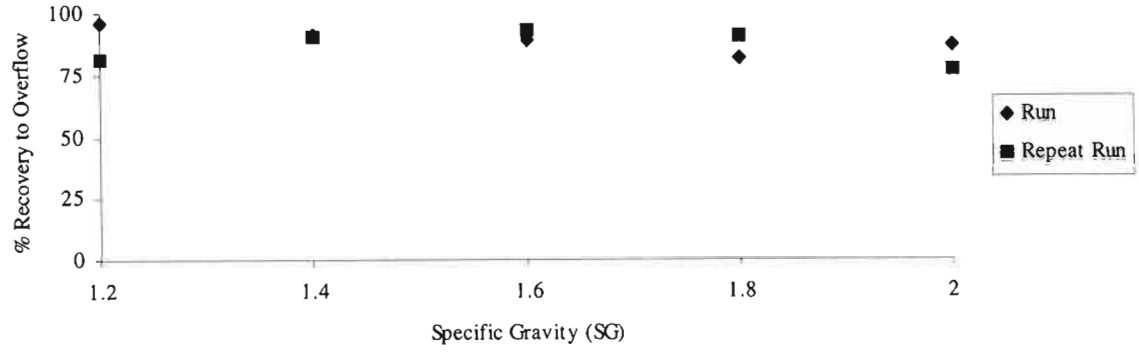

Figure C81: Partition Curve Comparisons for Plate 2 - 8 l/min

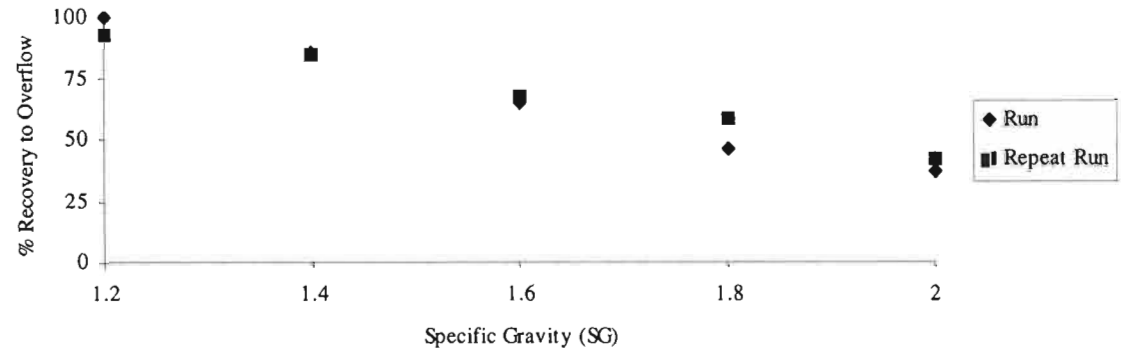

Figure C82: Partition Curve Comparisons for Plate 3 - 3 l/min

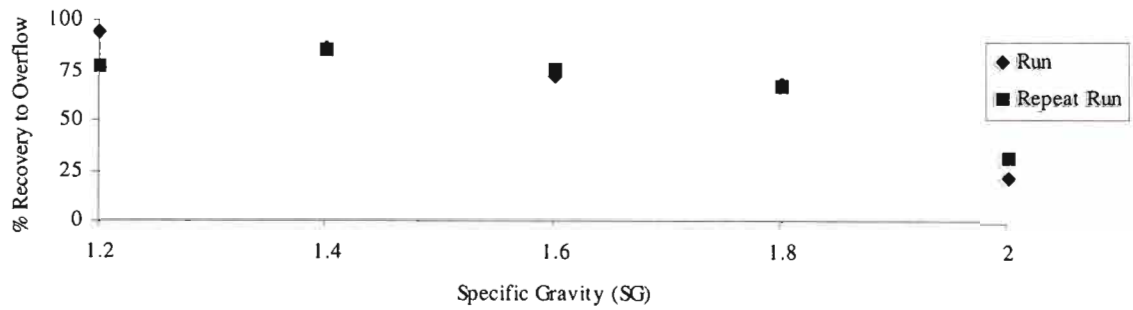

Figure C83: Partition Curve Comparisons for Plate 3 - 8 l/min

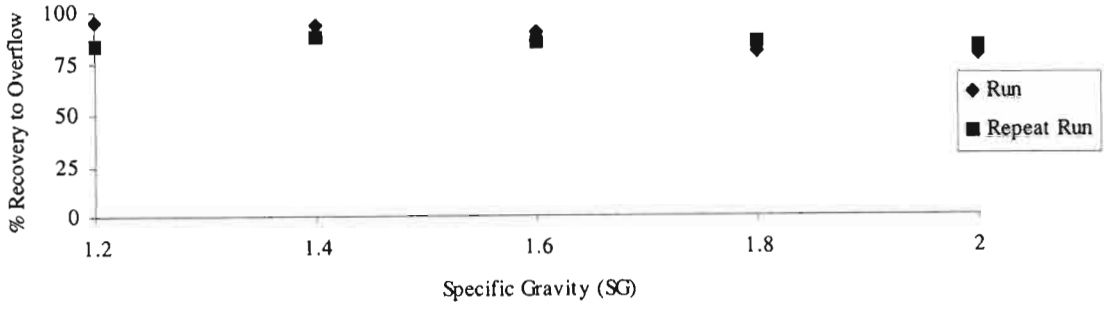

Figure C84: Partition Curve Comparisons for Plate 4 - 6 l/min

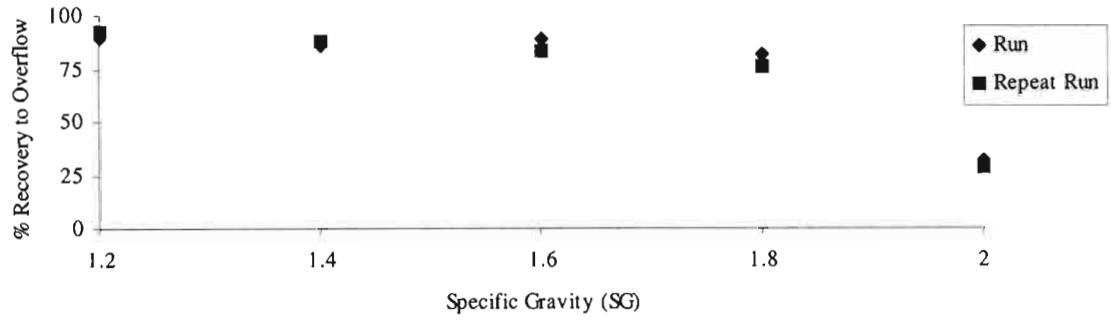

Figure C85: Partition Curve Comparisons for Plate 4 - 3 l/min

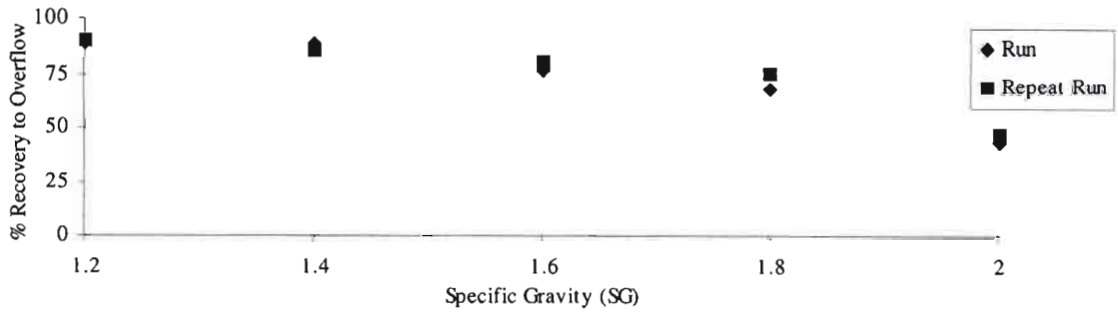

Figure C86: Partition Curve Comparisons for Plate 4 - 8 l/min

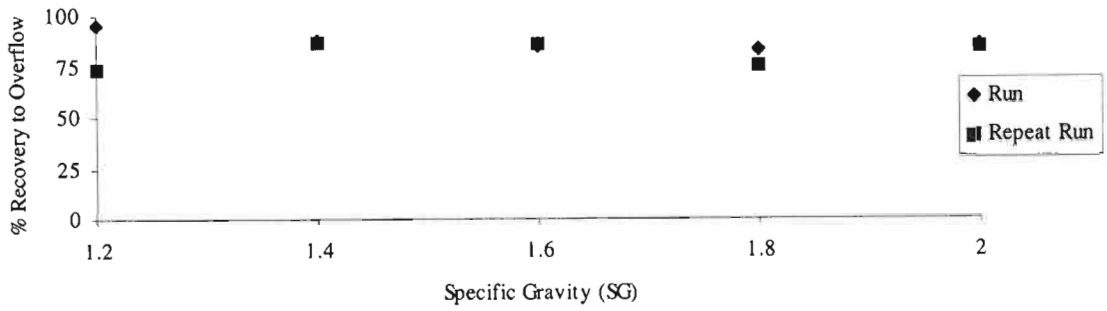

Figure C87: Partition Curve Comparisons for Plate 5 – 6 l/min

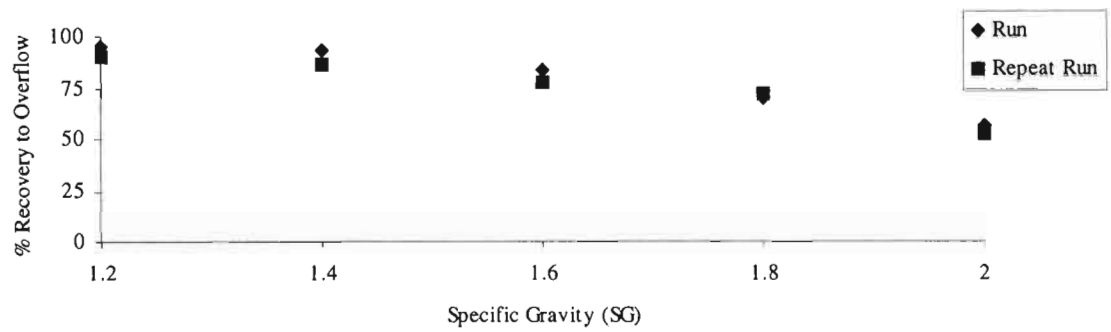

Figure C88: Partition Curve Comparisons for Plate 5 – 3 l/min

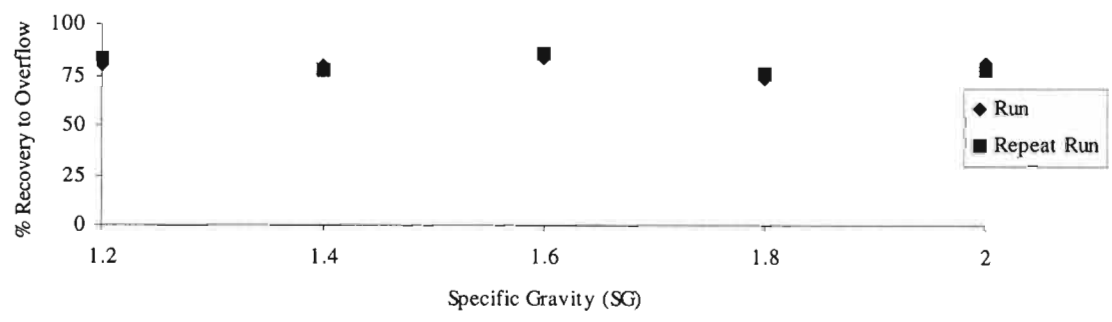

Figure C89: Partition Curve Comparisons for Plate 5 – 8 l/min

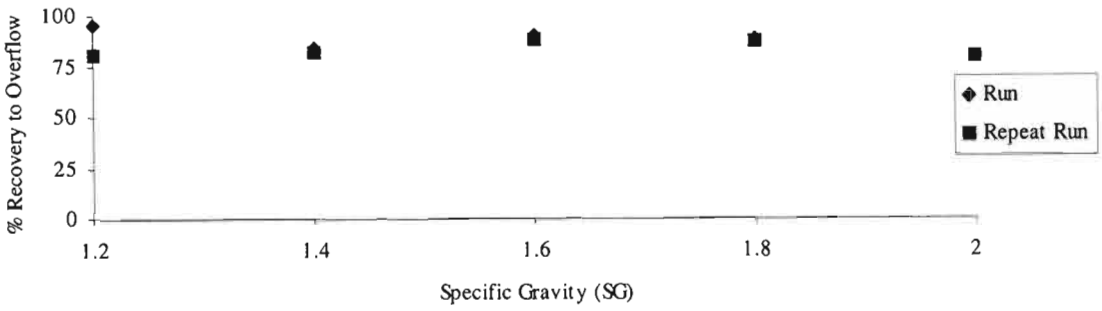

Figure C90: Partition Curve Comparisons for Plate 6 – 6 l/min

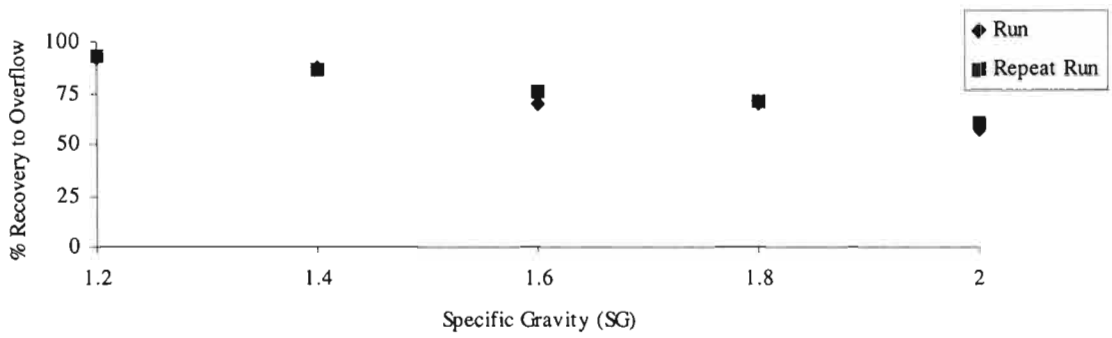

Figure C91: Partition Curve Comparisons for Plate 6– 3 l/min

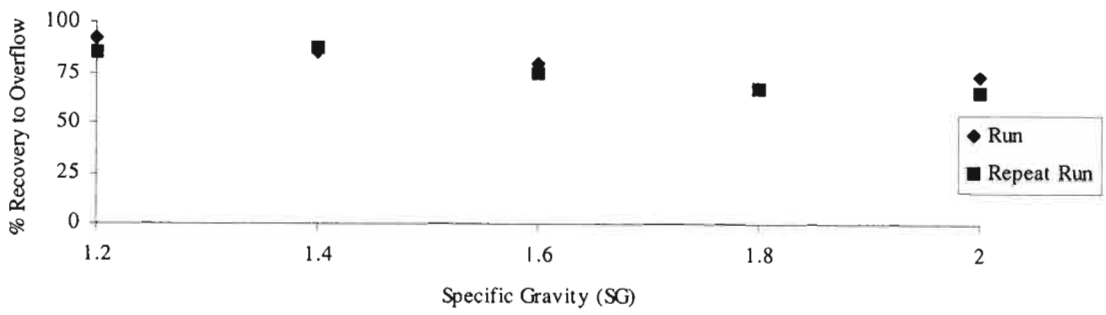

Figure C92: Partition Curve Comparisons for Plate 6 – 8 l/min

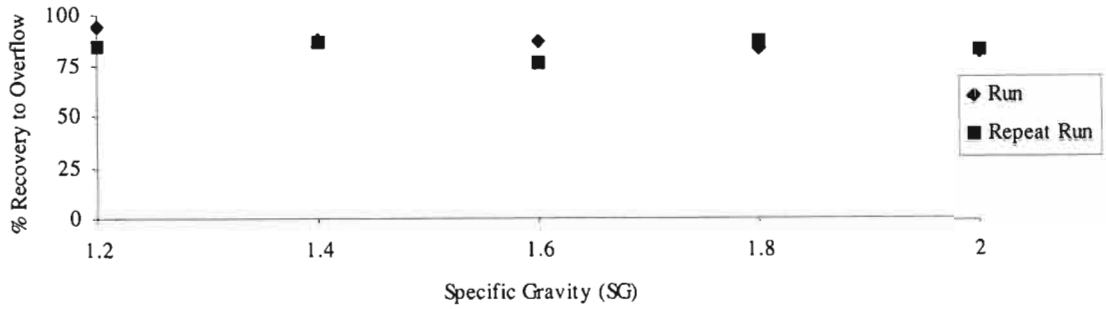

Figure C93: Partition Curve Comparisons for Plate 7 – 6 l/min

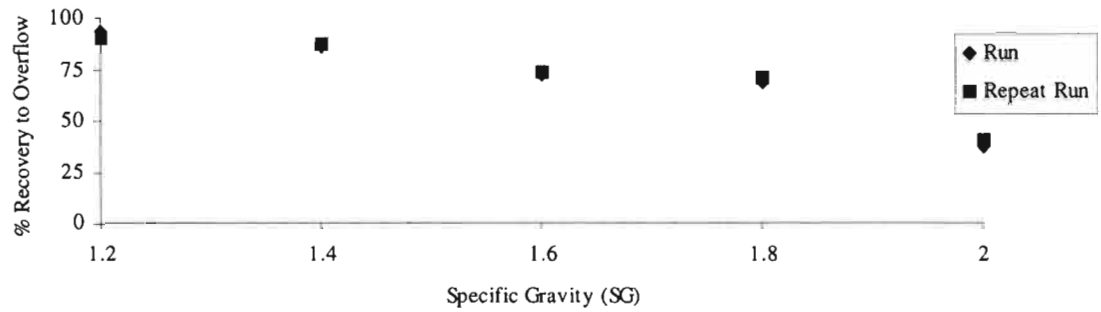

Figure C94: Partition Curve Comparisons for Plate 7 – 3 l/min

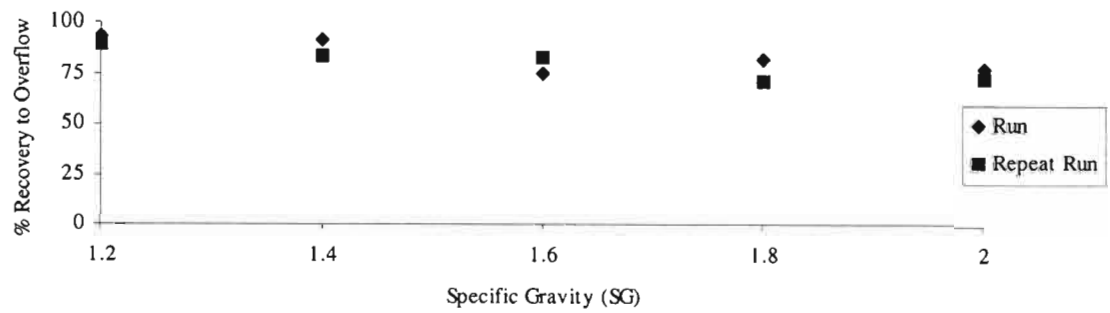

Figure C95: Partition Curve Comparisons for Plate 7 – 8 l/min

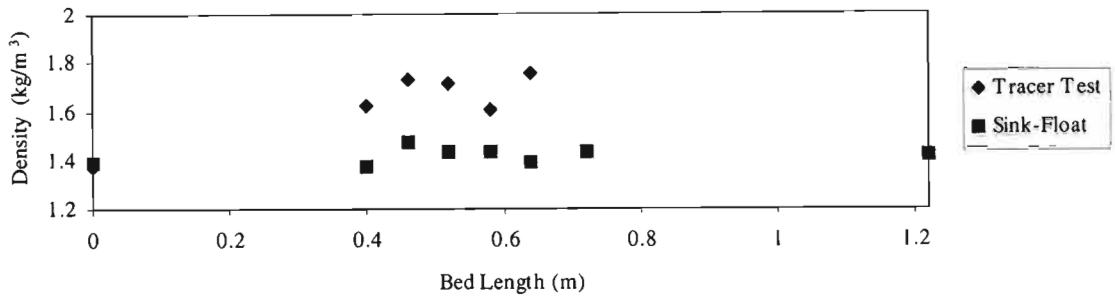

Figure C96: Comparison of the Tracer & Sink-Float Profiles through Teeter Bed for Plate 2 at 6 l/min

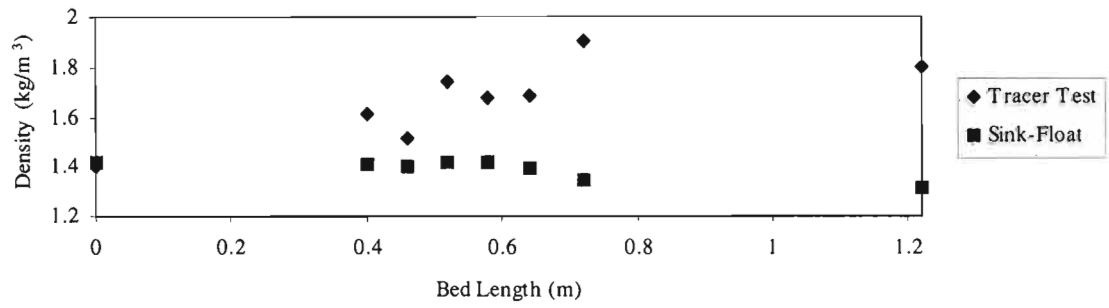

Figure C97: Comparison of the Tracer & Sink-Float Profiles through Teeter Bed for Plate 2 at 3 l/min

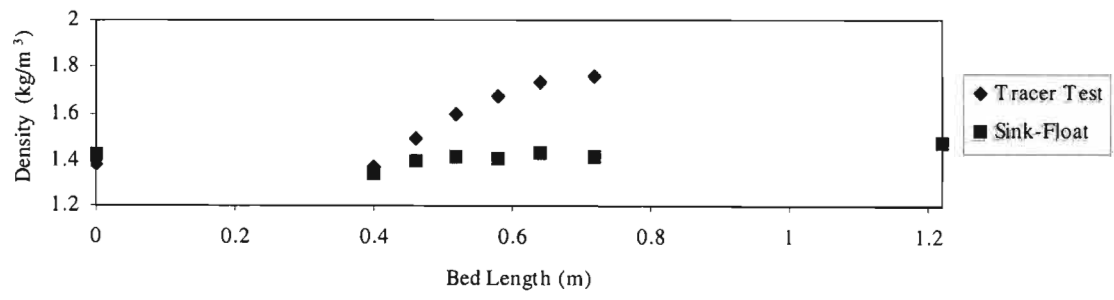

Figure C98: Comparison of the Tracer & Sink-Float Profiles through Teeter Bed for Plate 2 at 8 l/min

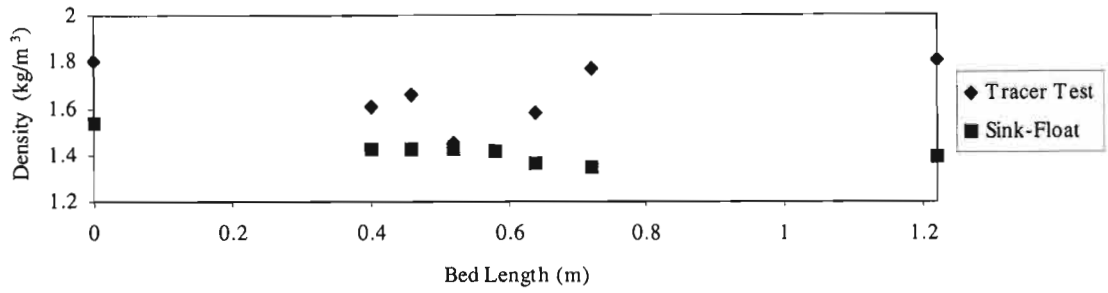

Figure C99: Comparison of the Tracer & Sink-Float Profiles through Teeter Bed for Plate 3 at 6 l/min

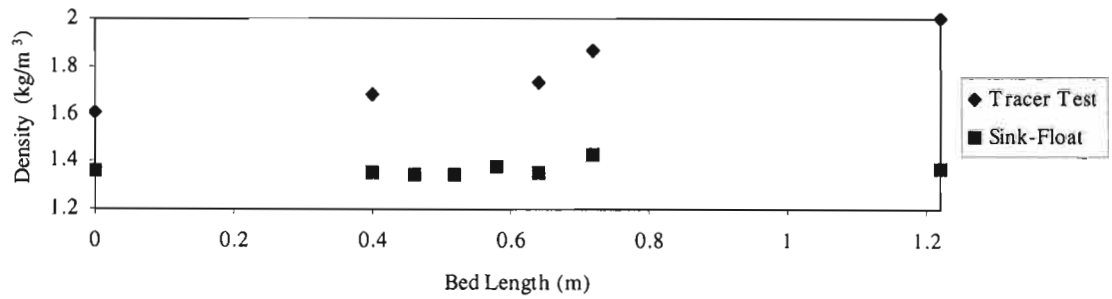

Figure C100. Comparison of the Tracer & Sink-Float Profiles through Teeter Bed for Plate 3 at 3 l/min

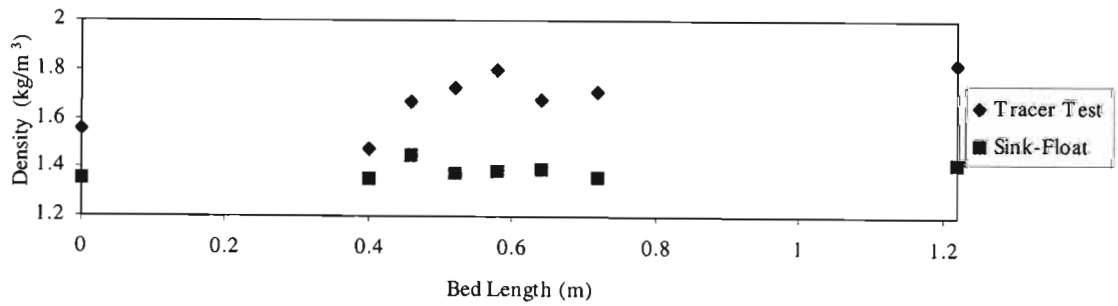

Figure C101: Comparison of the Tracer & Sink-Float Profiles through Teeter Bed for Plate 3 at 8 l/min

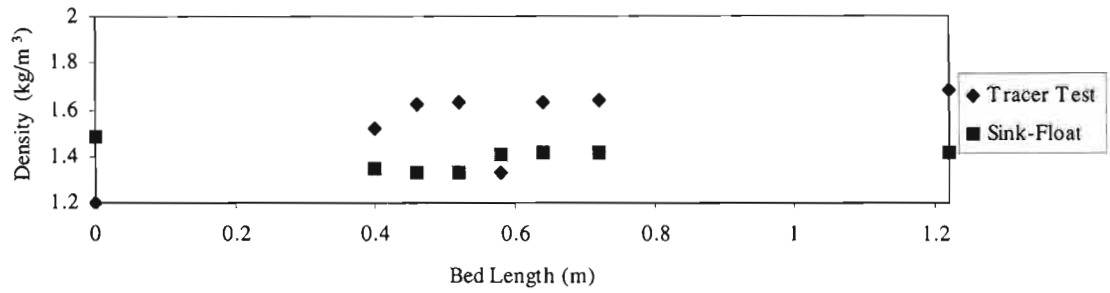

Figure C102: Comparison of the Tracer & Sink-Float Profiles through Teeter Bed for Plate 4at 6 l/min

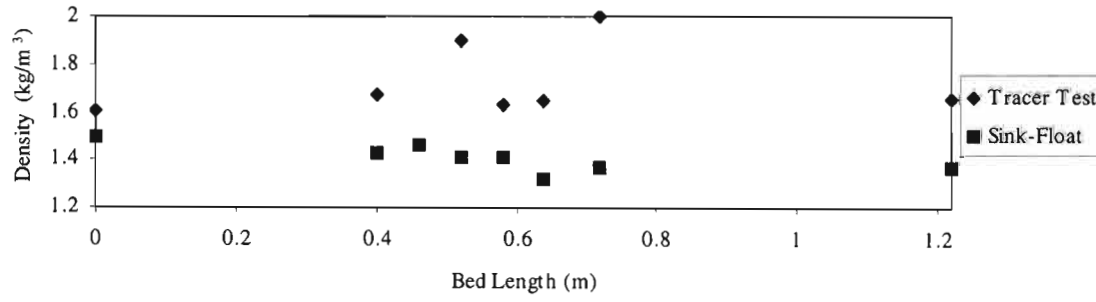

Figure C103: Comparison of the Tracer & Sink-Float Profiles through Teeter Bed for Plate 4 at 3 l/min

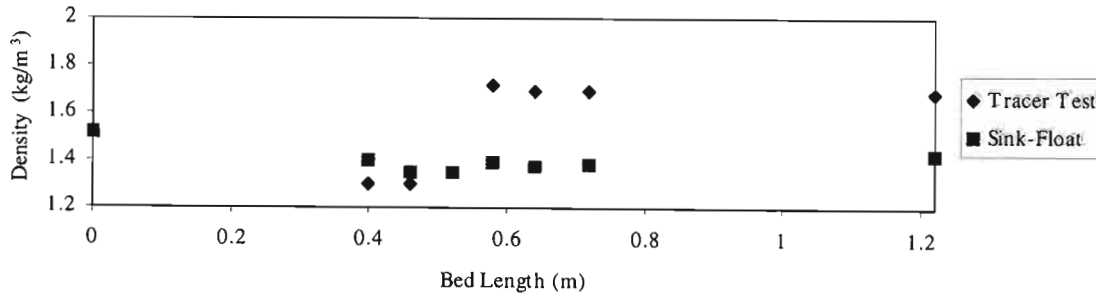

Figure C104: Comparison of the Tracer & Sink-Float Profiles through Teeter Bed for Plate 4 at 8 l/min

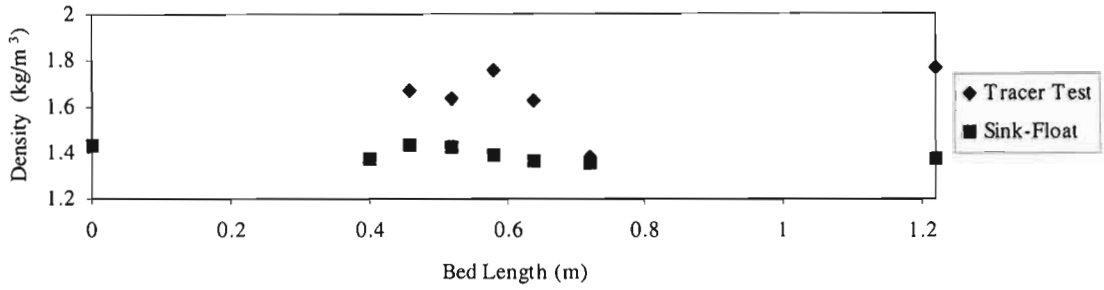

Figure C105: Comparison of the Tracer & Sink-Float Profiles through Teeter Bed for Plate 5 at 6 l/min

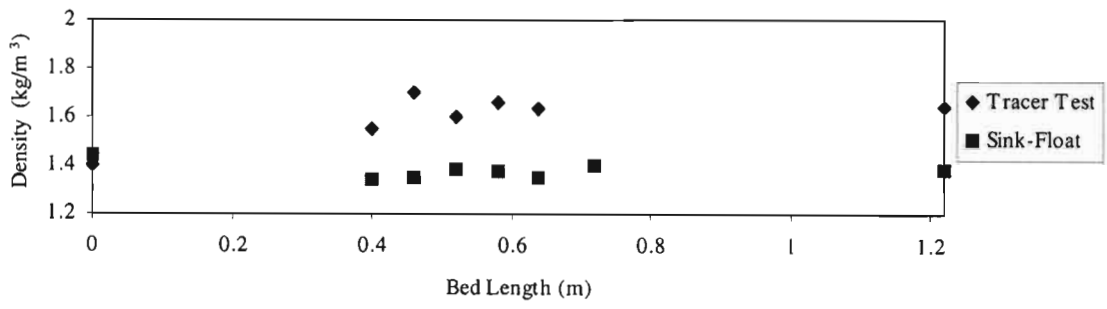

Figure C106: Comparison of the Tracer & Sink-Float Profiles through Teeter Bed for Plate 5 at 3 l/min

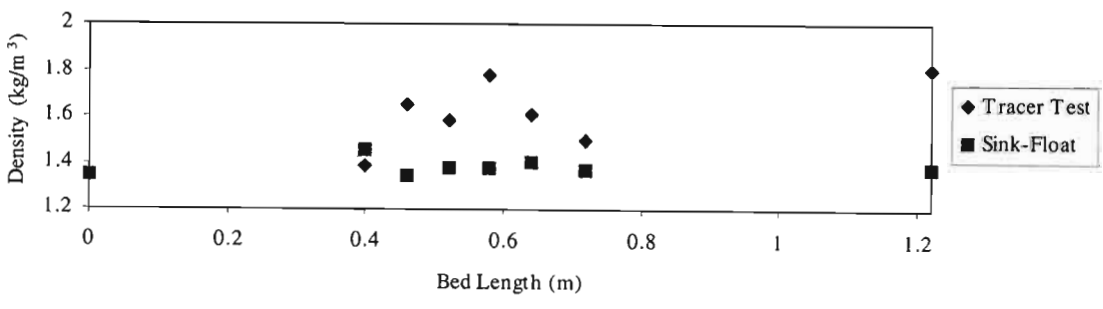

Figure C107: Comparison of the Tracer & Sink-Float Profiles through Teeter Bed for Plate 5 at 8 l/min

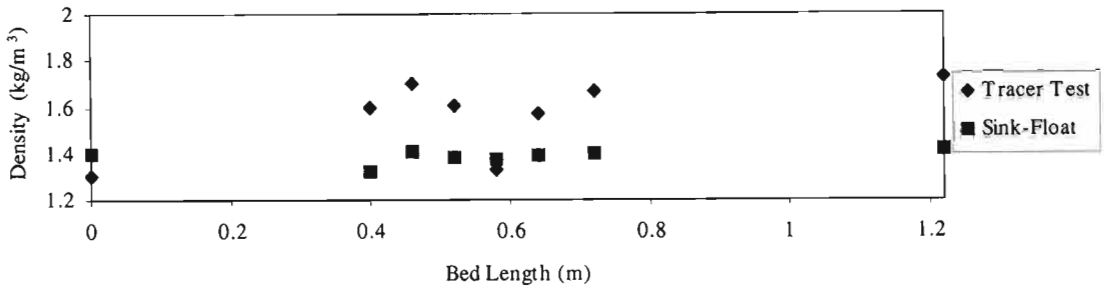

Figure C108: Comparison of the Tracer & Sink-Float Profiles through Teeter Bed for Plate 6 at 6 l/min

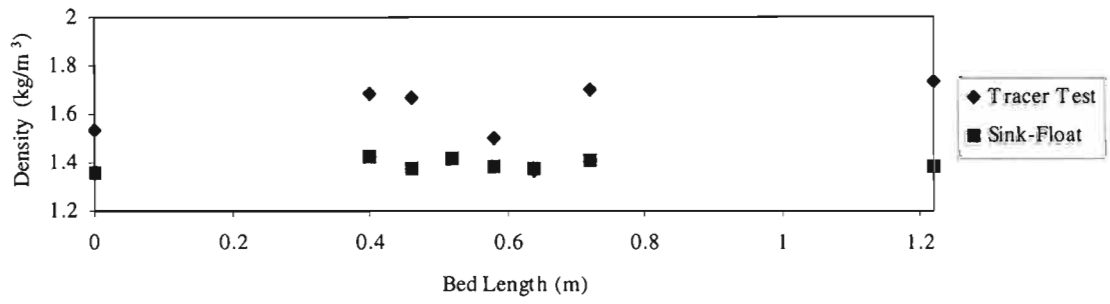

Figure C109: Comparison of the Tracer & Sink-Float Profiles through Teeter Bed for Plate 6 at 3 l/min

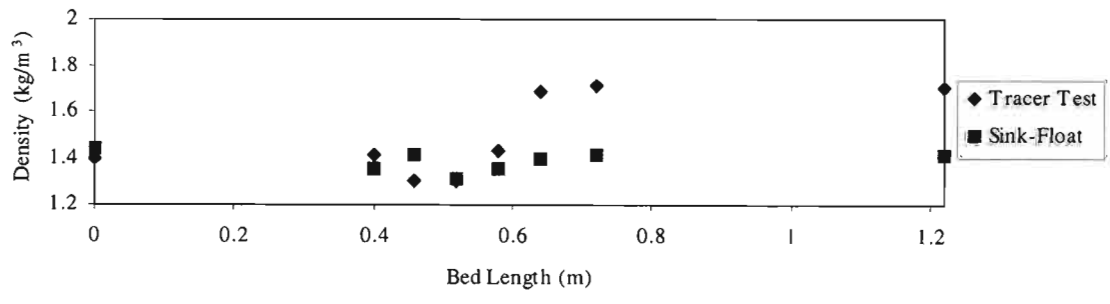

Figure C110: Comparison of the Tracer & Sink-Float Profiles through Teeter Bed for Plate 6 at 8 l/min

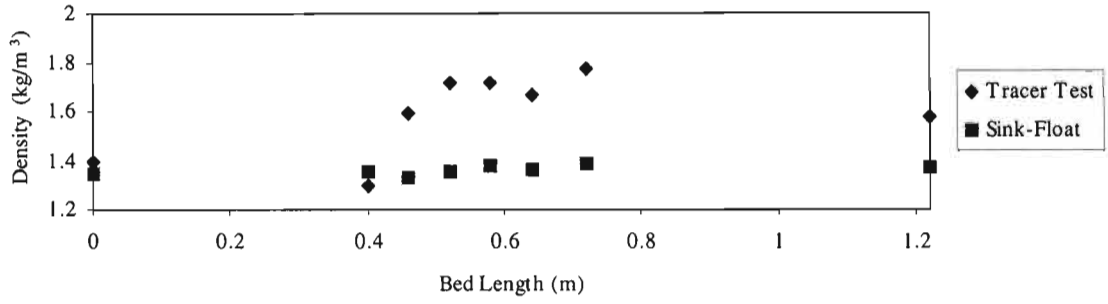

Figure C111: Comparison of the Tracer & Sink-Float Profiles through Teeter Bed for Plate 7 at 6 l/min

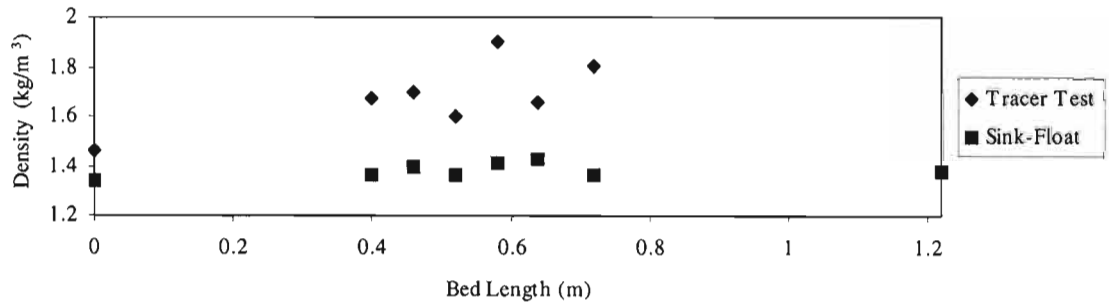

Figure C112: Comparison of the Tracer & Sink-Float Profiles through Teeter Bed for Plate 7 at 3 l/min

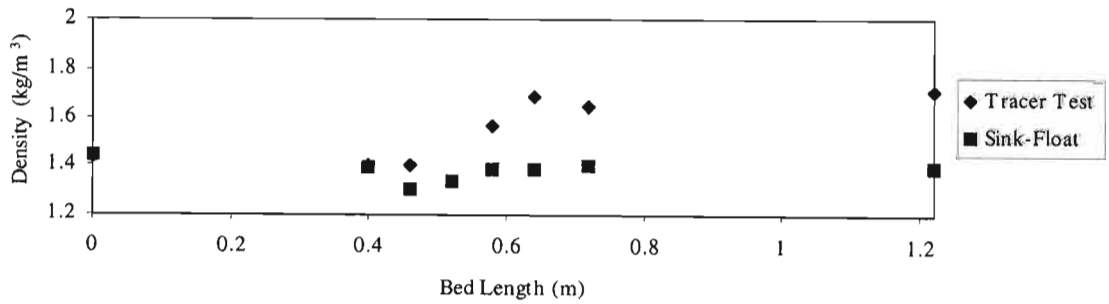

Figure C113: Comparison of the Tracer & Sink-Float Profiles through Teeter Bed for Plate 7 at 3 l/min

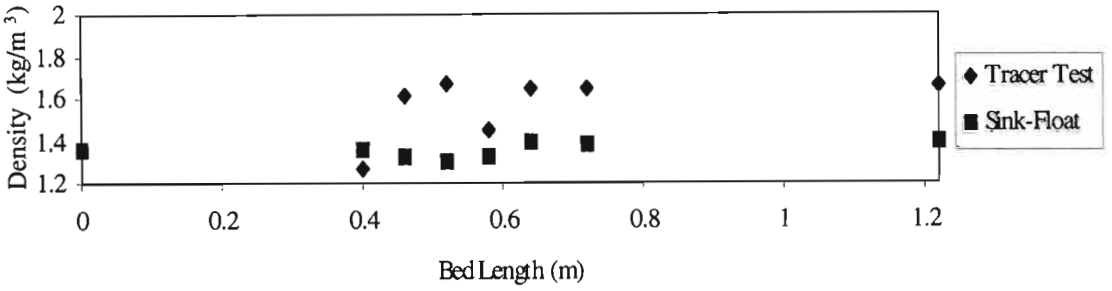

Figure C114: Comparison of the Tracer & Sink-Float Profiles through Teeter Bed for Plate 1a at 6 l/min

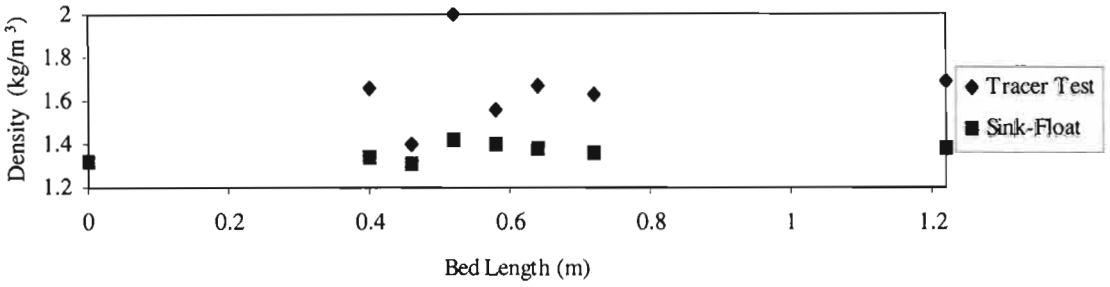

Figure C115: Comparison of the Tracer & Sink-Float Profiles through Teeter Bed for Plate 1a at 3 l/min

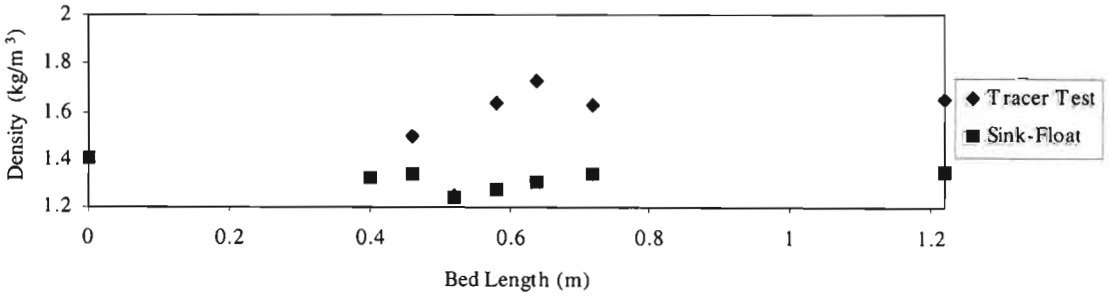

Figure C116: Comparison of the Tracer & Sink-Float Profiles through Teeter Bed for Plate 1a at 8 l/min

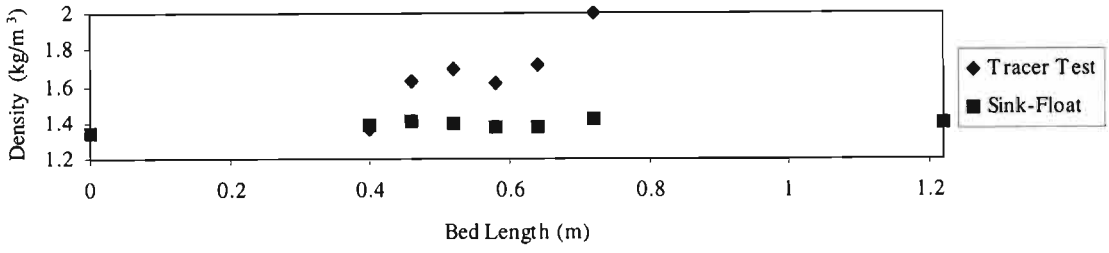

Figure C117: Comparison of the Tracer & Sink-Float Profiles through Teeter Bed for Plate 2a at 6 l/min

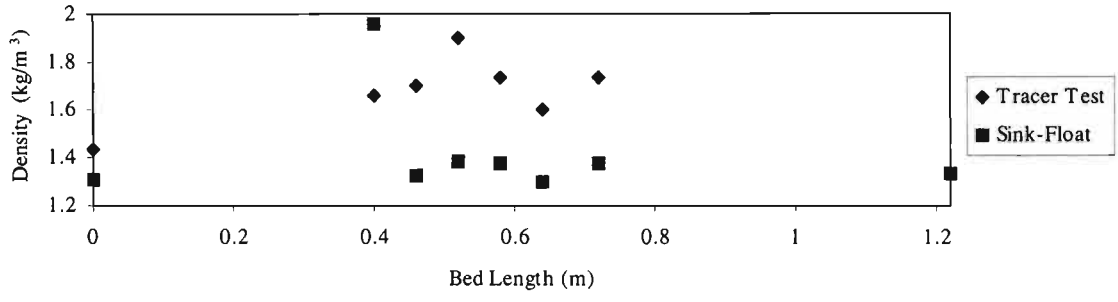

Figure C118: Comparison of the Tracer & Sink-Float Profiles through Teeter Bed for Plate 2a at 3 l/min

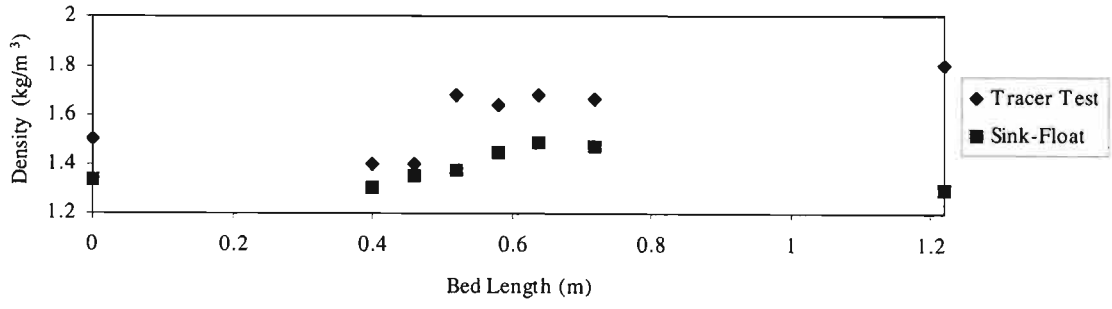

Figure C119: Comparison of the Tracer & Sink-Float Profiles through Teeter Bed for Plate 2a at 8 l/min

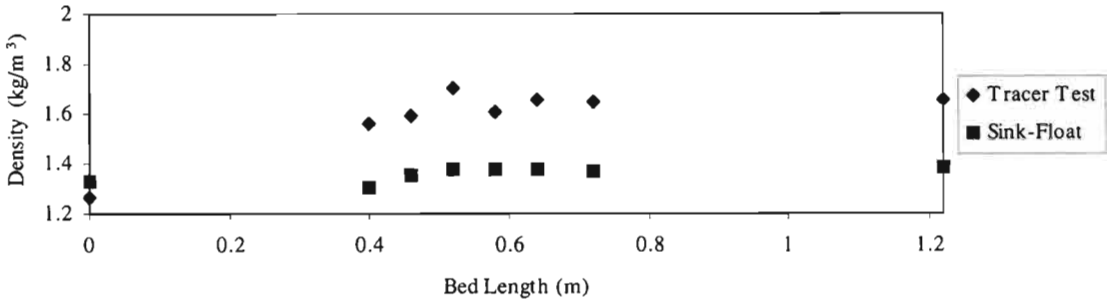

Figure C120: Comparison of the Tracer & Sink-Float Profiles through Teeter Bed for Plate 3a at 6 l/min

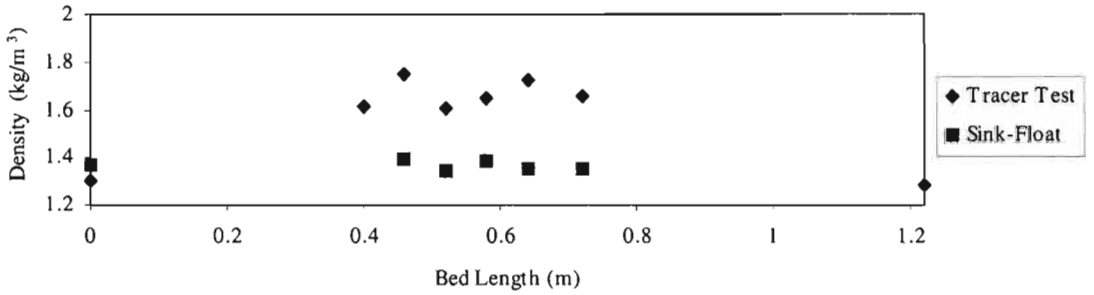

Figure C121: Comparison of the Tracer & Sink-Float Profiles through Teeter Bed for Plate 3a at 3 l/min

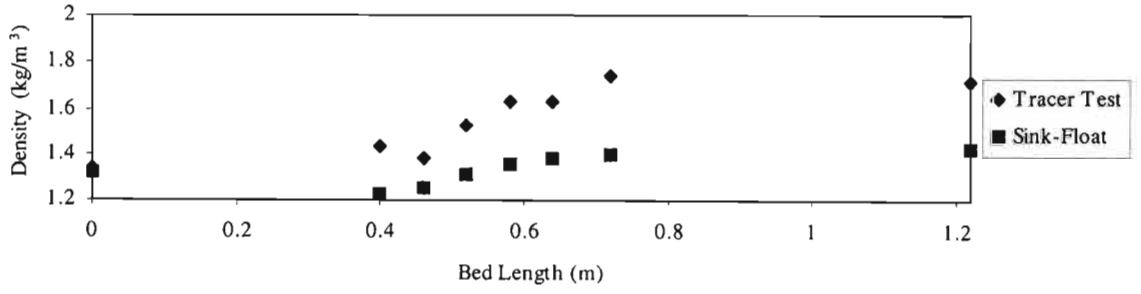

Figure C122: Comparison of the Tracer & Sink-Float Profiles through Teeter Bed for Plate 3a at 8 l/min

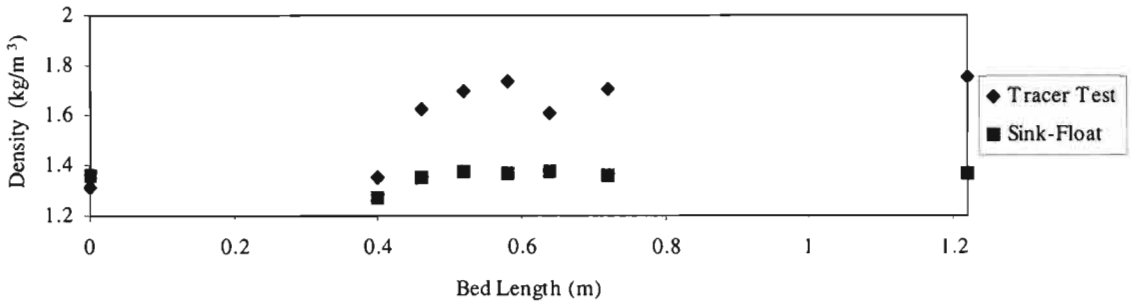

Figure C123: Comparison of the Tracer & Sink-Float Profiles through Teeter Bed for Plate 4a at 6 l/min

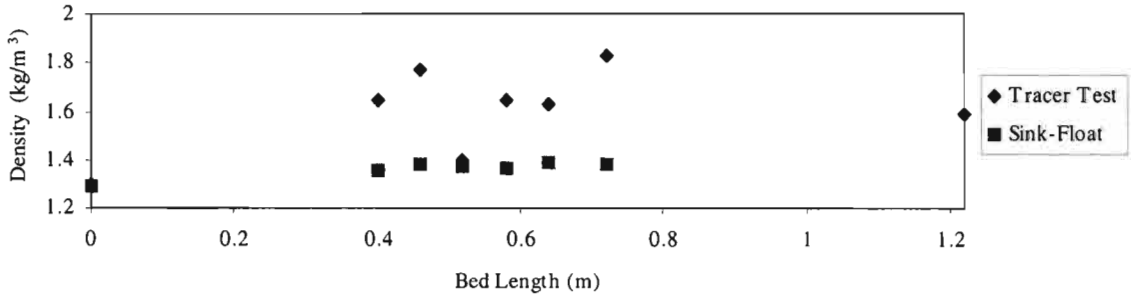

Figure C124: Comparison of the Tracer & Sink-Float Profiles through Teeter Bed for Plate 4a at 3 l/min

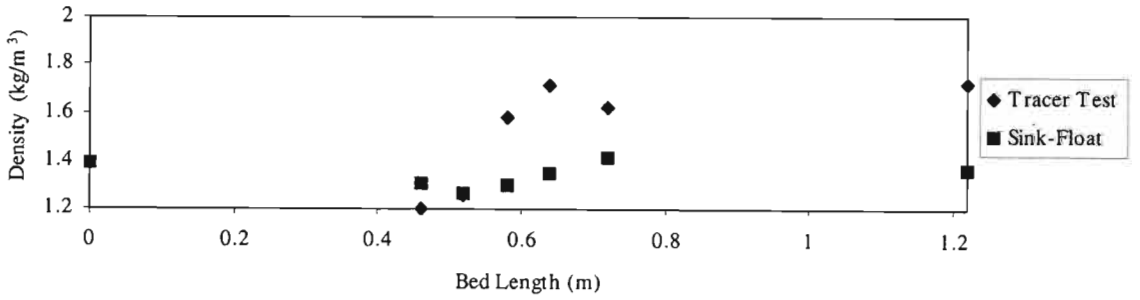

Figure C125: Comparison of the Tracer & Sink-Float Profiles through Teeter Bed for Plate 4a at 8 l/min

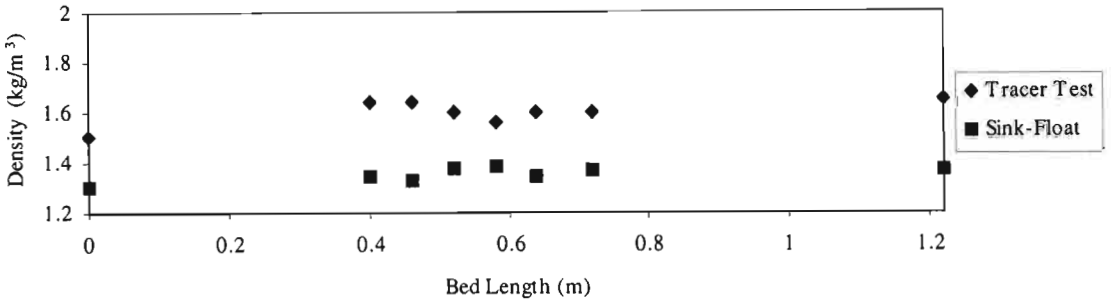

Figure C126: Comparison of the Tracer & Sink-Float Profiles through Teeter Bed for Plate 5a at 6 l/min

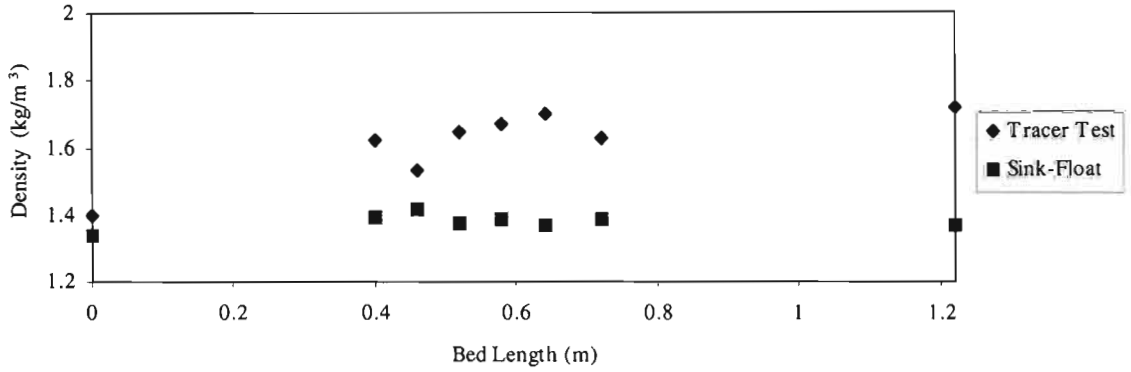

Figure C127: Comparison of the Tracer & Sink-Float Profiles through Teeter Bed for Plate 5a at 3 l/min

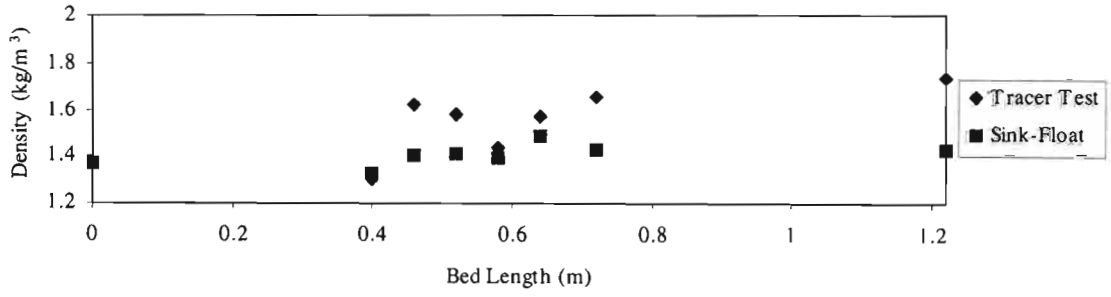

Figure C128: Comparison of the Tracer & Sink-Float Profiles through Teeter Bed for Plate 5a at 8l/min

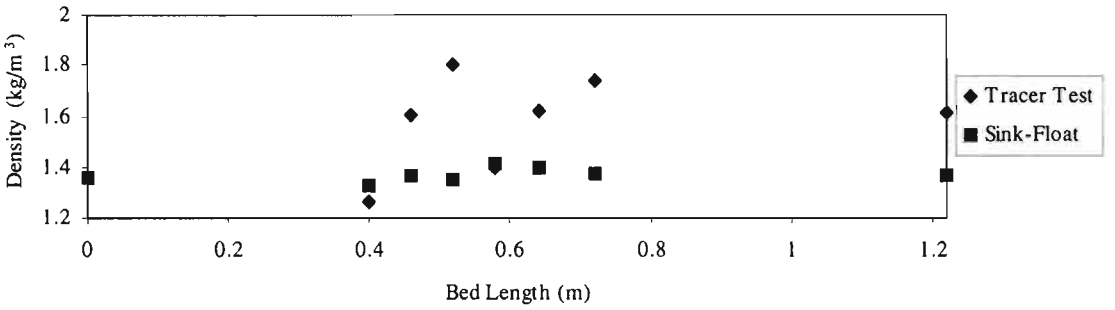

Figure C129: Comparison of the Tracer & Sink-Float Profiles through Teeter Bed for Plate 6a at 6 l/min

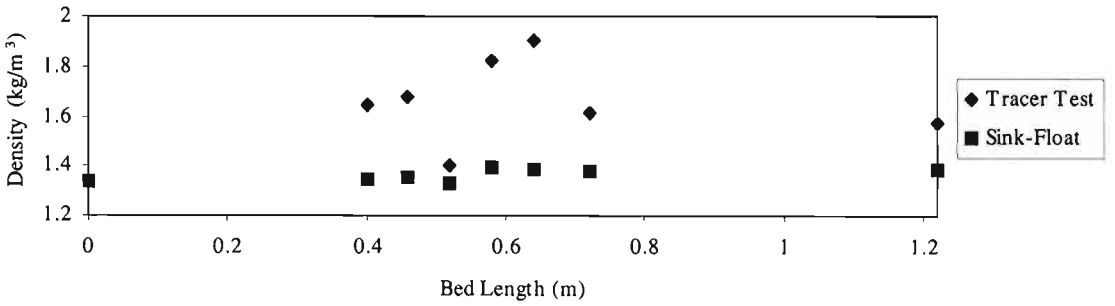

Figure C130: Comparison of the Tracer & Sink-Float Profiles through Teeter Bed for Plate 6a at 3 l/min

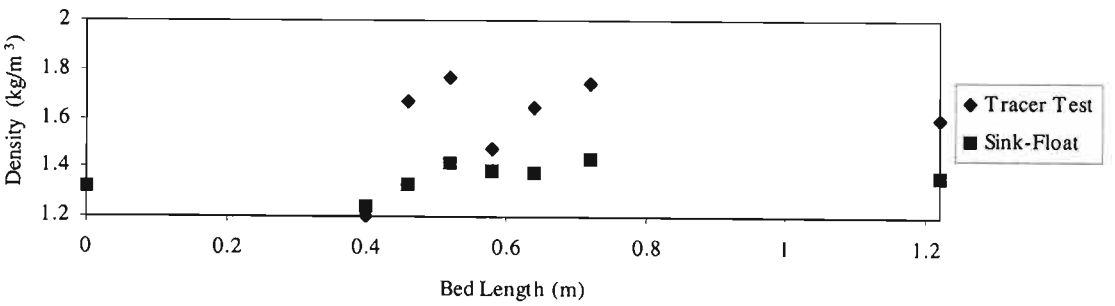

Figure C131: Comparison of the Tracer & Sink-Float Profiles through Teeter Bed for Plate 6a at 8 l/min

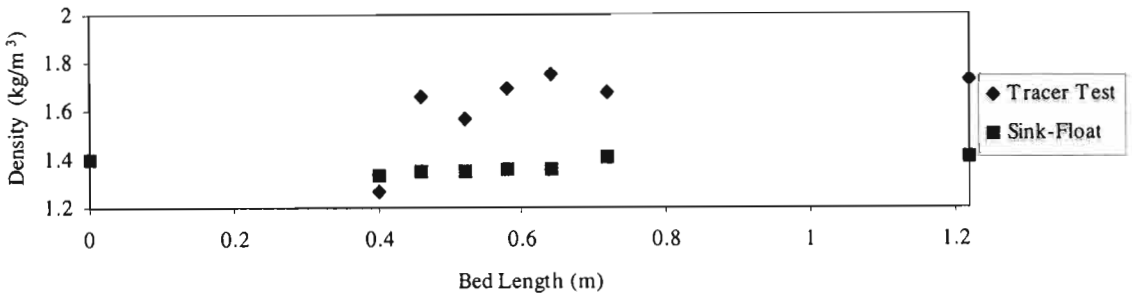

Figure C132: Comparison of the Tracer & Sink-Float Profiles through Teeter Bed for Plate 7a at 6 l/min

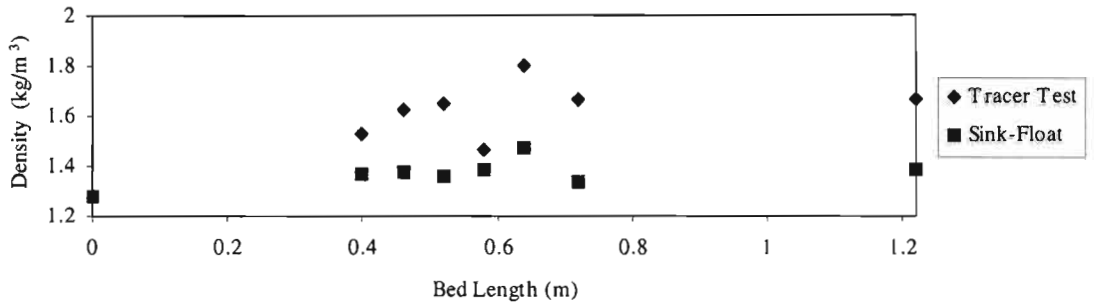

Figure C133: Comparison of the Tracer & Sink-Float Profiles through Teeter Bed for Plate 7a at 3 l/min

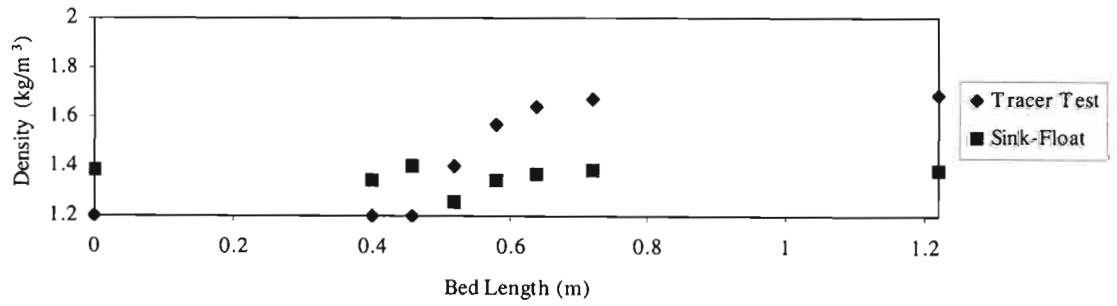

Figure C134: Comparison of the Tracer & Sink-Float Profiles through Teeter Bed for Plate 7a at 8 l/min

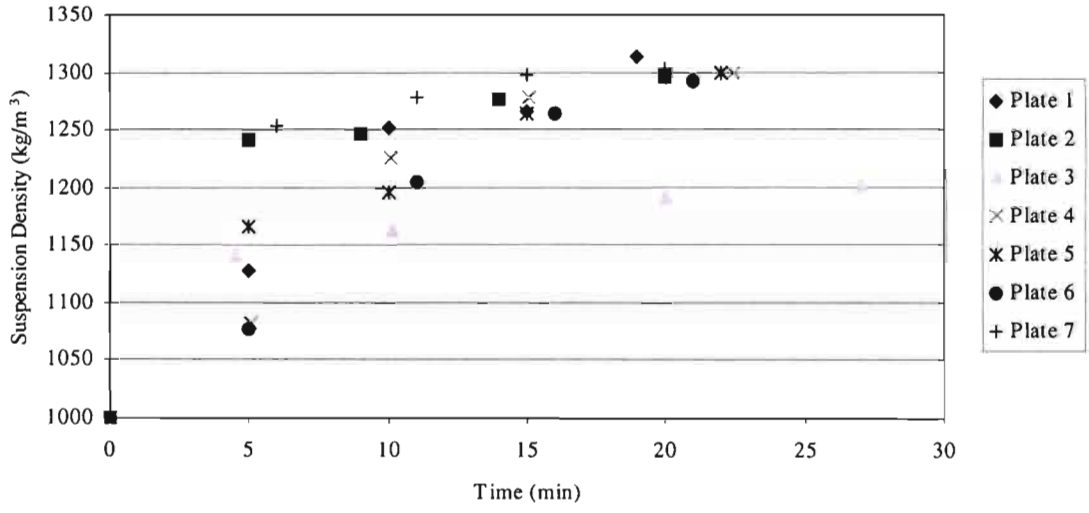

Figure C135: Suspension Density Variation with Time in the TBS at 6 l/min

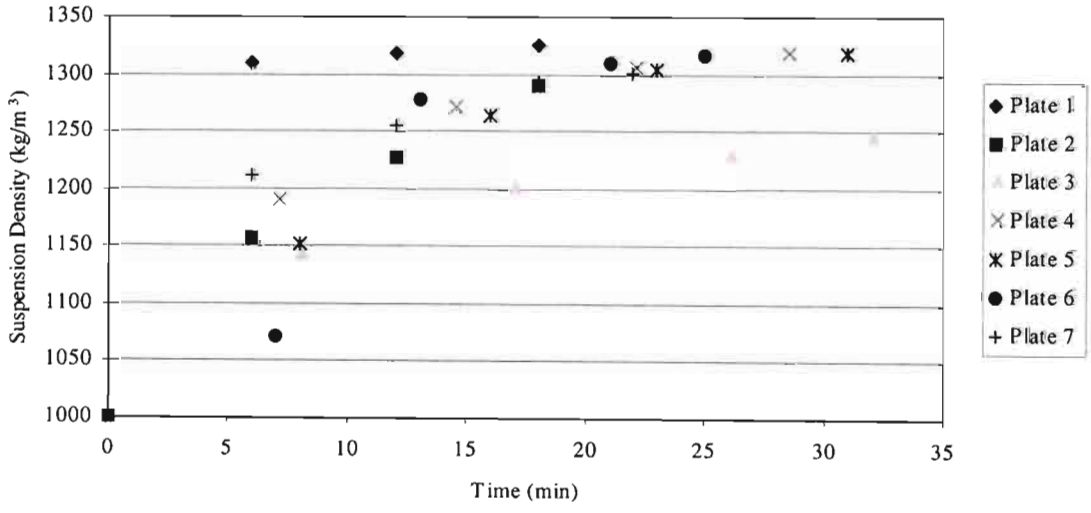

Figure C136: Suspension Density Variation with Time in the TBS at 3 l/min

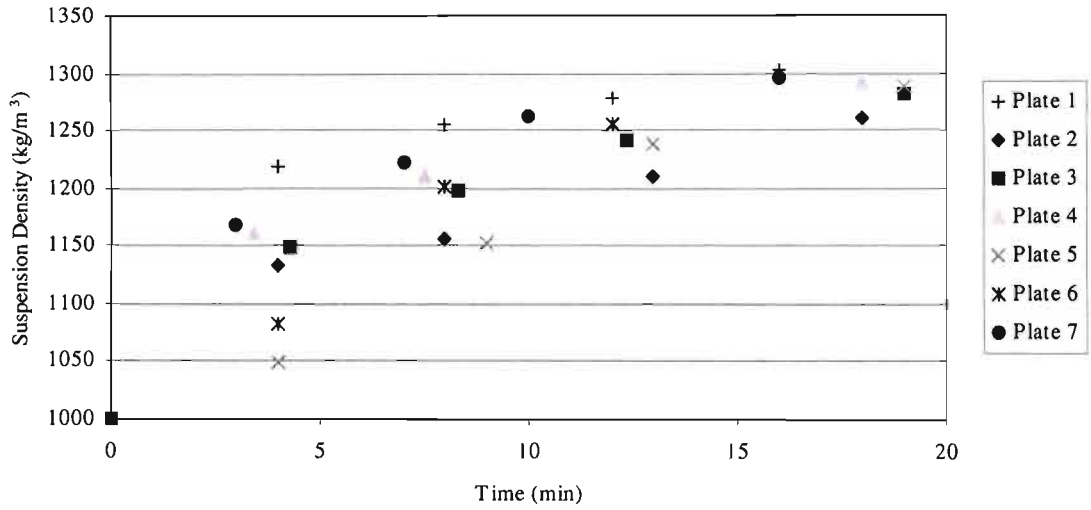

Figure C137: Suspension Density Variation with Time in the TBS at 8 l/min